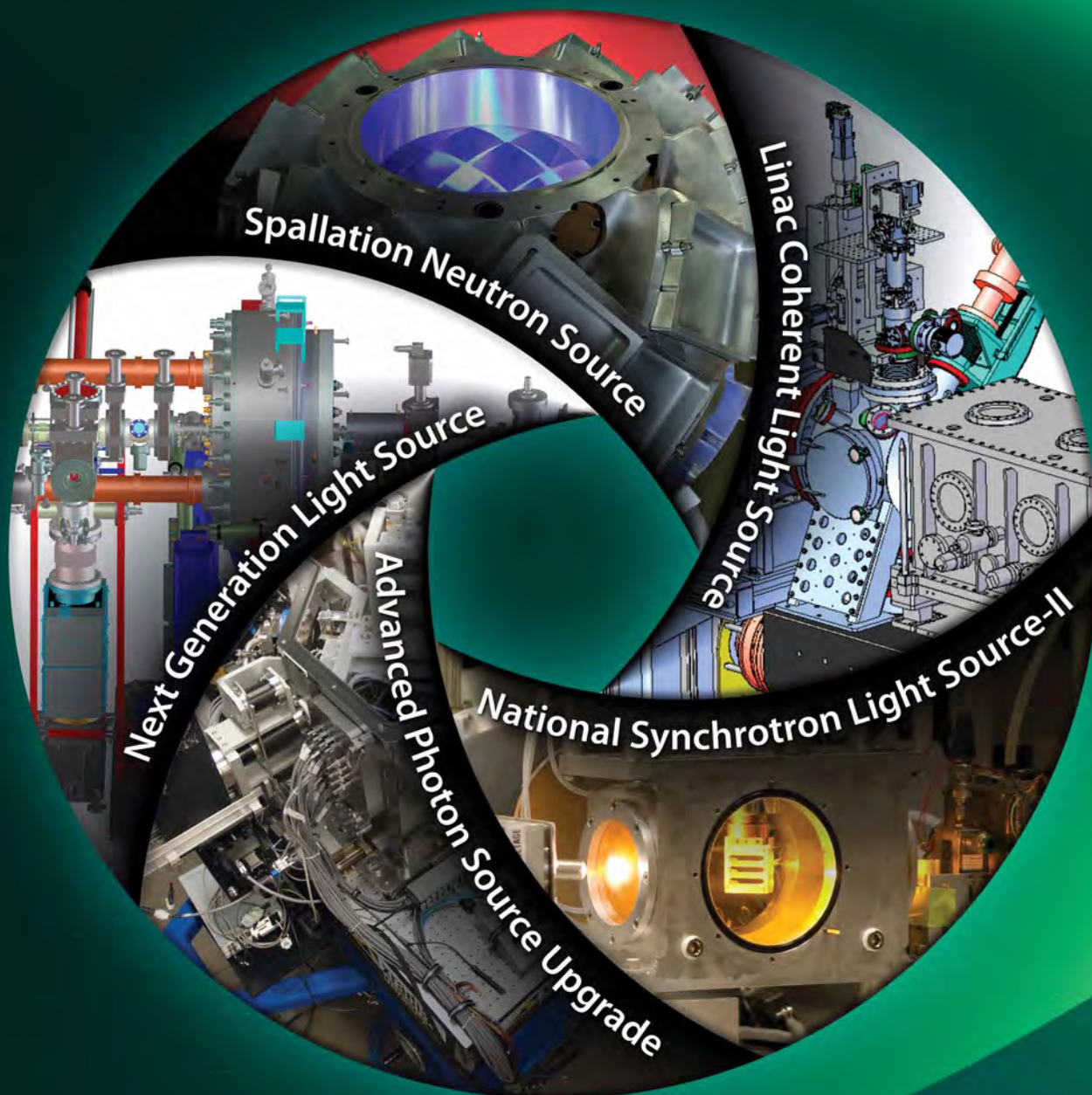


# Applications of New DOE National User Facilities in Biology

## Workshop Report



U.S. DEPARTMENT OF  
**ENERGY**

Office of  
Science

Office of Biological and Environmental Research

# Applications of New DOE National User Facilities in Biology Workshop

May 2011

Convened by

**U.S. Department of Energy**

**Office of Science**

**Office of Biological and Environmental Research**

## Co-chairs

**David Eisenberg**

University of California–Los Angeles

**Dagmar Ringe**

Brandeis University

## Organizers

**Roland Hirsch**

roland.hirsch@science.doe.gov

301.903.9009

**Susan Gregurick**

susan.gregurick@science.doe.gov

301.903.7672

---

**This report and more workshop information can be obtained at:  
[genomicscience.energy.gov/userfacilities/structuralbiologyworkshop/](http://genomicscience.energy.gov/userfacilities/structuralbiologyworkshop/)**



## About the Cover

### Image credits clockwise from top:

- Detector array for the TOPAZ instrument, Spallation Neutron Source at Oak Ridge National Laboratory.
- Coherent x-ray imaging system, Linac Coherent Light Source at SLAC National Accelerator Laboratory.
- Bio x-ray absorption spectrometer, National Synchrotron Light Source at Brookhaven National Laboratory.
- BioNanoprobe prototype, Advanced Photon Source at Argonne National Laboratory.
- Advanced photoinjector and initial acceleration section, Next Generation Light Source at Lawrence Berkeley National Laboratory.

## Suggested Citation for this Report

U.S. DOE 2012. *Applications of New DOE National User Facilities in Biology Workshop Report*, DOE/SC-0147, U.S. Department of Energy Office of Science. [genomicscience.energy.gov/userfacilities/structuralbiologyworkshop/report.pdf](http://genomicscience.energy.gov/userfacilities/structuralbiologyworkshop/report.pdf).

# Applications of New DOE National User Facilities in Biology

## Workshop Report

Published: February 24, 2012

**U.S. Department of Energy**  
**Office of Science**  
**Office of Biological and Environmental Research**





# PREFACE

This report represents the discussions and findings of a workshop held in May 2011 to consider the significance for biological science of five major Department of Energy (DOE) national user facilities that either have recently begun full operations (Linac Coherent Light Source and Spallation Neutron Source), are under construction (National Synchrotron Light Source-II), or are being designed (Advanced Photon Source Upgrade and Next Generation Light Source).

The Office of Biological and Environmental Research (BER), a program office in DOE's Office of Science, initiated support for researcher access to major user facilities for structural biology in 1990, when DOE was engaged in a similar program for constructing and upgrading these facilities. That initiative was focused on DOE synchrotron light sources and neutron beam facilities.

The workshop took place May 9–11 in Rockville, Maryland. Two months before the meeting, leaders from each of the five facilities submitted papers describing the facilities and potential applications in biology (these papers are included in Appendices A–E of this report). A panel of experts in the design, operation, and management of these facilities, as well as in several key nonfacility technologies used in biological research and in major areas of biology supported by BER, read these reports prior to the meeting (see Appendix F for participants list). At the meeting, the entire panel separately heard presentations from and engaged in discussions with representatives of each facility and then developed outlines for the chapters of this report.

The Executive Summary and the five chapters were prepared after the meeting by panel members and circulated to the entire panel for comments and editing prior to completion of the report. BER appreciates the involvement of all panel members, especially the co-chairs, Dagmar Ringe of Brandeis University and David Eisenberg of the University of California–Los Angeles.

The appendices describing the five facilities were prepared by staff of the respective national laboratories. In some cases, comments from panel members led to revisions of a paper; however, the final version included in this report represents the views of the national laboratory, not the panel members. The efforts of national laboratory staff members to prepare their papers are very much appreciated.

All of the written materials in this report were edited and prepared for publication by members of the Biological and Environmental Research Information System group at Oak Ridge National Laboratory. BER is indebted to the members of this group who devoted extensive time and much thought to preparation of all report components for publication.

Comments on this report will be welcomed by Roland Hirsch and Susan Gregurick, the BER program managers involved in the workshop.





# TABLE OF CONTENTS

Executive Summary .....	vii
Chapter 1. Advanced Photon Source Upgrade .....	1
Chapter 2. Linac Coherent Light Source.....	5
Chapter 3. National Synchrotron Light Source-II .....	11
Chapter 4. Next Generation Light Source .....	15
Chapter 5. Spallation Neutron Source.....	19
Appendices .....	25
Appendix A: Advanced Photon Source Upgrade .....	27
Appendix B: Linac Coherent Light Source .....	45
Appendix C: National Synchrotron Light Source-II .....	63
Appendix D: Next Generation Light Source.....	81
Appendix E: Spallation Neutron Source .....	99
Appendix F: Workshop Agenda and Participants .....	115
Acronyms and Abbreviations.....	Inside back cover



# EXECUTIVE SUMMARY

**B**iology has benefited greatly from resources enabling atomic-level investigations of matter. Biological questions that can only be addressed using high-intensity photon and neutron beams are now being explored. Particle accelerators developed over decades of research in high-energy physics have led to synchrotron light sources that offer very intense beams with tunable energies. Important contributions to the current understanding of a cell's biological infrastructure and the chemistry underpinning cellular function are based on results from experiments conducted at these synchrotrons.

An estimated 30% to 40% of light source users are from the biological sciences, and Nobel Prizes awarded in 1997, 2003, 2006, and 2009 recognized biochemical discoveries enabled by light sources. In fact, the biology community probably represents the largest single user group, even though synchrotron facilities in the United States generally were developed to support research in a variety of other fields, particularly materials science, geoscience, chemistry, and nanoscience.

In the United States, large scientific user facilities relevant to biological science are supported by many federal and state agencies. This report concerns facilities funded by the Department of Energy's (DOE) Office of Science, which develops and operates the largest base of national user facilities in the country. Within the Office of Science, the Office of Advanced Scientific Computing Research supports several of the world's fastest leadership computing facilities, with significant applications in biological science. The Office of Basic Energy Sciences (BES) maintains 17 user facilities including synchrotron radiation light sources, high-flux neutron sources, electron beam microcharacterization centers, and nanoscale science research centers. BES facilities enable progress in many scientific and technological disciplines and are used by more than 14,000 researchers annually. The Office of Biological and Environmental Research (BER) operates three major user facilities (the Atmospheric Radiation Measurement Climate Research Facility, the Environmental Molecular Sciences Laboratory, and the DOE Joint Genome Institute) that serve more than 3,000 users annually. The Offices of Fusion Energy Sciences, High Energy Physics, and Nuclear Physics also operate key facilities for research in physics that, in some cases, also have applications in the

life sciences (for example, experiments for development of particle beam therapies).

BER has played a major role in enabling new capabilities for biological research at existing Office of Science facilities. The primary focus of BER's Structural Biology activity is to support specialized instrumentation for biology at synchrotron light sources and neutron facilities. The light sources produce intense beams of x-rays and other wavelengths extending into the infrared to terahertz region, while particle accelerators and nuclear reactors produce neutron beams. These beams are directed into experimental stations housing instruments configured for specific biological investigations. This infrastructure provides user access to beamline instrumentation for studies of biological organisms and molecules in all areas of life science research. BER has supported development and operation of many of the instruments at the facilities, in close coordination with counterpart programs at other agencies and in the private sector.

These research facilities enable scientific studies aimed at understanding the structure and properties of matter at the atomic, molecular, and cellular levels, experiments not possible with instrumentation available in university, institute, or industrial laboratories. Several major techniques play a dominant role in structural biology: macromolecular crystallography, scattering from noncrystalline and semicrystalline materials, x-ray spectroscopy, and imaging using x-rays or other parts of the spectrum. Each of the five facilities described in this report will offer advanced capabilities for these techniques. Experimental results from such facilities have become critical parts of many investigations into the properties of biological systems from the molecular to cellular level. Facility use has become so important and widespread in biology that support staff have been specifically designated to assist novice users in accessing these resources.

Facility capabilities are essential for studies at the frontiers of science as well as for industrial research and development. Transfer of the knowledge gained from basic biological research at these facilities often leads to advances in industry and commerce. For example, the pharmaceutical industry has benefitted from these facilities in developing cancer treatments (including a recent therapy for melanomas) and new drugs for combating infections such as HIV. Collaboration

between facilities and scientific users ultimately benefits both. Continued involvement of academic scientists working at DOE national user facilities ensures development of advanced methods, and ongoing facility access allows new scientists to be trained in the design and building of new instrumentation. In fact, the training of new scientists familiar with the potential of these facilities is essential for future cutting-edge science in biology and all other fields.

## New Capabilities for Biological Research

With recent advances in synchrotron physics and advanced laboratory automation, national user facilities can now be upgraded to investigate new frontiers of biology. Planning for such enhancements thus is timely. Indeed, recent upgrades to European and Japanese synchrotrons are attracting some American investigators to compete for time on these remote facilities to perform advanced experiments not yet possible in the United States.

The Office of Science has a long-term plan for development of new or upgraded national user facilities with capabilities beyond those currently delivered. Two such facilities with important implications for biological science recently began full operation, and three others are in various stages of construction or planning:

- **Advanced Photon Source Upgrade (APS-U)** at Argonne National Laboratory — planning stage.
- **Linac Coherent Light Source (LCLS)** at SLAC National Accelerator Laboratory — operating.
- **National Synchrotron Light Source-II (NSLS-II)** at Brookhaven National Laboratory — under construction, with full operations expected to begin in 2015.
- **Next Generation Light Source (NGLS)** at Lawrence Berkeley National Laboratory — planning stage.
- **Spallation Neutron Source (SNS)** at Oak Ridge National Laboratory — operating.

To identify the new experimental capabilities that these facilities will provide and assess their potential impact on biological research, BER convened the *Applications of New DOE National User Facilities in Biology* community workshop from May 9–11, 2011, in Rockville, Maryland. The workshop was co-chaired by David Eisenberg (University of California, Los Angeles) and Dagmar Ringe (Brandeis University) and included a panel of experts in biological research enabled by synchrotron light sources, neutron facilities, and free-electron lasers, as well as in other types of key instrumentation used in biological research (see Appendix F for the workshop agenda and a list of participants). Scientists from each of the national laboratories prepared preworkshop papers about the new facilities (see Appendices A–E) and made presentations and engaged in

discussions with panel members during the meeting. The panel then wrote chapters describing each facility and its potential for supporting high-impact biology. The following brief summaries capture the key points in the five chapters.

### Advanced Photon Source Upgrade

APS, the largest synchrotron facility in the United States, runs an extremely successful user program, especially for structural biology. It is the only U.S. light source that can provide high-energy x-ray undulator radiation now and in the near future. APS has been in operation for more than 10 years, and the timely upgrade will allow major advances in synchrotron technology to be integrated into existing or new beamlines. The upgraded facility will provide x-rays with the highest flux and brightness at energies above about 10 and 20 kiloelectron volts (keV), respectively. Such capabilities will be achieved through long, straight sections; revolver and superconducting undulators; higher electron current; and improved beam stability. Novel “crab cavities” will enable 1 picosecond pulses in time-resolved experiments. Complementing the machine upgrade is a forefront instrumentation and beamline development program for ultrafast, high-energy imaging, and *in situ* studies. The proposed beamline and instrument upgrades build on world-leading programs and fully exploit unique APS properties. Importantly, in view of APS’s pivotal role in academic and industrial structural biology, machines will be upgraded with minimal loss of operating hours for ongoing programs. Two infrastructure projects—an automated crystallization facility and the Cryo Sample Preparation Facility—will meet the increasingly important need for onsite sample preparation in biological research. In summary, the proposed upgrade program is essential for restoring APS as a leading synchrotron source among new and recently upgraded facilities with significant impacts in biology.

### Linac Coherent Light Source

LCLS is the world’s first x-ray free-electron laser (XFEL) user facility. The machine produces extremely bright x-ray pulses as short as 10 femtoseconds over the energy range of ~500 to 10,000 eV with  $\sim 10^{12}$  photons per pulse. LCLS is capable of producing x-ray pulses of the highest energy of any XFEL worldwide. Five of the six planned multidisciplinary experimental stations are open to the user community and have produced exciting results; the sixth (Matter in Extreme Conditions) is in commissioning and will begin serving users in May 2012. The initial success of experiments on femtosecond nanocrystallography at LCLS has generated great excitement among structural biologists. Structure determination is based on collection of thousands of femtosecond x-ray diffraction snapshots collected on a stream of nanocrystals by femtosecond pulses. As diffraction is recorded in femtoseconds before the sample is destroyed, this method (1) overcomes the radiation damage problem in x-ray crystallography, (2) enables data collection on crystals that contain less than 1,000 unit cells,

(3) allows data collection at room temperature, and (4) may open the way for a new era of x-ray crystallography from nanocrystals. The first time-resolved femtosecond crystallography experiments indicate that LCLS will enable the determination of time-resolved x-ray data that could lead to molecular movies of biomolecules at work on a subpicosecond time scale. Early results from coherent x-ray imaging of single virus particles indicate that single particles can be imaged at LCLS and that the higher peak brilliance of the facility's planned expansion (LCLS-II) may extend single-particle analysis to atomic resolution. Plans for LCLS-II, to be completed in 2018, include increasing the peak brilliance of x-ray pulses, extending the energies accessible to a range from 200 eV to 20 keV, and supporting up to six simultaneous experiments. LCLS holds great potential for enabling researchers to obtain high-resolution structural data from biological samples free of radiation damage. Realizing this exciting promise will require further development of new detectors, rapid and low-consumption sample delivery techniques, and improved data analysis methods.

### **National Synchrotron Light Source-II**

Currently under construction, NSLS-II is set to begin operations in 2014. This synchrotron radiation source, located near the original NSLS, will accommodate at least 58 beamlines covering a wide range of disciplines, including the life sciences. Completely new, NSLS-II will deliver an extremely bright beam from the far infrared to the very hard x-ray region. By providing the world's brightest light source x-ray beams ranging from 2 to 10 keV, NSLS-II will be uniquely positioned to provide capabilities in this energy range, such as bright coherent beams for imaging and spectroscopy. For higher-energy x-rays, NSLS-II will be comparable to the best light sources. This facility will open new frontiers in photon sciences and engender development of new instruments and techniques to exploit fully its beam characteristics with cutting-edge projects such as a 1 nm hard x-ray nanoprobe. Planned biological beamlines at NSLS-II encompass macromolecular crystallography, scattering, spectroscopy, and imaging, ensuring that NSLS-II will play a major role in future biological research. In addition, the NSLS-II design includes a Biology Village or community of highly integrated groups working in different but related areas of the life sciences. This Village will provide a unified and synergistic environment for life science experiments and change the way researchers interact and work at a synchrotron radiation user facility. NSLS-II promises to be an outstanding source for many new types of experiments in various disciplines and will help the U.S. maintain a strong leadership position in synchrotron-based biological research.

### **Next Generation Light Source**

NGLS is a new facility in the early stages of planning (anticipated first light is in 2022). With an array of 10 independently configurable XFELs powered by a superconducting linear

accelerator, NGLS will be capable of delivering ultrafast, high-brightness, and high-resolution pulses of low-energy x-rays at high repetition rates. Each of these features distinguishes NGLS from any existing synchrotron or XFEL and contributes to its currently envisaged suite of transformative scientific capabilities for biology. For example, macromolecules, molecular assemblies, organelles, and cells will be imaged in real time and in real biological contexts. Individual biological objects will be imaged, rather than averaged over a large sample, to enable new understanding of the role of biological heterogeneity. Selective enhancement of scattering from specific chemical groups will permit simultaneous investigations of the structure and chemistry of molecular systems in solution. Additional powerful applications undoubtedly will emerge once this unique light source comes online.

### **Spallation Neutron Source**

SNS approached its designed operational capability about a year ago, becoming one of the world's two most powerful sources for investigating the structure and dynamics of biomolecular systems by elastic and inelastic neutron scattering. Isotopic substitution, specifically deuterium for hydrogen in the case of biological systems, coupled with contrast matching of selected components, provides a distinct advantage for these neutron-scattering techniques. This method can reveal key aspects of structure and dynamics over a wide range of length and time scales within complex macromolecular systems. Although important for studying biological macromolecules in single crystals, these techniques are essential for investigating more complex, noncrystalline systems, including multicomponent macromolecular assemblies in solution and liquid-crystalline membranes. Two important upgrades have been proposed and built into the SNS design. One would expand the proton accelerator's power, increasing by two to three times the flux of spallation-produced neutrons. This increase is highly significant because most neutron-scattering experiments are "flux-starved" (i.e., limited only by the available neutron flux). The other upgrade would add a second target station optimized for producing longer-wavelength "cold" neutrons important for structural studies of large macromolecular systems at longer length scales. This upgrade also will provide much needed additional capacity, including instruments optimized for studying biological systems.

### **The Path Forward**

This workshop report describes in detail these five major national user facilities and identifies their potential for significant impacts on biological research. The facilities—which have begun initial operations or are expected to move from planning to upgraded or new construction in the coming decade—will support a wide range of biological experiments. Such experiments include those that can be planned now and others that can be planned only after capabilities of the new facilities emerge. These facilities are expected to offer

new technologies that will advance not only biology, but also many other disciplines such as chemistry, geology, physics, and materials science.

For optimal service to the scientific community, the facilities also must consider the collateral needs of users. Of paramount importance will be development of a new generation of detectors, as well as advanced approaches for specimen mounting, preservation, and changing, including robotic devices for high-throughput applications. These capabilities will maximize the output of the experimental

stations at the facilities. Advances in technology and methods for data processing and storage will be critical, and adequate plans to recruit, house, and train new users are essential.

By focusing on the present and potential future capabilities of the five facilities, this report seeks to increase awareness of them among scientists in all areas of biology and related disciplines. Informing researchers about such capabilities and how they can be used to advance individual research is a challenge for each facility.

## Chapter 1

# ADVANCED PHOTON SOURCE UPGRADE

### Brief Facility Description

As the largest synchrotron facility in the United States, the Advanced Photon Source (APS) at Argonne National Laboratory runs an extremely successful user program, serving almost 3,800 researchers in 2010. APS generates synchrotron radiation of unrivaled brightness and is the only U.S. light source that can provide high-energy x-ray undulator radiation now and in the near future. The facility has contributed to numerous scientific advances, particularly in structural biology. This success is demonstrated by the impact of APS-enabled insights into, for example, ribosome structures and G protein-coupled receptors, as well as the number of publications and Protein Data Bank depositions resulting from APS work. Protein crystallography with picosecond temporal resolution was pioneered at APS and the European Synchrotron Radiation Facility, and the introduction of microprotein crystallography and related beamline instrumentation and automation was paramount in several high-profile projects. More recently, APS provision of micrometer-sized beams enabled the demonstration of their radiation damage-mitigating properties. The elemental and chemical specificity of x-ray fluorescence and microprobe x-ray absorption near-edge spectroscopy has been established in microscopy and tomography techniques at APS and successfully applied to biological research, environmental studies, and the imaging of nanoparticles. The current APS beam size is about 200 nanometers (nm), and studies are carried out mainly on freeze-dried samples in two dimensions. Recently, the first three-dimensional (3D) distribution maps of trace elements in a freshwater diatom were determined in a groundbreaking experiment.

An upgrade of the APS (in operation for more than 10 years) is timely and will allow major advances in the field to be integrated into existing or new beamlines. The upgraded facility will provide x-rays with the highest flux and brightness at energies above 10 and 20 kiloelectron volts (keV), respectively. Such capabilities will be achieved through long straight sections; revolver and superconducting undulators; higher electron current; and improved beam stability. Novel “crab cavities” will enable 1 picosecond pulses in time-resolved experiments. The machine upgrade is

complemented by a forefront instrumentation and beamline development program for ultrafast, high-energy, imaging, and *in situ* studies. Importantly, in view of APS’s pivotal role in academic and industrial structural biology, the machine upgrade will be realized with minimal loss of operating hours to ongoing programs. The proposed upgrade is essential for restoring APS as a leading synchrotron source among new and recently upgraded facilities.

### Facility Capabilities and Potential for High-Impact Experiments

The APS Upgrade (APS-U) has two scientific themes:

- (1) *Mastering hierarchical structures through imaging* and
  - (2) *Real materials under real conditions in real time*.
- As part of the overall scientific strategy for the upgrade, the APS Scientific Advisory Committee strongly endorsed proposals for new biology facilities. These proposals include a new beamline for microfocus protein crystallography, a new x-ray fluorescence microscope (BioNanoprobe II), a new beamline for small- and wide-angle x-ray scattering, and two infrastructure projects focused on sample preparation. These life science beamlines and infrastructure projects are not included in the scope of APS-U (funded by the DOE Office of Basic Energy Sciences) and hence will require separate funding.

### Microfocus Macromolecular Crystallography Beamline

Microcrystallography is the latest transformative advance in macromolecular crystallography (MX). Facilities around the world are scrambling to meet user demand by developing new microbeamlines, which require an order-of-magnitude greater precision in beam delivery and sample positioning than conventional beamlines. The proposed microfocus beamline will complete APS’s MX beamline portfolio. By providing the highest-energy microfocus beam for MX in the world, this beamline will take full advantage of APS’s unique source properties and complement the planned microfocus beamline at the National Synchrotron Light Source-II (NSLS-II) under construction at Brookhaven National Laboratory. High-energy microbeams enable improved signal-to-noise and, when combined with microcrystals, offer

the largest potential to reduce radiation damage to samples. With appropriate infrastructure, software, and support (see following sections), this beamline will enable data collection from crystals currently discarded as too small or imperfect, thereby reducing the need for time-consuming crystal optimization to avoid complete failure of structure solution. The new beamline will complement existing MX microbeams at APS and other microfocus beams under development, adding capacity to meet the strong and rapidly growing demand for dedicated microcrystallography facilities.

APS's importance for the U.S. structural biology community cannot be overestimated. NSLS-II construction is currently ahead of schedule, and early access to some beamlines will be available in 2014. However, other beamlines will not be available until 2015 or 2016, and the facility's full capacity may not be reached until 2017. Thus, both the APS-U project and continued availability of APS beamlines operating at the highest performance level are of great importance. Furthermore, APS and NSLS-II have complementary energy spectra, and, for x-ray energies above ~13 keV, APS will remain the nation's highest-flux synchrotron source even after NSLS-II is operational. For these reasons, the workshop panel endorses implementing the upgrade over 6 years with minimal instrument downtime for users.

### ***BioNanoprobe II: An X-Ray Fluorescence Microscope***

A second topic highlighted in the APS-U presentation is the use of nanofocused beams to perform x-ray fluorescence microscopy (XFM). The proposed BioNanoprobe II will offer a spatial resolution of 20 nm and improve elemental sensitivity by two orders of magnitude over current levels. Importantly, the high energy of APS will be fully exploited to probe all relevant absorption edges with high flux (5 to 30 keV). These higher energies also will be beneficial for studying thick or highly absorbing samples, both in the biological sciences and in the geosciences. The microscope will be operated in-vacuum, and samples will be held at cryogenic temperatures to minimize photoreduction and structural changes. It also will offer correlative optical cryomicroscopy (e.g., for complementary visualization of fluorophores). Dose fractionation enabled by simultaneous phase-contrast imaging is an important development to shorten exposure times and reduce radiation damage. Moreover, 3D reconstruction of the sample structure from the phase-contrast signal significantly facilitates interpretation of the spatial distribution of trace elements.

BioNanoprobe II will provide unique imaging capabilities for biological, biomedical, and environmental studies. It addresses the current gap in resolution between optical microscopies and electron microscopy and offers elemental and chemical specificity on thicker samples. The instrument's impact will be limited only by its throughput. Achieving the highest possible throughput will be critically important because studies of

genetically modified bacteria or cells require the measurement of a large number of samples to be conclusive.

### ***SAXS and WAXS Beamline***

Solution small-angle x-ray scattering (SAXS) has become an important method in structural biology. SAXS provides information complementary to data obtained with protein crystallography (e.g., the stoichiometry of large complexes and the conformational dynamics of proteins and complexes in solution). This technique also is useful if samples cannot be crystallized or for verifying that the crystal structure corresponds to the solution structure. Although SAXS can provide the molecular envelope of a sample, wide-angle x-ray scattering (WAXS) is more sensitive on shorter distances. Combined with computational simulations, they can reveal conformational changes and dynamic processes. A fully automated SAXS and WAXS beamline is proposed with an additional grazing incidence SAXS (GISAXS) capability. APS lacks a dedicated beamline for biological solution scattering, so the SAXS and WAXS beam would be a central element of a comprehensive suite of instruments for biological research.

### ***Infrastructure for Improved Sample Preparation***

Two infrastructure projects will complement the proposed life science beamlines and greatly benefit biological research at APS: (1) an automated crystallization facility and (2) the Cryo Sample Preparation Facility. The suggested XFM studies of frozen hydrated biological samples rely on state-of-the-art freezing protocols. Current vitrification techniques for protein crystals frequently compromise crystal quality, but optimized protocols may result in samples that are less mosaic and thus able to produce higher-resolution diffraction. Because crystallization and cryofreezing are subsequent steps in sample preparation and to foster interdisciplinary exchange, the workshop panel recommends that the two facilities work in close synergy and, if possible, as one unit.

The crystallization facility, housed in a building adjacent to APS that will be funded by the state of Illinois, should be connected as intimately as possible to the beamline facilities. This would enable a fully automated process of crystallization and crystal screening, followed by x-ray data collection, ideally under "native" crystallization conditions. Such a facility would have the greatest scientific impact if the research community could access its automated, robotic technology in a variety of ways. For example, researchers could bring samples for crystallization and then take the resulting crystals for analysis to any APS beamline instead of simply submitting a sample at one end and obtaining a structure from the other.

## Special Capabilities and Ancillary Facilities for Biology

Protein microcrystallography relies heavily on optimal sample visualization and adequate beamline automation. To this end, implementation of an advanced optical or x-ray method should be investigated. Such methods include, for example, the newly developed SONICC (second-order nonlinear optical imaging of chiral crystals) technology or x-ray tomography. Beamline automation should make any manual sample alignment unnecessary. Since the scattering of micrometer-sized crystals is extremely weak, low-background mounting techniques and a helium sample environment need to be considered to minimize background. Current detectors for MX are optimized to energies around 12 keV, and fully exploiting the potential of hard x-ray microbeams for reducing radiation damage will require the ability to optimize detectors accordingly. Moreover, software for merging multicrystal datasets will be needed to solve structures from microcrystals. Synergies with work done in the context of nanocrystallography at XFEL facilities should be exploited. Finally, optimal use of the automated crystallization facility should include the possibility of *in situ* diffraction screening and room-temperature data collection.

Raman, fluorescence, and ultraviolet–visible spectroscopy can provide specific chemical information that typically cannot be inferred from electron density alone. Moreover, radiation damage may alter oxidation states and binding length. Thus, the installation of multimode spectrometers at APS’s MX beamlines would significantly extend their capabilities.

X-ray fluorescence microscopy and tomography are scanning techniques and hence very slow compared to full-field techniques. High throughput and sensitivity completely rely on optimized detectors currently unavailable at APS. Since detector development requires substantial resources, a joint program should be considered that includes detector groups at different laboratories and, ideally, industrial partners. Likewise, an industrial partnership is encouraged for further development of the BioNanoprobe end station.

Implementation of an automated crystallization facility and Cryo Sample Preparation Facility is strongly supported. These facilities should be operated as general user facilities accessible during all stages of the user projects. To maximize their impact, the facilities need to make user training and education integral parts of their operation. In fact,

the workshop panel suggests that APS go a step further by implementing a support laboratory for biological research. This “biology village”—similar to a concept planned for NSLS-II—would be important for fostering multitechnique and multilength-scale approaches. As biological research becomes increasingly specialized and as newer, more powerful techniques emerge for application to biological problems, providing this type of support to biologists unfamiliar with such techniques will be important. This laboratory thus would be instrumental in ensuring that a broad audience can use the tools and that their scientific potential is known to the wider biomedical community. As techniques become more powerful, such facilities will help develop new biological applications, even among regular users. With increasingly sophisticated beamline instrumentation and progressively shorter runs, thorough user training is of utmost importance for efficient facility use. In addition, the crystallization facility could be an ideal platform for an APS *in situ* diffraction capability that allows recording of diffraction data directly from protein crystals in their growth environment.

Currently no central depository for x-ray fluorescence microscopy maps and tomograms exists. This hampers the development of the field because neither methods developers nor biologists can easily access recent results. In view of the anticipated rapid growth of XFM, implementing a database similar to Protein Data Bank or gene data banks would be timely. Similarly, a central repository of software for data collection and postcollection image preparation would facilitate more rapid development of the community.

## Support for Users, Existing Beamlines

Regular beamline access by users is key in MX but requires a high staffing level to cope with shorter individual runs. Although automation and remote access alleviate the problem with respect to scientific staff, significantly more technicians and engineers are needed to guarantee high availability of these services. Specific concerns involve the level of support for XFM data analysis and the availability of analysis software offsite for external users.

As the upgrade takes place, support for existing beamlines will be needed to adapt optics and front ends to the higher power and power density delivered by APS. An essential part of APS-U will be to ensure APS’s many current beamlines are fully operational when the upgrade is completed.



## Chapter 2

# LINAC COHERENT LIGHT SOURCE

### Brief Facility Description

The Linac Coherent Light Source (LCLS) at SLAC National Accelerator Laboratory is the world's first operational hard x-ray free-electron laser (XFEL). Using the last kilometer of SLAC's 3 km-long linear accelerator (or linac), LCLS accelerates electrons and passes

them through up to 112 m of undulators. These electrons initiate the self-amplified spontaneous emission (SASE) laser process.

LCLS has six end stations for experiments in a variety of science areas (see Table 2.1 for key facility parameters). Summaries of LCLS (e.g., Boutet and Williams 2010; Emma et al. 2010) include a description by Galayda et al. (2010) that places the facility in a historical and projected worldwide context.

Specific LCLS characteristics enabling new types of synchrotron radiation experiments are the spatially coherent, exceedingly intense x-ray pulses ( $>10^{12}$  photons/pulse) in very short time intervals of  $<100$  femtoseconds (fs). These intense, short pulses can provide useful x-ray signals that probe specimens on time scales far faster than typical atomic motions. When focused to micron diameters, the x-ray pulses are intense enough to turn all matter into plasma. However, in many cases, the scattered x-rays have escaped the specimen before the sample suffers atomic displacements, thereby enabling so-called “diffract before destroy” methods. This capability opens new opportunities in structural biology for nanocrystallography (Chapman et al. 2011), single-particle structural methods (Neutze et al. 2000; Seibert et al. 2011), and correlation solution scattering (Kam 1977). If the beam is expanded over larger areas, the specific peak power per unit area is reduced in proportion. Thus, beams spanning several hundred microns allow samples to survive but still are able to probe on subpicosecond time scales, a capability that offers new applications in biological pump-probe crystallography (Schotte et al. 2003). In addition, the very fast time scales

**Table 2.1 Summary of Key LCLS Parameters**

	Symbol	Hard X-Rays	Soft X-Rays	Unit
<b>Photon beam parameters</b>				
Fundamental wavelength	$\lambda_r$	$\geq 1.4$	$\leq 17$	Å
Photon energy	$\omega$	9,000	750 to 2,000	eV
Final linac $e^-$ energy	$\gamma mc^2$	14.2	4.1	GeV
FEL 3D gain length	$L_G$	3.3	1.5	m
Photons per pulse	$N_\gamma$	2	20	$10^{12}$
Peak brightness	$B_{pk}$	20	0.3	$10^{32\text{a}}$
Average brightness (30 Hz)	$\langle B \rangle$	40	2	$10^{20\text{a}}$
Photon bandwidth	$\Delta\omega/\omega$	$\sim 0.2$	$\sim 0.4$	%
Bunch charge	$Q$	0.25	0.25	nC
Final pulse duration (FWHM)	$\Delta\tau_f$	80	240	fs
<b>Electron beam parameters</b>				
Single bunch repetition rate	$F$	120	120	Hz
$e^-$ energy stability (rms)	$\Delta E/E$	0.04	0.07	%
$e^-$ x, y stability (rms)	$x/\sigma_x$	15, 10	25, 20	%
$e^-$ timing stability (rms)	$\Delta t$	50	n/a	fs
Peak current stability (rms)	$\Delta I/I$	10	6	%
Charge stability (rms)	$\Delta Q/Q$	2.5	2.5	%
FEL pulse energy stability	$\Delta N/N$	$<10$	$<10$	%

<sup>a</sup>Brightness units are photons $^{-1}$  s $^{-1}$  mm $^2$  mrad $^2$  0.1% BW. [Modified from Boutet, S., and G. J. Williams. 2010. “The Coherent X-Ray Imaging (CXI) Instrument at the Linac Coherent Light Source (LCLS),” *New Journal of Physics* **12**, 035024. (Open-access article distributed under a Creative Commons license.)]

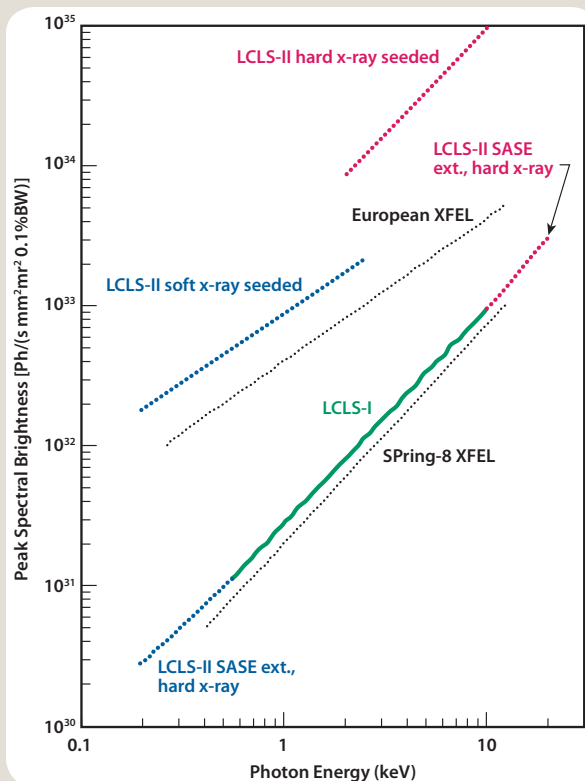


**Fig. 2.1. Peak brightness of current and planned LCLS radiation sources in comparison with other XFELs in construction or commissioning.** [Courtesy of SLAC National Accelerator Laboratory]

present new opportunities in time-resolved biological soft and hard x-ray spectroscopies. Frontier experiments at the now operational LCLS are investigating the feasibility of these novel methods.

The availability of the remaining two-thirds of the SLAC linac opens new and exciting possibilities for a second set of free-electron laser stations (see Fig. 2.1, this page). Many of these capabilities (e.g., hard x-ray seeding<sup>1</sup>) have yet to be demonstrated. Indeed, an important use of LCLS facilities, as the first hard XFEL in the world, is to explore the feasibility of new methods and capabilities, both for biology and many other science areas. Although other XFELs will begin operation in the coming years (Galayda et al. 2010), LCLS has a special obligation as the first hard x-ray laser to continue

<sup>1</sup>LCLS and other XFELs operate by the self-amplified spontaneous emission process (i.e., x-ray pulses arise from random fluctuations in microbunches). Consequently, each laser pulse is a statistical collection of micropulses that varies slightly from one another, leading to lots of pulse-to-pulse variation. In theory, the process could be made more coherent by “seeding” the pulse with a pre-existing “weak” x-ray pulse fed into the undulator. The new pulse then grows coherently around this seed pulse. This technique has been demonstrated at long x-ray wavelengths but not yet at short ones, which place far more stringent constraints on the process.

being very open-minded about biological experiments with low initial feasibility but potentially big payoffs if successful. It may seem strange to say this at this time, but there is a distinct danger that a few highly successful experiments will displace more speculative experiments. Researchers will continue to devise ideas for novel types of experiments, and thus the workshop panel believes LCLS should remain a facility for exploring such experiments and conducting proof-of-concept work. This would help ensure that a few successful experiments not displace newer, more speculative types of research. To meet this challenge, facility management must be strict and transparent about the procedure for selecting and prioritizing experiments.

Beam time at LCLS is highly competitive, and experiments frequently will involve untested and difficult experimental equipment. The presence of the Stanford Synchrotron Radiation Lightsource (SSRL) on the SLAC site can be beneficial in allowing users to set up experiments that can be partially debugged at SSRL and then quickly installed at LCLS. In at least the short term, LCLS will not be a production facility because it can accommodate only a very limited number of experiments. If very successful, LCLS may help justify construction of additional XFELs, but LCLS itself will not be able to accommodate more than a limited number of experiments. For this reason, traditional synchrotron sources will remain the workhorses for many different types of experiments.

## Facility Capabilities and Potential for High-Impact Experiments

X-ray laser beams, such as those at LCLS, offer three unique features that cannot be realized by storage ring-based x-ray light sources:

- **Extremely high peak brightness, currently at  $\sim 10^{12}$  photons/pulse at 8 keV** (more than four orders of magnitude brighter than any storage ring-based x-ray source).
- **Ultrashort x-ray pulses down to  $< 10$  fs** (more than a factor of 1,000 shorter than those from storage ring-based sources).
- **Nearly complete spatial coherence of x-rays** (in contrast to the small coherence fraction of storage ring sources).

These new features have the potential to revolutionarily impact biology, not only by extending the capabilities of existing technology, but also by opening up outstanding new research opportunities. Success of the highest-impact experiments by no means is assured, and considerable research will be required to test the feasibility of many experiments. In this respect, the x-ray laser is a “sandbox” for future biology research.

LCLS covers a wide variety of experimental methods, including diffraction, scattering, and spectroscopy. The planned experiments are at many stages of development, from “nearly ready for broad use” to “in the feasibility sandbox”, with

macromolecular crystallography being the most certain experiment during this initial stage of LCLS.

## Nanocrystallography

X-ray laser pulses of extremely high flux and short duration enable nanocrystallography, and recent publication of the first feasibility results at LCLS generated great excitement in this community (Chapman et al. 2011). In nanocrystallography, data are collected on nanocrystals containing only 100 to 10,000 molecules, avoiding the need for growing large single crystals. Each randomly oriented nanocrystal diffracts x-rays from one pulse of the XFEL. Nanocrystallography may enable structure determination of biologically important samples (e.g., membrane proteins and large protein complexes) that cannot be examined with crystallography using conventional synchrotron radiation because of the difficulty in obtaining crystals of sufficient size. Enabling broad use of nanocrystallography will require systematic studies on methods to grow and deliver nanocrystals of suitable diffraction quality and to reduce tens of thousands of single-pulse diffraction images to full diffraction datasets.

## Time-Resolved Crystallography and Damage-Free, Atomic-Resolution Structure Analysis

Using LCLS's ultrashort x-ray pulses for these types of experiments also has great potential to impact biology research. Time-resolved crystallography on a time scale of femtoseconds would reveal the correlated molecular motions of the chemical processes of enzyme catalysis. The principle of “diffract before destroy” allows collection of virtually damage-free data, thereby overcoming the problem of x-ray damage in crystallography. Damage-free, atomic-resolution structures would describe an enzyme reaction in unprecedented detail, potentially having significant impact in biochemistry. Considerable development of better ways for very quick initiation of the chemical process under study would be required to take advantage of this method.

## Coherent X-Ray Imaging (CXI) and Correlated X-Ray Scattering (CXS)

Studies exploiting the spatial coherence of LCLS x-rays have the potential for a very high impact and are true sandbox experiments because, prior to LCLS, existing x-ray sources could provide only a low flux of coherent x-rays. The capability for single-molecule structure determination (i.e., CXI) is among the most remarkable and exciting experiments for an XFEL. Unlike in conventional crystallography, resolution in single-particle experiments does not depend on the quality of a bulk sample but rather is a function of beam intensity, pulse duration, wavelength, and the sample's scattering power. The first biological CXI experiment targeted the mimivirus and demonstrated LCLS's potential for scattering experiments on biological samples (Seibert et al. 2011); no

other research facility in the world currently offers comparable capabilities.

Three-dimensional (3D) imaging (i.e., tomography) is key to evolving CXI into a widely used structure analysis method. A 3D dataset must be assembled from many diffraction patterns recorded when numerous copies of a reproducible sample are exposed to the beam one by one in random orientations (Huldt, Szoke, and Hajdu 2003; Bortel and Faigel 2007). Determination of molecular orientation and nonreproducible samples will be challenges for CXI experiments, as will be competition from cryo-electron microscopy.

CXS is another unique experiment exploiting the coherence of extremely brilliant x-ray pulses. CXS has the potential for time-resolved or static exploration of 3D structures of biological macromolecules in solution and should provide much more information about molecular structure than conventional small-angle x-ray scattering.

## X-Ray Spectroscopy

X-ray spectroscopy experiments also will take advantage of the ultrashort x-ray pulses at LCLS. Time-resolved spectroscopy of biological processes is important in monitoring, for example, the chemical reaction of enzymes. X-ray spectroscopy can be used in combination with crystallography to determine the chemical states of metal centers or color pigments involved in catalysis, and room-temperature spectroscopy and crystallography enable light-induced “snapshot” time-dependent studies.

## Future Experiments

Hard x-ray laser beams—never used prior to LCLS operation—have numerous capabilities and potential. In addition to the previously outlined experiments, LCLS and its planned expansion (LCLS-II) will be pioneers for discovering innovative technologies and methods beyond the expectations envisioned for x-ray lasers. To fully exploit x-ray lasers for biology, more beamlines and beam time will be needed. LCLS-II is an excellent start in this direction, particularly if emphasis is placed on the higher-energy x-rays (>10 keV) needed for most of the described experiments.

## Special Capabilities and Ancillary Facilities for Biology

The unique LCLS beams enable many novel and important biological experiments. However, any successful experiment requires more than just the appropriate x-ray beams (e.g., upstream XFEL and x-ray optics). Also needed are (1) methods to prepare and deliver specimens into the beam, (2) *in situ* probes (e.g., lasers for pump probe and simultaneous spectroscopy probes), (3) suitable detectors to capture x-ray signals, and (4) advanced methods to handle and analyze resultant data. In many biologically important experiments,

these nonbeam factors will be very challenging and certainly rate limiting in terms of delivering scientific results. Only representative examples of such factors can be given in this short report, and specifying detailed future needs in the rapidly evolving XFEL field is premature. However, support for ancillary equipment and methods research and development (R&D) clearly is essential if LCLS's biological promise is to be realized.

The model in which university groups develop experiments and experimental equipment has been successful at LCLS. Development within the universities builds robust connections, trains the next generation of instrument scientists, and vastly increases the human capital available to develop new ideas. This has been true in such areas as equipment for specimen handling and *in situ* specimen assays, novel detectors, and data handling and analysis.

### Specimen-Handling Methods

Both offline and online specimen handling are critical for biological experiments at LCLS. Offline considerations include standard equipment as well as R&D. Biological materials frequently require standard wet-lab capabilities and equipment currently not at the SLAC site. The needed wet-lab capabilities should be provided without presenting R&D challenges.

By contrast, much R&D is needed to learn how to prepare specimens for the unique requirements of LCLS experiments. For example, recent LCLS nanocrystallography experiments were enabled by the development of offline second harmonic microscopy [second-order nonlinear optical imaging of chiral crystals (SONICC); Wampler et al. 2008]. This technique helped identify materials as crystalline, even if the crystals were too small to be optically resolved. Online methods R&D also will be required. For example, nanocrystallography experiments to date have relied on the development of novel fluid jet methods to deliver nanocrystals into the x-ray beam (Weierstall et al. 2007). This method needs further development to enable wider use, and other methods should be investigated also.

### In Situ Probes

The means to prepare and probe the state of samples will be of utmost importance. For example, time-resolved “movies” of protein structure (Schotte et al. 2003) typically require both *in situ* lasers to pump the protein process and, ideally, *in situ* optical methods to monitor the spectroscopic state of crystals.

### Detectors

Perhaps the single most important lesson from the last two decades of biological research at synchrotrons is that better x-ray detectors are needed to take full advantage of x-ray sources. Aside from the development of synchrotron radiation sources themselves, no other ancillary equipment has been as rate limiting—or as important in increasing scientific

results—as advanced x-ray detectors. XFEL detectors will need capabilities considerably beyond the current state of the art, requiring a consistent long-term program of advanced R&D. In the past, the development of synchrotron x-ray detectors was greatly facilitated by the fact that many beamlines at different synchrotrons could use the same detector for crystallography, thereby making detector development attractive to commercial firms. This is less likely to be the case for XFEL detectors because they will need to be tailored for the specific needs of each XFEL experiment and thus will not enjoy a mass market. In this sense, XFEL detector R&D will be much more like R&D for other parts of the XFEL. This situation presents special challenges because development of new detectors is very expensive and takes many years for each new detector. Nonetheless, without several parallel detector R&D projects, LCLS simply will be unable to realize its promise.

A second lesson from the last few decades is that successful detector development is limited when confined to Department of Energy laboratories. As in the past, future success will require R&D wherever detector expertise exists, whether in national laboratories, industry, or academe.

### Data Handling and Analysis Procedures

Typical LCLS experiments each deliver terabytes of data. R&D is needed to establish better methods for handling and analyzing these huge volumes of data. Novel procedures will be required to analyze, for example, images from single protein molecules that will be severely Poisson noise limited. Although research has shown that this is not an insurmountable obstacle in principle (Elser 2009; Elser and Eisebitt 2011; Loh et al. 2010), much work remains to be done on practical methods for reducing large datasets so that structures can be obtained. Collaborations with the electron microscopy (EM) community, which has considerable expertise in determining molecular orientation from noisy images, could be highly beneficial. At some point, experiments at LCLS and other XFELs will transition from isolated demonstrations of feasibility to more routine delivery of structural or other services. This transition will require reduction of data at the point of generation (i.e., via the use of smart detectors and online computational procedures).

## Support for Personnel to Enable Collaboration Between X-Ray Experts, Biologists

LCLS has enormous promise to produce biological results of great impact. New experimental methodologies are needed to test the feasibility of the boldest LCLS experiments and enable the facility to reach its full potential for all biological experiments. These methodologies lie at the interface of the x-ray source and the sample, thus requiring collaboration between LCLS scientists and biological researchers. However,

a mismatch of knowledge exists between these two communities because experts in each field need a better understanding of the other. X-ray physicists and engineers with expertise in the production, delivery, and properties of LCLS's pulsed, coherent, and brilliant beams are not steeped in the complexities and subtleties of biological systems, nor are they up to date with the constantly evolving understanding of biological processes. Conversely, the most challenging and significant problems in structural biology require careful target selection and involve samples that are extremely difficult to produce. Very few researchers who are adept at project development and sample preparation also have expertise in x-ray physics at the level required to develop experiments at LCLS. The knowledge and training gap exists for many scientific communities who will use LCLS but is perhaps widest and most critical in biology. One approach to addressing this gap would be to identify "glue" personnel from each community

and embed them in the other, perhaps in a minisabbatical format. Another approach would be to convince groups with adequate expertise to participate in experiments, for example, by inviting more experienced crystallography and EM group leaders to visit and discuss new experiments. This would address the current challenge of making more people aware of LCLS and its capabilities.

"Gap" or "glue" personnel will be needed to support biologists using LCLS even after new experimental methodologies are established. The success of this approach is evident at SSRL, where a large and highly effective support staff has streamlined crystallography beamline use, leading to major biological results from true biologist users in contrast to past biophysicist users. The proximity of SSRL is a great advantage for LCLS, offering a good opportunity to develop staff expertise in biological experiments and user support.

## References

- Bortel, G., and G. Faigel. 2007. "Classification of Continuous Diffraction Patterns: A Numerical Study," *Journal of Structural Biology* **158**(1), 10–18.
- Boutet, S., and G. J. Williams. 2010. "The Coherent X-Ray Imaging (CXI) Instrument at the Linac Coherent Light Source (LCLS)," *New Journal of Physics* **12**, 035024.
- Chapman, H. N., et al. 2011. "Femtosecond X-Ray Protein Nanocrystallography," *Nature* **470**(7332), 73–77.
- Elser, V. 2009. "Noise Limits on Reconstructing Diffraction Signals from Random Tomographs," *IEEE Transactions on Information Theory* **55**(10), 4715–22.
- Elser, V., and S. Eisebitt. 2011. "Uniqueness Transition in Noisy Phase Retrieval," *New Journal of Physics* **13**, 023001.
- Emma, P., et al. 2010. "First Lasing and Operation of an Ångstrom-Wavelength Free-Electron Laser," *Nature Photonics* **4**, 641–47.
- Galayda, J. N., et al. 2010. "X-Ray Free-Electron Lasers—Present and Future Capabilities," *Journal of the Optical Society of America B—Optical Physics* **27**(11), B106–18.
- Huldt, G., A. Szoke, and J. Hajdu. 2003. "Diffraction Imaging of Single Particles and Biomolecules," *Journal of Structural Biology* **144**(1–2), 219–27.
- Kam, Z. 1977. "Determination of Macromolecular Structure in Solution by Spatial Correlation of Scattering Fluctuations," *Macromolecules* **10**(5), 927–34.
- Loh, N. D., et al. 2010. "Cryptotomography: Reconstructing 3D Fourier Intensities from Randomly Oriented Single-Shot Diffraction Patterns," *Physical Review Letters* **104**(22), 225501.
- Neutze, R., et al. 2000. "Potential for Biomolecular Imaging with Femtosecond X-Ray Pulses," *Nature* **406**, 752–57.
- Schotte, F., et al. 2003. "Watching a Protein as it Functions with 150-ps Time-Resolved X-Ray Crystallography," *Science* **300**(5627), 1944–47.
- Seibert, M. M., et al. 2011. "Single Mimivirus Particles Intercepted and Imaged with an X-Ray Laser," *Nature* **470**(7332), 78–81.
- Wampler, R. D., et al. 2008. "Selective Detection of Protein Crystals by Second Harmonic Microscopy," *Journal of the American Chemical Society* **130**(43), 14076–77.
- Weierstall, U., et al. 2007. "Droplet Streams for Serial Crystallography of Proteins," *Experiments in Fluids* **44**(5), 675–89.

## Chapter 3

# NATIONAL SYNCHROTRON LIGHT SOURCE-II

### Brief Facility Description

The National Synchrotron Light Source-II (NSLS-II) is a new synchrotron radiation source still under construction and planned to come online in March 2014. It is located at Brookhaven National Laboratory (BNL) on Long Island, New York, near the original NSLS synchrotron radiation source. NSLS-II is a large 3 gigaelectron volt (GeV) ring of 791.5 m in circumference, which will accommodate at least 58 beamlines including 27 insertion devices and 27 bending magnet lines. NSLS-II is not just an upgrade to NSLS; it is a completely new source. It will deliver an extremely bright beam ( $>10^{21}$  ph/mm<sup>2</sup>/mrad<sup>2</sup>/0.1%BW) in the 2 to 10 keV range, approaching a fully coherent, diffraction-limited source in the vertical plane. In addition, NSLS-II will have a very wide spectral range, from the far infrared (0.1 meV) to the very hard x-ray region (100 keV). In the medium term, NSLS-II will deliver the brightest low-energy x-ray beams in the world and will surpass other sources, such as the Advanced Photon Source (APS), in the 2 to 10 keV range. For higher-energy x-rays, NSLS-II will be comparable to many other sources. This suggests that NSLS-II will be in a unique position to dominate the low-energy x-ray range while still being a major player at higher energies. NSLS-II promises to be an outstanding source for many new types of experiments in a wide range of disciplines, including life sciences. NSLS-II will provide many new capabilities useful for Department of Energy (DOE) Office of Science research programs.

Allocation of all NSLS-II beamlines is still in progress. Initial construction plans include six insertion device lines, and over 30 more are in the approval process. Final approval will require identification of funding sources. Of the six initial lines, all of them funded by the DOE Office of Basic Energy Sciences, none are intended for biological sciences. Of the proposed beamlines, 11 have a biological science emphasis and are in the approval process; four more proposals are at the Letter of Intent stage. All these beamlines span a large cross-section of modern synchrotron-based biological research and include beamlines devoted to imaging, crystallography, spectroscopy, and scattering. This heavy involvement of the biological sciences community in NSLS-II reflects the wide interest in the capabilities that will be afforded by the new source.

NSLS-II plans include a Biology Village, or a community of highly integrated groups working in different but related areas in life sciences. As such, the Biology Village will play a role in bringing together all the different biological sciences present at NSLS-II, thus ensuring synergy and interconnection. The village will also ensure that experimenters have easy access to many different but complementary techniques available either at the biology beamlines or in the associated laboratories and will make researchers aware of the different experimental tools available to answer their particular biological question. Initial plans call for many of the beamlines with a biological focus to be in close physical proximity. In addition, planned laboratory space in the Laboratory Office Buildings will also bring life scientists together. Nevertheless, due to different constraints, the Biology Village may largely operate as a virtual one, which is not the most ideal situation. The concept of the Biology Village is very interesting and exciting and promises to change the way life scientists interact and work at a synchrotron radiation user facility. This is true not only for the life scientists at NSLS and BNL, but also for outside users and collaborators. It is thus very important to continue to elaborate and solidify the concept of the Biology Village and to strive to maintain physical connectivity among life scientists. In addition, it will be very important to plan for adequate laboratory space in support of both long- and short-term collaborative projects and guarantee a healthy involvement of the user community in NSLS-II and any future developments.

### Facility Capabilities and Potential for High-Impact Experiments

NSLS-II is still at the construction stage, so it is not possible to gauge fully its capabilities. Nevertheless, it is possible to anticipate areas where its designed capabilities potentially will have a large impact. As mentioned before, these areas encompass macromolecular crystallography (MX), scattering, spectroscopy, and imaging. Beamlines in all these areas are part of the current building and planning process, and additional beamlines also are being considered. The beamlines represent a healthy mix of established techniques, such as MX, and less developed areas, such as coherent x-ray diffraction. In terms of its unique capabilities, NSLS-II is

designed to be the synchrotron radiation source with the highest average spectral brightness in the world in the 2 to 10 keV range. At 8 keV, NSLS-II will be an order of magnitude brighter than APS. This will have a major impact on techniques requiring a high coherent flux, such as coherent x-ray diffraction imaging (CXDI). At much higher energies NSLS-II brightness will still be considerable but not as high as that of APS. In addition, NSLS-II is designed to have excellent energy resolution and very high beam stability, making it an ideal source for scattering, imaging, and spectroscopy experiments including nanobeam techniques.

### **Macromolecular Crystallography**

MX will be very well represented at NSLS-II. There are several beamlines planned, including one in “frontier MX,” one for correlated spectroscopy and diffraction, and one for microdiffraction led by the New York Structural Biology Consortium. In addition, plans for a low-energy anomalous x-ray diffraction beamline would strongly enhance the cohort of crystallography beamlines. This last beamline would be a very welcome addition, as it would take full advantage of the unique characteristics of NSLS-II and provide access to energies rarely used in anomalous x-ray scattering experiments due to the lack of facilities that can access low-energy x-rays at an adequate brightness. The planned beamline correlating MX with a variety of spectroscopic techniques will provide exciting complementary local information on protein structure and dynamics. Standardized online microspectrometry should, however, become optionally available on all MX beamlines. The use of microbeams ( $<100 \mu\text{m}^2$ ) is starting to revolutionize some MX experiments because these very small beams permit collection from very small crystals or very small areas of larger crystals. These emerging crystallography approaches will allow reaching the smallest crystal volumes and establishing fruitful collaborations with the upcoming generation of x-ray free-electron laser (XFEL) sources. NSLS-II will provide microbeam capabilities in several beamlines. This characteristic, together with planned automation and other developments, will make the MX facilities extremely competitive and likely to be in large demand, particularly with users in the surrounding area. The planned MX beamlines are all well designed and likely to make NSLS-II a major hub for structural biology.

### **Imaging**

Imaging is another area that will take full advantage of NSLS-II capabilities. NSLS-II will be ideally suited for x-ray fluorescence imaging of many elements difficult or impossible to access at other facilities. In addition, the beam characteristics will make it very well suited for microprobe imaging and CXDI. Thus, it will be possible to image at the nanometer scale using a variety of techniques to study different levels of organization and correlate this information with that from, for example, atomic-level elemental analyses. For instance, ptychography promises to provide

images of whole cells or organelles at nanometer resolution. In addition, fluorescence imaging of specific elements will help map their location in biological materials at nanometer resolution, thus providing information on the spatial distribution of key elements (e.g., carbon, nitrogen, phosphorus, and sulfur) for biological function.

### **Spectroscopy**

The characteristics of NSLS-II make it an excellent source for spectroscopy studies. Plans for beamlines dedicated to x-ray absorption spectroscopy (XAS), submicron resolution x-ray spectroscopy (SRX), and infrared spectroscopy ensure that NSLS-II will have a strong presence in this area. NSLS-II will provide access to a wide energy spectrum, making it possible to access the very low energy (infrared) spectrum. The advanced infrared microspectroscopy (AIM) beamline will provide unique capabilities for vibrational spectroscopy imaging at the submicron level. Finally, the ability to combine spectroscopic techniques with other approaches is likely to have a very high impact, as it will provide information on important biological processes by a variety of complementary techniques. For example, the ability to collect not only diffraction data but also near-simultaneous spectroscopic information is likely to have an enormous impact on mechanistic studies of enzymes and other important biological molecules.

### **Scattering**

Finally, several planned beamlines for scattering studies will exploit the exceptional brilliance and beam stability of NSLS-II. Indeed, in recent years, small-angle x-ray scattering (SAXS) has resurged as an important tool that provides low-resolution information on complex biological systems. The plans for an automated solution SAXS beamline are excellent, as it will ensure fast and easy access to a technique rapidly growing in popularity. In addition, other planned beamlines will ensure that NSLS-II stays at the forefront in this area. There is likely to be an increasing demand for solution scattering experiments in the coming years that, when combined with other imaging techniques, promise to provide nanometer-scale information on complex and relatively large macromolecular complexes. Nevertheless, to stay competitive, a strong R&D effort will have to be maintained to integrate the rapid advances in microfluidics technology for sample preparation and delivery, particularly for time-resolved SAXS studies. Ultrasmall sample volumes will also require exploring microbeam and possibly nanobeam SAXS probes.

## **Special Capabilities and Ancillary Facilities for Biology**

The Biology Village may be the key to the success of NSLS-II as a major hub for biological studies. The village promises to provide a unified and synergistic environment for life science

experiments. For this reason, it will be extremely important to ensure the success of the Biology Village. The village is likely to be most successful if it goes beyond a virtual one and instead forms a real community that physically brings together the equipment and personnel needed to conduct successful, multidisciplinary experiments. Successful biological experiments depend on more than just access to state-of-the-art facilities; they also require excellent onsite support for preparing materials needed for experiments as well as tools for characterizing samples before and after experiments at the synchrotron. While many experiments can be done by simply bringing the specimens to the synchrotron, many others are time sensitive and will require preparation onsite. It is thus very important that both BNL and outside users of NSLS-II have access to offices and laboratories to prepare for their experiments. Current plans call for 120 offices, conference rooms, and 10 laboratories for user support at NSLS-II, with additional laboratory space in the NSLS building. It is not clear how much of this space will be devoted to biology, but, given the strong need for onsite sample preparation for some experiments, it is important that sufficient space be allocated for biological laboratories. In addition, the ability to provide space for outside users engaged in long-term experiments may also be beneficial. The exact configuration of the laboratory space is very important to ensure success of the village concept, but the characteristics of this space should be determined by local users, keeping in mind the need of both outside and local users and the importance of maximizing collaboration and synergy. All of these features ideally should be contained in the Biology Village.

The advent of XFELs will have an impact on synchrotron radiation sources, but for many types of experiments, synchrotron radiation sources will continue to dominate and be essential because they provide higher beam stability and access to higher energies. In addition, the “diffract and destroy” limitation of XFELs means that certain types of experiments, such as those that probe the evolution of parameters in time or across a heterogeneous sample, will continue to be more suitable for synchrotron radiation sources. Moreover, phasing by anomalous dispersion will remain a mainstay of synchrotron radiation sources and an area in which NSLS-II is likely to play a very important role. Overall, while XFELs are likely to engender new and powerful techniques for studying biological samples, they will not replace or supplant synchrotron radiation sources such as NSLS-II in the near or medium future.

The characteristics of NSLS-II make it ideal for experiments using very small beams. Beamlines are planned with beams down to micron-level sizes. This is an artificial limit not dictated by instrumental limitations. For many experiments, even smaller beams (nanometer-scale sizes) would be ideal, especially if they are coupled with sample manipulation and positioning instrumentation congruent with the ultrasmall beam sizes. Nanobeams have potentially groundbreaking applications in biological SAXS, CXDI, and MX. Active R&D in

this area is important and desirable, and the aim of reaching a 1 nanometer focal spot at the hard x-ray nanoprobe is a well-chosen challenge for NSLS-II.

The success of many synchrotron-based biological experiments depends largely on the ability to preserve the samples and minimize radiation damage. NSLS-II will be an extremely bright synchrotron, and some of the problems with radiation damage may be exacerbated. For this reason, it is extremely important to have an active R&D program for sample preservation and preparation and assessment of radiation damage, with suitable experimental facilities for these tasks.

Existing detectors and detector technology very likely will not be optimized for the new generation of synchrotron radiation sources, including NSLS-II. For this reason, striving for a leadership position in detector R&D is important. It is unlikely that one type of detector will be ideal for the many different experiments and beamlines planned at NSLS-II, and thus it may be necessary to build specialized detectors for different applications. To satisfy many applications, future detectors will need to have low noise, small pixel size, and high readout speeds. Whereas some areas, such as x-ray crystallography and SAXS, are large enough to attract the interest of detector development companies, others are more specialized and likely will require in-house detector developments or partnerships with academic groups. Detectors are likely to continue to be major impediments to many experiments, and hence it is important to have a strong presence in this area through internal R&D, partnerships with academic groups, and active involvement of commercial companies.

Almost all experiments at NSLS-II will create enormous amounts of data, most of it stored and processed in digital form. For this reason, careful consideration should be given to the capabilities for storing and distributing the data and to the types of data processing capabilities that will be provided. Currently, there are plans to support data collection, storage, and analysis, but the details of the implementation are still being worked out. Information from similar facilities will be used to design the computational infrastructure. The plan to allow remote data collection, processing, and access is a welcome development. All these developments will necessitate implementation of state-of-the-art networks and strong computational support.

## Support for Beamline Staff, User Community

As mentioned, the impact of NSLS-II in the life sciences hinges to a great extent on the success of the Biology Village. The most important component of the Biology Village will be the personnel comprising it. On one hand, many of the most challenging experiments will require the involvement of highly specialized beamline scientists to conduct them. On the other hand, the experiments also require strong involvement from biological scientists to prepare samples and

analyze and interpret results. For this reason, ensuring excellent collaboration between beamline scientists and experimenters is extremely important. This can be accomplished not only by the availability of physical space for interaction and sample preparation and manipulation, but also by giving beamline scientists time to engage in productive collaborations with users, local researchers, or scientists from other institutions and embark on beamline-related, Ph.D.-type projects. In addition, the presence of local scientists with strong research programs in relevant areas will help maintain a vibrant atmosphere conducive to forefront research. Limited funding for internal research is available, but additional research support is expected to come from external sources. For this reason, it is very important that NSLS-II scientists are competitive not only internally, but also externally. A strong emphasis should be placed on ensuring that the scientific staff actively engages the research community and seeks outside support.

Projected staffing levels include one to two Ph.D.-level scientists, one engineer, and 0.5 FTE (full time equivalent) technicians per beamline. This staffing level is similar to that at other U.S. facilities but more modest than at comparable facilities elsewhere, such as the European Synchrotron Radiation Facility–Grenoble, which has on average two scientists at the postdoctoral level and a 0.5 FTE beamline operation manager. Furthermore, the staffing level at NSLS-II may need to expand as demand increases, especially if remote operations become routine. It is important to note that staff support will depend on outside funding and hence is likely to be uneven across different beamlines. Exploring alternative ways of supporting staff to achieve a more even staffing of all beamlines is likely to be important.

## Chapter 4

# NEXT GENERATION LIGHT SOURCE

### Brief Facility Description

The Next Generation Light Source (NGLS) at Lawrence Berkeley National Laboratory is a scientifically transformative new facility in the early stages of planning (anticipated first light is 2022). As currently envisioned, it will include an array of 10 independently configurable x-ray free-electron lasers (XFELs) powered by a superconducting linear accelerator and capable of delivering ultrafast (attosecond to femtosecond), high-brightness (up to  $10^{12}$  photons/pulse), and high-resolution pulses of soft x-rays [ $\leq 3$  kiloelectron volts (keV), with reduced flux at higher energies]. These pulses will be delivered at high rates of repetition (as short as microsecond intervals, or 1 MHz) because of the superconducting accelerator design (see Figs. 4.1, this page, and 4.2, p. 16). Each of these features defines the experimental potential of this planned facility and distinguishes it from existing synchrotron and XFELs, including the Linac Coherent Light Source (LCLS), which has a repetition rate four orders of magnitude lower (see Fig. 4.2). The high pulse repetition rate is a singular feature of NGLS that will enable time-resolved experiments and acquisition of billions of x-ray “snapshots” within experimentally practical time frames (hours, not days).

NGLS also will allow a greater average photon flux than is currently available at existing x-ray laser sources, including LCLS. In contrast, LCLS produces pulses whose peak brightness is one to two orders of magnitude higher, and it has significantly higher brightness at the high-energy/hard x-ray energies. Uniform spacing of NGLS x-ray pulses will further allow for shot-by-shot sample replacement and data collection, in contrast to the burst mode design of the European XFEL. Hence, NGLS will have useful and distinct features.

These capabilities are likely to have profound impacts on future biological research (see Table 4.1, p. 17). Some of the most exciting experimental capabilities of NGLS for biology include:

1. Observation of structure and spectra on the *real time scales* (including  $\leq$  femtosecond) of biological events.
2. Imaging of single molecular complexes, membrane protein complexes, macromolecular assemblies, organelles, and cells—outside the context of a large crystal and, in some cases, prior to the onset of molecular damage.
3. Simultaneous observation of the structure and spectroscopy of single biological objects or molecular complexes, including scattering experiments at energies that provide

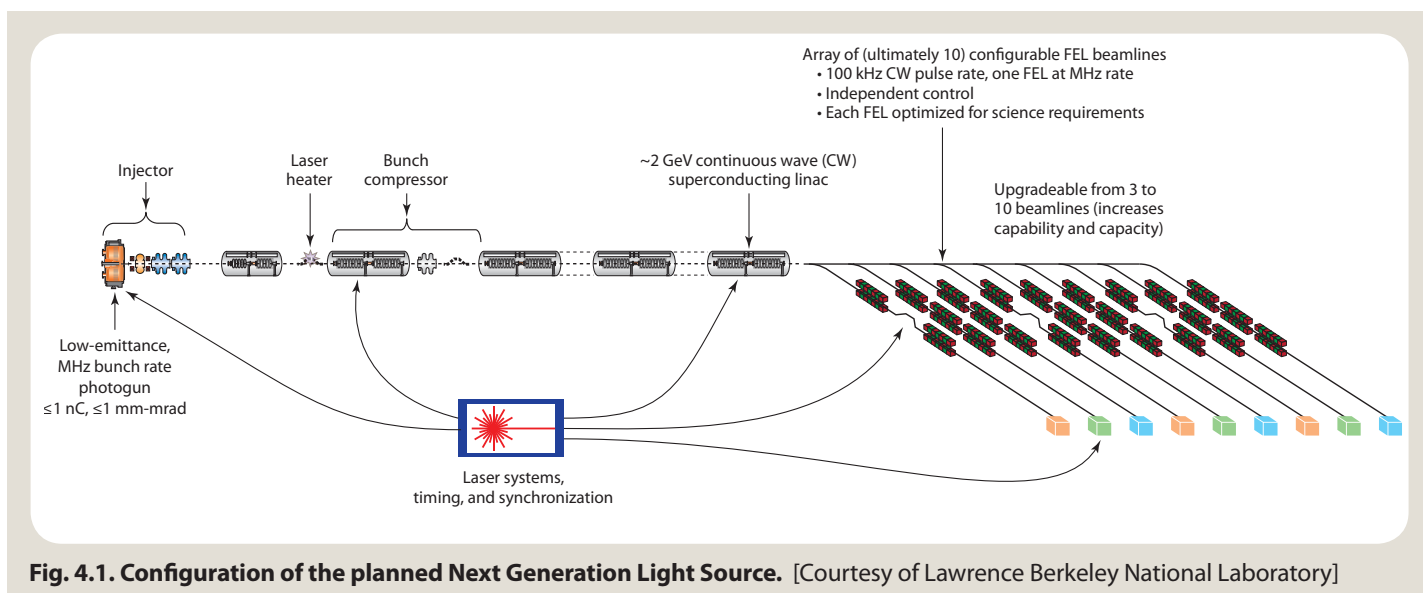


**Fig. 4.1. Configuration of the planned Next Generation Light Source.** [Courtesy of Lawrence Berkeley National Laboratory]

selective enhancement of specific chemical groups, simultaneously providing information about the chemistry of molecular systems in solution.

- Imaging and understanding of conformational heterogeneity and its role in biological function.
- Higher-throughput experimentation and broader access of the scientific community to these technologies because of the ability to operate 10 XFELs concurrently.

While features 1, 4, and 5 are unique to NGLS, 2 and 3 are shared with LCLS and its planned upgrade, LCLS-II. However, NGLS and LCLS, as currently planned, would differ in the kinds of biological systems observable by each due to differences in their wavelength ranges of optimal photon flux (see Table 4.1, p. 17). Specifically, LCLS produces high-brightness x-ray pulses of short duration in the  $<1$  to  $>10$  keV energy range. As planned, NGLS, by contrast, is a soft x-ray source where harder x-rays would be available only via harmonics of the fundamental wavelength, which are expected to be of lower intensity. However, NGLS's performance at x-ray harmonic energies is yet to be optimized, and it is possible that some attention to such optimization could enable more productive use of the hard x-rays in experiments. Importantly, both conventional diffraction experiments and high-resolution single-molecule imaging would require harder x-rays to observe features less than  $\sim 4$  angstroms ( $\text{\AA}$ ) in scale. NGLS would therefore be of greatest use not for determining atomic-resolution structures of molecules, but for imaging macromolecular topologies and objects up to the cellular size scale. It seems likely that many important biological applications of NGLS are yet to be determined and will deliver types of information unlike any yet available.

## Facility Capabilities and Potential for High-Impact Experiments

Several NGLS experiments such as x-ray scattering, “diffract and destroy” nanocrystallography, and spectroscopy could have a high impact on biological science.

### X-Ray Scattering: Biological Objects in Native Environments and in Real Time

Small-angle x-ray scattering (SAXS) in the soft x-ray wavelength range currently gives only low-resolution structural information about biomolecules in solution, in part because diffracting objects rotate too fast to allow sufficient scattering data from each object to be obtained. The speed and brightness of the NGLS source will allow multiple scattering snapshots to be collected within the time scale of a molecular rotation, eliminating the “spherical averaging” necessitated by existing, slower soft x-ray sources. Coupled with the appropriate detectors and needed computational tools for image reconstruction, such scattering techniques will enable imaging of biomolecules and molecular assemblies in motion and outside the context of a crystal.

The soft x-ray source likewise will be amenable to element-specific imaging of the lightweight bioelements, including carbon, oxygen, and nitrogen, as well as phosphorus and sulfur (the latter being potentially important for phasing scattering patterns). Resonant x-ray reflectivity for enhancing either the sensitivity to selected light elements or the e-density contrast matching of light elements (as possible in the *soft x-ray* regime) may be particularly valuable for determining the structure of membrane proteins vectorially oriented in single lipid bilayer membranes. It also would aid

investigation of the dynamics of these structures via pump-probe approaches (the latter facilitated by NGLS's high repetition rate).

Finally, the high-intensity NGLS source can provide significant structural information using scattering data from single molecules or molecular assemblies (e.g., delivered to the x-ray beam via a microfluidic jet or viewed by rastering a beam across a crystal surface) rather than averaged information from many molecules in a crystalline array. This will enable visualization of intrinsic structural heterogeneity in biological systems,

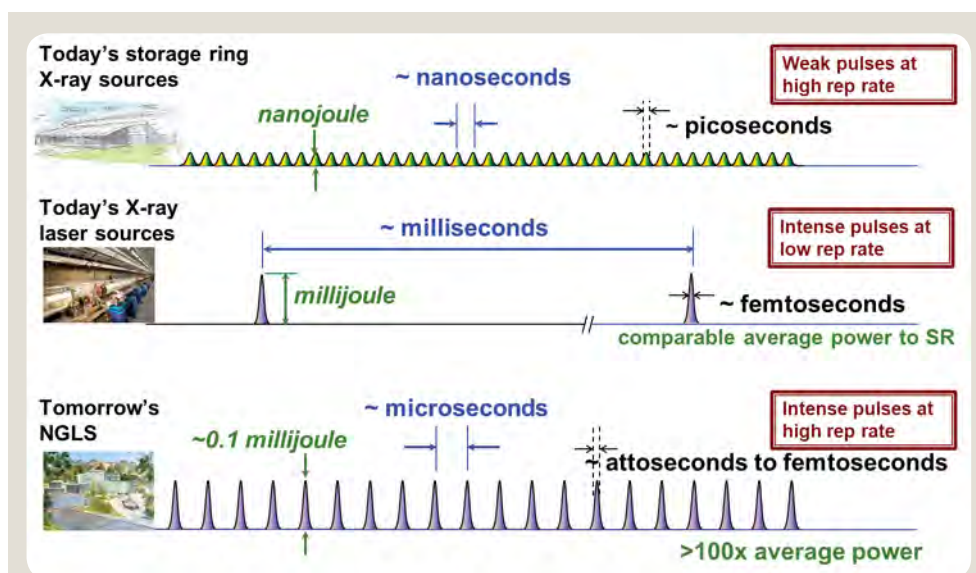


**Fig. 4.2. Comparison of pulse characteristics at existing and planned light sources.**  
[Courtesy of Lawrence Berkeley National Laboratory]

**Table 4.1. Length Scales of Relevant Cellular Structures of Interest\***

System	Length Scale	Remarks
Cell	10 $\mu\text{m}$	NGLS gigascale imaging
Major subsystems	1 $\mu\text{m}$	
Clusters and regulons	100 nm	
Protein complexes	10 nm	
Molecular shape	1 nm	
Molecular structure	0.1 nm	LCLS

\*Adapted from Lerman, J., and B. O. Palsson. 2010. "Topping off a Multiscale Balancing Act," *Science* **330**, 1058. Reprinted with permission from AAAS.

an important and as-yet unexplored experimental frontier. Such measurements will need to take advantage of existing and improving technologies for sample delivery currently in use at LCLS. Collectively, these capabilities will revolutionize biological science.

### ***Diffraction and Destroy Nanocrystallography***

As also described for LCLS, diffraction experiments using smaller nanocrystals will be possible with NGLS. Such experiments are desirable in the biological context because large, well-ordered crystals of many biomolecules (and particularly large complexes such as molecular machines) are not readily obtainable.

The optimal wavelengths for these experiments (hard x-ray) may fall outside the range of high-brightness wavelengths for NGLS. Hence it is unclear whether sufficiently well resolved diffraction images on nanocrystals may be obtained with NGLS (see Limitations and Needs section).

### ***Spectroscopy***

The high pulse rate and high brightness of NGLS offer new opportunities for time-resolved x-ray absorption spectroscopy (XAS). Element-specific imaging of the lightweight bioelements via their characteristic absorption wavelengths was mentioned above. Also, conventional *K*- and *L*-edge XAS on metalloenzyme solutions can be carried out in a time-resolved fashion.

## **Limitations and Needs**

For biology, NGLS is ideally suited to the study of larger biological objects, such as molecular complexes, in time-resolved ways and in close-to-native environments (e.g., in solution) using scattering methods such as fluctuation SAXS (fSAXS). As presently planned, NGLS would enable diffraction or other experiments aimed at the subnanometer-length scale, via the use of harder x-rays generated as harmonics of higher-brightness pulses at longer wavelengths.

Averaging data from several pulses could lead to sufficient hard x-ray flux, but using NGLS this way would provide data akin to what could be gathered from a synchrotron source. However, the coherence of NGLS, along with the specific pulse structure, enables measurement approaches quite different from synchrotrons, even at harder x-ray energies where data might be accumulated from multiple pulses. Although they exploit information from multiple pulses, these approaches are very different from simply averaging the data from multiple pulses.

For instance, in specific experiments, a user would like to accumulate many individual fSAXS snapshots and then combine them in an intelligent way (e.g., so that the azimuthal correlation patterns are properly oriented). Manifold mapping is another example of a powerful analysis method that exploits coherent scattering data accumulated from multiple pulses. Again, this requires individual snapshots and is quite different from what can be achieved by simply averaging over many pulses, as might be done at a synchrotron source.

For example, accumulation of data from multiple pulses has the potential to recover phases and possibly calculate *ab initio* structures for molecules in solution. In current synchrotron-based SAXS experiments the scattering data are spherically averaged, in effect projecting the three dimensions of the structure onto one dimension. The restricted information available from these one-dimensional projections is insufficient for unambiguous structure determination. The ability to collect many millions of scattering patterns from x-ray pulses at NGLS will provide information about the fluctuations around the mean SAXS signal (i.e., modulations in the nominally radially symmetric SAXS signal). Calculations show that extraction of the single molecule autocorrelation function from these data will provide significantly more observations (two orders of magnitude) than traditional SAXS methods. This will greatly improve the ability to generate atomic models based on scattering data. Ultimately, it may be possible to recover phases from the continuous scattering pattern and calculate *ab initio* structures for the molecule(s) in solution.

It would, therefore, be useful to address two issues as the NGLS project goes forward. First, optimizing the brightness of the hard x-ray harmonics may be of some use because the very high pulse repetition rates of NGLS may thus be brought to bear at smaller length scales, at least to a practical extent. Second, since NGLS offers such unique capabilities relative to synchrotrons, LCLS, or any existing light source, it will be exceedingly important to communicate with the biological community and cultivate a cadre of potential users who can develop new applications and techniques. NGLS is not merely a brighter synchrotron, a faster LCLS, or a new Advanced Light Source, but a brand new entity for which the possibilities are yet to be fully conceived.

Development of NGLS experimental capabilities will certainly benefit from soliciting and maintaining input from two

groups: LCLS users and staff and the cryo–electron microscopy community. The latter will be of particular importance in developing computational methods for image reconstruction from scattering data of heterogeneous samples. In addition, because many NGLS hardware, software, and detector needs will be rather unique, the production of certain specialized equipment is expected to be unattractive to industry vendors. Thus, the academic physics community will need to be engaged not only in NGLS use, but also in its development.

## Special Capabilities and Ancillary Facilities for Biology

Six areas deserving consideration are:

- 1. Experimental stations.** These are essential components of the facility. Having sufficient funds available is crucial so that stations can be planned, constructed, and ready when the light source is operational.
- 2. Data management and software development.** Very large amounts of data, including data from time-resolved “stroboscopic” measurements (as also proposed for the upgraded Advanced Photon Source), will require substantial software development, data management, and commensurate hardware for high-performance parallel computing and storage.
- 3. New algorithms for image reconstruction.** New algorithms, such as manifold embedding as proposed by Abbas Ourmazd, are very promising and will be necessary to make full use of the data obtained from large numbers of scattering experiments. Testing of such algorithms with phantom data already has been started, well before the new facilities are in place.

- 4. Biological preparative lab.** A laboratory for preparation and parallel characterization of samples with experienced staff must be made available onsite. Equipment for such a laboratory could include centrifuges, refrigerators and a cold room, dark room, chromatography and high-performance liquid chromatography equipment, mass spectrometers, light scattering, and an electron microscope.
- 5. Detectors and related equipment.** Detectors matching the speed of the source and having a large pixel number must be available. While LCLS could provide significant input in this area, the measurement time scales will be much faster at NGLS. Additionally, equipment should be available for tandem measurements of fluorescence or other kinds of spectroscopy.
- 6. Technique development.** NGLS will offer capabilities that are not dreamt of yet. Dedicated beam time and support for ongoing technique development should be available.

## Support

With new-generation light sources, a large and sophisticated team is required because every facet of the experiment is non-trivial—from sample preparation and handling (e.g., injection and mounting) to data collection, processing, and archiving. Staff scientists in particular are essential because they serve as the connection between the users, facility, and beam. Adequate funding to support these positions thus is needed. Since experimental needs will be well beyond the state of the art, multidisciplinary collaborations in the areas listed above will be vital. As with synchrotrons, having staff with biological as well as facility expertise will be vital to bridge the gap for biologists who may want to use the x-ray source but require assistance to do so. Finally, once experimental time is ready to be allocated, having different panels that review proposals focusing on spectroscopy, imaging, crystallography, and technique development will be important.

## Chapter 5

# SPALLATION NEUTRON SOURCE

### Brief Facility Description

The Spallation Neutron Source (SNS) at Oak Ridge National Laboratory (ORNL) is becoming one of the world's most powerful sources of neutrons for investigating the structure and dynamics of biomolecular systems by elastic and inelastic neutron scattering. Isotopic substitution, specifically deuterium for hydrogen in the case of biological systems, coupled with contrast matching of selected components provides a distinct advantage for neutron scattering techniques. This reveals key aspects of the structure and dynamics within complex macromolecular systems over a wide range of length and time scales. While these techniques are important for studying biological macromolecules in single crystals, they are essential for investigating more complex, noncrystalline systems, including multicomponent macromolecular assemblies in solution and liquid-crystalline membranes. Two important proposed upgrades were built into the design of SNS. One would boost the power of the proton accelerator, increasing the flux of spallation-produced neutrons by a factor of two to three times. This increase is highly significant because most neutron scattering experiments are “flux-starved” (i.e., limited only by the neutron flux available). The other upgrade would add a second target station optimized for the production of longer-wavelength “cold” neutrons, important for structural studies of large macromolecular systems. This station would provide much-needed additional capacity, including instruments optimized for the study of biological systems.

Sources of thermal and cold neutrons [ $\lambda = 1$  to 20 angstroms ( $\text{\AA}$ )] include nuclear fission<sup>1</sup> and proton accelerator-based nuclear spallation<sup>2</sup>. Both are polychromatic, with the former being continuous and the latter inherently pulsed. Importantly, the neutron flux densities (neutrons/sec/mm<sup>2</sup>) available from even the most powerful of these sources are dramatically lower (by many orders of magnitude) than the photon flux densities available from synchrotron radiation-based x-ray sources. As a result, neutron scattering techniques, both *elastic* and *inelastic or quasielastic*, are generally utilized only when they can provide either the best or the only approach to a specific structural or dynamical problem.

In accelerator-based spallation sources, negatively charged hydrogen ions are produced by an ion source and stripped of their electrons, producing protons. The protons are injected into a linear accelerator—composed of both normal and superconducting radio frequency (RF) cavities—that accelerates the protons to an energy of 1 gigaelectron volt (GeV), providing a total proton beam power of 1.4 megawatts (MW). SNS currently is operating somewhat below this primary design parameter at ~1.0 MW. The high-energy protons are then injected into an accumulator storage ring that bunches them into 1 microsecond pulses. These are directed to a liquid mercury target, chosen for its superior capabilities in dissipating thermal energy and shock effects arising from the pulsed proton bombardment. The target is surrounded above and below by a collection of moderators, either liquid water or liquid hydrogen (20 K) that cool the high-energy neutrons produced by nuclear spallation to produce room-temperature, or thermal neutrons, and cold neutrons, respectively.

Importantly, the initial design of SNS can accommodate increases in both proton beam energy (1.0 to 1.3 GeV) and current (1.4 to 2.3 milliamperes (mA)), resulting in an increase in total proton beam power to 3.0 MW, thereby tripling the currently available neutron flux. In addition, a second target

<sup>1</sup>Nuclear fission is an exothermic nuclear reaction, either induced by neutron bombardment or spontaneous, resulting in a heavy nucleus splitting into two lighter nuclei with the release of energy, neutrons, and photons ( $\gamma$ -rays). Under appropriate conditions, this can become a chain reaction resulting in an intense source of “fast” neutrons. This “hot” Maxwellian distribution can be cooled (“moderated”) to produce a distribution of “slow” neutrons with de Broglie wavelengths ( $\lambda = 1$  to 20  $\text{\AA}$ ) suitable for elastic and inelastic scattering experiments. Because the nuclear fission process occurs randomly among the ensemble of heavy nuclei, the fission neutron source is effectively continuous.

<sup>2</sup>Nuclear spallation is the production of neutrons via the bombardment of heavy nuclei (e.g., Ta, W, and Hg) with a beam of high-energy protons from a particle accelerator. Again, the energies of the spallation neutrons are adjusted via “moderation” to produce a distribution of “slow” neutrons with de Broglie wavelengths ( $\lambda = 1$  to 20  $\text{\AA}$ ) suitable for elastic and inelastic scattering experiments. Because the proton accelerator is inherently pulsed, the spallation neutrons are similarly pulsed.

station also can be accommodated, approximately doubling the number of neutron scattering instruments.

## Specific Facilities at SNS

**Macromolecular Neutron Crystallography.** Two single-crystal diffractometers—TOPAZ (available 2012) and MaNDi (available 2013)—will enable the investigation of three-dimensional (3D) macromolecular structure at both lower resolution ( $>10$  Å), relevant to macromolecular solvent structure (e.g., lipids and detergents for membrane proteins), and high resolution (1.5 to 2.0 Å) for determining protein structure. Data acquisition rates of these facilities will exceed current capability by 10 to 50 times. Unit cell dimensions of up to 150 Å can be investigated at 2.0 Å spatial resolution by utilizing crystal volumes as small as 1 mm<sup>3</sup>, or down to 0.125 mm<sup>3</sup> for perdeuterated proteins with TOPAZ and potentially down to 0.001 to 0.01 mm<sup>3</sup> with MaNDi. These instruments also are well suited to structural studies of partially ordered systems, protein and nucleic acid fibers in particular.

**Reflectometry.** Two reflectometers, the “magnetism reflectometer” with a horizontal reflection plane and the “liquids reflectometer” with a vertical reflection plane, are operational at SNS. The magnetism reflectometer instrument enables direct phasing of reflectivity data by employing a magnetic reference structure adjacent to the layered bio-organic structure to be determined, for example a membrane at the solid-liquid interface, with the solid incorporating the reference structure. The liquids reflectometer allows structural studies of macromolecular systems at the liquid-gas and liquid-liquid interfaces relevant to the study of biological membranes. Both instruments access a broad range of momentum transfer up to 0.3 to 0.4 Å<sup>-1</sup>, with a dynamic range of reflectivity extending down to the level of  $5 \times 10^{-8}$  and data acquisition times of a few hours.

**Small-Angle Neutron Scattering (SANS).** One SANS instrument, the Extended Q-range SANS (EQ-SANS), can access a broad range of momentum transfer of  $0.004 \text{ Å}^{-1} < q < 1.5 \text{ Å}^{-1}$ , or a somewhat more limited range of  $0.003 \text{ Å}^{-1} < q < 0.4 \text{ Å}^{-1}$  in a single configuration for time-resolved studies utilizing a 30 Hz pulse repetition rate.

**Inelastic Scattering.** Three instruments are available for inelastic scattering. The Cold Neutron Chopper Spectrometer (CNCS) accesses the shorter time scales of  $10^{-13}$  s to  $3 \times 10^{-10}$  s with 100 times higher flux than previously available. The Backscattering Spectrometer (BaSiS) accesses somewhat longer time scales of  $10^{-12}$  s to  $2 \times 10^{-9}$  s with a flux 60 times higher than previously available. The Neutron Spin Echo Spectrometer (NSE) accesses much longer time scales extending to  $5 \times 10^{-7}$  s (and 1 to  $2 \times 10^{-6}$  s by 2012).

**Biodeuteration Facility.** Deuteration is key to the applications of neutron scattering in structural biology. Currently, a substantial facility exists at ORNL for the *biodeuteration* of biomolecules, including proteins and nucleic acids. For

proteins, the biodeuteration facility can provide (1) perdeuteration of an entire protein; (2) perdeuteration of all copies of one or more selected amino acids throughout a protein; and (3) “segmental labeling,” namely the selective perdeuteration of tertiary structural components within a quaternary structure or covalently linked domains within a multidomain tertiary structure, the latter achieved via chemical ligation.

## Facility Capabilities and Potential for High-Impact Experiments

### Macromolecular Neutron Crystallography

Due to its much higher sensitivity to hydrogen atom locations, *neutron diffraction from single crystals* is capable of accurately determining these locations under physiological conditions with significantly lower-resolution data (e.g.,  $\sim 1.5$  to  $2.5$  Å) compared to x-ray diffraction, which requires a very high resolution (e.g.,  $<1.0$  Å), cryotemperatures, and very accurate data to locate the hydrogen atoms in a macromolecule. The major advantage of *neutron* crystallography of proteins lies in its unique capability for detecting the locations of hydrogen atoms, or protons, within the overall 3D structure. The number of significant challenges in structural biology benefiting from this approach is potentially quite large. For proteins, they range from investigating:

- The mechanism of action of enzymes in which hydrogen atoms or protons play a key role, including the ionization states and hydrogen bonding of residues and water within the catalytic site.
- The mechanism of protein folding, including the roles of hydrogen bonding and solvation.
- Small-molecule or macromolecular ligand binding involving essential hydrogen bonding.

Insights provided by such investigations would be key in enabling the genetic engineering of enzymes to improve their performance and stability in nonnatural hosts for industrial applications and the rational design of pharmacological agents for modulating protein physiological function. While the number of such problems investigated has been relatively few to date, they include the classic contribution establishing the protonation state of the charge relay system in serine proteases.

A significant disadvantage of neutron crystallography for proteins traditionally has been the requirement for relatively large crystal volumes. This is associated with the low flux densities available from fission sources and utilization of the Bragg method for collecting neutron diffraction data, appropriate for continuous neutron radiation but requiring only a very narrow bandwidth of the available continuous radiation. The time-of-flight quasi-Laue method for collecting neutron diffraction data from macromolecular single crystals—required for the most effective utilization of the polychromatic, inherently pulsed neutron radiation from

spallation sources—was first developed at the Los Alamos Neutron Science Center at Los Alamos National Laboratory in the United States. Importantly, this method also has significantly reduced the crystal volume now required with the newest instruments at SNS, namely down to the level of  $\geq 0.1 \text{ mm}^3$ . These developments ultimately could enable analysis of the proton-pumping mechanism of membrane protein complexes responsible for biological energy transduction, an area of continued controversy and significance.

In spite of the quite broad range of potentially significant problems in structural biology, the current perception is that they represent a relatively small subset of biological crystallography. However, it is important to stress that the primary reason for this perception likely lies in the past requirement for comparatively large crystal volumes due to the relatively low incident neutron flux densities available. Thus, important to note is that the crystal volume required for this capability at SNS will be substantially reduced to the level of  $\geq 0.1 \text{ mm}^3$  with the commissioning of the TOPAZ instrument in 2012 and further reduced to  $0.001$  to  $0.01 \text{ mm}^3$  with the MaNDi instrument in 2013. Nevertheless, even the greatly reduced crystal volume required by these new SNS instruments remains at the high end of what is now needed for x-ray crystallography. As a result, continued development of coupling the neutron spallation source and moderator to effective neutron optics is essential for increasing neutron flux density, thereby further decreasing the minimal crystal volume needed.

## Reflectometry

The major advantage of *neutron scattering from partially ordered, noncrystalline macromolecular systems* (e.g., fibers and membranes) lies in its unique ability to determine macromolecular conformations within complex, multicomponent assemblies. A key example is provided by the case of *neutron reflectivity*, here broadly defined to include specular<sup>3</sup> and off-specular<sup>3</sup> neutron reflectivity from oriented membranes (i.e., oriented in the laboratory frame at a solid-liquid or solid-gas interface, ranging from thick multilayers down to the level of a single membrane). Deuteration of a particular macromolecular component, or submolecular portions thereof, coupled with contrast matching of the remaining components can reveal the conformation of the selected component within a complex membrane system. The conformation of a functional *integral* membrane protein component within a single phospholipid bilayer membrane at the solid-liquid interface can be investigated as a function of the transmembrane electrochemical potential, providing key information into its mechanism of action. For a membrane-associated protein,

<sup>3</sup>“Specular reflectivity” refers to elastic scattering from an oriented multilayer structure with momentum transfer perpendicular to the layer plane. “Off-specular reflectivity” refers to elastic scattering with the momentum transfer parallel to the layer plane.

whose function is to alter the physical-chemical properties of the membrane’s lipid bilayer matrix, the conformations of both the protein and lipid components can be investigated separately as a function of their interaction. However, determining the conformation of the protein and/or lipid depends upon detailed computer modeling. For protein structure, this is based on the 3D crystal structure, which is determined independently and then critically constrained by the available structural information from the reflectivity experiments. The latter are limited to the projection of the protein’s (or lipid’s) 3D structure onto the normal to the membrane plane, and, in some cases, also the projection onto the membrane plane. For biological membranes, the membrane protein’s environment in the fully hydrated, noncrystalline lipid bilayer is more biologically relevant than that within a single crystal.

Within the overall range of currently perceived significant problems in structural biology, those in *membrane* biology would appear to gain the greatest advantage from the *neutron reflectivity* approach. This derives mostly from the ability to investigate functionally relevant conformations and conformational changes of selected macromolecular membrane components under physiological conditions. Currently, those working in this field remain limited to a relatively small number of more-expert users. Nonetheless, the breadth of potential problems in membrane structural biology uniquely accessible via neutron reflectivity would appear to justify a substantial extension to effectively address the significant problems of interest to less experienced users.

## Small-Angle Neutron Scattering

The major advantage of *SANS from macromolecules and supramolecular assemblies in isotropic solution* again lies in its unique capability for determining macromolecular conformations within complex, multicomponent assemblies. As for the case with membranes, deuteration of a particular macromolecular component (or submolecular portions) coupled with contrast matching of the remaining components can reveal the conformation of the selected component within a complex supramolecular system. For several macromolecular components in isotropic solution, conformations can be separately investigated as a function of their interactions in forming binary, tertiary, and higher-order complexes. These complexes can be composed of oligomers of a single protein component, different protein components, and protein and nucleic acid components. For a single macromolecular component in isotropic solution, its conformation also can be investigated as a function of its interactions with one or more small-molecule ligands centrally related to its biological function. Importantly, determining the conformation of a macromolecular component again depends upon detailed computer modeling, based on the respective 3D x-ray crystal structures determined independently and critically constrained by the available, spherically averaged structural information from SANS experiments. For macromolecular biological components, or supramolecular complexes thereof

in isotropic aqueous solution, the environment is more biologically relevant than that within a single crystal.

Within the overall range of currently perceived significant challenges in structural biology, those concerning the conformations of macromolecular components in isotropic solution, or selected macromolecular components within supramolecular complexes in isotropic solution, would appear to gain the greatest advantage with the SANS approach. Again, this derives mostly from the ability to investigate functionally relevant conformations and conformational changes of selected macromolecular components under physiological conditions. Currently, researchers working in this field include a substantial number of more-expert users as well as nonexpert users. Furthermore, the breadth of potential problems in structural biology uniquely accessible via SANS would appear to justify a substantial extension to effectively address these significant problems of interest to the broader scientific community.

### Inelastic Scattering

The major advantage of *inelastic and quasielastic neutron scattering* lies in the extremely broad range of time scales of periodic motions over a wide range of length scales [0.1 nanometer (nm) to 100 nm] that can be accessed. Specific applications in structural biology include the investigation of (1) light-induced exciton diffusion in photosynthetic complexes at the faster extreme, (2) local motions in proteins affected by small-molecule ligand binding and the relative motions of protein domains associated with the function in the intermediate regimes, and (3) diffusive and undulatory motions in macromolecular ensembles (e.g., in membranes at the slower extreme). Molecular dynamics computer simulations are very important for quantitatively interpreting the scattering data to provide detailed information on the dynamics of protein motions down to the level of specific elements of secondary structure and individual residues. Otherwise, there is no special advantage here with regard to investigating the dynamics of biological macromolecular systems in physiologically relevant environments, given that neither the inelastic and quasielastic neutron scattering techniques nor other physical techniques such as nuclear magnetic resonance and isotopic exchange require a three-dimensionally ordered structure.

Although *inelastic neutron scattering* clearly has already had a major impact in condensed matter science, its promise for structural biology remains largely unfulfilled. This is likely due to the low-incident neutron flux available at the sample, as limited principally by the nature of the neutron source. Investigations of protein dynamics in various environments, including within lipid bilayer membranes, have provided some interesting results. However, it would now appear that application of the neutron spin echo technique to investigations of physiologically relevant factors affecting undulatory motions in membranes may offer a needed breakthrough in this area. Importantly, this situation may

improve substantially with SNS development that provides an enhancement of 10 to 50 times in incident neutron flux most relevant for the investigations of slower motions evidenced by proteins and membranes.

Lastly, the 30 to 60 Hz repetition rate of pulsed spallation neutron sources provides the possibility of “pump-probe” studies of the structural evolution of biological macromolecular systems *if* the mechanism of action is relatively slow ( $>10^{-5}$  s) and is (or can be made to be) cyclic. This would enable the collection of statistically significant scattering data via signal-averaging for a specified pump-to-probe delay time. One such example is provided by voltage-gate ion channel proteins vectorially oriented within a single membrane at the solid-liquid interface, where the protein can be cycled between closed and open states via the applied transmembrane voltage to investigate the mechanism of electromechanical coupling at the submolecular level.

### Additional Biological Applications of Elastic Scattering

It is important to note that there are many other biological applications of primarily *elastic neutron scattering techniques* highly relevant to the missions of the Department of Energy and National Institutes of Health. Notable examples would include:

- Structural studies of the interactions of natural and artificial functional protein systems with inorganic surfaces and polymer matrices relevant to solar energy conversion (solar to power and solar to fuel).
- Interactions of enzymes with cellulosic materials relevant to biomass to biofuel conversion.
- Mechanism of enzymes for carbon sequestration and renewal energy.
- Development of biocompatible polymer scaffolds and drug delivery systems.

### Plans for Upgrading SNS

Many technical margins were built into the SNS design and hardware to facilitate a power upgrade from the current baseline 1.4 MW level to the 3 MW range. The upgrade plan builds upon recent progress in SNS development programs to improve superconducting cavity performance in the linear accelerator (linac), mitigate intensity thresholds in the accumulator ring, and reduce cavitation damage in the mercury target. Because key elements of the upgrade rely on replicating existing designs, the upgrade is positioned for aggressive deployment. The proton beam energy will be increased by 30% from 1.0 GeV to 1.3 GeV, and the time-averaged accelerator output beam intensity will be increased by 65% from 1.4 mA to 2.3 mA for 3.0 MW of beam power.

Because the vast majority of neutron scattering experiments are flux limited, even modest improvements in source

intensity can lead to scientific measurements that were previously out of reach. An increase in power by a factor of two will enable the study of smaller samples and real-time studies at shorter time scales. It also will allow a modest increase in resolution on most instruments and enable more experiments to take advantage of the highest resolution available on each instrument. Importantly, by providing beam power to support a second target station, the power upgrade facilitates a significant expansion of capacity and substantial performance gains for long-wavelength applications of neutron scattering techniques (see below). Although the second target station can be implemented without the power upgrade, its power level—and hence scientific performance—will be significantly curtailed if its operation were to come at the expense of the existing target station.

SNS was designed to accommodate a second target station *optimized to produce longer-wavelength “cold” neutrons*. This station would be a “long-pulse” facility that uses the full millisecond proton pulse length from the linac, providing a 50% increase in proton flux on target. Focusing the resulting cold neutrons would provide at least an *order of magnitude improvement* compared to the instruments now operating on the first target station. In particular, the intense cold neutron beams will enable the extension of kinetic studies (e.g., via SANS and reflectivity) down to the 10 microsecond regime utilizing sample modulation techniques. Revolutionary new capabilities would enable investigation of the lateral structure of interfaces and membranes at length scales from 10 to 1,000 nm via reflectivity. Tightening the angular resolution will permit focusing down to 10 micron–size neutron beams, thereby greatly facilitating the investigation of much smaller samples, including protein crystals, and providing totally new neutron imaging capabilities. The high-intensity cold neutron beams also will extend dynamical studies employing spin echo techniques by an order of magnitude for the study of slow motions up to 10 microseconds on length scales up to a micron. Importantly, adding this extended capability to the ones already (or soon to be) available in the first target station could allow for the *addition of instruments optimized for and (at least partially) dedicated to structural biology*. These could include, for example, a bioreflectometer enabling magnetic phasing and vertical reflection plane and a Bio-SANS instrument.

## Support

**Substantial Expansion of the Deuteration Facility.** Given the critical importance of deuteration to neutron scattering in structural biology, the current biodeuteration facility at ORNL should be substantially expanded. This should include an extension to site-directed labeling at the tertiary structure level via both chemical synthesis (e.g., to selectively labeled lipids, polysaccharides, and peptides) and to protein semisynthesis. Importantly, protein semisynthesis may provide a key breakthrough needed for investigations of protein conformations directly involved in their mechanisms of action.

**Expanding the Protein Crystallography Users Group.** For macromolecular neutron crystallography, it is essential to continue the development of coupling the neutron spallation source and moderator to effective neutron optics as required to increase neutron flux density, thereby further decreasing the minimal crystal volume necessary. A relevant example is provided by Ice et al. (2005). As long as we continue to not understand, and therefore not control, the crystallization process, we can neither control the size nor the degree of periodic order in 3D crystals. Both are key in determining the positions of hydrogen atoms in the overall 3D structure—the former (crystal volume) for the case of neutrons, and the latter (degree of periodic order) for the case of x-rays. Importantly for the neutron case, the crystal size accessible for perdeuterated proteins is often smaller than that for the fully hydrogenated case.

**Expanding the Neutron Scattering Community in Structural Biology.** To make the most significant impact on important biological problems, a major sustained effort is required—ranging from the production of optimal biological materials to the utilization of fully integrated structural techniques. As a means of engaging a larger user community, SNS might consider stronger collaborations with institutions already possessing such integrated programs in structural biology. Establishing such a “structural biology village” of major users with the necessary capabilities might greatly facilitate the dissemination of the overall utility of neutron scattering techniques in biological research.

## Reference

Ice, G. E., et al. 2005. “Kirkpatrick–Baez Microfocusing Optics for Thermal Neutrons,” *Nuclear Methods in Physics Research A* **539**, 312–20.



# APPENDICES

Appendix A: Advanced Photon Source Upgrade .....	27
<i>Facilities for Biological Science for the Next Decade at APS</i> .....	27
<i>Life and Environmental Science Enabled by APS-U</i> .....	35
Appendix B: Linac Coherent Light Source .....	45
<i>Facilities, Operations, and Future Perspective of LCLS-I and LCLS-II</i> .....	45
<i>LCLS: Impacts and Future Potential in Biology</i> .....	53
Appendix C: National Synchrotron Light Source-II.....	63
<i>Opportunities for Biological Sciences at NSLS-II</i> .....	63
<i>Overview of Significant New Biological Research at NSLS-II</i> .....	72
Appendix D: Next Generation Light Source .....	81
<i>NGLS: A Transformative Tool for X-Ray Science</i> .....	81
<i>New Biological Research Enabled by NGLS</i> .....	89
Appendix E: Spallation Neutron Source.....	99
<i>SNS: A Powerful Tool for Biological Research</i> .....	99
<i>SNS: Addressing the Next Challenges in Biology</i> .....	105
Appendix F: Workshop Agenda and Participants .....	115
Acronyms and Abbreviations.....	Inside back cover



## Advanced Photon Source Upgrade

# Facilities for Biological Science for the Next Decade at APS\*



## Biological Science at APS

The Advanced Photon Source (APS) at Argonne National Laboratory (ANL) is the largest user facility operated by the U.S. Department of Energy (DOE) Office of Science. For more than a decade, APS has been providing the brightest hard x-ray beams available in the Western Hemisphere to the most users of any U.S. synchrotron radiation source. In 2010, almost 3,800 users performed experiments at 62 beamlines.

Biological science is a vital component of the research activity at APS. Currently, 41% of users are in the biological and life sciences field, 3% in environmental sciences, and 2% in medical science. Funding for this community is quite diverse, with more than 50 institutes, states, and agencies—including the DOE Office of Biological and Environmental Research (BER)—contributing funds for construction and operation of beamlines managed by Collaborative Access Teams and for some enhancements of APS-managed beamlines. In 2010, over 1,100 users received funding from the National Institutes of Health (NIH), and about 50 were supported by BER. As shown by colored ovals in Fig. A1, half the sectors at APS primarily serve this community with techniques such as macromolecular crystallography (MX); small-angle x-ray scattering (SAXS), wide-angle x-ray scattering (WAXS), and fiber diffraction; spectroscopy; and microprobes. Although the majority of biological and life sciences research is conducted at beamlines managed by Collaborative Access Teams, some biological research is performed on every beamline at APS. For example, 31% of the microprobe facility users at beamline 2-ID were funded by NIH or BER, and 43% were classified as life scientists. Biological research at APS results in about half the facility's

\*Argonne National Laboratory prepared this and a companion document (p. 35) and approved post-workshop revisions to each.



[Courtesy of Argonne National Laboratory]

publications (~600 per year) and accounts for 20% of the worldwide deposits into the Protein Data Bank.

## APS Upgrade Project

Over the next decade, the facilities at APS will be improved to stay at the forefront of x-ray science. The primary vehicle for this improvement will be the APS Upgrade project (APS-U), a major accelerator and beamline equipment upgrade approved by the DOE Office of Science in April 2010 at an

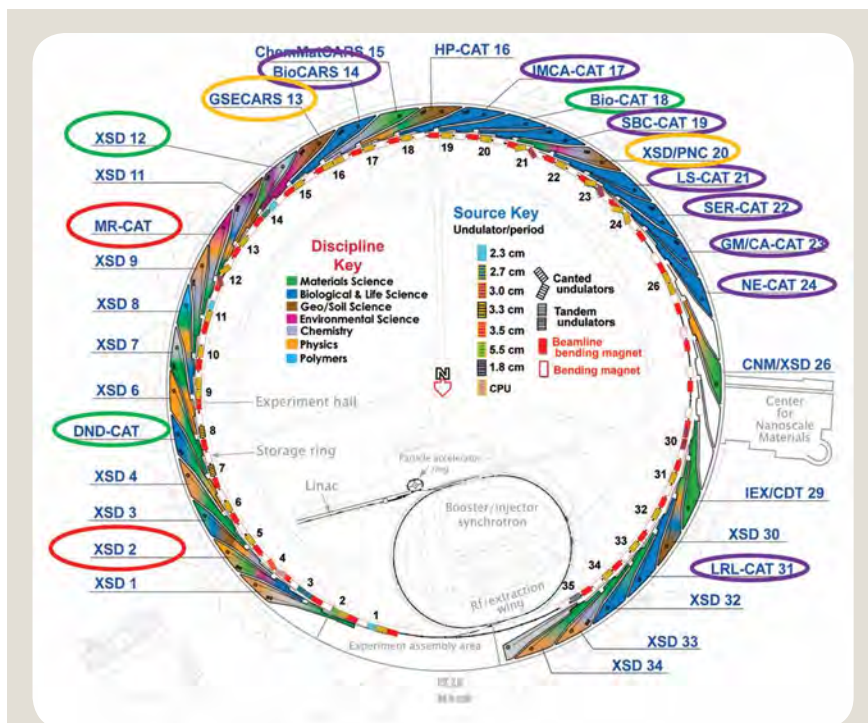


**Fig. A1. Current APS sector layout.** Ovals show primary beamlines serving environmental science (yellow) and biological science via macromolecular crystallography (purple), scattering (green), and imaging (red). [Courtesy of Argonne National Laboratory]

estimated cost of \$300M to \$400M (APS 2010). APS-U has been designed to complement the National Synchrotron Light Source-II (NSLS-II) project at Brookhaven National Laboratory. The upgrade will provide the highest flux and brightness in the world at x-ray energies above 10 and 20 kilo-electron volts (keV), respectively (see Table A1, this page). These qualities will be achieved through improvements to the accelerator, increased electron current, and undulator sources such as “revolver” undulator systems and innovative superconducting undulators. APS-U also will provide the higher stability needed for imaging, microfocus, and high-resolution studies. Other outstanding capabilities will be available for time-resolved studies through flexible operational modes of x-ray pulses with a duration of 100 picoseconds (ps) provided to all beamlines and a unique accelerator system that will produce 1 ps x-ray pulses for a subset of beamlines. In addition to these source improvements, APS-U will enable major enhancements in experimental capability and capacity through a suite of new and improved beamlines. A large expansion in the number of forefront beamlines is made possible by implementing “canted” undulators that provide sources for two independent high-brightness beamlines from a single APS sector.

These improvements will allow APS to continue to provide leading-edge x-ray capabilities to the biological sciences community through the next decade and beyond. The vision for biological sciences has been developed in the “Proteins to Organisms” theme of the APS-U Conceptual Design. This theme addresses the grand challenge of identifying how proteins and other macromolecules, under the influence of environmental factors or inherent genetic programming, determine function at every level of organization—from biomolecular interactions to an organism’s higher functions. As described in more detail below, APS-U will enable a significant extension of the ability to probe protein structure and dynamics and to image directly and indirectly nonperiodic soft structures spanning length scales from millimeters to 10 nm (i.e., from tissues to cells to subcellular structures). This will be the first time since the beginning of biology that the same imaging technique can be used with increasing resolution from microns to 10 nm and with samples cryogenically preserved in their native state.

Several characteristics of the upgraded APS provide advantages to biological science research. A primary feature is the excellent source flux and

brightness at high x-ray energies. As described below, higher energies can reduce the effects of radiation damage in macromolecular crystallography studies. The deeper penetration of higher-energy x-ray beams enables *in situ* observations critical for environmental science and whole-organism and tissue studies. For fluorescence microscopy, higher energies provide access to all elements in the periodic table. APS has a strong existing suite of beamlines, many optimized for biological science applications and all available to the biological research community. APS-U’s improved electron-beam stability and current will benefit all beamlines. New specialized beamlines for phase-, absorption-, and fluorescence-contrast imaging; microfocus macromolecular crystallography; SAXS and WAXS; and time-resolved studies will complement this existing base. The large floor area available at APS also provides space for important ancillary facilities.

**Wide-Field Imaging Beamline.** Funded as part of APS-U, this new facility will strengthen the capabilities for biological science at APS. The high flux and partial coherence of the x-ray beam enable synchrotron x-ray imaging to combine the penetrative power of hard x-rays with high sensitivity and exceptional spatial and temporal resolutions. No other imaging technique has this combination of properties. For example, optical techniques do not have the same penetrating power, and magnetic resonance imaging (MRI) and ultrasounds do not have the same spatial and temporal resolutions. Synchrotron-based x-ray phase-contrast imaging (as shown in Fig. A2, p. 29) has enabled direct visualization of the dynamics of millimeter-sized animal physiology in *real time* at the micron scale (Westneat et al. 2003; Kaiser et al. 2007; Lee and Socha 2009; Simon et al. 2010). The Wide-Field Imaging beamline of the APS-U will expand current full-field imaging capabilities at APS in three crucial ways: (1) increase beam size to the centimeter scale, (2) increase the sensitivity for phase-contrast imaging, and (3) reduce the source-size blurring contribution to spatial resolution. The increased beam size will allow the study of important biomedical models (e.g., rats and mice) and accommodate a much wider

**Table A1. Spectral Flux ( $10^{14}$  ph/s/0.1%bw) and Brightness ( $10^{18}$  ph/s/0.1%bw/mm<sup>2</sup>/mrad<sup>2</sup>) for Key Sources Worldwide\***

Country	Name	E (GeV)	8 keV		25 keV		60 keV	
			Flux	Brightness	Flux	Brightness	Flux	Brightness
Japan	SPring-8	8	11	150	4.6	83	1.1	24
England	Diamond	3	11	50	N/A	N/A	N/A	N/A
France	ESRF	6	1.9	120	0.64	8.4	0.064	0.49
France	ESRF-U	6	9.6	240	2.6	83	0.29	7
Germany	PETRA-III	6	4.5	800	0.94	59	0.14	3.5
USA	SPEAR3	3	3	0.015	N/A	N/A	N/A	N/A
USA	APS	7	5	70	1.4	17	0.29	1.3
USA	APS-U	7	12	105	8	113	2.1	32
USA	NSLS-II	3	16	1,200	0.25	9.9	0.0008	0.012

\*As shown, the APS Upgrade Project (APS-U) will provide the highest flux and brightest x-rays at energies above 10 and 20 keV, respectively (APS 2010).

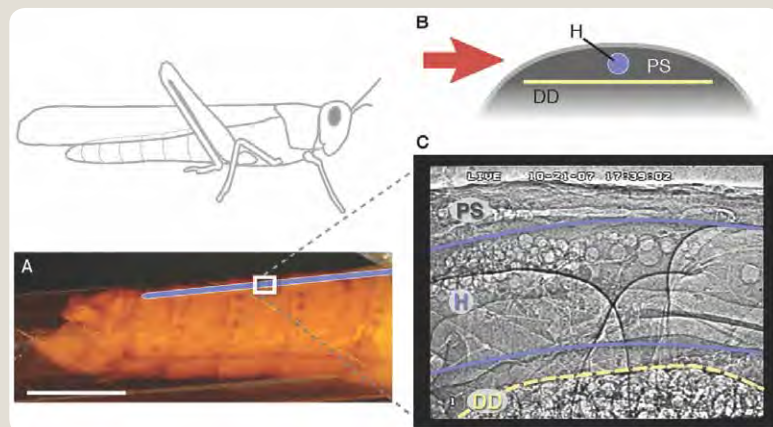
variety of animals and plants. Due to the high photon flux, obtaining full three-dimensional (3D) images of centimeter-sized living animals with micron resolution in less than 0.1 s will be possible. Thus, researchers will be able to see a beating mouse heart in 3D at high spatial resolutions *in real time*. Current techniques for 3D visualization of heart dynamics depend on “retrospective-gating” (i.e., postsynchronization of images using other physiological monitors) of 2D images averaged over many heartbeats. The ability to view small-animal physiology with high resolution in real time will open up avenues of biomedical research currently unavailable.

**High-Energy Tomography Beamline.** This second imaging facility, funded as part of APS-U, is significant for biological science. The importance of this capability to understand biological systems can be illustrated via studies of bone and biomineralization. Example challenges that could benefit from materials-based research on mineralized tissue and its replacements are (1) bone fragility in osteoporosis, (2) implant stability and wear resistance in joint replacements, and (3) impaired fracture healing in the elderly. Such research will have a major role in improving health and reducing morbidity and mortality. The roles of genetics, biology, and epidemiology in the study of mineralized tissue dysfunction are not to be underestimated, but bone is a composite of protein, calcium phosphate mineral, and water—each of whose constituent functions remain poorly understood. Understanding the basic processes in biomineralization is important in establishing what constitutes “good” versus “poor” bone quality, a basic materials question. Systemic interactions *in vivo* complicate direct studies of bone, and much progress has been made with invertebrate models whose mineralization-related proteins are close analogs of those in bone. Because soft tissues surround and produce the mineral in echinoderms, attaining enough phase contrast from soft tissue in the presence

of heavy absorption from the mineral and from the long fluid path length is a challenge. High-energy imaging is the solution because it decreases absorption contrast relative to phase contrast; however, such imaging is practical only at hard x-ray light sources like APS. The High-Energy Tomography beamline will provide that solution by developing a 20 to 60 keV beamline and suitable area detectors.

**Advanced Protein Crystallization Facility (APCF).** Also important to the future of biological science at APS and in conjunction with APS-U will be construction of the APCF. This facility will be a highly automated state-of-the-art laboratory—integrated with a scientific collaboration and user facility—for the production and characterization of proteins and macromolecular crystals and the design of proteins with new activities. The APCF building, funded by the state of Illinois, will be adjacent to APS to provide streamlined access to beamlines and take full advantage of ANL’s capabilities for determining the 3D structure of macromolecules and characterizing their functions. Focusing on the most challenging classes of proteins and macromolecular assemblies, APCF will be home to several research groups and will provide highly flexible laboratory and office space for outside users. These laboratory activities will be supported by common core facilities. The space is designed to facilitate discussion, interaction, and collaboration as defined by its users. The facility is expected to produce many microcrystals requiring the capabilities of the upgraded APS and the new microfocusing beamline. Similar facilities are operating at the Hauptman-Woodward Institute, Structural Biology Research Center at the Photon Factory, Protein Production Facility at Oxford, and the European Molecular Biology Laboratory’s high-throughput crystallization facility at Deutsches Elektronen Synchrotron (DESY) in Hamburg.

**Fig. A2. Flow visualization in the heart of a grasshopper (*Schistocerca americana*) using 25 keV x-rays. (A) Side view of the grasshopper abdomen showing the approximate location of the heart (blue) and the relative size of the imaging window (white rectangle, 1.3 by 0.9 mm). The abdomen is encapsulated in an x-ray transparent Kapton tube (scale bar, 5 mm). (B) Cross-sectional schematic of the dorsal abdomen showing the relative sizes and locations of the heart (H), dorsal diaphragm (DD), and pericardial sinus (PS). The red arrow indicates the orientation of the x-ray beam. (C) an x-ray video still of a region in the dorsal third abdominal segment in lateral view. Round structures are air bubbles used to visualize patterns of heartbeat and hemolymph flow. [From Lee, W.-K., and J. J. Socha. 2009. “Direct Visualization of Hemolymph Flow in the Heart of a Grasshopper (*Schistocerca americana*),” *BMC Physiology* 9(2). (Open-access article distributed under the Creative Commons Attribution License.)]**



## Biological Science Beamline Plans

In addition to the improvements in x-ray source performance provided by APS-U (e.g., increased current and stability and new undulator sources) that will benefit all existing APS beamlines, the biological science community has proposed several new beamlines and beamline upgrades. Although these projects will be funded separately from APS-U, their scientific cases have been reviewed and recommended by the APS Scientific Advisory Committee, and space has been allocated on the “roadmap” for future APS plans. Highlighted below are some projects that have been proposed by the user community and included in planning for APS-U. The synergy of the excellent properties of the upgraded APS source, the active APS biological science community, the existing beamlines’ high capacity and wide range of capabilities, and the location of the planned forefront capabilities at APS will enable cutting-edge biological research for years to come.

### Microfocus Macromolecular Crystallography Beamline

Many macromolecules, complexes, and cellular assemblies are very difficult to produce, and their crystals tend to be small, imperfect, and weakly diffracting. A micron-sized x-ray beam enables researchers to study and optimize data collection from very small macromolecular crystals and potentially ordered intracellular arrays and microcompartments within cells. An x-ray beam size of 5 to 20  $\mu\text{m}$  can be obtained by collimating the beam produced by a typical undulator beamline at a third-generation synchrotron source. Because crossfire in the beam converges to the focus, the collimating pinhole must be close to the sample. However, distance and aperture limits result in unacceptably long exposure times. Furthermore, these “fixed-size” collimated beams can be adjusted to crystal sizes only in fixed-step sizes, resulting in high background scattering for very small crystals. This problem can be solved by using highly demagnifying optics capable of imaging the source into a natural focal spot of 1 to 2  $\mu\text{m}$  while still accepting most of the source divergence. The greatly increased flux density compensates for the decreased exposed volume, resulting in reasonably short exposure times.

The microfocus facility will be highly complementary to existing APS MX beamlines and the BioNanoprobe, as well as capabilities developed at the Linac Coherent Light Source (LCLS) and the planned microfocus beamline at NSLS-II. By providing a microbeam capability, the facility will improve data quality and efficiency for very small samples. In addition, research at APS has demonstrated that radiation damage and its deleterious effects on data quality can be reduced with a micron-sized beam because damaging photoelectrons deposit their energy outside the diffracting volume of the crystal, as shown in Fig. A3, this page (Finrock et al. 2010; Sanishvili et al. 2011). Also, the best-quality data predictably

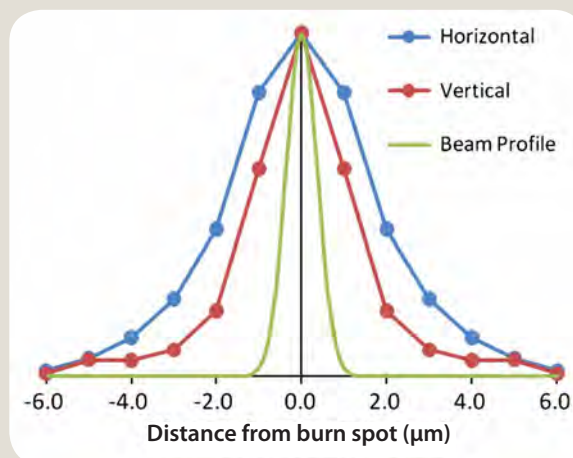


**Fig. A3. Comparison of spatial extent of radiation damage and beam size at 18.5 keV.** Widths of the damage distributions (blue and red curves) are significantly larger than the width of the x-ray beam (green curve) and are slightly anisotropic. [From Sanishvili, R., et al. 2011. "Radiation Damage in Protein Crystals is Reduced with a Micron-Sized X-Ray Beam," *PNAS* **108**(15), 6127–32.]

could be obtained at higher x-ray energies (20 to 30 keV), of which the upgraded APS will be the ideal source. Other benefits of the microfocus facility are reduction of background and increase of signal-to-noise for small crystals, as well as the use of more ordered regions of crystals for data collection. The substantial increase in x-ray beam stability and current provided by APS-U will make the proposed microfocus beamline reliable and productive.

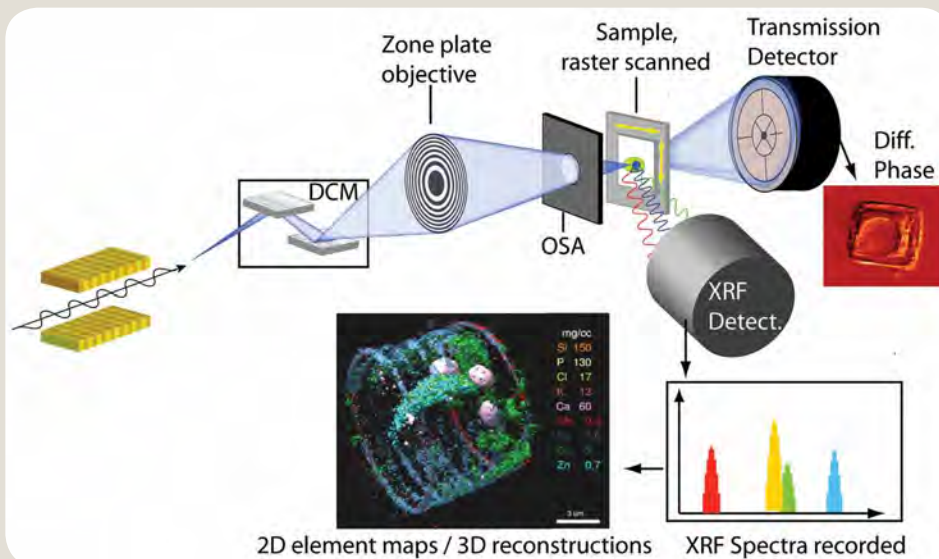
### BioNanoprobe I and II

The presence of metals and trace elements is essential for the existence of life as we know it. In any organism, there are very few intracellular processes not dependent on the presence of metals or other trace elements. Yet environmental contaminants—both heavy metals and radionuclides—can have considerable negative impacts on living systems.

The BioNanoprobe I is a scanning fluorescence nanoprobe with cryotransfer capabilities and sub-50 nm spatial resolution. Funded by NIH and the American Recovery and Reinvestment Act, BioNanoprobe I was delivered to APS in summer 2011. Moreover, the instrument was commissioned for the first time in November 2011. Users obtained images of a cell with its surface decorated with nanoparticles at 70 nm resolution and of cryogenically frozen cells imaged at cryogenic temperatures. As the first of its kind, the BioNanoprobe I will significantly advance the ability to probe and understand the role of trace metals in biology and environmental science. In addition to investigating dynamic changes in the concentrations and localization of metals in cells and organelles, this instrument will enable 3D visualization of the elemental content in the spatially heterogeneous microenvironment around cells.

**Fig. A4. Schematic of the**

**BioNanoprobe II.** *Hard x-rays are focused onto a specimen that is raster-scanned through the focus. Ultrastructural information is acquired by exploiting phase contrast, while trace elemental information is simultaneously acquired using x-ray fluorescence. 3D specimen reconstructions, including both structural and elemental information, are calculated from numerous individual projections. Dose fractionation (Hegerl and Hoppe 1976) is exploited to minimize dose and acquisition time. [From de Jonge, M. D., et al. 2010. "Quantitative 3D Elemental Microtomography of Cyclotella meneghiniana at 400-nm Resolution," PNAS 107(36), 15676–80.]*



The nanoprobe will considerably improve the achievable spatial resolution in biological samples and soft materials, such that precise 3D elemental maps can be acquired even in small organelles, vesicles, and within and adjacent to actively metabolizing cell surfaces and membranes (de Jonge et al. 2010; de Jonge and Vogt 2010). X-ray phase-contrast methods, largely developed at APS (Holzner et al. 2010; de Jonge et al. 2008; Hornberger et al. 2008) will simultaneously provide the ultrastructural context. A cryogenic specimen environment, with cryotransfer, will minimize radiation damage and permit imaging of frozen-hydrated specimens preserved as closely as possible to their natural state. After gaining some years of operational experience with BioNanoprobe I, a second-generation instrument with new and enhanced capabilities will be developed. *In situ* fluorescence light microscopy—at cryogenic temperatures and with high numerical aperture—will permit correlative studies such as the correlation of select fluorophores [including green fluorescent protein (GFP)] with specimen ultrastructure and trace metal content. This combination of features, illustrated in Fig. A4, this page, will make the BioNanoprobe II a unique instrument for biological and environmental sciences, enabling, in particular, the following upgraded (1–3) or new (4–5) capabilities:

1. Throughput and sensitivity improved by up to a factor of 20 through increased beam current, optimized undulators and monochromators, and better detectors compared to BioNanoprobe I.
2. Spatial resolution improved to 10 to 20 nm by building upon BioNanoprobe I experience to work with shorter-focal length, higher-aperture x-ray optics.
3. (Semi)automated x-ray fluorescence tomography using phase contrast to make dose fractionation feasible without the use of fiducial markers.

4. Visualization of the trace elemental content of specimens in the context of their ultrastructure by using novel approaches to exploit Zerniucke-type phase contrast in scanning x-ray microscopy (Holzner et al. 2010).
5. Correlative microscopy combining trace elemental content with protein localization by permitting *in situ* visualization of fluorophores (e.g., GFP fusion proteins) using optical cryomicroscopy.

### Enhanced SAXS and WAXS

It is becoming increasingly clear that a complete description of biomolecular activity requires an understanding of the nature and role of conformational dynamics for proteins, DNAs, RNAs, and their assemblies in solution. The resounding success of the worldwide macromolecular crystallographic effort over the last few decades has led to a burgeoning of high-resolution structures. These structures raise new questions about how macromolecules react in solution to changing environmental conditions, bind to ligands, and especially how they assemble into larger macromolecular complexes. The ability of SAXS to yield low-resolution macromolecular envelopes allows high-resolution structures and fragments to be assembled into high-resolution model structures, inaccessible by crystallographic means, that can yield insight into their function. Another growing area is the combination of global orientational information from nuclear magnetic resonance (NMR) residual dipolar coupling measurements with the global dimensional information from small-angle scattering restraints. Used together, these two complementary techniques form a powerful combination for structure characterization, determination (Wang et al. 2009), and refinement (Grishaev et al. 2005). The combined use of SAXS and NMR measurements has been applied to proteins

(Grishaev et al. 2005), protein-protein complexes (Zuo et al. 2008; Wang et al. 2009), RNAs, and an RNA–RNA complex (Zuo et al. 2008). These emerging applications—along with traditional pair distribution function  $P(r)$  and radius of gyration  $R_g$  analysis—have been major driving forces for the exponential increase in the use of SAXS and WAXS for biological research in recent years. Consequently, SAXS and WAXS have played a critical role in experiments resulting in many high-profile publications from 2000 to 2011. For example, they were used in research described in approximately 20 papers in the *EMBO Journal*, 20 in *Science*, 50 in *Cell*, 50 in the *Nature* group, and 90 in *Proceedings of the National Academy of Sciences*. About two-thirds of these papers had U.S. scientists as corresponding authors.

WAXS extends the range of SAXS to spacings comparable to those of crystallography ( $\sim 2.0$  Å), greatly expanding the range of possible experiments (Fischetti et al. 2003; Makowski 2010). The intensity falls off rapidly with scattering angle; therefore, high-brilliance undulator beamlines such as those available at APS are required to record accurate scattering intensities from macromolecules to these spacings. When combined with the capability of calculating solution scattering data from atomic coordinates (Park et al. 2009), WAXS becomes a powerful technique for testing structural models constructed by other means, such as molecular dynamics, homology modeling, or *ab initio* approaches (Zuo et al. 2006). WAXS data have proven highly sensitive to small changes in protein structure induced by ligand binding (Fischetti et al. 2004; Rodi et al. 2007), changes in oxidation state (Tiede, Zhang, and Seifert 2002), and the effect of mutations (Yang et al. 2010). Time-resolved WAXS studies have been highly informative in tracking conformational changes (Cammarrata et al. 2008; Choa et al. 2010) and have proven effective in the study of membrane proteins (Anderson et al. 2009) as well as dynamics in systems through research on changes in protein ensembles. WAXS studies can be used to investigate protein folding and unfolding in great detail (Hirai et al. 2004); are sensitive to modulation of structural fluctuations (Makowski et al. 2008); and can be used to monitor shifts in the character of a protein ensemble in response to environmental changes, ligand binding, or mutations (Makowski et al. 2011).

The high quality of data achievable with SAXS and WAXS instruments using third-generation undulator radiation will be further enhanced by the improved beam stability and higher beam current from APS-U, potentially opening new avenues of study. The proposed new beamline will enable capabilities for anomalous SAXS (ASAXS), an approach basically equivalent to the multiwavelength anomalous dispersion (MAD) method in crystallography. This beamline would also permit grazing incidence SAXS (GISAXS) measurements that could be used to determine accurate molecular envelopes of biomacromolecules in model membranes (Andersson et al. 2009). Furthermore, WAXS offers the prospect of collecting detailed structural information concerning

structural intermediates that exist only in the presence of other structural forms. By adjusting the solution conditions that determine the relative abundances of different intermediates, structural information can be obtained about transient forms involved in, for instance, enzymatic regulation (Yang et al. 2010; Bernado and Blackledge 2010).

The ease with which proteins under different conditions can be studied opens up a wide range of possibilities for the future. However, no APS beamline currently is fully dedicated to biological solution scattering studies. The planned beamline is a fully automated, dedicated undulator beamline capable of simultaneously recording SAXS and WAXS data with high flux and tunable high x-ray energy. Together with the improved beam stability and higher beam current from APS-U, this beamline has the potential to revolutionize the application of scattering in biological research and accelerate our understanding of biology at the molecular level under near-physiological solution conditions.

### **Enhanced 100 ps High-Flux Pump-Probe Facility**

BioCARS, a national research resource currently funded by NIH, conducts time-resolved studies that probe problems of interest to structural biologists. The BioCARS 14-ID beamline is optimized to perform laser pump, x-ray probe experiments at 100 ps time resolution with the first harmonic of a focused undulator polychromatic (Laue) beam. A 100 ps x-ray probe pulse is isolated by an x-ray chopper to deliver nearly  $4 \times 10^{10}$  photons within a bandwidth ( $\Delta E/E$ ) of  $\sim 4\%$  to a tightly focused area at the sample of  $90(\text{H}) \times 20(\text{V}) \mu\text{m}^2$ . The x-ray probe pulses are synchronized with the picosecond laser pump pulses. The BioCARS per-pulse flux is similar to that delivered by free-electron laser (FEL) sources such as LCLS ( $10^{11}$  to  $10^{12}$  photons per pulse within a pulse of 10 to 100 fs and  $\Delta E/E$  of  $\sim 0.4\%$ ), albeit with longer time and wider energy resolution. BioCARS specializes in coupling this high-flux, time-resolved capability to well-established x-ray scattering techniques such as crystallography, WAXS, and general diffraction. For experiments that require narrow energy bandwidth ( $\Delta E/E$  of  $\sim 0.01\%$ ), a Si (111) monochromator is available. With these key capabilities, BioCARS is uniquely positioned to contribute to ultrafast dynamical studies in the biological sciences complementary to those at the highly oversubscribed FEL sources.

Despite the demonstrated successes of time-resolved macromolecular crystallography, an important and major challenge involves studies of biologically interesting but irreversible reactions. All previous ultrafast time-resolved experiments at beamline 14-ID, beamline ID09 at the European Synchrotron Radiation Facility (ESRF), and elsewhere have studied reversible systems in which the initial state is thermally re-established within, at most, a few seconds after reaction photoinitiation. Examples of irreversible biological systems studied by BioCARS users include (1) bacteriophytochromes

(regulate histidine kinase activity by light); (2) fluoroacetate dehalogenases (microbial enzymes of considerable environmental significance with the rare ability of breaking the carbon-fluorine bond, the strongest covalent bond in organic chemistry); and (3) human quinone reductase 2 (a potential molecular target for the development of cancer chemopreventive compounds for which resveratrol is a potent inhibitor).

The main limitation on studies of irreversible systems is the absence of large-area x-ray detectors with a fast frame rate, which consequently has constrained all time-resolved x-ray diffraction experiments to date to a single pump–single probe approach. This approach is particularly inefficient for irreversible reactions that require a new sample (or new sample microvolume) for each pump-probe event. For such reactions, a time-slicing detector would allow the much more efficient single pump–multiple probe approach. Following a single reaction initiation with a pump laser pulse, the reaction could be probed with a sequence of x-ray pulses. Currently available detectors, such as the photon-counting Pilatus, are not appropriate for this application due to the 1 MHz count rate limit, which is several orders of magnitude too low for Laue x-ray diffraction experiments. The proposed enhancement to the BioCARS facility includes the development and implementation of a large-area, fast-readout, analog-integrating pixel array detector (the so-called APAD) to open the new horizon of irreversible processes to the biological science community. Because this capability is also of strong interest to the physical sciences community, joint funding across agencies is anticipated.

### ***Cryo Sample Preparation Facility***

To image biological materials as closely as possible to their native state, they typically must remain hydrated to maintain structural fidelity and reflect the true location of diffusible ions. However, x-ray imaging (as well as macromolecular crystallography) also involves exposing molecules, cells, and tissues to extremely high doses of ionizing radiation. These would seem to be mutually incompatible requirements, yet a well-known solution exists: by maintaining the specimen at about 110 K or below, structural degradation due to irradiation is reduced by many orders of magnitude. Ultrafast or high-pressure freezing prevents the formation of ice crystals in suitable specimens and preserves them in vitreous ice as closely as possible to their native state. Working with cryogenic specimens requires preparing and understanding them, purposes for which the Cryo Sample Preparation Facility has been planned for APS-U.

While the damage resistance of cryospecimens is well known, only the most rudimentary cryopreparation methods have been available to the APS user community. Macromolecular crystals can be cryocooled onsite by dipping into liquid nitrogen a loop containing the crystal and a cryoprotectant liquor. The loop can then be viewed at a

resolution of several micrometers using the alignment telescope in an MX end station. In microscopy, no cryopreparation facilities have been available, and specimens have been viewed only at room temperature. This has remained the case at APS in spite of a long history of advances elsewhere in cryospecimen preparation, including high-pressure cooling to produce low-mosaicity protein crystals (Kim, Kapfer, and Gruner 2005) and well-preserved tissues (Richter 1994) and cryo-ultramicrotomy to generate sections from tissues for high-resolution analysis (Erk et al. 1998).

The Cryo Sample Preparation Facility will have wide impacts on biomedical and environmental science research at APS. Considerable effort has gone into the development of automated sample-loading robots for handling already-frozen crystals at APS, so MX beamlines are well positioned to take immediate advantage of improved crystal freezing techniques. In microscopy, the BioNanoprobes described on p. 30 will be complemented by cryospecimen capabilities planned for (1) the transmission x-ray microscope for nanotomography and (2) coherent diffraction imaging studies of cellulose crystallinity in biomass for beyond-lens-limit high spatial resolution. The Cryo Sample Preparation Facility will play an essential role in complementing these efforts by providing a full suite of capabilities including:

- Facilities for cell and tissue culture.
- High-pressure cryocooling for crystallography.
- High-pressure and plunge freezing for microscopy.
- Cryosectioning for preparation of tissues.
- Cryo-focused ion beam (cryo-FIB) for tissues and for producing isolated crystal slabs.
- Research into timed freezing of dynamic biological processes.

Because the compressed time frame of tightly scheduled competitive beamtime proposals does not favor the patient development of optimized freezing protocols, the Cryo Sample Preparation Facility also will include room-temperature and cryogenic light microscopy as well as cryo-electron microscopy. (This also will enable correlative microscopy studies of hierarchical processes.) Finally, by being located at APS or in a possibly interconnected imaging institute, the facility will benefit research in ANL's Center for Nanoscale Materials and the Electron Microscopy Center. APS in turn will benefit through interaction with researchers using similar sample preparation protocols in these other centers.

In summary, APS-U will provide enhancements to the accelerator (e.g., improved current, stability, and undulator sources) and beamlines (e.g., for imaging and time-resolved studies) that will enable APS to remain at the forefront of the life and environmental sciences. Exciting new beamline facilities being proposed by the user community are well matched to exploit the extended capabilities and capacity at APS to advance the forefront of biological science in the coming decade.

## References

- Andersson, M., et al. 2009. "Structural Dynamics of Light-Driven Proton Pumps," *Structure* **17**(9), 1265–75.
- APS, Argonne National Laboratory. 2010. "Mission Need Statement for the Advanced Photon Source Upgrade."
- Bernado, P., and M. Blackledge. 2010. "Structural Biology: Proteins in Dynamic Equilibrium," *Nature* **468**(7327), 1046–48.
- Cammarata, M., et al. 2008. "Tracking the Structural Dynamics of Proteins in Solution Using Time-Resolved Wide-Angle X-Ray Scattering," *Nature Methods* **5**(10), 881–86.
- Choa, H. S., et al. 2010. "Protein Structural Dynamics in Solution Unveiled via 100-ps Time-Resolved X-Ray Scattering," *Proceedings of the National Academy of Sciences of the United States of America* **107**, 7281–86.
- de Jonge, M. D., et al. 2008. "Quantitative Phase Imaging with a Scanning Transmission X-Ray Microscope," *Physical Review Letters* **100**(16), 163902.
- de Jonge, M. D., et al. 2010. "Quantitative 3D Elemental Microtomography of *Cyclotella meneghiniana* at 400-nm Resolution," *Proceedings of the National Academy of Sciences of the United States of America* **107**(36), 15676–80.
- de Jonge, M. D., and S. Vogt. 2010. "Hard X-Ray Fluorescence Tomography—An Emerging Tool for Structural Visualization," *Current Opinion in Structural Biology* **20**(5), 606–14.
- Erk, I., et al. 1998. "Electron Microscopy of Frozen Biological Objects: A Study Using Cryosectioning and Cryosubstitution," *Journal of Microscopy* **189**, 236–48.
- Finrock, Y. Z., et al. 2010. "Spatial Dependence and Mitigation of Radiation Damage by a Line-Focus Mini-Beam," *Acta Crystallographica, Section D: Biological Crystallography* **66**, 1287–94.
- Fischetti, R. F., et al. 2003. "High-Resolution Wide-Angle X-Ray Scattering of Protein Solutions: Effect of Beam Dose on Protein Integrity," *Journal of Synchrotron Radiation* **10**(5), 398–404.
- Fischetti, R. F., et al. 2004. "Wide-Angle X-Ray Solution Scattering as a Probe of Ligand-Induced Conformational Changes in Proteins," *Chemistry and Biology* **11**(10), 1431–43.
- Grishaev, A., et al. 2005. "Refinement of Multidomain Protein Structures by Combination of Solution Small-Angle X-Ray Scattering and NMR Data," *Journal of the American Chemical Society* **127**(47), 16621–28.
- Hegerl, R., and W. Hoppe. 1976. "Influence of Electron Noise on Three-Dimensional Image Reconstruction," *Zeitschrift für Naturforschung* **31a**, 1717–21.
- Hirai, M., et al. 2004. "Hierarchical Map of Protein Unfolding and Refolding at Thermal Equilibrium Revealed by Wide-Angle X-Ray Scattering," *Biochemistry* **43**(28), 9036–49.
- Holzner, C., et al. 2010. "Zernike Phase Contrast in Scanning Microscopy with X-Rays," *Nature Physics* **6**(11), 883–87.
- Hornberger, B., et al. 2008. "Differential Phase Contrast with a Segmented Detector in a Scanning X-Ray Microprobe," *Journal of Synchrotron Radiation* **15**(4), 355–62.
- Kaiser, A., et al. 2007. "Increase in Tracheal Investment with Beetle Size Supports Hypothesis of Oxygen Limitation on Insect Gigantism," *Proceedings of the National Academy of Sciences of the United States of America* **104**(32), 13198–203.
- Kim, C., R. Kapfer, and S. Gruner. 2005. "High-Pressure Cooling of Protein Crystals without Cryoprotectants," *Acta Crystallographica, Section D: Biological Crystallography* **61**, 881–90.
- Lee, W.-K., and J. J. Socha. 2009. "Direct Visualization of Hemolymph Flow in the Heart of a Grasshopper (*Schistocerca americana*)," *BMC Physiology* **9**(2). DOI: 10.1186/1472-6793-9-2.
- Makowski, L., et al. 2008. "Molecular Crowding Inhibits Intramolecular Breathing Motions in Proteins," *Journal of Molecular Biology* **375**(2), 529–46.
- Makowski, L. 2010. "Characterization of Proteins with Wide-Angle X-Ray Solution Scattering (WAXS)," *Journal of Structural and Functional Genomics* **11**(1), 9–19.
- Makowski, L., et al. 2011. "X-Ray Solution Scattering Studies of the Structural Diversity Intrinsic to Protein Ensembles," *Biopolymers* **95**(8), 531–42.
- Park, S., et al. 2009. "Simulated X-Ray Scattering of Protein Solutions Using Explicit-Solvent Models," *Journal of Chemical Physics* **130**(13), 134114.
- Richter, K. 1994. "High-Density Morphologies of Ice in High-Pressure Frozen Biological Specimens," *Ultramicroscopy* **53**(3), 237–49.
- Rodi, D. J., et al. 2007. "Detection of Functional Ligand-Binding Events Using Synchrotron X-Ray Scattering," *Journal of Biomolecular Screening* **12**(7), 994–98.
- Sanishvili, R., et al. 2011. "Radiation Damage in Protein Crystals Is Reduced with a Micron-Sized X-Ray Beam," *Proceedings of the National Academy of Sciences of the United States of America* **108**(15), 6127–32.
- Simon, M., et al. 2010. "Visceral-Locomotory Pistoning in Crawling Caterpillars," *Current Biology* **20**(16), 1458–63.
- Tiede, D. M., R. Zhang, and S. Seifert. 2002. "Protein Conformations Explored by Difference High-Angle Solution X-Ray Scattering: Oxidation State and Temperature Dependent Changes in Cytochrome C," *Biochemistry* **41**(21), 6605–14.
- Wang, J., et al. 2009. "Determination of Multicomponent Protein Structures in Solution Using Global Orientation and Shape Restraints," *Journal of the American Chemical Society* **131**(30), 10507–15.
- Westneat, M. W., et al. 2003. "Tracheal Respiration in Insects Visualized with Synchrotron X-Ray Imaging," *Science* **299**(5606), 558–60.
- Westneat, M. W., J. J. Socha, and W.-K. Lee. 2008. "Advances in Biological Structure, Function, and Physiology Using Synchrotron X-Ray Imaging," *Annual Review of Physiology* **70**, 119–42.
- Yang, S., et al. 2010. "Multidomain Assembled States of Hck Tyrosine Kinase in Solution," *Proceedings of the National Academy of Sciences of the United States of America* **107**, 15757–62.
- Zuo, X., et al. 2006. "X-Ray Diffraction 'Fingerprinting' of DNA Structure in Solution for Quantitative Evaluation of Molecular Dynamics Simulation," *Proceedings of the National Academy of Sciences of the United States of America* **103**(10), 3534–39.
- Zuo, X., et al. 2008. "Global Molecular Structure and Interfaces: Refining an RNA:RNA Complex Structure Using Solution X-Ray Scattering Data," *Journal of the American Chemical Society* **130**(11), 3292–93.

## Advanced Photon Source Upgrade

# Life and Environmental Science Enabled by APS-U

Life and environmental science experiments at APS range from working with macromolecules in solution or crystalline forms to studying whole cells and whole organisms. The types of current experiments and those projected for the future generally can be sorted into one of two categories: macromolecular structure determination and cell or elemental imaging. The APS Upgrade (APS-U) will provide enhanced capabilities enabling experiments in both categories that are currently challenging or even impossible to execute. APS-U will allow the probing of biological systems on a scale from several to a few thousand angstroms. This capability therefore will bridge the gap between x-ray crystallography and electron microscopy while addressing an overarching theme of APS-U: “Mastering hierarchical structures through imaging.” APS-U will provide new opportunities to investigate macromolecular structures using single-crystal diffraction with micron-size beams, a technology currently in its infancy. Addition of the micron beam facility will bridge APS-U capabilities between regular-size beams and the x-ray BioNanoprobe used to study biological systems. A large biological user community thus will be able to take advantage of this expanded portfolio of APS capabilities in their research. Future APS capabilities can be envisioned to allow the integration of macromolecular structure determination and imaging in experiments aimed at characterizing single macromolecules in dynamic biological systems.

## Next-Generation Macromolecular Structure Determination

### Current Challenges

Macromolecular x-ray crystallography has already provided structural representatives for the majority of proteins associated with key cellular processes (Marsden, Lewis, and Orengo 2007) and for numerous complexes and multicomponent assemblies such as the ribosome, RNA polymerase, nucleosome, molecular chaperones, and intact viruses (Schmeing and Ramakrishnan 2009; Wang et al. 2009; Reddy et al. 2010). Enabled by the genome sequencing revolution, next-generation sequencing is producing at unprecedented rates an order of magnitude more genome sequences that are publicly available. Not only are sequences of individual organisms being released to public databases, but so are genome sequences from entire environmental, human, animal, and microbial communities. These new sequences are predicted to provide a new wealth of knowledge and understanding about biological and macromolecular systems pertinent to human health, remediation and sustainability of the environment, bioenergy production, and carbon biomanagement.

Macromolecular x-ray crystallography is currently the most powerful method available for determining the 3D structures of macromolecules. However, significant challenges still remain for experiments aimed at increased high-throughput structure determination to capitalize on larger amounts of genome sequences as well as for studies seeking to determine structures of important macromolecular targets such as membrane proteins and macromolecular complexes. For example, some excellent progress has been made for several classes of membrane proteins such as G protein-coupled receptors (see Case 1, p. 36; Cherezov, Abola, and Stevens 2010; Rasmussen et al. 2011) transporters, and ion channels (Lunin et al. 2006). But despite these advances, new approaches and technologies are needed to elevate our understanding of membrane protein structure, interactions, and function to the same level as that for soluble proteins. Drug target discovery and structure-based drug design are other important and challenging areas, as well as altering and tuning enzyme catalytic properties and specificities for a variety of applications. The tremendously expanded genome sequence databases will provide thousands of new promising drug target candidates and potential new catalytic functions. Structural coverage of several important human drug targets in recent years is remarkable (e.g., kinases, phosphatases, and proteases). However, both the design and implementation of high-throughput experiments to accelerate structure-based drug discovery for human targets and for combating human pathogens are currently constrained by available x-ray and computational capabilities. Thus, expanded competence provided by APS-U combined with Argonne National Laboratory’s (ANL) advanced computing capabilities will provide new opportunities for critical insights in macromolecular structure and drug discovery. APS-U will enable researchers to address many new macromolecules and assemblies discovered through the integration of genomic, structural, and biological research.

### Facility Required to Address the Challenges

Obtaining quality crystals for x-ray diffraction is the most significant limitation of macromolecular crystallography (Bolanos-Garcia and Chayen 2009). Many macromolecules and complexes are very difficult to produce, and their crystals tend to be small, imperfect, and weakly diffracting. Some samples may show significant differences in crystalline order across the crystal, and the diffraction may be highly anisotropic. A mixture of static and dynamic disorder may lead to diffuse scattering, resulting in high temperature factors

and poor diffraction. If structures could be determined from initial crystallization trials that produce microcrystals, the throughput of structure determination would be accelerated and much more cost-effective. The capability to collect data from very small crystals or from multiple sites within larger crystals, together with reduced radiation damage, will provide new opportunities for experiments on membrane proteins and macromolecular complexes.

### Microfocus Macromolecular Crystallography Beamline.

Proposed for APS, the microfocus beamline will provide this capability via the use of micron-size beams. This beamline will be central to increased throughput in macromolecular structure determination and to successful data collection from projects currently considered impossible. The feasibility of using a small x-ray beam to produce high-quality data leading to crystal structure determination has been demonstrated. For example, the crystal structure of xylanase II was determined at 1.5 Å resolution with a flux of about  $3 \times 10^{10}$  photons per second and a beam size of around  $1 \mu\text{m}^2$  at the sample (Moukhametzianov et al. 2008). Also promising are preliminary data from Japan's  $1 \mu\text{m}$ -wide beamline BL32XU at SPring-8 and beamline B1-A at the Photon Factory, as well as results with diffraction from protein nanocrystals at LCLS at Stanford University (Hunter et al. 2011; Chapman et al. 2011). APS-U will provide highly brilliant, very stable, and small x-ray beams with a broad range of energies that will enable data collection from micron-size macromolecular crystals. These capabilities will allow optimization of diffraction experiments while reducing the radiation damage to samples. The revolver undulators implemented by APS-U will deliver high-brilliance beams ranging from low to high photon energies ( $>40$  keV), without gaps between the harmonics, at relatively low total power on the monochromator, which will improve thermal stability. The doubling of the beam current and the greatly increased beam stability together will provide ideal conditions for data collection from small crystals by using micron-size x-ray beams, making the APS microfocus beamline truly unique.

### Microfocus Beamline Experiments

Experiments enabled by the microfocus beamline will include structural analysis of (1) large transmembrane proteins and multicomponent assemblies or multidomain eukaryotic proteins; (2) viral particles and assemblies; (3) *in vivo* crystals and cell crystalline microcompartments as they form (e.g., viral assemblies, carboxysomes, and enterosomes); and (4) crystals only a few microns in size. The following sections describe several examples of cutting-edge areas in which a dedicated microfocus beamline will contribute to landmark scientific discovery.

### Case 1: Large Transmembrane Proteins

**G protein-coupled receptors** (GPCRs) are the largest family of signaling membrane proteins in the human genome and play a critical role in the signaling of extracellular stimuli. GPCRs have been linked to the differentiation of stem cells and tissue-specific progenitor cells during development. They also regulate numerous cellular processes and have been implicated in many human diseases. In addition, GPCRs interact with small ligands and other proteins during signaling and thus represent a class of proteins that form complexes (see Fig. A5, this page). For that reason, these proteins are highly targeted for drug development, and structure determination of the complexes they form is of high importance. However, obtaining high-quality samples of GPCRs is a significant challenge for structural studies, which have been hampered by crystals that are very small, difficult to reproduce, and poorly ordered. Recently, though, the crystallization of human membrane GPCRs in lipidic cubic phase was discovered to produce very small but highly ordered crystals. High-quality diffraction data from such microcrystals were collected for the first time (Cherezov, Abola, and Stevens 2010; Rasmussen et al. 2011) using the sub- $10 \mu\text{m}$  minibeam at the APS GM/CA-CAT (the National Institute of General Medical Sciences and National Cancer Institute Collaborative Access Team) facility. The resulting diffraction patterns had a significant reduction in background, with strong intensities and improved diffraction resolution compared with patterns from data collected using larger beam sizes, providing evidence for the utility of small beams (Cherezov, Abola, and Stevens 2010; Rasmussen et al. 2011). Structure determination of membrane proteins is recognized as a grand challenge in macromolecular structure determination, and

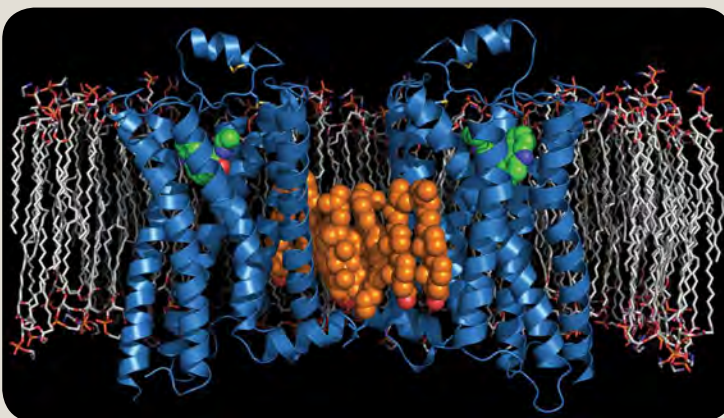


**Fig. A5. The 2.4 Å crystal structure of human  $\beta$ 2-adrenergic receptor.** The structure of the adrenaline receptor in complex with cholesterol and carazolol was obtained using the minibeam at GM/CA-CAT at APS [From Authors' Summary section in Cherezov, V., et al. 2007. "High-Resolution Crystal Structure of an Engineered Human  $\beta$ 2-Adrenergic G Protein-Coupled Receptor," *Science* **318**(5854), 1258–65. Reprinted with permission from AAAS. See also Cherezov, Abola, and Stevens 2010.]

these initial studies using the minibeam demonstrate the importance of continued development of this technology. GPCRs belong to a class of proteins that appears, at present, to principally benefit from the use of micron-size beams for data collection. In fact, the development of minibeam at APS is driven by GPCRs science, since such beams as well as technologies developed for sample handling, data collection, and processing enable structure determination of these biomedically important membrane proteins. Combining the low background of small x-ray beams with the reduction in radiation damage offered by microbeam technology may be the most important contribution to this important biomedical field. Results from these approaches indicate their great promise in enabling future studies of even larger and more complex assemblies.

**Integrins** are large, heterodimeric membrane-spanning proteins comprising the largest family of adhesion receptors that mediate eukaryotic cell-cell, cell-extracellular matrix, and cell-pathogen interactions. A large part of the receptor dimer is extracellular, but both subunits traverse the membrane and contain short cytoplasmic domains. Integrins have evolved to allow cells to sense and respond to changes in their environment. These proteins are very difficult to crystallize, and their crystals diffract poorly. A number of researchers study integrins, their domains, and various complexes. For example, in collaboration with Dr. Amin Arnaout from Harvard Medical School, researchers determined the crystal structure of the extracellular portion of integrin  $\alpha V\beta_3$ , both free and in complex with a cyclic peptide, Arg-Gly-Asp (Xiong et al. 2002; Xiong et al. 2001). Twelve integrin domains assemble into an ovoid “head” and two “tails.” The ligand binds at the major interface between the  $\alpha V$  and  $\beta_2$  subunits. These structures presented the first view of this very important molecule needed for cell signaling and provided a structural basis for the divalent cation-dependent binding of heterodimeric alpha and beta integrins to their ligands. The Springer laboratory at Harvard Medical School investigates integrins and their interactions. Integrin alpha and beta subunits form a head and two long legs in the ectodomain and span the membrane. Using a new crystal form, this lab was able to define the atomic basis for allosteric regulation of the conformation and affinity for ligand of the integrin ectodomain and determine how fibrinogen-mimetic therapeutics bind to platelet integrin  $\alpha_{IIb}\beta_3$  (Zhu et al. 2009; Zhu et al. 2008; Baram et al. 2005). Active research on integrins and their complexes will continue to present huge challenges both in crystallization and crystallography for the foreseeable future. Continued advances in our understanding of this class of poorly diffracting crystals will require a microfocus beam to reduce background scattering and thus improve the signal-to-background ratio.

### Case 2: Multicomponent Assembly

**The ribosome** is a large ribonucleoprotein assembly composed of both RNA and protein molecules. Bacterial

ribosomes consist of a large (50S) and small (30S) subunit that combine to form the 2.5 megadalton (MDa) 70S functional assembly composed of 23S RNA, 5S RNA, 16S RNA, and about 50 proteins. The eukaryotic ribosome is even larger, with a 60S large subunit and 40S small subunit forming the 80S assembly. Because of the ribosome’s universal role in protein synthesis and a difference between bacterial (pathogen) and human ribosomes, these assemblies are very important targets for developing antimicrobial agents (Schmeing and Ramakrishnan 2009). Although the molecules are very large (0.8 to 2.5 MDa), their crystals are small and diffract weakly. Recent experiments with 10 and 7  $\mu\text{m}$  beams at GM/CA-CAT beamlines showed the benefits from a very low background and high flux density, revealing the structure of the N-terminal domain of trigger factor (TF) in complex with the large ribosomal subunit from the eubacterium *Deinococcus radiodurans* (Baram et al. 2005). These results suggest that the availability of a microfocus beamline with increased stability provided by APS-U will (1) reduce background and allow for data collection from weakly scattering crystals, (2) provide the ability to locate the best part of an inhomogeneous crystal, and (3) even allow structure determination of individual components in multicomponent assemblies.

### Case 3: Bacterial Microcompartments

**Bacterial microcompartments** are new organelle-like structures discovered inside bacterial cells (Yeates, Thompson, and Bobik 2011). Genomic sequence data reveal that these microcompartments are widely distributed in many bacterial species—specifically, in over 40 genera (Kerfeld, Heinhorst, and Cannon 2010). These capsid-like protein assemblies consist of a few thousand evolutionarily related shell proteins. The microcompartments appear to enhance or provide a protective environment for key metabolic pathways inside the cell; metabolic functions include carbon dioxide fixation, degradation of small organic molecules such as propanediol and ethanolamine, and elimination of toxic metabolites. The microcompartments seem to encapsulate several sequentially acting enzymes to enhance or sequester certain metabolic pathways, particularly those involving toxic or volatile intermediates. These specialized metabolic functions may be particularly relevant to biofuel production and synthesis of specialized chemicals. The Yeates laboratory determined a number of shell protein structures (Yeates, Thompson, and Bobik 2011), and the DOE Joint Genome Institute’s Genomic Encyclopedia of Bacteria and Archaea project, funded by BER, generated several novel microcompartment-related proteins. Several structures from some new bacterial species also have been determined in collaboration with the Midwest Center for Structural Genomics. These and other crystal structures of shell proteins from distinct types of microcompartments have provided keys for understanding how the shells are assembled and how they conduct molecular transport into and out of microcompartments. The structural data show a high level of complexity and

mechanistic sophistication and direct further studies on this intriguing but poorly understood class of subcellular assemblies. The distribution and diversity of these unique structures have been underestimated because many are not formed during growth on standard laboratory media. Relatively little is known about their assembly, turnover, and molecular evolution and how these processes are achieved at the molecular level. Given the microcompartments' complexity and distinctive structure, the biochemical mechanism may be unique for this class of crystalline-like subcellular assemblies, and *in situ* studies of their structure and assembly may require a micron-size beam.

## X-Ray Fluorescence Imaging

### Current Challenges

With current developments in genomics and proteomics, our knowledge of the enormous number of pathways in which metals and trace elements are necessary for life is ever increasing. However, this knowledge is largely static because we still do not have appropriately sensitive approaches to follow the fluctuations in normal metal homeostasis that accompany the processes of, for example, development, differentiation, senescence, and stress response. Equally important is the interaction of biological systems with metals in the environment, a process that impacts the geochemistry of ecosystems as well as human health. Likewise, the elemental content of nanodevices and nanoparticles and their interfaces with cells, tissues, and whole organisms represent a major field in which hard x-ray fluorescence microscopy (XFM) imaging can play a significant role. Due to the nanoscale dimensions of these systems, a requirement for nanometer-scale resolution is implicitly necessary. For that reason alone, bionanotechnology investigators currently rely on atomic force microscopy and electron microscopy, neither of which is optimally suited for determining elemental components of either the nanomaterials used or the cells with which they interact.

From an environmental perspective, the chemical speciation of carbon greatly influences the partitioning and reactivity within its solid, liquid, and gas phases as well as its role in global climate change. Similarly, the mobility of heavy metal and radionuclide contaminants in subsurface environments is greatly influenced by the chemical speciation of the contaminants, especially their oxidation state. Predictions of future global climate change and contaminant fate and transport are highly dependent upon fundamental biochemical and biogeochemical interactions. Yet, much remains to be learned about the key processes that determine the rate and extent of cycling of these elements, particularly with regard to the coupling of biotic (microbial) and abiotic (geochemical) processes. The 3D, spatially heterogeneous microenvironment within and adjacent to actively metabolizing cell surfaces and membranes (~0.01 to 10  $\mu\text{m}$ ) can be

significantly different from ensemble averages for environments across larger spatial scales. Metabolic products can set up steep chemical gradients over very short distances. Furthermore, characteristics of the chemical gradients created at the microbe-mineral interface might differ under different biogeochemical conditions. Predicting the behavior of elements in such microenvironments is currently very challenging because the chemistry of the environments has been difficult or impossible to define. The transformations of elements in such microenvironments can affect their macroscopic fates. Therefore, information about heterogeneous biogeochemical interactions within, at, or near the microbial cell, its membrane, and the microbe-mineral microenvironment is paramount for predicting the fate of carbon and heavy metal and radionuclide contaminants. (See Case Study 3, p. 39.)

### Facilities Required to Address the Challenges

The BioNanoprobe will be designed to address the need to image, in tomographically 3D and with high resolution, the distribution and chemical status of metals and trace elements in environmental, biological, and medical samples cryopreserved to avoid radiation damage (at a resolution possibly as good as 5 nm in 10 to 15 years). Moreover, hard x-ray imaging with the BioNanoprobe II will be particularly suitable for heavier elements across the periodic table, and the addition of cryocapacity and an optical fluorescence microscope should make this instrument uniquely equipped for co-localization studies of optical fluorophores and trace elements. Development of nanoscale-resolution XFM will complement not only atomic force microscopy, transmission electron microscopy, and analytical electron microscopy, but also the existing lower-resolution XFM beamlines at APS. The BioNanoprobe II will provide the unique opportunity to study samples across numerous length scales, from nanometers to centimeters, at trace elemental sensitivity.

### BioNanoprobe Experiment Examples

A combination of unique features will make the BioNanoprobe II the first instrument of its kind and will build upon an x-ray fluorescence nanoprobe for life sciences recently funded by the NIH National Center for Research Resources; it is being installed at the Life Sciences Collaborative Access Team (sector 21) at APS. Areas of research opened by the use of XFM fall into two major categories: studies of "natural" metal and trace element distributions in health and disease and studies of distributions of metals, nanovectors, and trace elements deliberately or unintentionally introduced into organisms, cells, or the environment. Both areas are of great biological, medical, and environmental significance. The following sections describe examples of a few cutting-edge areas in which the BioNanoprobe II will provide much scientific growth and development.

### Case 1: Tomography for Metallomics

#### Imaging Cryopreserved Biological Samples in Their Natural State.

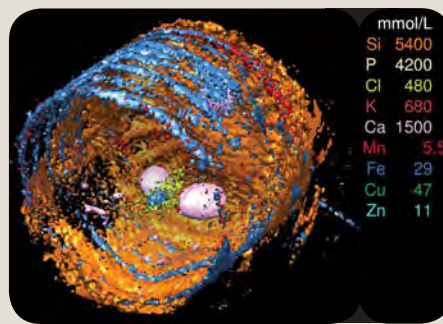
Responses to trace element concentrations in natural algae and protozoan cells suggest strong linkages among the elements. For example, when iron is a limiting nutrient, cellular concentrations of manganese and zinc are also low, and when cellular iron increases, so do cellular concentrations of the other metals. One hypothesis is that iron limitation causes a physiological cascade that affects all metals involved in cell metabolism and reproduction. Likewise, low availability of iron limits the assimilation of nitrate by diatoms (Milligan and Harrison 2000). Nanoscale maps of metal distribution within the cell coupled with other spectroscopic and microscopic techniques would allow evaluation of these hypotheses. For example, the function of manganese and iron ring distributions within the silicon frustules is not known. Capabilities expected to significantly help elucidate the role of these metal rings are (1) higher spatial resolution (e.g., to determine whether manganese or iron are embedded in the silicon frustule), (2) higher throughput with automated x-ray fluorescence tomography, and (3) phase contrast for ultrastructural visualization. These improvements thus should lead to a better understanding of key nutrients in global biomass cycling. High spatial resolution will be required to understand the role metals play on the molecular level in an organism, tomography is needed to understand the 3D arrangement of trace metals within the cell (see Fig. A6, this page), and a cryogenic specimen environment is necessary to achieve appropriate specimen preservation without artifacts.

### Case 2: Bionanotechnology

**Imaging Nanoparticles Physically and Functionally.** Recent studies using multifunctional nanocomposites of titanium dioxide (TiO<sub>2</sub>) and DNA have shown that these particles are functional inside cells and can be used both in facilitating biomedical imaging and for gene therapy by removing harmful genes from genomes (Endres et al. 2007; Paunesku et al. 2008; Paunesku et al. 2003a,b; Paunesku et al. 2007; Brown et al. 2008). Following the patterns of degradation (either engineered or “natural”) and stability or release of the nanocomposites and their constituents inside cells (Thurn et al. 2009), cells, tissues, and organisms will be critical for preclinical testing of such “nanocomposite therapies.” All these approaches require a probe with nanometer-scale spatial resolution to resolve organelles within cells and a high elemental sensitivity to detect minute amounts of nanoscale materials. At the same time, understanding the diversity of cell reactions to the introduction of these agents is crucial (e.g., to understand toxicity), including the events that occur only at low probabilities. Achieving this understanding will require the use of high-throughput approaches to survey large tissue areas.

Also at the crossroads of nanotechnology and environmental sciences are studies of nanoparticle distribution in plants. One such recent study focused on TiO<sub>2</sub> nanoparticles

**Fig. A6. Rendering of trace elements in a freshwater diatom (*Cyclotella meneghiniana*) with its dense siliceous cell wall partially (virtually) removed. The diatom was shock-frozen, freeze-dried, and then imaged with an x-ray beam focused to 270 nm. Spectra were recorded at each of 24 angles at 150 nm intervals (de Jonge et al. 2010). The ring-like distribution of iron and manganese could not have been detected by any other imaging approach. These unexpected patterns may elucidate the role of metals in diatom biology**



and the role of diatoms in oceanic element cycles. [Courtesy of Argonne National Laboratory]

as well, but, in this case, their distribution in *Arabidopsis thaliana* cells was followed by XFM (Kurepa et al. 2010). In general, plant samples require high-resolution XFM (Kim et al. 2006), particularly when elemental information on different subcellular compartments is required.

Nanoparticle development efforts are focused especially on development of multifunctional “third-generation” nanovectors made of combinations of inorganic and organic materials. Recently, an XFM microprobe was used to image TiO<sub>2</sub> nanoparticles decorated with a peptide that matches the amino acid sequence of epidermal growth factor (EGF). These nanoparticles bind to but do not activate the epidermal growth factor receptor (EGFR) signaling cascade, since the peptide used cannot induce EGFR phosphorylation. To demonstrate co-localization of nanoparticles with EGFR (to the best resolution possible with the current XFM microprobe), the intracellular membrane component of the receptor was labeled with EGFR-specific antibodies, and the cells treated with immunogold protein A. Interesting to note is that the first-ever BioNanoprobe I image (showing a cell with nanoparticles at 70 nm resolution) was obtained with the same type of sample. Co-localization of titanium and gold (albeit with a 300 nm beam spot size) suggests that there is indeed an interaction between the nanoconjugates and the EGFR (see Fig. A7, p. 40) and that patching and capping may take place even when the ligand is bound to a nanoparticle.

### Case 3. Imaging Metal Contaminants in Biological Systems

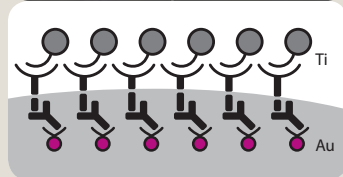
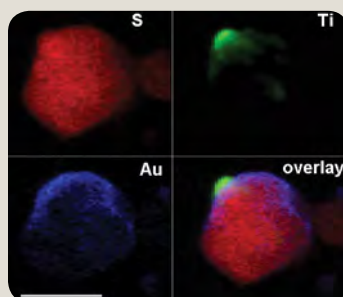
**Environmental Contaminant Transformations.** The mobility of heavy metal and radionuclide contaminants in soil and subsurface environments is greatly influenced by the chemical speciation of the contaminants, especially their oxidation state. Many general points about biochemical and biogeochemical

**Fig. A7. (Top) Elemental maps of a HeLa cell treated with nanoparticles containing titanium (Ti) and gold (Au) and a schematic of nanoparticle distribution at the cell membrane (bottom).**

Although the sulfur (S) image shows an outline of the whole cell, distribution of the protein epidermal growth factor receptor is outlined as Au signal because Au nanoparticles react with it. A peptide

bound to  $\text{TiO}_2$  nanoparticles serves as a ligand for epidermal growth factor receptor, hence Ti and Au signals largely co-localize at the cellular membrane. [Top image reprinted with permission from Yuan et al. 2011. "Interrogation of EGFR-Targeted Uptake of  $\text{TiO}_2$  Nanoconjugates by X-Ray Fluorescence Microscopy," AIP Conference Proceedings **1365**, 423–26.

©2011, American Institute of Physics.]



interactions are known, but much remains to be learned about the key processes determining the rate and extent of the cycling of these contaminants, particularly with regard to the coupling of biotic (microbial) and abiotic (geochemical) processes. The 3D, spatially heterogeneous microenvironment within and adjacent to actively metabolizing cell surfaces and membranes ( $\sim 0.01$  to  $10 \mu\text{m}$ ) can be significantly different from ensemble averages for environments across larger spatial scales (for more details, refer back to Current Challenges, p. 38, and see Fig. A8, this page). Probing the vast majority of the heavy metal and radionuclide contaminants of concern to DOE (e.g., Cs, Sr, Tc, Hg, Pb, U, and Pu) via x-ray absorption processes requires x-ray energies greater than 15 keV. The projected significant increases in incident photon flux resulting from APS-U, in conjunction with anticipated improvements in x-ray detector technologies, will enable chemical speciation measurements of elements at more environmentally relevant dilute concentrations than presently possible. The very high spatial resolution (down to 20 nm and below), combined with cryogenic sample preservation, and the corresponding minimization of radiation damage will permit localized measurement of the oxidation state of relevant heavy metals and radionuclides. That is, researchers will be able to not only determine where trace metals are located in and around a single cell, but also pinpoint their oxidation state.

**Mammalian Cells and Heavy Metals.** A key reason for diligent studies on heavy metal and radionuclide contamination is the anticipated uptake of these contaminants by humans and other species, leading to health complications that may be avoidable. In the past 60 years, interest in radioactive actinides, in particular, has passed through different phases. The difficulty

**Fig. A8. Schematic (top) and electron microscopy image of a microbe-mineral interface illustrating spatial scale and some complex interactions occurring in this microenvironment.**

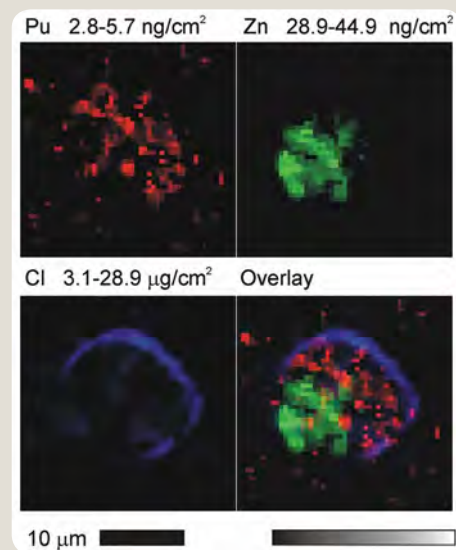
[Top image from Kemner, K. M., et al. 2005. "Synchrotron X-Ray Investigations of Mineral-Microbe-Metal Interactions," Elements **1**(4), 217–21. Bottom image from Marshall, M. J., et al. 2006. "c-Type Cytochrome-Dependent Formation of U(IV) Nanoparticles by *Shewanella oneidensis*," PLoS Biology **4**(8), e268. DOI: 10.1371/journal.pbio.

0040268. (Open-access article distributed under the Creative Commons Attribution License.)]



of handling these elements has slowed progress of this field greatly, compared to studies of many other environmental contaminants. The importance of plutonium in weapon development and its rich chemistry led to an initially prolific research thrust that eventually slowed down significantly due to the difficulties of handling and the resulting safety issues. Although, for example, plutonium is known to accumulate in the liver and bones of mammals, the chemical form of plutonium present *in vivo* and the identities of biomolecules that associate with this element in mammals are primarily conjectural. Therefore, a group of ANL actinide chemists led by Lynne Soderholm and Mark Jensen has focused on investigating the accumulation of plutonium by mammalian cells, with the goal of uncovering which chemical form of plutonium is found in cells and which macromolecules associate with it. The group's method of choice was x-ray fluorescence, as it is the only approach that allows mapping of plutonium in cells. To identify its oxidation state, which is a critical determinant of the elemental chemistry, micro-x-ray absorption near-edge spectroscopy ( $\mu$ -XANES) was done as well (see Fig. A9, p. 41; Gorman-Lewis et al. 2011). This work documented that plutonium offered to the cells in different oxidation states and chemical forms does not have the same capacity for intracellular accumulation. The XANES spectra of the intracellular plutonium deposits were always consistent with a single valence state of plutonium. This surprising finding forms

**Fig. A9. Three-element co-localization maps of a cell incubated with plutonium.** Microprobe x-ray absorption near-edge spectroscopy was used to determine directly, for the first time, the oxidation state of intracellular plutonium in individual  $0.1 \mu\text{m}^2$  areas within single rat pheochromocytoma cells (PC12). These maps of a PC12 cell show the accumulation of plutonium



in the cytoplasm (outlined as the area with chlorine signal). [From Gorman-Lewis, D., et al. 2011. "Direct Determination of the Intracellular Oxidation State of Plutonium," *Inorganic Chemistry* **50**(16), 7591–97. Copyright 2011 American Chemical Society. See also Jensen et al. 2011.]

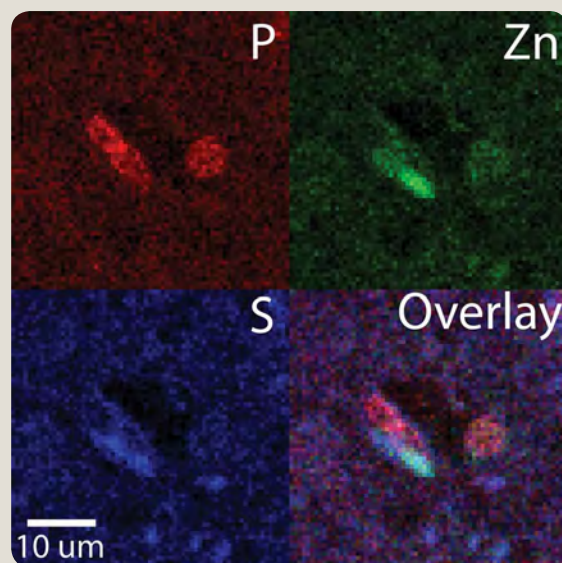


**Fig. A10. A neurofibrillary tangle in a brain sample from a patient with Alzheimer's disease.** Phosphorus (red), sulfur (blue), and zinc (green) elemental distribution maps are shown. [Courtesy of E. Bigio, T. Paunesku, M. Mishra, and G. Woloschak (Northwestern University Feinberg School of Medicine) and S. Vogt, B. Lai, and J. Maser (ANL).]

a basis for an upcoming interrogation of archival lung tissues containing plutonium in different chemical (and physical or particulate) forms. These archival tissues were collected through the concerted efforts of several national laboratories and institutes investigating the effects of plutonium uptake on animal models. A conglomeration of all such existing tissues has been stored in an archive at Northwestern University; efforts to complete this collection were funded by DOE BER over the past 5 years.

## The Future: APS Capabilities Enable Integrated Molecular and Whole-Cell Studies of Cellular Dynamics

A concept underlying biological and biochemical studies today is that macromolecular interactions govern both cell and organism fate. From coping with DNA-damaging stresses to cognition, it is molecular interactions that regulate how an impulse will be detected and what its effects will be for the whole organism. The overwhelming complexity of these interactions lies at the core of all the problems faced by life scientists. Conversely, any technique that brings us closer to a systematic understanding of these interactions advances biology, medicine, and environmental science further toward those insights for which every science strives. On one end of the spectra of experimental possibilities lie approaches geared to isolate multiple copies of single macromolecules or macromolecular complexes; on the other are techniques focused on context-dependent changes in macromolecules

as they perform their functions *in situ*, in different subcellular compartments, in different cell types, and in tissues and organs of different organisms. At present, most of these approaches look at multiple copies of macromolecules. Few techniques carried out in biological systems can boast of single-molecule sensitivity, yet a number of synchrotron-dependent techniques could reach that goal with the boosted sensitivity and resolution resulting from synchrotron modifications possible now or in the very near future. Moreover, by reaching toward single-molecule resolution, these (now disparate) techniques arrive at the same destination—visualization of individual interactions between macromolecules and the downstream molecular effects of these interactions. The Microfocus Macromolecular Crystallography beamline and BioNanoprobe II represent two techniques that could reach such a common ground.

**Neuropathology and Neurodevelopmental Abnormalities.** Studies of metal accumulation in brains of patients with Alzheimer's, Parkinson's, and other diseases and in the spinal cords of patients with Lou Gehrig's disease (amyotrophic lateral sclerosis) have already demonstrated that some metals are associated with disease progression and possibly disease onset (Campbell et al. 2001). Nevertheless, the precise cellular and subcellular locations—and in some cases even the regional brain locations—of these metals are not known. For instance, an important contribution to understanding the pathogenesis of Alzheimer's disease (AD) would be defining the precise locations of copper or zinc in plaques, tangles, (see Fig. A10, this page), nontangle-bearing neurons, and synapses in AD brain

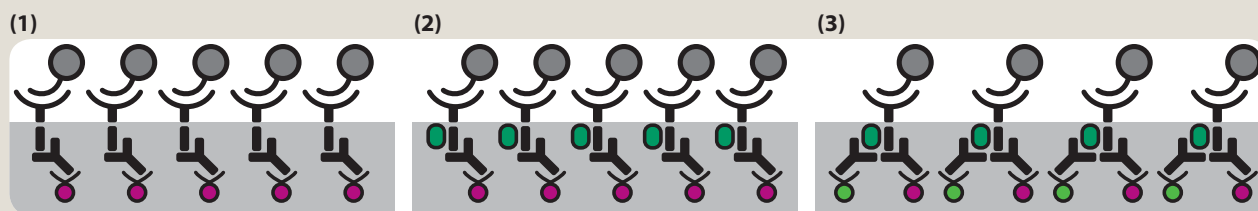


**Fig. A11. Schematic representation of possible influence of nanoconjugate interaction with EGFR on further interactions of EGFR with GPCRs (green oval).** (1) The lack of EGFR phosphorylation and possible change of conformation due to nanoconjugate binding may preclude EGFR interaction with GPCR. (2) Conversely, GPCR binding may be impervious to nanoparticle binding. (3) If the latter is the case, nanoparticles of yet another makeup can be used to immunolabel the GPCR for imaging at the BioNanoprobe II, or the diffraction patterns can be observed at the microfocus beamline. [Courtesy of Woloschak laboratory, Northwestern University (credit revised April 2012)]

tissue by imaging with the hard x-ray BioNanoprobe II. At the same time, such studies could lead to the development of new diagnostic procedures, particularly when complemented by protein fingerprinting using Fourier transform infrared (FT-IR) spectroscopy or microdiffraction *in situ*. The nanometer-scale resolution possible with the hard x-ray BioNanoprobe II will be particularly useful for investigating changes at the synapse level, since synapses are less than 1  $\mu\text{m}$  in size. Although, the decrease in synapses has, for some time, been known to be the major correlate with the cognitive decline observed in AD (Terry et al. 1991), the sequence of events leading to this decline remains unclear. Notably, the microfocus beamline—in keeping with the “proteins to organisms” theme—engages in studies of the same proteins and reaches toward sensitivity and resolution required for *in situ* analysis of complex protein and protein-membrane assemblies. This and many other examples of complementary work at other APS-U beamlines will enable deeper understanding of results in each of these studies.

**Cell Signaling Research: Investigating EGFR-GPCR Dynamics.** Another example of a cellular systems project that provides an interesting overlap of BioNanoprobe II imaging capabilities with the science anticipated to be done at the microfocus beamline is shown in Fig. A7, p. 40. HeLa cancer cells were exposed to  $\text{TiO}_2$  nanoparticles conjugated with a peptide that matches the amino acid sequence of epidermal growth factor. These nanoparticles were shown to co-localize and interact with the EGF receptor. Currently, it is not known if this interaction further includes interactions between EGFR and G protein-coupled receptors. GPCRs are

key research areas of the microfocus beamline, and a large family of GPCRs has been reported to transactivate EGFR via both ligand-dependent and -independent mechanisms (Thomas et al. 2006). Therefore, combined studies at the BioNanoprobe II and microfocusing beamline may include, for example, investigation on whether EGFR molecules bound to the nanoconjugate mimics still undergo transactivation by GPCRs or if such transactivation requires the receptor be free from its ligand. While these studies may be done on one level using “classical” molecular biology approaches such as Western blots, upgraded APS facilities would enable qualitatively different scientific investigation. Indeed, the ability to acquire and compare complementary data on the EGFR-GPCR protein “complex” through its co-localization (from BioNanoprobe II) and diffraction (from the microfocus beamline) may provide new paradigms in cell-signaling research (see Fig. A11, this page).

Coupling the imaging and spectroscopy capabilities proposed for APS-U with existing capabilities will allow us to address scientific questions that cannot be addressed elsewhere. Specifically, in 15 years, the use of these nanoprobe will enable high-resolution 2D and 3D imaging of the spatial distribution of elements within hydrated or frozen regions in, at, or near the microbial cell, its membrane, and the microbe-mineral microenvironment via tomographic reconstruction. Similarly, coupling x-ray absorption spectroscopy measurements with these nanoscopy measurements is envisioned to enable the imaging of the chemical speciation of elements in these critical regions.

## References

- Baram, D., et al. 2005. "Structure of Trigger Factor Binding Domain in Biologically Homologous Complex with Eubacterial Ribosome Reveals its Chaperone Action," *Proceedings of the National Academy of Sciences of the United States of America* **102**(34), 12017–22.
- Bolanos-Garcia, V. M., and N. E. Chayen. 2009. "New Directions in Conventional Methods of Protein Crystallization," *Progress in Biophysics and Molecular Biology* **101**(1–3), 3–12.
- Brown, E., et al. 2008. "Methods for Assessing DNA Hybridization of Peptide Nucleic Acid–Titanium Dioxide Nanoconjugates," *Analytical Biochemistry* **383**(2), 226–32.
- Campbell, A., et al. 2001. "Mechanisms by which Metals Promote Events Connected to Neurodegenerative Diseases," *Brain Research Bulletin* **55**(2), 125–22.
- Chapman, H. N., et al. 2011. "Femtosecond X-Ray Protein Nanocrystallography," *Nature* **470**(7332), 73–77.
- Cherezov, V., E. Abola, and R. C. Stevens. 2010. "Recent Progress in the Structure Determination of GPCRs, a Membrane Protein Family with High Potential as Pharmaceutical Targets," pp. 141–68. In *Membrane Protein Structure Determination: Methods and Protocols*, the Methods in Molecular Biology series, **654**.
- Cherezov, V., et al. 2007. "High-Resolution Crystal Structure of an Engineered Human  $\beta_2$ -Adrenergic G Protein–Coupled Receptor," *Science* **318**(5854), 1258–65.
- de Jonge, M. D., et al. 2010. "Quantitative 3D Elemental Microtomography of *Cyclotella meneghiniana* at 400-nm Resolution," *Proceedings of the National Academy of Sciences of the United States of America* **107**(36), 15676–80.
- Endres, P. J., et al. 2007. "DNA-TiO<sub>2</sub> Nanoconjugates Labeled with Magnetic Resonance Contrast Agents," *Journal of the American Chemical Society* **129**(51), 15760–61.
- Gorman-Lewis, D., et al. 2011. "Direct Determination of the Intracellular Oxidation State of Plutonium," *Inorganic Chemistry* **50**(16), 7591–97.
- Hunter, M. S., et al. 2011. "X-Ray Diffraction from Membrane Protein Nanocrystals," *Biophysical Journal* **100**(1), 198–206.
- Jensen, M. P., et al. 2011. "An Iron-Dependent and Transferrin-Mediated Cellular Uptake Pathway for Plutonium," *Nature Chemical Biology* **7**, 560–65.
- Kemner, K. M., et al. 2005. "Synchrotron X-Ray Investigations of Mineral-Microbe-Metal Interactions," *Elements* **1**(4), 217–21.
- Kerfeld, C. A., S. Heinhorst, and G. C. Cannon. 2010. "Bacterial Microcompartments," *Annual Review of Microbiology* **64**(1), 391–408.
- Kim, S. A., et al. 2006. "Localization of Iron in *Arabidopsis* Seed Requires the Vacuolar Membrane Transporter VIT1," *Science* **314**(5803), 1295–98.
- Kurepa, J., et al. 2010. "Uptake and Distribution of Ultrasmall Anatase TiO<sub>2</sub> Alizarin Red S Nanoconjugates in *Arabidopsis thaliana*," *Nano Letters* **10**(7), 2296–302.
- Lunin, V. V., et al. 2006. "Crystal Structure of the CorA Mg<sup>2+</sup> Transporter," *Nature* **440**(7085), 833–37.
- Marsden, R. L., T. A. Lewis, and C. A. Orengo. 2007. "Towards a Comprehensive Structural Coverage of Completed Genomes: A Structural Genomics Viewpoint," *BMC Bioinformatics* **8**(86). DOI:10.1186/1471-2105-8-86.
- Marshall, M. J., et al. 2006. "c-Type Cytochrome-Dependent Formation of U(IV) Nanoparticles by *Shewanella oneidensis*," *PLoS Biology* **4**(8), e268. DOI: 10.1371/journal.pbio.0040268.
- Milligan, A. J., and P. J. Harrison. 2000. "Effects of Non-Steady-State Iron Limitation on Nitrogen Assimilatory Enzymes in the Marine Diatom *Thalassiosira weissflogii* (Bacillariophyceae)," *Journal of Phycology* **36**(1), 78–86.
- Moukhametzianov, R., et al. 2008. "Protein Crystallography with a Micrometre-Sized Synchrotron-Radiation Beam," *Acta Crystallographica, Section D: Biological Crystallography* **64**(2), 158–66.
- Paunesku, T., et al. 2003a. "Biology of TiO<sub>2</sub>–Oligonucleotide Nanocomposites," *Nature Materials* **2**(5), 343–46.
- Paunesku, T., et al. 2003b. "Intracellular Localization of Titanium Dioxide–Biomolecule Nanocomposites," *Journal de Physique IV* **104**, 317–19.
- Paunesku, T., et al. 2007. "Intracellular Distribution of TiO<sub>2</sub>–DNA Oligonucleotide Nanoconjugates Directed to Nucleolus and Mitochondria Indicates Sequence Specificity," *Nano Letters* **7**(3), 596–601.
- Paunesku, T., et al. 2008. "Gadolinium-Conjugated TiO<sub>2</sub>–DNA Oligonucleotide Nanoconjugates Show Prolonged Intracellular Retention Period and T1-Weighted Contrast Enhancement in Magnetic Resonance Images," *Nanomedicine* **4**(3), 201–07.
- Rasmussen, S. G., et al. 2011. "Structure of a Nanobody-Stabilized Active State of the  $\beta_2$  Adrenoceptor," *Nature* **469**(7329), 175–80.
- Reddy, V. S., et al. 2010. "Crystal Structure of Human Adenovirus at 3.5 Å Resolution," *Science* **329**(5995), 1071–75.
- Schmeing, T. M., and V. Ramakrishnan. 2009. "What Recent Ribosome Structures Have Revealed about the Mechanism of Translation," *Nature* **461**, 1234–42.
- Terry, R. D., et al. 1991. "Physical Basis of Cognitive Alterations in Alzheimer's Disease: Synapse Loss is the Major Correlate of Cognitive Impairment," *Annals of Neurology* **30**(4), 572–80.
- Thomas, S. M., et al. 2006. "Cross-Talk Between G Protein–Coupled Receptor and Epidermal Growth Factor Receptor Signaling Pathways Contributes to Growth and Invasion of Head and Neck Squamous Cell Carcinoma," *Cancer Research* **66**(24), 11831–39.
- Thurn, K. T., et al. 2009. "Labeling TiO<sub>2</sub> Nanoparticles with Dyes for Optical Fluorescence Microscopy and Determination of TiO<sub>2</sub>–DNA Nanoconjugate Stability," *Small* **5**(11), 1318–25.
- Wang, D., et al. 2009. "Structural Basis of Transcription: Backtracked RNA Polymerase II at 3.4 Angstrom Resolution," *Science* **324**(5931), 1203–06.
- Xiong, J.-P., et al. 2001. "Crystal Structure of the Extracellular Segment of Integrin  $\alpha V\beta_3$ ," *Science* **294**(5541), 339–45.
- Xiong, J.-P., et al. 2002. "Crystal Structure of the Extracellular Segment of Integrin  $\alpha V\beta_3$  in Complex with an Arg-Gly-Asp Ligand," *Science* **296**(5565), 151–55.
- Yeates, T. O., M. C. Thompson, and T. A. Bobik. 2011. "The Protein Shells of Bacterial Microcompartment Organelles," *Current Opinion in Structural Biology* **21**(2), 223–31.

Zhu, J., et al. 2008. “Structure of a Complete Integrin Ectodomain in a Physiologic Resting State and Activation and Deactivation by Applied Forces,” *Molecular Cell* **32**(6), 849–61.

Zhu, J., et al. 2009. “The Structure of a Receptor with Two Associating Transmembrane Domains on the Cell Surface: Integrin  $\alpha_{11b}\beta_3$ ,” *Molecular Cell* **34**(2), 234–49.

## Linac Coherent Light Source

# Facilities, Operations, and Future Perspective of LCLS-I and LCLS-II\*



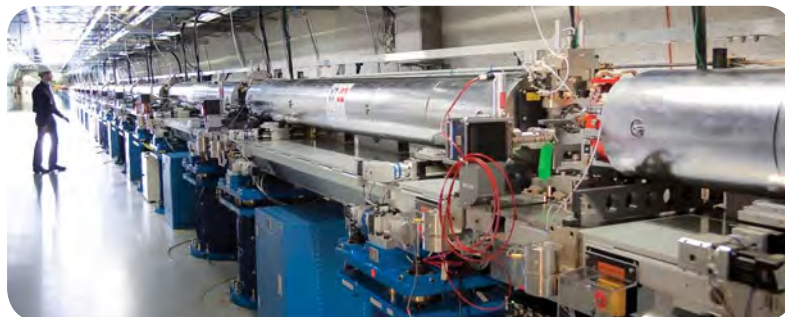
## Introduction and Overview

The Linac Coherent Light Source (LCLS) is the world's first operational x-ray free-electron laser (XFEL). Over the last 5 years, the construction of LCLS—supported by the Office of Basic Energy Sciences (BES) within the U.S. Department of Energy (DOE)—and its transition to full operations, which started with user-assisted commissioning in late 2009, have been accomplished. A vigorous user program is already well established. Four of the six instruments planned for LCLS-I are operational or in commissioning, and the complete facility will be finished in FY 2012. At this point, DOE will have invested ~\$500M in construction and supports the LCLS operations with an annual budget in excess of \$100M. LCLS also has played a key role in the transformation of the SLAC National Accelerator Laboratory from a predominantly high-energy physics laboratory to a true multiprogram laboratory with strong core capabilities in x-ray facilities and related enabling cutting-edge science.

Today LCLS, together with SLAC's third-generation synchrotron, SPEAR3 at the Stanford Synchrotron Radiation Lightsource (SSRL), is the basis for SLAC's current and future plans for growth and delivery of new science and user capabilities enabled by x-rays for understanding the structure and function of materials on the atomic and nanoscale levels. A suite of LCLS and SSRL instruments provides the capabilities for research at SLAC to span a range of dimensions (from microns to subnanometer) and time (from milliseconds to femtoseconds). LCLS is the key, new revolutionary element, opening up research opportunities in areas that include the emerging fields of ultrafast x-ray science, structural dynamics on the fastest time scales, imaging of nanocrystalline and nonperiodic materials at or near atomic resolution, and creation and study of new states of matter heretofore inaccessible.

There is significant potential for future applications of LCLS in the biosciences, including areas of mission relevance to DOE's Office of Biological and Environmental Research (BER). The first part of Appendix B, the Facility Paper, is one of two LCLS documents that have been prepared for the BER panel assessing the future potential of new DOE Office of Science scientific user facilities. It focuses on LCLS-I

\*SLAC National Accelerator Laboratory prepared this and a companion document (p. 53) and approved post-workshop revisions to each.



[Courtesy of SLAC National Accelerator Laboratory]

and its capabilities and on the expansion of LCLS (LCLS-II) that already is approved by BES and is in advanced stages of conceptual design. The companion document, beginning on p. 53, discusses the scientific case and potential of LCLS-I and LCLS-II as related to the biosciences and BER mission objectives.

## Brief History of LCLS

LCLS was conceived in 1992 by Claudio Pellegrini of the University of California–Los Angeles; over the years, design studies were carried out at SSRL under the leadership of Pellegrini, Herman Winick, and Max Cornacchia. Following completion of the scientific case, documented in the report *LCLS: The First Experiments* ([www-ssrl.slac.stanford.edu/lcls/papers/lcls\\_experiments\\_2.pdf](http://www-ssrl.slac.stanford.edu/lcls/papers/lcls_experiments_2.pdf)) and a presentation to the Basic Energy Sciences Advisory Committee (BESAC) in October 2000, the LCLS project was awarded CD0 (critical decision 0) status in 2001. After breaking ground in 2006, the accelerator part was completed by early 2009. First light was observed on April 10, 2009, and, after only 2 hours, hard x-ray lasing and saturation were observed at 8 kiloelectron volts (keV). Immediately thereafter, LCLS demonstrated reliable operations so rapidly that by August, the first instrument built for Atomic, Molecular, and Optical (AMO) Science was commissioned. By early October, users were gathering their first data during “user-assisted commissioning,” much earlier than projected and well before CD4, which was officially achieved in April 2010. Early involvement of users during the stepwise commissioning of the first three instruments proved so successful that it is being implemented on all the remaining LCLS instruments, with the last one scheduled to begin operation in early 2012. LCLS presently operates in the 480 to 10,000 electron volt region. SLAC's goal is to retain a leadership position of LCLS through strategic investments and innovative developments in accelerator, x-ray, and laser technologies and science, with a long-range plan that has the next step being LCLS-II (2018 completion) on the way to a vision for the facility that extends to 2025.

## LCLS Science

In contrast to storage ring–based light sources, LCLS offers extreme peak brightness and full transverse coherence in its ultrashort x-ray pulses, brightness sufficient to capture a signature (diffraction or absorption/emission pattern) of electronic bonding or atomic structure in a single shot. This enables production of time-resolved rather than time-averaged information on the subpicosecond time scale. More specifically, LCLS x-ray pulses down to less than 10 femtoseconds (fs) are more than a factor of 1,000 shorter than those from storage ring–based x-ray sources, while containing about  $10^{12}$  photons per pulse at 8 keV (more than four orders of magnitude higher than any other x-ray source). Such pulses allow the observation of phenomena on the fundamental length and time scale of the motion of atoms and the associated charge and spin distributions.

Breakthrough discoveries are expected in understanding the structure and function of materials on the atomic and nanoscale levels, as LCLS x-ray laser beams will, for the first time, enable the simultaneous investigation of their electronic and structural properties on the size (subnanometer) and time (femtosecond) scales that determine their function. LCLS experiments will reveal the speed limits enforced by nature that, in spite of the best human ingenuity, impose absolute constraints on technological advances (e.g., those that occur in the switching of magnetization bits required for magnetic recording of data). The experiments will provide the opportunity to understand and ultimately control chemical processes, such as those central to the process of photosynthesis, which supplies our world with oxygen, or the catalytic reactions that underlie conversion of raw materials for energy production. LCLS will enable determination of key reaction intermediates in chemical pathways that influence the environment and climate, as well as the structure of countless biological systems not accessible to current imaging techniques.

Over its spectral range, LCLS offers almost fully spatially coherent x-rays instead of the small fraction offered at storage-ring sources. While the largely incoherent or “disordered” x-ray beams of the latter sources require “ordered” samples, as exemplified by the need for crystals in protein crystallography, the coherent or ordered x-rays from LCLS can be used to determine the structure of disordered samples and nonperiodic materials, including biological materials, glasses, and liquids. Early experience with LCLS has demonstrated that it has met and exceeded all its performance goals; no other research facility in the world currently offers comparable capabilities. The stage is set for subsequent breakthroughs across a range of scientific disciplines.

## LCLS-I Accelerator, Operations, Instruments, and Users

### The LCLS Accelerator

LCLS currently uses the last one-third of the 3 km–long SLAC linear accelerator, or linac, operating at 2,856 MHz (s-band) radio frequency (RF) fields. A perspective of LCLS is shown in Fig. B1, p. 47. The facility has been designed to allow future expansion, with use of the entire linac and up to eight undulators and separate x-ray beamlines. The LCLS-II project will take advantage of these capabilities.

To create LCLS, the last one-third of the linac was modified to include a new high-brightness photocathode electron injector, followed in the main linac by two magnetic bunch compressor chicanes that increase the peak current of the electron beam in stages through magnetic electron beam compression as the beam is accelerated along the linac. The new injector utilizes a copper photocathode illuminated by ultraviolet (UV) light from a frequency-tripled pulse from an amplified Ti:Sapphire laser system to produce an extremely bright electron beam in a single bunch at a rate of up to 120 Hz. Each bunch has a typical charge of ~250 picocoulombs (pC). For ultrashort x-ray bunch production, the charge can be made as short as ~20 pC in which the compressors operate more effectively with lower space-charge effects, allowing the production of shorter pulses. In fact, the pulse length can be readily varied between these values as user experiments dictate.

The pair of new bunch compressors shortens the electron bunch and thereby magnifies the peak current from the injector by a factor of ~100. The high peak current is required to efficiently generate x-rays in the undulator and saturate at the shortest x-ray wavelengths. The electron bunch length is measured using a transverse RF s-band deflecting cavity, which works like a femtosecond-resolution streak camera for electrons and is capable of resolving bunch lengths as short as 25 fs full width at half maximum (FWHM). A special “laser heater,” the first of its kind in a linac-based free-electron laser (FEL), is located in the injector at 135 MeV. This adds a small level of energy spread to the electron beam to damp a microbunching instability before it potentially breaks up the high-brightness electron beam.

Many beam-stabilizing feedback loops are in operation, with RF- and beam-based loops. The most critical loop uses linac RF phases and voltage levels to control the energy and bunch length after each compressor. The bunch length measurements are based on coherent edge radiation from the last dipole magnet of each compressor chicane, and this critical loop stabilizes the final peak current at any selected value. Because the x-ray pulse length is similar to the electron bunch length, the closed-loop control allows the operator to simply enter the user-requested pulse length into the computer.

## The LCLS Undulator and Photon Source

At the end of the linac, a new 350 m-long transport line was built to deliver the 3.5 to 15 GeV compressed electron beam to the undulator located in a tightly climate controlled underground tunnel (with  $<1^\circ\text{C}$  variations) shown in the upper right of Fig. B1, this page. The LCLS undulator system is 132 m long, including breaks for quadrupole focusing magnets, resulting in 112 m of active undulator. It is composed of 33 planar, permanent-magnet (neodymium iron boron) undulator segments 3.4 m long with a period of 3 cm, full gap height of 6.8 mm (fixed), and undulator magnetic deflection parameter  $K = 3.5$  (corresponding to a peak magnetic field of 1.25 T). The undulators and focusing magnets are mounted on cam-based submicrometer controlled horizontal and vertical translation stages to allow beam-based alignment. A 5 by 12 mm<sup>2</sup> quasirectangular vacuum chamber within each segment has a highly polished aluminum surface to minimize electron beam interactions. Located at each of the 33 breaks are a focusing quadrupole magnet, a cavity-type electron beam position monitor (BPM), an insertable alignment and beam-size monitoring wire, and a flexible vacuum bellows. To maintain spatial overlap and relative phasing with the x-rays, the electron beam

trajectory along the 132 m-long undulator is required to be absolutely straight at the level of  $\sim 5 \mu\text{m}$  rms over an FEL gain length of  $\sim 4 \text{ m}$  [at 1.5 angstroms ( $\text{\AA}$ )]. Beam-based alignment requires a few hours and is repeated every 2 to 3 weeks as necessary to maintain FEL power.

The Front End Enclosure (FEE) contains a range of monitors and diagnostics, including pulse-energy detectors that rely on absorption of x-rays in low-pressure nitrogen gas. The downstream half of the FEE is occupied by an x-ray beam switchyard based on grazing incidence mirrors. In addition to directing the FEL beam to various experimental stations, the mirrors serve as low-pass filters that separate the FEL radiation from higher-energy spontaneous undulator radiation and the Bremsstrahlung background radiation. Two mirror systems are used: a soft x-ray mirror system with the reflectivity cutoff at 2 keV and a hard x-ray mirror system with the cutoff at 25 keV. Moving the first soft x-ray mirror into the beam directs it to one of two soft x-ray experimental stations. Moving the first soft x-ray mirror out of the beam allows it to intercept two hard x-ray mirrors arranged in a periscope geometry and thence to several hard x-ray experimental stations. The soft x-ray mirrors are coated with boron carbide and the hard x-ray

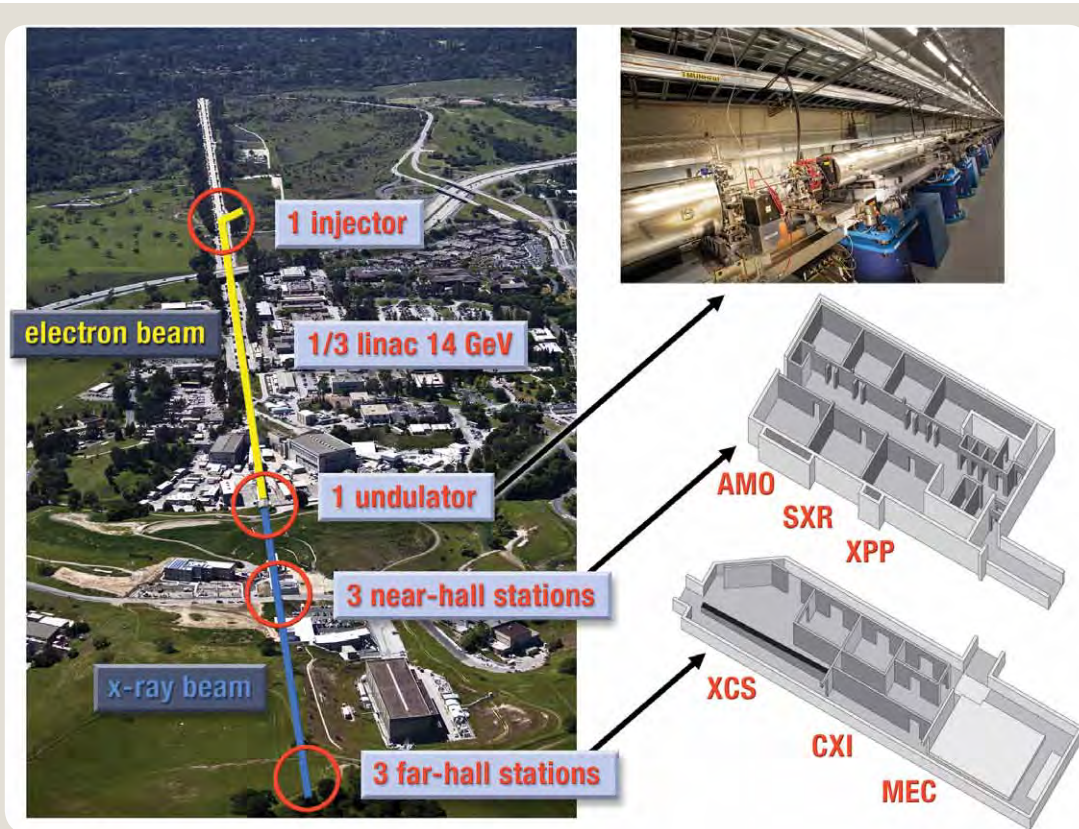


**Fig. B1.** (Left) Overview of LCLS showing the locations of the injector, linac, underground undulator hall, and the near and far experimental halls. (Right, top) Undulator hall looking toward the linac. (Right, bottom) Schematic showing locations of the six instruments described later in the text—AMO, SXR, and XPP (near hall) and XCS, CXI, and MEC (far hall). [Courtesy of SLAC National Accelerator Laboratory]

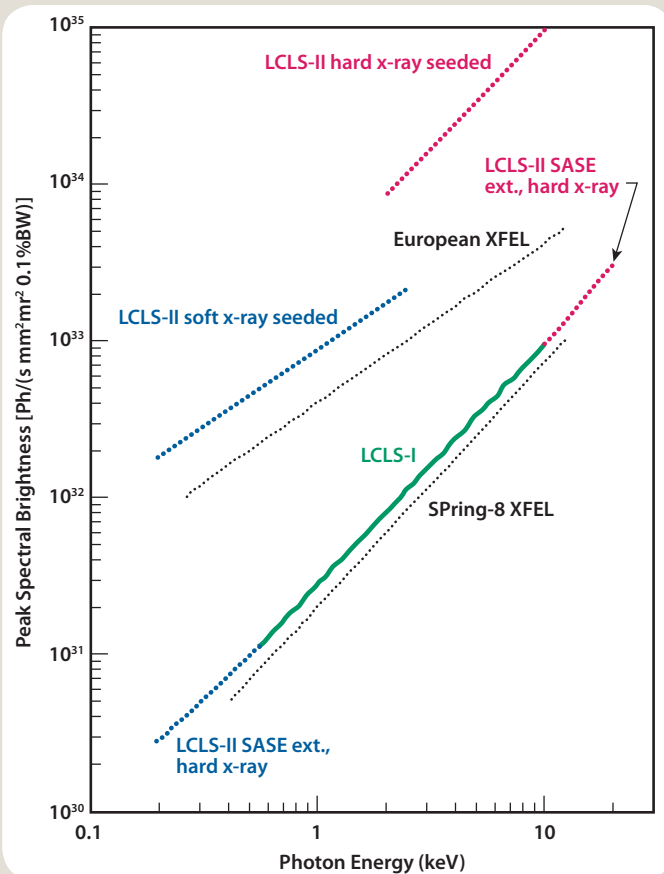


**Fig. B2. Peak brightness of LCLS-I and LCLS-II radiation sources in comparison with other XFELs in construction or commissioning.** Dotted colored lines are estimates for LCLS-II based on electron beam parameters already achieved. Gray dotted lines represent future facilities, and solid lines are based on measurements. [Courtesy of SLAC National Accelerator Laboratory]

mirrors with silicon carbide. The mirrors were polished to extreme flatness to preserve the coherent x-ray FEL wavefront.

The peak brightness curves for LCLS-I are shown in Fig. B2, this page. For comparison, the figure includes the expected performance of the European XFEL (operation planned for 2016) and the Japanese XFEL facility SACLA, which is located adjacent to the SPring-8 synchrotron source. Likewise, the projected brightness performance for LCLS-II is shown. Not shown are peak brightness curves from a typical undulator on a third-generation synchrotron source. The peak brightness from such sources is in the  $10^{20}$  to  $10^{22}$  range on this scale.

## LCLS Instruments

As previously noted (see also Fig. B1, p. 47), the initial-phase LCLS scientific user facility includes six instruments. Five of these instruments are now in regular user-scheduled operation; the remaining one is in the installation phase and is anticipated to be operational during FY 2012. Each instrument is supported by a team led by two staff scientists.

Currently, the instruments operate in a serial mode, but techniques for beam sharing in the hard x-ray region are being developed, in particular large offset monochromators equipped with a thin Bragg crystal that transmits part of the x-ray beam. Space limitations in this document allow only a brief overview of each instrument, but more detail is provided for three instruments that have or potentially will have more biological applications. Detailed optical configuration, operational parameters, and other information for all six instruments can be found online: [slacportal.slac.stanford.edu/sites/lcls\\_public/instruments/Pages/default.aspx](http://slacportal.slac.stanford.edu/sites/lcls_public/instruments/Pages/default.aspx).

## Atomic, Molecular, and Optical (AMO) Science Instrument – in operation

The AMO instrument is located on one of the soft x-ray branches of LCLS and delivers soft x-rays (480 to 2,000 eV). Instrumentation is designed to minimize losses and deliver the maximum possible soft x-ray intensity (up to 1,013 photons per pulse) to the interaction region. The AMO instrument can be configured with a variety of sampling systems and detectors. Gaseous targets of atoms, molecules, clusters, and other nanoscale objects such as protein crystals or viruses typically are used in the AMO instrument. Electrons and ions are detected with a variety of time-of-flight and imaging spectrometers. Large charged-coupled device (CCD) area detectors sensitive to x-rays are used for x-ray diffraction measurements. Science performed with the AMO instrumentation includes fundamental studies of light-matter interactions in the extreme x-ray intensity and high fields of the LCLS FEL beam; time-resolved photoionization; x-ray diffraction of nanocrystals; and single-shot,

nanometer-resolution imaging of nonreproducible objects. A minimal set of optics is used to preserve the high peak brightness and deliver the LCLS beam to the target in the AMO instrument. Three soft x-ray offset mirrors direct the beam to the soft x-ray branches, and two planar, elliptically bent Kirkpatrick-Baez mirrors are used to focus the beam to  $\sim 1 \mu\text{m}$  in the first interaction region within the high-field physics chamber. The mirrors can be bent to various radii, allowing the focus to be moved along the beam or the size of the beam in the interaction region to be varied as desired by the experiment. At the more downstream interaction region in either the “CAMP chamber” or the “Diagnostics chamber,” focal spot sizes of  $\sim 3$  to  $5 \mu\text{m}$  can be achieved. [Note that the Center for Free-Electron Laser Science (CFEL) Advanced Study Group Multipurpose Chamber (CAMP) was provided by a consortium of German institutions.] A high-power, synchronized Ti:Sapphire optical laser is available for all experiments using the AMO instrument, and a variety of wavelengths can be provided. Typically, an 800 nm beam is delivered to the AMO hutch,

with wavelength conversion carried out in the hutch with doubling and tripling crystals for shorter wavelengths and an optical parametric amplifier (OPA) for longer wavelengths. Additional lasers have been installed in the hutch (e.g., a Nd:YAG laser) for specific experiments.

### **Soft X-Ray Materials Science (SXR) – in operation**

The SXR instrument was designed and built by a consortium of institutions in collaboration with LCLS. Located in the near experimental hall, SXR provides intense, ultrashort soft x-ray LCLS pulses. The instrument provides for a highly diverse set of experimental configurations using established and powerful tools such as x-ray emission, coherent imaging, resonant scattering, photoelectron spectroscopy, and x-ray absorption spectroscopy. The science that can be performed at the SXR beamline covers widespread fields such as catalysis, astrophysics, magnetism, correlated materials, clusters, and biological structure at lower resolution. The instrument is equipped with a monochromator whose energy range (500 to 2,000 eV) covers several of the important *K* and *L* edges of the second- and third-row elements for resonant excitation with a resolving power on the order of 4,000. Consortium members and various collaborators can roll up and connect different end stations and detectors to the instrument for the experimental program. These capabilities are also available to general users.

### **X-Ray Pump Probe (XPP) – in operation**

The XPP instrument is located in Hutch 3 of the near experimental hall and is designed for pump-probe experiments. In these studies, a synchronized fast optical laser (Ti:Sapphire) is used to generate transient states of matter, and the hard x-ray pulses from LCLS (4 to 25 keV using first and third undulator harmonics) are used to probe the structural dynamics initiated by the laser excitation. The x-ray scattering and emission are detected via a custom area detector designed to operate at a repetition rate of 120 Hz and capable of integrating thousands of photons per pixel in a single shot. The instrument design emphasizes versatility. To maximize the range of phenomena that can be excited, manipulating the laser pulse energy, frequency, and temporal profile is possible. X-ray scattering is the dominant tool for probing the laser-induced structural changes. These experiments require the union of four experimental capacities: generation and delivery of x-ray and laser pulses to the sample, preparation of the excited state in the sample, and detection of the x-ray scattering pattern. Scientific objectives include the study of biological, chemical, and physical processes that involve the time-dependent transformation of matter on the atomic scale. Examples of these processes with technological and environmental significance are photosynthetic generation of chemical energy, catalytic production of fertilizer, chemical degradation of pollutants, and melting of ice. These structural transformations involve the motion of electrons, atoms, and molecules over very short distances ( $10^{-9}$  m) and time scales ( $10^{-12}$  s). Though much has been learned about these dynamical processes

from previous work, particularly studies using optical lasers, no existing technology can provide direct observation of atomic motions on ultrafast time scales.

### **Coherent X-Ray Imaging Instrument (CXI) – in operation**

The CXI instrument is located in the far experimental hall and is designed to deliver hard x-ray pulses from LCLS (4 to 10 keV fundamental and up to 25 keV using higher harmonics) for diffraction and imaging experiments with submicron periodic and nonperiodic materials. The transverse coherence of LCLS allows single nanoscale particles to be imaged at high resolution, while the short pulse duration will limit radiation damage during the measurement through an approach often referred to as “diffract and destroy.” Maximum per-pulse fluxes delivered by the CXI instrument are in the range of  $10^{11}$  to  $10^{12}$  photons per pulse, and pulse lengths are as short as ~5 to 80 fs. Samples can be inserted into the beam using several means, including those fixed on substrates or free-standing particles injected into the beam. High-quality focusing optics will generate three foci: ~100 nm, 1 to 2  $\mu$ m, and 10  $\mu$ m. The two smallest focal spot sizes are achieved using Kirkpatrick-Baez mirror systems with the highest-achievable surface quality to preserve the LCLS wavefront.

Two complete end stations, capable of operating in series and including vacuum sample chambers and sample delivery systems, exist at the CXI instrument. These end stations contain custom-made pixel array detectors known as CS-PADs (Cornell SLAC Pixel Array Detectors). Each CS-PAD contains 1,520 by 1,520 pixels of 110  $\mu$ m pitch that are individually read out at 120 Hz, allowing each shot of LCLS to be measured and stored independently. Each pixel contains the electronics necessary to convert the analog photon signal created in its sensor to a digital signal, which is suitable for transmission to the data acquisition system. This design enables researchers to change the behavior, specifically the dynamic range and sensitivity, on a pixel-by-pixel basis. In the so-called low-gain mode, each pixel has a dynamic range corresponding to almost  $10^4$  at a photon energy of 8 keV; while in the high-gain mode, the dynamic range is  $10^3$  and a single photon event can be detected with a >3 signal-to-noise ratio. The design of each end station allows multiple, identical copies of reproducible objects to be sequentially illuminated by the LCLS beam. With each sample oriented randomly, the high data rate and single-shot readout of the detector are critical to building the complete, three-dimensional (3D) set of diffracted intensities required for any structural determination.

One objective of the bioscience experiments on the CXI instrument is to allow imaging of biological samples beyond the damage limit that cannot be overcome with synchrotron sources. The first CXI user experiments performed in February 2011 demonstrated the unique capabilities of the instrument with great success. In particular, during a period of roughly 1 week, protein nanocrystals were injected into the LCLS x-ray beam, resulting in the unambiguous observation

of Bragg peaks up to better than 3 Å in all cases and better than 2 Å in some cases. Promisingly, in these latter cases the resolution was primarily limited by the clear aperture of the sample injector that can be removed in future experiments, potentially increasing the resolution of the final structure even further. This experiment collected over 120 terabytes (TB) of data, highlighting the challenges in data processing and analysis at LCLS. These experiments benefit from the highest x-ray intensities achievable; that is, the greatest number of photons per unit area per unit time, with pulses ideally about 10 fs in duration. LCLS-II will increase the intensities achievable for such experiments.

### ***X-Ray Correlation Spectroscopy (XCS) – in operation***

The XCS instrument is located in Hutch 4 of the LCLS far experimental hall, about 420 m away from the source. Characteristic time scales ranging from 10 milliseconds (ms) to thousands of seconds can be explored using a sequential mode of operation. Ultrafast time scales ranging from ~100 fs to several nanoseconds can be probed using a novel “split and delay” mode of operation. The unprecedented brilliance and narrow pulse duration of LCLS provide a unique opportunity to observe dynamical changes of large groups of atoms in condensed matter systems over a wide range of time scales using coherent x-ray scattering in general and x-ray photon correlation spectroscopy (XPCS) in particular. The XCS instrument will allow the study of equilibrium and nonequilibrium dynamics in disordered or modulated materials.

### ***Matter in Extreme Conditions (MEC) – in installation, operation in 2012***

The MEC instrument also is located in the far experimental hall. It is designed to combine the unique LCLS x-ray beam with high-power optical lasers to create and study unique phases of matter under extreme conditions. In particular, states of matter that have solid density but temperatures ranging from a couple to hundreds of electron volts, with corresponding pressures of multiple megabars, will be studied. The main body of MEC users will come from the research disciplines studying warm dense-matter physics, high-pressure physics, shock physics, and high-energy density science. The MEC instrument will include a suite of dedicated diagnostics tailored for these fields of science, including an x-ray Thomson scattering spectrometer, an extreme ultraviolet (XUV) spectrometer, a Fourier domain interferometer, and a velocity interferometer system for any reflector (VISAR). All diagnostics will be located in a large vacuum target chamber, making the end station very versatile for any investigation of laser-pumped matter that needs a vacuum.

## ***LCLS Early Operations Phase***

For many years, it has been recognized that the “interaction” between the XFEL user and “the machine” would be different, more interactive for free-electron laser facilities compared with synchrotron radiation storage ring–based facilities. Just how different it turned out to be may not have been fully appreciated. During the design of LCLS, emphasis was placed on creating a facility capable of maximum single-shot brightness. During commissioning, emphasis was placed on early achievement of well-defined performance goals with stability and reliability. Early attainment of these goals opened the door to exploration of other flexibilities. From its inception, the science community and the LCLS machine designers knew that the baseline wavelength range, 800 eV to 8 keV, could be extended if the electron beam quality was good enough. LCLS now routinely operates at energies from 480 eV (below the oxygen *K* edge) up to 10 keV. Recently, the high energy limit has been further extended with the installation of a section of undulators that are tuned to the second harmonic (“afterburner”). This second harmonic afterburner (SHAB) provides up to 10% of the first harmonic pulse energy at photon energies up to 18 keV.

The most welcome surprise to LCLS users has been the easy adjustability of pulse length and the availability of <10 fs pulses based on the “low-charge” mode of operation mentioned earlier. Options for producing very short LCLS x-ray pulses were developed and tested from 2006 to 2008 while LCLS construction was under way. Implementation for user experiments began in late 2009. LCLS can now deliver pulse lengths for soft x-rays from below 10 fs up to 500 fs, and for hard x-rays from below 10 fs to 100 fs. The users immediately took advantage of this capability in the very first experiments. LCLS today runs much more like a “laser in the lab,” where experimenters vary photon wavelength, per-pulse energy, and pulse duration—not on an experiment-by-experiment but on a shift or even hourly basis—as they explore the new potential and scientific possibilities that LCLS provides. As the LCLS science program is now showing, a stable and reliable wavelength reach is only one ingredient of success. Experimenters also need full control of the photon beam and the ability to vary all parameters in the course of a single experiment to understand the time scale of the dynamical processes they study or else to ascertain that they are measuring “static” properties unperturbed by the LCLS x-ray pulse itself. Real-time flexibility to change parameters has been critical to the success of the first LCLS experiments. This is clearly a paradigm shift for the design of LCLS upgrades and future facilities.

## ***LCLS User Program***

LCLS management works very closely with the LCLS Scientific Advisory Committee (SAC), LCLS Proposal Review Panel (PRP), and the LCLS Users’ Executive Committee (UEC) to develop a fair and transparent external peer-review process

for beam-time proposals and user access. LCLS proposal review and ranking are carried out by the PRP, which includes over 50 international experts grouped into seven subpanels: Atomic, Molecular, Optical, and Cluster Physics; Biology and Life Sciences; Chemistry; Materials—Hard Condensed Matter; Materials—Soft Condensed Matter; High Energy Density Science/Matter in Extreme Conditions; and Methods and Instrumentation. The work of the PRP for each run begins shortly after each call for proposals is closed and generally ends with an onsite meeting at SLAC twice per year, approximately 3 months after the proposal deadline, where a ranking of the proposals is provided. LCLS management and staff help to facilitate the review process but are not involved in the review and ranking. A description of the proposal review process can be found on the LCLS website ([www-ssrl.slac.stanford.edu/lcls/users/proposals.html](http://www-ssrl.slac.stanford.edu/lcls/users/proposals.html)).

Interest in using LCLS has been steadily increasing, with 427 proposals submitted to date. The LCLS scientific community is forming larger teams of collaborators than typically seen with experiments at synchrotron facilities. Some 1,100 different scientists are currently affiliated with these proposals, which have been received from 200 institutions in more than 20 countries. Of the 427 proposals submitted through the end of 2010, 87 have been scheduled. In addition, ~20% of the proposals submitted thus far are classified in the general area of structural biology or biosciences. Given the excitement in the community about the first published LCLS experiments on nanocrystals and large viruses (Chapman et al. 2011; Seibert et al. 2011), this percentage conceivably could grow substantially in the future.

## LCLS-II

Given the rapid commissioning and operation of LCLS-I, SLAC and DOE recognized the need to immediately begin planning for the future. The expansion of LCLS (the LCLS-II project) is hence already under way, and, given adequate and timely funding, completion is anticipated by 2018. DOE has provided CD0 (statement of mission need), and the DOE CD1 Lehman Review was held at SLAC in April 2011. The outcome was the recommendation to DOE for approval of CD1 for the LCLS-II project. Over the last 2 years, key advances and developments have led to the recognition that the capabilities and capacity of LCLS can be significantly improved, further enabling new scientific breakthroughs. The recognition of the capability gap between what exists and what is possible is due partly to the remarkable performance of LCLS, which has already far exceeded its design goals. The landscape has changed through (1) the demonstration of the self-amplified spontaneous emission (SASE) lasing process at the highest envisioned energy of 8 keV, (2) the reduced length of undulators needed because of the high quality and brightness of the electron beam, and (3) the operational stability and reliability of the SLAC linac in the >95% range, comparable to storage-ring sources.

LCLS-II will build on a reliable platform for future improvements and proceed with the construction of a second electron beam source, which will independently serve another undulator x-ray source. Variable gap undulators will be constructed to extend the photon energy range and control, and novel concepts like short undulator “afterburners” for energy extension, pulse control, and polarization control will be implemented. In addition, photon seeding techniques to produce x-ray beams with increased peak brightness that are completely longitudinally coherent will be pursued. The existence of more than one undulator x-ray source will offer the opportunity to combine two beams for two-color pump-probe studies of excited states. Such pump-probe studies are furthermore extended by use of high-field THz radiation to trigger chemical reactions and promote materials into new transient states. These concepts form the basis of LCLS-II, which also addresses the looming reality of insufficient capacity and limited capability of LCLS to accommodate the fast-growing number of users excited by the early success of LCLS. From the beginning, LCLS conventional facilities were designed to support rapid extension of their capabilities and capacity, and LCLS-II leverages this design to remain at the international forefront even as new facilities around the world are completed.

LCLS-II is also a natural next step in a larger DOE Office of Science photon science strategy that involves a suite of world-class complementary facilities and tools covering the x-ray energy spectrum with diverse timing capabilities. LCLS-II complements existing facilities—such as the Advanced Light Source, Advanced Photon Source (APS), National Synchrotron Light Source (NSLS), and SSRL—and planned facilities (APS-U and NSLS-II) based on storage rings by opening up the combined domain of ultrasmall and ultrafast. LCLS-II leverages the early LCLS success into continued U.S. leadership.

A limitation of LCLS is its limited user access, determined by the availability of only a single linac beam and one fixed-gap undulator source that can supply x-rays at a repetition rate of 120 Hz to only one of six experimental stations at a time. LCLS-II will overcome this roadblock by the creation of two independent linac beams of different and independent properties. The high-energy electron beam from one injector will be used to create hard x-rays by means of two in-series undulators, with the second one acting as a second harmonic afterburner that creates x-rays at twice the energy. By using semitransparent monochromator crystals to create offset x-ray beams, two LCLS hard x-ray instruments can be served simultaneously with monochromatic x-rays. The transmitted beam is not monochromatized and serves the other two hard x-ray instruments with a broader bandpass and higher power beam. This way, three of the four hard x-ray stations can operate simultaneously. The lower-energy beam from the second injector is converted by two independent undulators into two soft x-ray beams with independently tunable energies and slightly offset paths. These beams serve the two LCLS soft x-ray stations independently and simultaneously.

In summary, it will become possible to supply five of the six experimental stations simultaneously with 120 Hz x-ray pulses. This capacity increase of LCLS-II by a factor of 5 transforms the character of LCLS, initially scoped to be a facility with revolutionary capabilities serving a small number of specialized users, toward a higher-capacity general user facility.

The current spectral range of LCLS is limited to around 480 to 10,000 eV, and LCLS does not allow rapid energy tuning and full control of pulse properties such as intensity, length, and polarization. The present capabilities limit the scientific exploration of several important problems. Based on the initial performance of LCLS, we now have the confidence to overcome these limitations. Realistically, the hard x-ray limit can now be extended from 10 up to 20 keV in the fundamental (up to 24 keV in harmonics) and the soft x-ray limit from 480 eV down to 200 eV. LCLS-II will provide any desired polarization state of light—linear, circular, or elliptical instead of a single linear polarization state. This is accomplished by adding special short undulators (of order 5 m) that maintain the order within the electron bunch but redirect its motion. LCLS-II will provide the capability to control the pulse length and longitudinal coherence by “self seeding” (i.e., by monochromatizing radiation from a first SASE undulator and reinserting it superimposed on the electron bunch in a second undulator). The predicted peak brightness of LCLS-II with this seeding scheme is illustrated in Fig. B2, p. 48, in comparison with LCLS-I and the projected brightness of XFELs under construction. In the soft x-ray range, other seeding schemes also will be explored, such as Enhanced Echo Harmonic Generation (EEHG). The envisioned LCLS-II time scale with consecutive improvement steps between 2012 and 2017 overlaps international XFEL developments in Europe and Japan and constitutes a measured U.S. response to the international competition. It assures international competitiveness of the U.S. x-ray program beyond 2015.

To summarize, in the baseline scope LCLS-II is being planned to provide the following capabilities:

- Two independent injectors using two linac sections (14 GeV each).
- One fixed-gap hard x-ray undulator with seeding option (2 to 20 keV).
- One variable-gap hard x-ray SASE undulator (2 to 13 keV).
- One variable soft x-ray SASE undulator (200 to 2 keV).
- Six experimental stations, up to four operating simultaneously.

In addition, upgrades to the LCLS-II baseline scope that require nonproject funding include:

- High-field THz sources for novel pump-probe experiments.
- Rapid tuning ability of x-ray energy and polarization delivered by the soft x-ray undulator sources.
- Option of seeded soft and hard x-rays with improved pulse control and transform-limited pulses.

LCLS-II capitalizes on the remarkable early success of LCLS, the excitement and engagement of the international scientific user community, and the strong demand for additional capabilities. LCLS-II utilizes the existing infrastructure of SLAC and presents a measured response to international competition. SSRL upgrades and developments support its excellent user program in targeted areas and will further align this program with the science directions of LCLS (especially time-resolved studies), the SLAC-specific parts of U.S. energy initiatives, and the larger West Coast light source strategy. The synergistic SSRL and LCLS strategy couples the spatial and temporal regimes and helps optimize the limited availability of LCLS beam time to the collective benefit of the scientific user community.

## References

- Chapman, H. N., et al. 2011. “Femtosecond X-Ray Protein Nanocrystallography,” *Nature* **470**, 73–77.
- Seibert, M. M., et al. 2011. “Single Mimivirus Particles Intercepted and Imaged with an X-Ray Laser,” *Nature* **470**, 78–81.

## Linac Coherent Light Source

### LCLS: Impacts and Future Potential in Biology

LCLS is the world's first operational x-ray free-electron laser (the machine and instruments are described in the Facility Paper of this appendix, p. 45). This revolutionary x-ray light source, funded and operated by the DOE Office of Basic Energy Sciences, has significant discovery potential for biology that is only now just beginning to be realized with researcher access to instruments for experiments. The first section of this Science Paper describes recent experiments, opportunities, and challenges for nanocrystallography at LCLS and their likely impacts in biology. The second and third sections (p. 56 and p. 57) present two representative time-resolved experiments on macromolecules made possible by LCLS. In the fourth section (p. 58), the first imaging experiments of single particles at LCLS are discussed followed by a description in the fifth section of the prospects for correlated scattering experiments on macromolecules (p. 59). Taken together, these few selected projects (out of many other LCLS proposals) demonstrate the potentially large impact of x-ray free-electron light sources in biology. We are indebted to the individual project leaders for supplying information about their projects.

### Nanocrystallography and Mitigating Radiation Damage

#### LCLS Experiments with Photosystem I Nanocrystals

**Project Leaders:** Henry Chapman, Deutsches Elektronen Synchrotron (DESY), Hamburg, Germany; Petra Fromme and John Spence, Arizona State University; and many collaborators

Recent experiments with photosystem I (PS I) nanocrystals demonstrate that LCLS opens up exciting new possibilities in macromolecular crystallography, especially for crystals that are too small for synchrotron beamlines. Radiation damage is what limits structure determination at high resolution. For example, x-rays may ionize the sample and cause it to degrade. By using LCLS femtosecond pulses, many more photons can be delivered onto the sample than is possible with conventional light sources, thus providing strong diffraction patterns in a very short time. In the process, the crystal completely vaporizes in a plasma but only after the x-ray pulse has already passed through the sample if the pulse is short enough (the atoms have mass, and their inertia keeps them in place longer than the flash of x-rays takes to generate the diffraction pattern). There are about  $10^{12-13}$  photons in a single femtosecond LCLS pulse (depending on photon energy), which is enough to obtain diffraction patterns from much smaller crystals than those needed for synchrotron studies in a single LCLS shot.

Diffraction images have been obtained from PS I crystals of only 6 unit cells across ( $a = b = 281 \text{ \AA}$ ,  $c = 165 \text{ \AA}$ ), initially at relatively low resolution (see Fig. B3, this page; Chapman et al. 2011). In the most recent LCLS experiments on PS I, carried out at the CXI beamline using  $1.3 \text{ \AA}$  wavelength x-rays with a 40 fs pulse width, diffraction was observed to  $3 \text{ \AA}$  resolution (see the accompanying LCLS Facility Paper, p. 49, for a description of the CXI beamline and detector). Since the sample is completely destroyed in a single shot, the x-ray beam must be replenished constantly with new crystals. One approach carries the crystals in a liquid and then flows that suspension in a jet across the x-ray beam. However, to minimize absorption and background and ensure the crystals are targeted to the  $3 \text{ \mu m}$ -diam x-ray beam, the jet also must be of similar dimensions. Making such small-diameter water beams is a challenging problem and is even harder with crystals in solution, which can cause small nozzles to clog. As a first solution to this problem, DePonte and colleagues (DePonte et al. 2008) developed a liquid jet-injection method consisting of a coaxial gas flow to focus the water

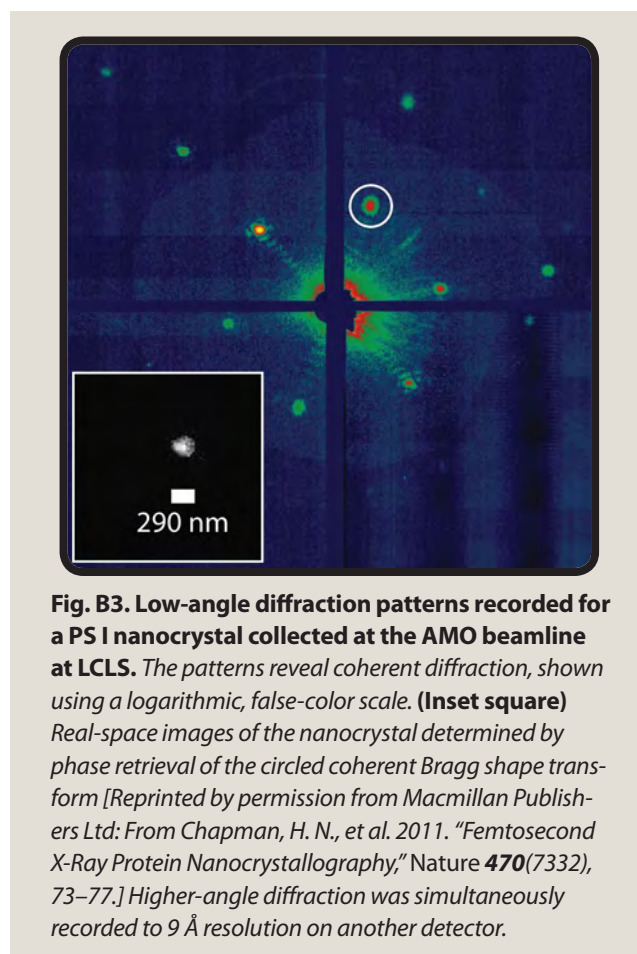


**Fig. B3. Low-angle diffraction patterns recorded for a PS I nanocrystal collected at the AMO beamline at LCLS.** The patterns reveal coherent diffraction, shown using a logarithmic, false-color scale. (Inset square) Real-space images of the nanocrystal determined by phase retrieval of the circled coherent Bragg shape transform [Reprinted by permission from Macmillan Publishers Ltd: From Chapman, H. N., et al. 2011. "Femtosecond X-Ray Protein Nanocrystallography," *Nature* **470**(7332), 73–77.] Higher-angle diffraction was simultaneously recorded to  $9 \text{ \AA}$  resolution on another detector.

into a narrow jet, an approach demonstrated to work well with LCLS experiments.

One way to think of a nanocrystal experiment is like powder diffraction measured one crystallite at a time. However, unlike in powder diffraction, the patterns from every single crystal can be indexed, oriented, and then merged into a dataset of three-dimensional (3D) structure factors. These data are roughly equivalent to those obtained by rotating a single crystal in a conventional monochromatic synchrotron beam. This approach was demonstrated for data collected on PS I at the AMO beamline at LCLS in June 2010, resulting in 15,000 usable diffraction patterns (out of about 1.5 million images) at a resolution of  $\sim 9$  Å. Upon indexing each individual pattern, the partial intensities were summed for each Bragg index. On average, each structure factor in the entire 3D dataset was observed in about 1,000 patterns. Accordingly, the sum of all these partial intensities is related to an average over all the random orientations and different shapes and sizes of crystals. Just as a powder ring gives an accurate measure of a structure factor (if it is well separated from other rings), these summed partial intensities give potentially similarly accurate measurements for each Bragg peak. Refinement of the PS I structure against the merged LCLS diffraction data produced electron density maps at  $\sim 9$  Å resolution. These maps were comparable to diffraction data (truncated to 9 Å resolution) collected at the Advanced Light Source at Lawrence Berkeley National Laboratory (Chapman et al. 2011).

## Key Opportunities and Challenges for Nanocrystallography

The PS I LCLS studies (Chapman et al. 2011) and more recent experiments carried out by Boutet, Chapman, Fromme, Schlichting, and collaborators demonstrate the feasibility of nanocrystallography experiments. These experiments also indicate a number of potential advantages of this method (compared to conventional synchrotron-based data collection) that could transform structural studies in biology. Advantages include:

- Diffraction data can be acquired from crystals too small or too radiation-sensitive for meaningful collection of diffraction data at synchrotron beamlines.
- Crystals that are very mosaic when grown to micron size might be significantly less mosaic when grown to a size of a few hundred nanometers, potentially producing higher-quality and higher-resolution diffraction patterns.
- Crystal diffraction is measured at room temperature rather than cryogenic temperatures. Furthermore, the crystals can be studied in their crystallization buffer without having to add cryoprotectants.
- Mixing experiments can be performed to flow samples under different conditions into the x-ray beam.
- The method can be used for time-resolved measurements ( $\sim 100$  fs) for the study of optically triggered reactions.

- The method might enable low-resolution phasing based on oversampling the diffraction pattern (e.g., Spence and collaborators, Arizona State University).

Despite these advances, many challenges need to be addressed to make nanocrystallography useful for the most difficult problems in biology (see below for a particular example). These challenges provide rich opportunities for research and development (R&D) at LCLS, with strong connection to the facilities and R&D activities within the Structural Molecular Biology program at SSRL. Furthermore, LCLS is establishing general user facilities for such studies, again resting on the rich tradition and strong expertise at SSRL.

**Characterization of Nanocrystals.** If crystals are too small to allow visualization in a standard optical microscope, other techniques must be developed to characterize such crystals. SSRL Structural Molecular Biology beamline 4-2 now enables automatic collection of small-angle x-ray diffraction patterns of a large number of samples. The appearance of a pseudopowder diffraction pattern can be used as an indicator for the presence of small crystals in the solution. Such an approach could include the exploration of lipidic cubic phase matrices to correlate precipitant, protein, and lipidic phases in sample holders that contain a large number of individual samples to identify protocols that provide the best crystallization conditions. This approach could be coupled with optical spectroscopy measurements to characterize the samples.

**Experimental Phasing.** An adaptation of multiwavelength anomalous dispersion (MAD)/single-wavelength anomalous dispersion (SAD) methods conceivably can be applied to the high-intensity regime of femtosecond LCLS experiments at different wavelengths. Based on a nonrelativistic Hartree-Fock-Slater method, the fluence-dependent scattering factors of heavy elements have been computed (Chapman and collaborators). Despite the extensive (and varied) electronic reconfiguration of these elements that occurs during intense x-ray LCLS pulses, existing MAD/SAD phasing algorithms can be applied to the analysis of MAD/SAD LCLS diffraction data. Furthermore, the high intensity can increase the anomalous signals, and the “bleaching” of scattering factors potentially may provide useful information (e.g., radiation damage-induced phasing, or “RIP”). However, a major challenge will be posed by the relatively small anomalous and dispersive signals from such MAD/SAD experiments. Since “inverse beam” or crystal alignment approaches will not be possible, this method might be restricted to relatively strong anomalous scatterers, such as those in the lanthanide series. Exploratory experiments are planned to assess this question by Chapman (DESY) in collaboration with the Weis and Brunger groups at Stanford University.

**Sample Delivery.** The current sample requirements for a liquid jet-injection system must be reduced. For example, in the nanocrystal experiment on PS I (Chapman et al.

2011), the liquid jet injector was operated for 17 hours at 10 microliters ( $\mu\text{L}$ ) per minute (equaling 10 mL of solution utilized). The overall protein concentration was 1 mg/mL, so the total sample requirement was 10 mg of nanocrystals. For this experiment, LCLS operated at 30 Hz; thus at 120 Hz (currently used at LCLS), the sample requirement would have been  $\sim 2.5$  mg of nanocrystals. Still, this is a large amount of sample, especially for the difficult cases of large protein complexes or membrane proteins. Currently, most of the suspension flows past the beam without ever being exposed to x-rays. The volume of liquid that interacts with a single pulse is about  $4^3$  microns, 120 times per second, or  $5 \times 10^{-4}$   $\mu\text{L}$  per minute. Thus, only about  $5 \times 10^{-5}$  of the suspension is utilized. This wasteful situation could be improved by pulsing the jet, although efforts to do so have produced larger-sized drops that give higher background. Alternatively, by recirculating the suspension, more of the crystals would have a chance to be hit by the LCLS x-ray pulses, which will slowly deplete the suspension of crystals. Furthermore, Spence and collaborators are developing mixing jets, consisting of double-bored capillaries.

As crystal sizes get smaller, the scattering from the fluid medium becomes an increasingly important source of noise. The requirement for a jet with submicron diameters has been demonstrated (DePonte et al. 2008). Another method is to aerosolize the crystals and introduce them to the beam through an aerodynamic lens stack. Used to image virus particles, this method recently has achieved high hit rates by redesigning the gas flow (see *Nonperiodic Imaging of Biological Particles*, p. 58).

Sample delivery by liquid jets will not be easy for membrane protein crystals grown in lipidic cubic phases. Thus, other sample-delivery systems must be developed by using, for example, chip-based technologies that allow automated rapid translation between individual crystals. All these sample delivery systems are areas of opportunity for R&D at LCLS and could leverage similar ongoing R&D at SSRL.

**Single-Crystal Data Analysis.** The nanocrystallography data-reduction method used for PS I employed a relatively straightforward scheme consisting of autoindexing each suitable diffraction pattern individually and then summing the resulting partial reflections for each individual Bragg index. Numerical calculations showed that summing such “random sampling” of partial Bragg intensities eventually converges to the full Bragg intensity (Kirian et al. 2010). However, there is a practical issue in space groups with an inherent indexing ambiguity, giving rise to a “pseudo-twinned” dataset when using the simple summation method of individually indexed diffraction patterns. A potentially more serious problem arises when summing partial intensities from many individual crystals because the absorption properties of the individual crystals might vary. Use of “pink” pulses versus monochromatic pulses would enable collection of at least some fully recorded Bragg

intensities for each diffraction pattern, enabling so-called postrefinement schemes to resolve the indexing ambiguity and to allow scaling between different diffraction patterns. Such a method makes use of several decades of experience in multocrystal data collection. Changes to the way LCLS generates x-rays (utilizing energy-chirping of the electron beam) can produce a somewhat broader bandwidth. Research and development in this area are ongoing at LCLS. (It also is important for spectroscopy applications.)

## Example of a Difficult System: Mediator Complex

**Project Leaders:** Roger Kornberg and David Bushnell, Stanford University

This project exemplifies an important biological system that thus far has eluded structure determination by x-ray crystallography with synchrotron light sources. This representative example shows the difficulties encountered on other systems by many leading research groups worldwide. It also illustrates the potentially transformative impact that LCLS will have in biology by enabling the imaging of systems that are out of reach with current methods.

The ultimate goal of transcription research is an understanding of transcription control. In the case of bacteria and bacteriophage, this goal has been largely achieved. Transcriptional repressor and activator proteins, responsive to environmental stimuli, bind to DNA sequences adjacent to promoters and directly affect RNA polymerase. Repressors prevent polymerase binding to the promoter, while activators contact polymerase and increase its affinity for the promoter or stimulate the transition from a closed to an open polymerase-promoter complex (i.e., formation of a “transcription bubble” in which the DNA double helix is melted to facilitate the initiation of transcription).

The central components of the transcription machinery are the same in bacteria and eukaryotic cells. The RNA polymerases share a conserved core and common transcription mechanism. Initiation factors—sigma in bacteria and a set of general transcription factors (GTFs) in eukaryotes—are more distantly related but function similarly in promoter recognition, promoter melting, abortive initiation, and promoter escape. Where bacterial and eukaryotic systems truly diverge is in the targets of regulatory proteins. In contrast with the direct targeting of RNA polymerase in bacteria, there are intermediary factors in eukaryotes: chromatin and Mediator. The chromatin of eukaryotes, based on a histone octamer enveloped by DNA, and Mediator, a giant multiprotein complex, have no counterparts in bacteria. They represent a new layer interposed between regulatory proteins and RNA polymerase. This layer must account for the far greater complexity of regulation in eukaryotes and the consequent capacity for cell differentiation and development.

With a reconstituted transcription assay as a guide, Mediator was first purified to homogeneity in the yeast *Saccharomyces cerevisiae* (Kim et al. 1994). The purified protein complex had several notable characteristics. It was large and complex, comprising 21 polypeptides, with a total mass of 1 million daltons (Da). It was isolated in two forms, either alone or in an even larger complex with RNA polymerase II. The purified Mediator not only was required for response to a transcriptional activator, but it stimulated basal transcription tenfold in the absence of an activator.

The Kornberg group has extended the structural study of Mediator along two lines—crystallization of the entire Mediator and expression and crystallization of Mediator sub-complexes. After some years of effort, the group developed a procedure for obtaining Mediator in a form and amount suitable for crystallization. About 2 mg of pure protein can be obtained from 200 L of cell culture. Crystal conditions were discovered, and, after several rounds of crystal refinement, reproducible growth of  $300 \times 200 \times 5$  micron plates, which diffract to  $20 \text{ \AA}$ , was achieved. The thinness of the plates, along with radiation damage, could possibly limit the diffraction. Thus, the use of a femtosecond pulse of very high beam intensity might allow collection of meaningful data. This system, therefore, is a potential candidate for liquid jet–injection experiments at the CXI beamline at LCLS. A conventional goniometer also could be used, along with translation of the crystal after each LCLS pulse.

## X-Ray Damage–Free Atomic Resolution Structures

**Project Leaders:** S. Michael Soltis, SSRL, and David Fritz, LCLS

Recent LCLS experiments demonstrate that crystals of myoglobin can produce high-resolution data. Using the XPP station, data to  $1.4 \text{ \AA}$  were recorded from  $\sim 50 \text{ }\mu\text{m}$ -thick myoglobin crystals [ $\sim 10^{12}$  photons per second ( $\gamma/s$ )]. The diffraction data showed no evidence of radiation damage despite vaporization of the sample after each exposure. Although this resolution can be achieved on a conventional synchrotron source with the same number of photons, a structure based on LCLS data could be expected to be free from the effects of radiation damage. Damage-free structures could have considerable impact on detailed mechanistic studies of metalloproteins with metals in high valent states, which are particularly susceptible to photoreduction. Higher resolution would also improve time-resolved studies in which subtle structural changes and changes in electron density distributions are anticipated. Methods to prealign samples, perhaps by probing part of the crystal with a conventional synchrotron source, could be developed to reduce the number of samples required to collect a complete dataset, with sample delivery through the use of crystallization containment. Another area of R&D would be the development of fluid, jet spray, or crystal suspension systems that could

deliver crystals 100 to  $500 \text{ }\mu\text{m}$  in size to the LCLS beam target area rapidly and efficiently. Such a benefit could be found, for example, in the studies of photosystem II (PS II) single crystals (as described in Time-Resolved Spectroscopy of Biological Processes, p. 57) or in many other examples in which the effects of radiation damage, including facile photoreduction in the crystalline state, are limiting.

## Time-Resolved Studies of Macromolecules

**Project Leaders:** Philip Anfinrud, Laboratory of Chemical Physics, National Institute of Diabetes and Digestive and Kidney Diseases, National Institutes of Health; Ilme Schlichting, Max Planck Institute for Medical Research, Heidelberg, Germany; Dwayne Miller, Max Planck Society, Center for Free-Electron Laser Science, Hamburg

LCLS provides the opportunity to extend time-resolved x-ray studies of correlated molecular motion to the chemical time scale. Since the first protein structure was determined just over 50 years ago, the structures of tens of thousands of proteins have been unveiled at or near atomic resolution. Many of these proteins function as molecular machines and are engaged in the making and breaking of chemical bonds. A grand challenge in the biosciences is to understand how such proteins function from a mechanistic point of view. Because the elementary steps in a chemical transformation generally occur on the chemical time scale of femtoseconds, direct observation of these steps requires ultrafast time resolution. In pursuit of this aim, the infrastructure required to conduct time-resolved pump-probe structural studies of proteins has been developed at the European Synchrotron Radiation Facility (Schotte et al. 2003) and more recently at the Advanced Photon Source. Unfortunately, the time resolution attainable at these third-generation synchrotron facilities is currently limited by the x-ray pulse duration to about 100 ps, which is insufficient to observe the primary events that lead to the globally distributed structural changes observed in proteins at the 100 ps time delay. Indeed, ultrafast time-resolved optical and infrared studies of proteins have detected changes occurring on the femtosecond and picosecond time scales (Lim, Jackson, and Anfinrud 1993; Lim, Jackson, and Anfinrud 1997), but these measurements are capable of probing structural changes only indirectly. During LCLS beam time in December 2010, substantial progress was made toward the goal of characterizing, with near-atomic spatial resolution, the ultrafast structural changes that ultimately lead to the efficient debinding of CO from the Fe-heme in myoglobin. The structural details unveiled from this and subsequent studies will provide stringent constraints for putative models of short-lived intermediates and structural transitions between them and will help describe in atomic detail the mechanisms of protein function. LCLS opens up

this area of structural dynamics in the femtosecond regime, complementing studies in the longer time regime possible with third-generation synchrotron sources.

The planned research described above on myoglobin is illustrative of the kinds of structural changes that occur on the femtosecond to picosecond time scale. Such changes are central to the mechanisms of action of many biological systems, including electron transport proteins; other small molecule-binding proteins like the cytochrome P450s; many metalloprotein enzymes; and photoactive proteins such as the photosynthetic reaction center, bacteriorhodopsin, and photoactive yellow protein (PYP). In general, the ability to funnel a local distortion into a concerted macroscopic transformation in these proteins represents one of the many fascinating attributes of biological systems. In PYP, for example, *trans*-to-*cis* isomerization about a single chromophore double bond, which occurs on the picosecond time scale, introduces strain into the chromophore and the surrounding protein residues. The relaxation from this strain drives all subsequent structural changes in this protein on the nanosecond to second time scale that ultimately lead to signal transduction as shown by the work of Moffat and collaborators (Rajagopal et al. 2004). Many of these processes are expected to have structural changes that occur in the femtosecond to picosecond time range and hence are not accessible using storage ring-based synchrotron radiation.

Identifying, for example, the atomic motions that occur during the photoisomerization reaction in PYP or other photoactive proteins would greatly expand the understanding of the influence of the protein environment in this and similar systems. By exploiting the laser-pulse pump and the femtosecond x-ray-pulse probe configuration together with ultrashort pulse x-rays from LCLS, characterizing the evolution of structure over the time course of femtoseconds to nanoseconds will be possible.

## Time-Resolved Spectroscopy of Biological Processes

**Project Leaders:** Vittal Yachandra and Junko Yano, Lawrence Berkeley National Laboratory; Uwe Bergmann, LCLS; and many collaborators

The “collect before destroy” approach for biological samples enabled by the extremely bright and ultrashort x-ray pulses from LCLS provides an opportunity to overcome the current limitations of synchrotron sources for both spectroscopy and crystallography. An LCLS experiment can be carried out at room temperature unlike the cryogenic conditions in synchrotron experiments. Only room-temperature spectroscopy and crystallography make feasible the light-induced “snapshot” time-dependent studies described below.

The oxygen-evolving complex (OEC) in PS II catalyzes the oxidation of water to dioxygen. The OEC contains a heteronuclear  $\text{Mn}_4\text{Ca}$  cluster that couples the four-electron

oxidation of water with the one-electron photochemistry occurring at the PS II reaction center by acting as the locus of charge accumulation. This complex cycles through a series of five intermediate S-states ( $S_0$  to  $S_4$ ), representing the number of oxidizing equivalents stored on the OEC, driven by the energy of four successive photons absorbed by the pigments of the PS II reaction center (Kok, Forbush, and McGloin 1970). Once four oxidizing equivalents are accumulated in the OEC ( $S_4$ -state), a spontaneous reaction occurs that results in the release of  $\text{O}_2$  and the re-formation of the  $S_0$ -state. Given the role of PS II in maintaining life in the biosphere and the future vision of a renewable energy economy, understanding the structure of the  $\text{Mn}_4\text{Ca}$  catalyst and the mechanism of the water oxidation reaction is considered a grand challenge in the biological sciences. Although the detailed chemistry involved in water oxidation is emerging slowly, there still are competing models of structures and mechanisms, and the data currently available have not provided a definitive answer.

Synchrotron radiation-based x-ray diffraction has been used to study structures of PS II, currently at a resolution of 1.9 Å (Zouni et al. 2001; Guskov et al. 2009; Umena et al. 2011; Ferreira et al. 2004). The geometric and electronic structural information of the intact  $\text{Mn}_4\text{Ca}$  cluster has been addressed primarily by spectroscopic methods, especially x-ray absorption and emission techniques (Yano et al. 2006). Among these methods, x-ray emission spectroscopy (XES) is a powerful tool for studying the charge and spin density and ligand environment of the metal site and has been used successfully to probe steady-state isotropic PS II samples. Methods using polarized x-rays and oriented samples were demonstrated to have the potential for significantly increasing the chemical information by orientationally selecting specific transitions, thereby detecting unresolved features (Yano et al. 2007; Bergmann et al. 2002). However, it is unrealistic with third-generation synchrotron sources to follow the time course of the water-oxidation reaction by the weak valence-to-core emission spectrum ( $K\beta_{2,5}$ , see below) or to collect polarized  $K\beta$  XES data ( $K\beta_{1,3}$ ) from single crystals within the threshold of radiation damage.

Spectroscopy provides a probe for the integrity of the catalytic  $\text{Mn}_4\text{Ca}$  site during crystallography, the electronic structure, and the advancement of S-states during the light-induced reaction, while crystallography provides the structures and orientational information crucial for polarized spectroscopy. The  $K\beta$  emission peaks of Mn ( $K\beta_{1,3}$  and  $K\beta_{2,5}$  regions) can be used because these transitions are sensitive to the charge and spin states ( $K\beta_{1,3}$ ), ligand environment ( $K\beta_{2,5}$ ) (Pushkar et al. 2010), and polarization (Bergmann et al. 2002). The dichroism is expected to be similar to what was observed in the previous single-crystal x-ray absorption near-edge structure (XANES) spectroscopy study at SSRL (Yano et al. 2006). The  $K\beta_{1,3}$  peak also will be used to determine the integrity for the PS II samples, as already demonstrated by Messinger et al. 2001. A laser

pump, x-ray probe setup is available at the CXI beamline at LCLS. Of particular interest is the  $S_3 - [S_4] - S_0$  transition, where the O-O bond formation and  $O_2$  release occur.

A dispersive XES setup on the LCLS CXI beamline will allow simultaneous collection of diffraction data and a certain energy range of the XES spectrum in one shot from each of the PS II crystals in the stream. The wavelength dispersive setup will use a set of 16 (4 by 4) cylindrically bent Si(440) analyzer crystals in von Hamos geometry and one or two modules of a pixel array detector (PAD) for collecting the emission spectrum in single-photon counting mode, a capability essential to minimize the background signal from the scattered photons (see Fig. B4, this page).

The primary goal is to develop a map of changes in the electronic and geometric structure of the  $Mn_4Ca$  cluster during the light-induced reaction cycle of water oxidation. Building on the information about the dark-stable  $S_1$ -state, researchers plan to determine the time evolution of the electronic structure of the  $Mn_4Ca$  cluster, protonation state of the ligated oxygen atoms, and changes in the ligand environment along the Kok-cycle. All these measurements are essential to elucidate the mechanism of O-O bond formation and water oxidation in this biological nanomachine.

## Nonperiodic Imaging of Biological Particles

**Project Leader:** Janos Hajdu, Uppsala University, and many collaborators

A grand challenge for 21st century biology involves molecular-level structural studies on a living cell, and a first step in this direction is to gain an understanding of key damage processes in micron-sized biological objects (Bergh et al. 2008). Recent results on imaging live picoplankton cells at LCLS show diffraction signal extending to about 10 Å resolution with a 60 fs FEL pulse of 2 keV energy (unpublished). The cell was alive at the time it met the x-ray pulse. Although further work is required, there is evidence that images at biologically useful resolutions can be obtained from this LCLS-enabled approach.

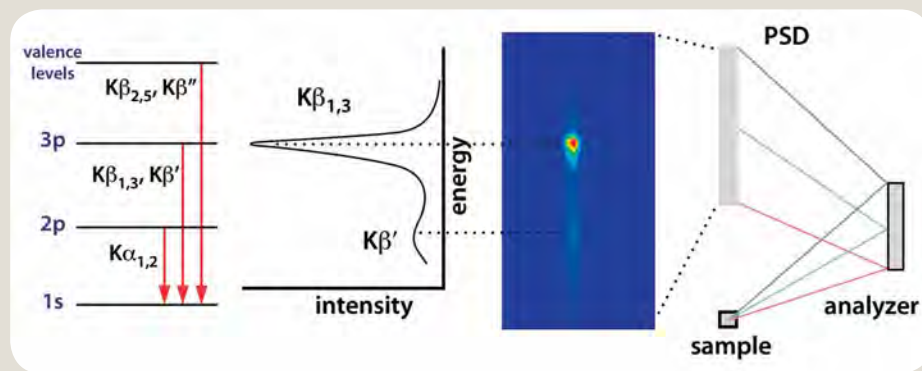


**Fig. B4. Mn  $K\beta$  x-ray emission spectrum from a manganese complex collected using an energy-dispersive spectrometer (energy-level diagram for emission processes is at left).** The spectrum was collected using only one analyzer crystal and a Pilatus position-sensitive x-ray detector (PSD) on SSRL beamline10-2. The spectrometer that will be used at LCLS for time-resolved studies will have 16 analyzer crystals and an energy-discriminating PSD. A collection time of  $\sim 10$  minutes is estimated for a high-quality  $K\beta_{1,3}$  spectrum from PS II crystals at LCLS. [Courtesy of SLAC National Accelerator Laboratory]

In another project enabled by LCLS, the first images of a single virus particle, the mimivirus, were obtained (see Fig. B5, p. 59). The figure shows the reconstructed exit wavefronts from two mimivirus particles injected into the AMO chamber at LCLS (Seibert et al. 2011). Mimivirus, the largest known virus, is visible in an optical microscope. It is too big for a full 3D reconstruction by electron microscopy (Xiao et al. 2009), and its core is surrounded by fibrils, preventing crystallization. A highly efficient aerosol injector was developed for sample delivery to the LCLS x-ray beam. The injector can be used to introduce living cells, viruses, or biomolecules at reduced pressure into the beam. In a more recent experiment at the LCLS AMO beamline (conducted from January to February 2011), a hit rate of 43% was achieved with an improved aerosol injector, producing 1.2 million hits on various viruses in 36 hours (see Fig. B6, p. 59).

The coherent diffraction pattern of a nonperiodic object is continuous; in principle, there is a direct way to determine the phases from the pattern for image reconstruction by “oversampling” (Fienup 1978). Resolution in single-particle experiments does not depend on sample quality in the same way as in conventional crystallography. Rather, resolution is a function of radiation intensity, pulse duration, and wavelength—all of which are factors controlling ionization and sample movement during exposure. A 3D dataset can be assembled from such diffraction patterns when copies of a reproducible sample are exposed to the beam one by one in random orientations (Huldt, Szoke, and Hajdu 2003; Bortel and Faigel 2007). Damage can be distributed over many copies of the sample in a similar manner as in “single-molecule” electron microscopy or in crystallography using multocrystal averaging. Diffraction data from reproducible objects can be enhanced by merging redundant data, and this should be possible even from very weak individual shots (Fung et al. 2009; Loh and Elser 2009). Averaging (in a redundant

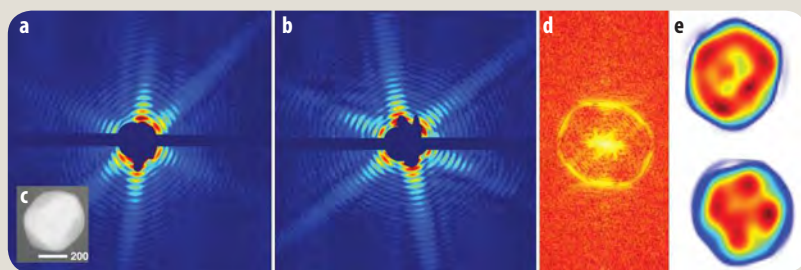
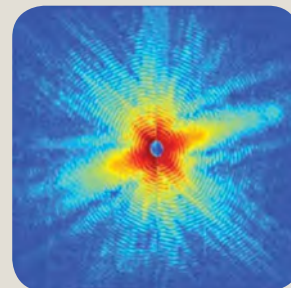


**Fig. B5. (a, b) Diffraction patterns of mimivirus collected at the LCLS AMO station at 1.8 keV. (c) A transmission electron micrograph of a single mimivirus particle. (d) Autocorrelation function for image a. (e) Reconstructions for a and b, giving a first glimpse at the structure of mimivirus in 2D projections enabled by LCLS. [Reprinted by permission from Macmillan Publishers Ltd: From Seibert, M. M., et al. 2011. "Single Mimivirus Particles Intercepted and Imaged with an X-Ray Laser," *Nature* **470**(7332), 78–81.] The diffraction patterns were recorded with 1.8 keV x-ray energy, 70 fs pulse length,  $6.5 \times 10^{15} \text{ W/cm}^2$  on the sample, and the patterns contained about 1.7 million scattered photons.**

**Fig. B6. Diffraction from a single mimivirus particle using a single 60 fs-long pulse of 2 keV radiation at the LCLS AMO beamline in January and February 2011. [Ekeberg et al., Uppsala University, unpublished]**



dataset) reduces the error in the signal by the square root of the number of patterns that sample the same pixel. The limiting factors here are the accuracy of the orientation information and heterogeneity in the sample population, both of which will blur the reconstructed image (Maia et al. 2009; Quiney and Nugent 2011). The first experimental demonstration of this concept of 3D structure determination from single shots was achieved using soft x-ray laser diffraction data from aerosolized ellipsoidal nanoparticles (Loh et al. 2010; Bogan et al. 2010). With a *nonreproducible object*, there is no chance of repeating the experiment to improve the signal, creating a resolution gap between structures for reproducible and nonreproducible objects. Interestingly, the highest possible resolution in a *single shot* is not necessarily at the shortest possible wavelength (Bergh et al. 2008). Experimental strategies, therefore, are different for high-resolution studies on reproducible and nonreproducible objects.

In the first experiments at the LCLS AMO beamline, background scattering in the vacuum chamber did not exceed the readout noise of the detectors, nor the noise of the diffuse photon background. This is quite remarkable considering that the number of photons in the LCLS pulse was nearly 100 billion times higher than this background. Analysis tools were developed to generate 2D and 3D images from coherent diffraction data (Maia et al. 2010), and new concepts developed for phase retrieval and holography (Marchesini et al. 2008).

As LCLS and imaging techniques develop, it will be possible to move toward more-demanding applications and extend the experiments to smaller particles and, ultimately, to single macromolecules. LCLS is rapidly developing to meet the requirements of such demanding scientific applications, and the first tests on single macromolecules were conducted in August 2011.

## Correlated X-Ray Scattering (CSX)

**Project Leaders:** Sebastian Doniach and Vijay Pande, Stanford University; John Spence, Arizona State University; and many collaborators.

CSX, in principle, should provide much more information about molecular structure than conventional small-angle x-ray scattering (SAXS) data. Recently, the first experimental *ab initio* image reconstruction of a single particle (gold nanorods) was created from the diffraction pattern of an ensemble of randomly oriented copies from its angular correlations. This reconstruction showed that effects of interparticle interference from the partially coherent incident radiation are essentially negated if the particles are also in random positions (Saldin et al. 2011). The measurement of correlated scattering events in which a given molecule in the ensemble can scatter two photons within the same x-ray pulse is made possible by the high x-ray brightness of the LCLS pulse. Furthermore, recent advances in control of droplet formation and transport into the LCLS beam allow droplets to be formed by mixing an enzyme and its substrate in a continuous flow mixer in a few tens of microseconds. The droplets are then injected toward the x-ray beam at 10 to 20 m/s. By varying the distance to the beam, a series of CSX snapshots may be obtained from mixing at times ranging from ~100 microseconds ( $\mu\text{s}$ ) to several milliseconds.

The incidence of such CSX events is greatly amplified by the number of macromolecules in the droplet. By correlating scattering events at different pixels in an area detector and defining a pair of scattering vectors ( $|q_1|$  and  $|q_2|$ ), these two-photon events define a cross-correlation function:

$$C4(q_1, q_2, \cos \theta_{12}) = \langle I(q_1)I(q_2) \rangle - \langle I(q_1) \rangle \langle I(q_2) \rangle$$

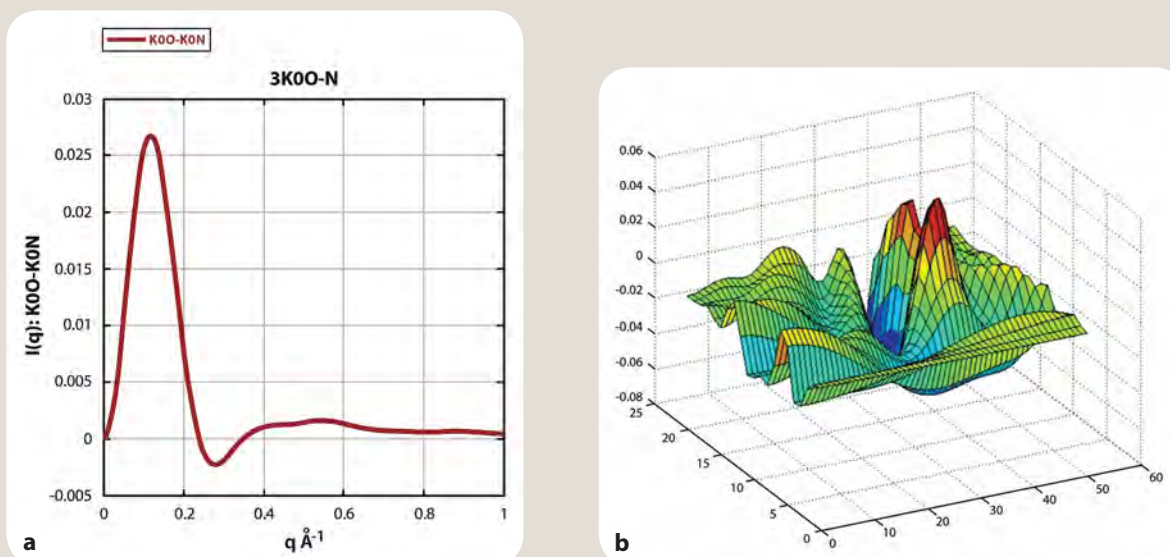


**Fig. B7. (a) Difference in calculated SAXS profiles for the initial and final states of CypA as estimated from the structures of the native versus a Ser99Thr mutant. (b) A slice through the difference of the calculated cross-correlation function  $C4$ .**

for a diffraction image obtained from a single x-ray pulse.  $I(q_1)$  measures the number of photon counts in the pixel defining a scattering vector  $q_1$ . The correlated average is over all pairs of pixels subtending a fixed relative angle  $\theta_{12}$  and a certain neighborhood around each vector.  $\langle I(q) \rangle$  represents the usual two-point SAXS scattering averaged over all orientations. There are an estimated  $10^8$  protein molecules per droplet, so the cross-correlation is the sum over the CSX profiles for all the conformational states of the molecule occupied at the instant of exposure. Since LCLS x-ray pulses have a duration on the order of 10 fs, the molecules in the droplet do not have time to undergo significant Brownian motion during exposure. Hence, two-photon scattering from any molecule in the ensemble happens for a given molecular orientation and internal conformation. Some  $10^7$  correlated two-photon CSX events could be expected from a single micrometer-sized droplet of protein solution at a concentration of 10 mg/mL exposed to a single LCLS x-ray pulse focused to an area of  $\sim 1 (\mu\text{m})^2$ . An advantage of CSX relative to the usual single-photon SAXS measurement is that background subtraction is self-generated by the act of correlating the data, with subtraction of the product of average scattering in the two wave vector channels  $|q_1|$  and  $|q_2|$ .

An algorithm has been developed to calculate the theoretical XCS profile given the coordinates of a macromolecule. In Fig. B7a, this page, the calculated change in the ordinary SAXS profile,  $I(q)$ , is shown for the enzyme cyclophilin A (CypA) as it goes from initial to final state conformations. In B7b, the calculated difference is shown for a slice through the cross-correlation function. The overall magnitude of the difference profile is of order 8% of the individual profiles. The data resulting from time-resolved CSX measurements can be analyzed using an approach in which macromolecular kinetics are simulated using Markov state models built from molecular dynamics simulations. Direct fitting approaches similar to those used for refinement at low resolution in macromolecular crystallography (Schroder, Levitt, and Brunger 2010) can also be employed.

## References

- Bergh, M., et al. 2008. "Feasibility of Imaging Living Cells at Subnanometer Resolutions by Ultrafast X-Ray Diffraction," *Quarterly Reviews of Biophysics* **41**(3–4), 181–204.
- Bergmann, U., et al. 2002. "Anisotropic Valence → Core X-Ray Fluorescence from a [Rh(en)<sub>3</sub>][Mn(N)(CN)<sub>5</sub>]-H<sub>2</sub>O Single Crystal: Experimental Results and Density Functional Calculations," *Journal of Chemical Physics* **116**(5), 2011–15.
- Bogan, M., et al. 2010. "Single-Shot Femtosecond X-Ray Diffraction from Randomly Oriented Ellipsoidal Nanoparticles," *Physical Review Special Topics—Accelerators and Beams* **13**(9), 094701. DOI: 10.1103/PhysRevSTAB.13.094701.
- Bortel, G., and G. Faigel. 2007. "Classification of Continuous Diffraction Patterns: A Numerical Study," *Journal of Structural Biology* **158**(1), 10–18.
- Chapman, H. N., et al. 2011. "Femtosecond X-Ray Protein Nanocrystallography," *Nature* **470**(7332), 73–77.
- DePonte, D., et al. 2008. "Gas Dynamic Virtual Nozzle for Generation of Microscopic Droplet Streams," *Journal of Physics D: Applied Physics* **41**, 195505. DOI: 10.1088/0022-3727/41/19/195505.
- Ferreira, K. N., et al. 2004. "Architecture of the Photosynthetic Oxygen-Evolving Center," *Science* **303**(5665), 1831–38.
- Fienu, J. 1978. "Reconstruction of an Object from the Modulus of its Fourier Transform," *Optics Letters* **3**(1), 27–29.
- Fung, R., et al. 2009. "Structure from Fleeting Illumination of Faint Spinning Objects in Flight," *Nature Physics* **5**, 64–67.
- Guskov, A., et al. 2009. "Cyanobacterial Photosystem II at 2.9-Å Resolution and the Role of Quinones, Lipids, Channels and Chloride," *Nature Structural and Molecular Biology* **16**(3), 334–42.
- Huldt, G., A. Szoke, and J. Hajdu. 2003. "Diffraction Imaging of Single Particles and Biomolecules," *Journal of Structural Biology* **144**(1–2), 219–27.
- Kim, Y. J., et al. 1994. "A Multiprotein Mediator of Transcriptional Activation and its Interaction with the C-Terminal Repeat Domain of RNA Polymerase II," *Cell* **77**(4), 599–608.
- Kirian, R. A., et al. 2010. "Femtosecond Protein Nanocrystallography—Data Analysis Methods," *Optics Express* **18**(6), 5713–23.
- Kok, B., B. Forbush, and M. McGloin. 1970. "Cooperation of Charges in Photosynthetic O<sub>2</sub> Evolution—I. A Linear Four Step Mechanism," *Photochemistry and Photobiology* **11**(6), 457–75.
- Lim, M., T. A. Jackson, and P. A. Anfinsen. 1993. "Nonexponential Protein Relaxation: Dynamics of Conformational Change in Myoglobin," *Proceedings of the National Academy of Sciences of the United States of America* **90**(12), 5801–04.
- Lim, M., T. A. Jackson, and P. A. Anfinsen. 1997. "Ultrafast Rotation and Trapping of Carbon Monoxide Dissociated from Myoglobin," *Nature Structural Biology* **4**(3), 209–14.
- Loh, N. T., and V. Elser. 2009. "Reconstruction Algorithm for Single-Particle Diffraction Imaging Experiments," *Physical Review E: Statistical, Nonlinear, and Soft Matter Physics* **80**(2), 026705. DOI: 10.1103/PhysRevE.80.026705.
- Loh, N. D., et al. 2010. "Cryptotomography: Reconstructing 3D Fourier Intensities from Randomly Oriented Single-Shot Diffraction Patterns," *Physical Review Letters* **104**(22), 225501.
- Maia, F. R., et al. 2009. "Structural Variability and the Incoherent Addition of Scattered Intensities in Single-Particle Diffraction," *Physical Review E: Statistical, Nonlinear, and Soft Matter Physics* **80**(3), 031905.
- Maia, F., et al. 2010. "Hawk: The Image Reconstruction Package for Coherent X-Ray Diffractive Imaging," *Journal of Applied Crystallography* **43**, 1535–39.
- Marchesini, S., et al. 2008. "Massively Parallel X-Ray Holography," *Nature Photonics* **2**, 560–63.
- Messenger, J., et al. 2001. "Absence of Mn-Centered Oxidation in the S<sub>2</sub> → S<sub>3</sub> Transition: Implications for the Mechanism of Photosynthetic Water Oxidation," *Journal of the American Chemical Society* **123**(32), 7804–20.
- Pushkar, Y., et al. 2010. "Direct Detection of Oxygen Ligation to the Mn<sub>4</sub>Ca Cluster of Photosystem II by X-Ray Emission Spectroscopy," *Angewandte Chemie International Edition* **49**(4), 800–03.
- Quiney, H., and K. Nugent. 2011. "Biomolecular Imaging and Electronic Damage Using X-Ray Free-Electron Lasers," *Nature Physics* **7**, 142–46.
- Rajagopal, S., et al. 2004. "Analysis of Experimental Time-Resolved Crystallographic Data by Singular Value Decomposition," *Acta Crystallographica, Section D: Biological Crystallography* **60**(5), 860–71.
- Saldin, D., et al. 2011. "New Light on Disordered Ensembles: *Ab Initio* Structure Determination of One Particle from Scattering Fluctuations of Many Copies," *Physical Review Letters* **106**(11), 115501.
- Schotte, F., et al. 2003. "Watching a Protein as it Functions with 150-ps Time-Resolved X-Ray Crystallography," *Science* **300**(5627), 1944–47.
- Schroder, G. F., M. Levitt, and A. T. Brunger. 2010. "Super-Resolution Biomolecular Crystallography with Low-Resolution Data," *Nature* **464**(7292), 1218–22.
- Seibert, M. M., et al. 2011. "Single Mimivirus Particles Intercepted and Imaged with an X-Ray Laser," *Nature* **470**(7332), 78–81.
- Umena, Y., et al. 2011. "Crystal Structure of Oxygen-Evolving Photosystem II at a Resolution of 1.9 Å," *Nature* **473**(7345), 55–60.
- Xiao, C., et al. 2009. "Structural Studies of the Giant Mimivirus," *PLoS Biology* **7**(4), e92.
- Yano, J., et al. 2006. "Where Water is Oxidized to Dioxygen: Structure of the Photosynthetic Mn<sub>4</sub>Ca cluster," *Science* **314**(5800), 821–25.
- Yano, J., et al. 2007. "Polarized X-Ray Absorption Spectroscopy of Single-Crystal Mn(V) Complexes Relevant to the Oxygen-Evolving Complex of Photosystem II," *Journal of the American Chemical Society* **129**(43), 12989–13000.
- Zouni, A., et al. 2001. "Crystal Structure of Photosystem II from *Synechococcus elongatus* at 3.8 Å Resolution," *Nature* **409**(6821), 739–43.



## National Synchrotron Light Source-II

### Opportunities for Biological Sciences at NSLS-II\*



#### Overview

The National Synchrotron Light Source-II (NSLS-II) is designed to provide a broadband source of synchrotron photons—from infrared light to x-rays—with a brightness unsurpassed by any synchrotron worldwide. The extreme brightness and coherence of NSLS-II will enable new techniques, such as nanoscale imaging, that currently are either in their infancy or not feasible with present sources. Moreover, NSLS-II will take widely used techniques, such as macromolecular crystallography (MX), x-ray scattering (XRS), and x-ray absorption spectroscopy (XAS), and extend them to new regimes in time and spatial resolutions that cannot be achieved today. With construction over 50% finished, NSLS-II is on track for completion in March 2014—15 months ahead of schedule (see Fig. C1, this page). When operational, it will replace the original NSLS.

The synchrotron storage ring for NSLS-II is designed for operating at 3 gigaelectron volts (GeV) and 500 milliamperes (mA) to produce electron beams of ultralow emittance [ $\epsilon_x, \epsilon_y = 0.6, 0.008$  nanometer-radians (nm-rad)]. The accelerator design that reaches this emittance features a large ring (circumference 791.5 m) with relatively soft bend magnets configured in a 30-cell, double-bend achromat that holds 15 long (9.3 m) high- $\beta$  straight sections and 15 short (6.6 m) straight sections, with damping wigglers in 8 of the 15 long straights. The baseline configuration implements damping wigglers in only three of the straights. The straight sections can accommodate a variety of insertion devices including undulators and superconducting wigglers, large-gap dipoles can be accommodated for infrared (IR) sources, and three-pole wigglers (3PWs) can be added at bend positions to shift the critical energy into a spectrum similar to that at the NSLS bends.

NSLS-II can accommodate at least 58 independently operating beamlines and potentially many more with canted insertion devices and multiple end stations per beamline. These could comprise insertion devices on 15 low- $\beta$  straights and on 12 high- $\beta$  straights, including:

- Damping wigglers as potent x-ray sources.
- Twenty-seven bend-magnet (BM) ports for IR.
- Ultraviolet or soft x-rays from the dipoles or hard x-rays from 3PWs.
- Four large-gap BM ports for far-IR.

\*Brookhaven National Laboratory prepared this and a companion document (p. 72) and approved post-workshop revisions to each.



**Fig. C1. NSLS-II under construction and ~50% complete on March 25, 2011.** The new facility will produce photon beams with a brightness and coherence unsurpassed by any synchrotron worldwide and will support a wide range of experiments in the biological and physical sciences. [Courtesy of Brookhaven National Laboratory]

As the brightest synchrotron in the world, NSLS-II will be more than 10,000 times brighter than NSLS. It is designed to enable  $\sim 1$  nm spatial resolution,  $\sim 0.1$  meV energy resolution, and diffraction-limited coherence in the vertical at 12 keV.

The baseline construction project for NSLS-II includes six insertion-device beamlines; others are being built with additional funding from the DOE Office of Basic Energy Sciences and other sources. A call for proposals in 2010 generated 54 Beamline Development Proposals, 34 of which were approved. Calls for additional proposals will recur annually, and the 2011 call generated 13 Letters of Intent, including resubmissions as well as new Beamline Development Proposals.

#### NSLS-II Beamlines for Biological Sciences

Biological sciences are prominent in the planning for NSLS-II beamlines. Four of the six project beamlines are intended to address biological research interests as well as physical and material science needs. Thirteen of the 34 approved beamlines include substantial biological applications, with biology predominating for 11 of these. Also, four of the new Letters of Intent are exclusively or substantially for biology (see Table C1, p. 64).

The beamlines planned for NSLS-II are intended to accommodate both existing science programs and those that will develop in response to new opportunities. Several NSLS-II beamlines currently under development do address future needs of current NSLS users. In addition, however, NSLS-II brightness brings new opportunities both for these disciplines and for techniques that take advantage of the unprecedented resolutions and coherence at NSLS-II, notably in imaging. The rest of this Facility Paper describes

some features of the currently envisioned beamlines. In the long run, NSLS-II will accommodate beamlines addressing other applications. The current beamlines are grouped in the following text into four categories: macromolecular crystallography, scattering, spectroscopy, and imaging.

Capabilities and science areas for each beamline now under development are briefly described. The divisions are somewhat arbitrary (e.g., a scattering beamline might examine crystals, and an imaging or MX beamline might use spectroscopic probes), but the beamline descriptions clarify this.

**Table C1. NSLS-II Beamlines for Biological Sciences**

Acronym	Application	Spokesperson or Beamline Scientist	Source
<b>Project Beamlines</b>			
CHX	Coherent hard x-ray scattering	Andrei Fluerasu	U
HXN	Hard x-ray nanoprobe	Yong Chu	U
IXS	Inelastic x-ray scattering	Yong Cai	U
SRX	Submicron resolution x-ray spectroscopy	Juergen Thieme	U
<b>Approved Beamline Development Proposals</b>			
ABS	Automated biomolecular solution scattering	Lin Yang	3PW
AIM	Advanced infrared microspectroscopy	Lisa Miller	BM
AMX	Flexible access macromolecular crystallography	Dieter Schneider	U
CDI	Coherent x-ray diffraction	Ian Robinson	U
FMX	Frontier macromolecular crystallography	Robert Sweet	U
FXI	Long beamline for full-field imaging	Jake Socha	SCW
IRI	Full-field infrared spectroscopic imaging	Lisa Miller	BM
LIX	X-ray scattering for life sciences	Lin Yang	U
NYX	NYSBC microdiffraction beamline	Wayne Hendrickson	U
SM3	Correlated spectroscopy and MX	Allen Orville	3PW
XAS	X-ray absorption spectroscopy	Mark Chance	3PW
XFM	X-ray fluorescence microprobe	Antonio Lanzirotti	3PW
XFP	X-ray footprinting	Mark Chance	DW
<b>Letters of Intent</b>			
HIT	Discoveries for chemical biology	Marc Allaire	U
LAX	Low-energy anomalous x-ray diffraction	Wayne Hendrickson	U
MIT	Medical imaging and radiation therapy	Avraham Dilmanian	SCW
STX	Scanning transmission x-ray microscope	Juergen Thieme	U

BM = bending magnet; DW = damping wiggler; SCW = superconducting wiggler; U = undulator; 3PW = three-pole wiggler.

## Macromolecular Crystallography

### FMX – Frontier Macromolecular Crystallography

This MX beamline will exploit the finest properties of NSLS-II and push the state of the art in x-ray optics. The tunable, 1 micron ( $\mu\text{m}$ ), and variable divergence beam handles small crystals and very large unit cells. Preserving beam coherence makes new experiments possible. Leading-edge cryogenic automation will provide convenience for users.

#### Examples of Science Areas and Impact

- **Structural biology.** The most interesting structures are often the most difficult to study. This beamline will push new limits in crystal size.
- **Biochemistry.** Knowledge of intermediates in enzymatic pathways expands our understanding of cellular and microbiological processes.
- **Physiology and medicine.** Knowing how drugs interact with their targets is essential to development of new pharmacologically effective compounds.

#### FMX Beamline Capabilities

Source:	Canted U20 undulator
Energy range and resolution:	5 to 20 keV; $\Delta E/E \sim 5 \times 10^{-4}$
Beam size:	From 1 by 1 $\mu\text{m}^2$ to 100 by 100 $\mu\text{m}^2$
Diffraction resolution:	To 1 Å resolution

### AMX – Flexible Access, Highly Automated Beamline for Macromolecular Crystallography

AMX at NSLS-II will provide structural biologists with ready access to an advanced facility for precise structure determinations at unprecedented rates. It will exploit source characteristics, deliver a very high flux in a suitably small focused beam, and be highly automated to support remote access and extensive experimental studies.

#### Examples of Science Areas and Impact

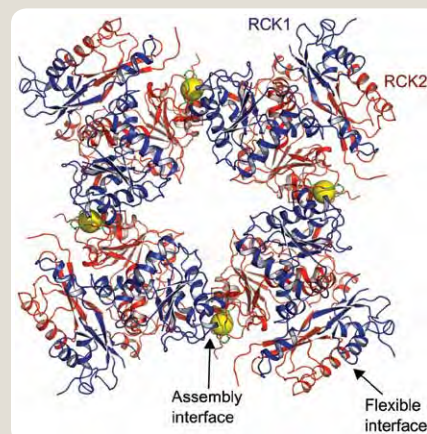
- **Structural biology.** Atomic structures of large protein and nucleic acid complexes, including membrane proteins, are prerequisites to gaining insights into their function, interaction, and dynamics, thus creating molecular movies.
- **Biochemistry.** Structural analysis of all intermediates in entire enzymatic cycles and pathways will expand our understanding of cellular and microbiological processes.
- **Physiology and medicine.** Crystallographic studies of the interactions of drugs with their targets are essential in the development of pharmacologically effective compounds.

#### AMX Beamline Capabilities

Source:	Canted U20 undulator
Energy range and resolution:	5 to 20 keV; $\Delta E/E \sim 5 \times 10^{-4}$
Beam size:	From 5 $\mu\text{m}$ to 300 $\mu\text{m}$
Diffraction resolution:	To 1 Å resolution

**Fig. C2. Ribbon diagram of the gating ring of the human BK channel  $\text{Ca}^{2+}$ -activation apparatus.**

(From Yuan, P., et al. 2010. "Structure of the Human BK Channel  $\text{Ca}^{2+}$ -Activation Apparatus at 3.0 Å Resolution," *Science* **329**(5988), 182–86. Reprinted with permission from AAAS.)



### NYX – NYSBC Microdiffraction Beamline

This is a Type II beamline built by the New York Structural Biology Center as a Partner User. It features:

- **Diffraction options.** Diffraction from micron-sized crystals and rastered scans for optimized diffraction from larger crystals of challenging biological macromolecules and complexes.
- **Anomalous diffraction.** Access to a broad range of resonant edges for anomalous diffraction (multi- and single-wavelength anomalous dispersion) phasing—from U  $M_V$  (3.5 keV) to Se K (12.7 keV) to U  $L_{III}$  (17.2 keV).
- **Light elements.** Optimization of anomalous scattering from high energy resolution for sharp transitions at resonant edges and lower energy for increased  $f''$  with light elements (sulfur).

#### NYX Beamline Capabilities

Source:	Undulator on a low- $\beta$ straight section
Energy range:	3.5 to 17.5 keV
Energy resolution:	Down to $\Delta E/E \sim 5 \times 10^{-5}$
Beam cross-section:	From 5 to 50 $\mu\text{m}$

### Examples of Science Areas and Impact

- **Membrane proteins.** These proteins present challenging structural problems with high relevance in neurobiology and metabolic disorders.
- **Macromolecular complexes.** Protein-protein interactions are essential in signaling complexes, and protein-nucleic acid complexes in transcription or replication.
- **Methods development.** Supports efforts for methods to improve phase evaluation and enhance resolution.

**Fig. C3. Homologue structure of the SLAC1 anion channel for closing stomata in plant leaves.** [Reprinted



by permission from Macmillan Publishers Ltd: From Chen, Y.-H., et al. 2010. "Homologue Structure of the SLAC1 Anion Channel for Closing Stomata in Leaves" *Nature* **467**, 1074–80.]

### SM3 – Correlated Spectroscopy and Macromolecular Crystallography

This is a unique facility for multidisciplinary, nearly simultaneous studies of single crystals. Options include macromolecular crystallography; electronic absorption spectroscopy; fluorescence spectroscopy; Raman spectroscopy; Fourier transform infrared spectroscopy; and XAS, x-ray absorption near-edge structure (XANES), and extended x-ray absorption fine structure (EXAFS) spectroscopy.

#### SM3 Beamline Capabilities

Source: Three-pole wiggler  
Energy range: 5 to 20 keV  
Flux:  $10^{13}$  ph/s at 12 keV

### Examples of Science Areas and Impact

- **Redox state.** Define redox states of metalloproteins using structures and spectroscopy from the same sample.
- **Mystery density.** Assign electron density where ambiguities exist using Raman spectroscopy.
- **Mechanisms.** Initiate and follow reactions. Trap and identify reaction intermediates.

## X-Ray Scattering

### LIX – High-Brilliance X-Ray Scattering for Life Sciences

This beamline will support simultaneous small- and wide-angle time-resolved x-ray scattering measurements of proteins, DNA, and RNA in solution using flow cells on time scales down to 10  $\mu$ s. It also will provide for grazing incident scattering from two-dimensional (2D) solutions of membrane proteins embedded in near-native membranes and will be able to perform 1- $\mu$ m-beam scanning probe imaging and tomography of biological tissues.

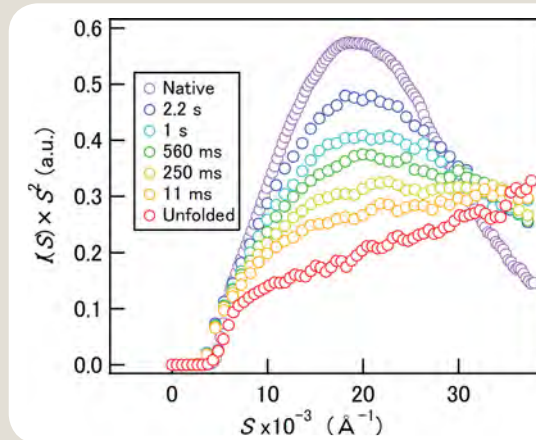
#### LIX Beamline Capabilities

Source: U23 undulator  
Energy range and resolution: 2 to 20 keV at 0.01%  
Wave vector transfer (Q) range: 0.002 to 3.0  $\text{\AA}^{-1}$  at 12 keV

### Examples of Science Areas and Impact

- **Protein dynamics.** Help understand the dynamic processes of protein conformation change (e.g., folding) and enzymatic reaction.
- **Membrane proteins.** Resolve the structure of membrane proteins at low resolution and reveal how their structures change in response to external stimuli.
- **Tissue engineering.** Help elucidate the relationship between the hierarchical structure in natural and engineered tissues and their functional properties.

**Fig. C4. Kratky profiles from time-resolved SAXS of barnase folding dynamics.** [Reprinted with permission from Elsevier from Konuma, T., et al. 2011. "Time-Resolved Small-Angle X-Ray Scattering Study of the Folding Dynamics of Barnase," *Journal of Molecular Biology* **405**(5), 1284–94.]



## ABS – Highly Automated Biomolecular Solution Scattering

This beamline will perform high-throughput static solution-scattering measurements at the rate of up to one sample per minute. It also will support automated data processing, including background subtraction, combining small-angle x-ray scattering (SAXS) and wide-angle x-ray scattering (WAXS) and extraction of basic parameters such as  $R_g$  and  $D_{max}$ .

### ABS Beamline Capabilities

Source:	Three-pole wiggler (or short undulator)
Energy range and resolution:	Fixed at 12 keV at 1% (3PW)
Q range:	0.005 to 3.0 Å <sup>-1</sup>

### Examples of Science Areas and Impact

- **Structural biology.** Complement other structural information (e.g., from MX, electron microscopy, and nuclear magnetic resonance) to provide a complete understanding of the structure of proteins and protein complexes in biologically relevant environments.
- **Structural genomics.** Identify the interacting partners of genomic products.
- **Engineered proteins.** Verify the structure of combinatorially engineered molecular machines for therapeutics and bioenergy applications.
- **Structure-based screening.** Identify functional ligands (e.g., drug molecules) based on the structural change they induce in the target protein.

## CHX – Coherent Hard X-Ray Scattering

This beamline is being designed and constructed within the NSLS-II project for studies of nanometer-scale dynamics in materials using x-ray photon correlation spectroscopy (XPCS) and other experimental methods enabled by bright coherent x-ray beams. XPCS measures time-correlation functions of the speckle fluctuations that occur when a coherent x-ray beam is scattered by a disordered sample. The CHX beamline will allow studies of dynamics ~100 times faster and on shorter length scales than ever before. Scattering geometries will include SAXS, WAXS, and grazing incidence SAXS. A versatile five-circle diffractometer will allow hosting a large selection of sample environments (e.g., cryo-furnace SAXS/WAXS chamber, microfluidic environments, shear cell, and Langmuir-Blodgett trough).

### Examples of Science Areas and Impact

- **Glassy materials.** Driven and out of equilibrium.
- **Colloids and polymers.** Nanostructured complex fluids.

- **Biological systems and processes.** Proteins, membranes, protein folding, and RNA folding.
- **Coherent diffraction imaging.** On near-native biological systems (frozen or hydrated).

### CHX Beamline Capabilities

Source:	U23 undulator
Energy range:	6 to 15 keV
Energy resolution:	$\Delta E/E \sim 10^{-4}$ to pink beam
Coherent beam size:	10 $\mu\text{m}$ by 10 $\mu\text{m}$ (SAXS) 1 $\mu\text{m}$ by 3 $\mu\text{m}$ (WAXS)
Coherent flux at sample:	$2 \times 10^{11}$ at 10 keV

## IXS – Inelastic X-Ray Scattering

This beamline is being designed and constructed within the NSLS-II project to access a broader dynamic range than currently available, filling the dynamic gap between high-frequency spectroscopies, such as IXS, and low-frequency ones. To achieve this goal, a new optics concept will be implemented. This concept involves an aggressive research and development effort that aims within the baseline scope to obtain 1 meV resolution with a sharp resolution tail and a momentum resolution better than 0.25 nm<sup>-1</sup>. Future developments of the IXS beamline will seek to achieve an ultimate goal of 0.1 meV resolution and a momentum resolution substantially better than 0.1 nm<sup>-1</sup>.

### Examples of Science Areas and Impact

- **Disordered systems.** Investigate relaxation dynamics, sound propagation, and transport properties in such systems including glasses, fluids, and polymers.
- **Lipid membranes and other biological systems.** Study their collective dynamics.

### IXS Beamline Capabilities

Source:	In-vacuum undulator
Energy:	9.132 keV (1.358 Å wavelength)
Energy resolution:	1 meV
Momentum transfer:	0.5 to 80 nm <sup>-1</sup>
Flux at sample:	$1.6 \times 10^{10}$ ph/s at 1 meV

## Spectroscopy

### XFP – X-Ray Footprinting

This beamline is designed for studies of x-ray-mediated hydroxyl-radical footprinting. It will provide a local probe of solvent accessibility for *in vivo* and *in vitro* structural studies of biomolecular complexes and their interactions. Time-resolved XFP studies will elucidate local structural dynamics from microsecond to millisecond time scales. The high flux density and beam energy range of NSLS-II damping wigglers will provide high-quality data from microliter volumes of dilute solution samples in near physiological conditions.

#### XFP Beamline Capabilities

Source:	Damping wiggler
Energy range and resolution:	White beam (5 to 20 keV)

#### Examples of Science Areas and Impact

- **In vivo studies.** Investigating real-time ribosomal biogenesis in living cells and receptor-ligand interactions at the cell surface (e.g., drug-protein and antibody-antigen interactions).
- **Membrane proteins.** Understanding the molecular-level structure and function of ion channels, receptors (e.g., G protein-coupled receptors), gated pores, H<sup>+</sup>-pumps, transporters, and membrane enzymes, as well as the dynamics of bound waters in pores, channels, and cavities.
- **Megadalton complexes.** Studying protein-protein interactions, which are essential in protein-nucleic acid and signaling complexes in transcription or replication.
- **Hybrid approach.** Using XFP (for local structural measures) and SAXS (for global measures) is important in deciphering the mechanism of biomolecular assemblies.

### XAS – X-Ray Absorption Spectroscopy for Biological, Environmental, and Energy Sciences

Enabling studies of low-concentration (<100  $\mu\text{m}$ ) samples, this beamline will be the best facility of its kind in the United States and the only such facility on the East Coast (with ~2 times the flux of beamline 9-3 at the Stanford Synchrotron Radiation Lightsource). The XAS beamline will provide continuity of service and expanded capabilities for an extensive, highly productive user community. It will feature a sagittally focusing monochromator, giving flexible beam size and tunable flux density (~0.2 by 0.5 mm to 2 by 10 mm, maintaining flux), and multiple end stations (e.g., cryogenic, *in situ*, and high throughput) with rapid changeover.

#### Examples of Science Areas and Impact

- **Biology.** Study freeze-quench intermediates in metallo- $\beta$ -lactamase reactions to understand antibiotic resistance.
- **Environment.** Observe Fe-TAML intermediates in the efficient catalysis of pollutant decomposition by hydrogen peroxide (H<sub>2</sub>O<sub>2</sub>).
- **Energy.** Use *in situ* electrochemical cell EXAFS to determine structure-property relationships of electroactive enzyme active sites for biological fuel cells.

#### XAS Beamline Capabilities

Source:	Three-pole wiggler
Energy range and resolution:	4.5 to 25 keV/1 to 4 eV ( $\Delta E/E$ )
Detector:	31-element germanium

## Imaging

### CDI – Coherent Diffraction Imaging

When ultimately configured, this beamline will provide both in-line and Bragg coherent diffraction imaging using independent undulators. It will support (1) diffraction imaging of crystal shapes in 3D at the nanometer scale; (2) diffraction imaging of cryofrozen cells and tissues; (3) imaging of strain fields inside crystals; (4) time evolution of shape and strain under working conditions; and (5) manipulation, deformation, and indentation at the nanometer scale.

#### Examples of Science Areas and Impact

- **Ptychographic imaging** of domains in materials and of biological samples using phase-contrast, dark-field, and phase-encoding methods.
- **Applications.** In nanoscale semiconductor devices, strain engineering, catalysis, and energy materials.

#### CDI Beamline Capabilities

Source:	U20 undulators, low $\beta$
Energy range:	2.5 to 20 keV (in-line CDI)

**Fig. C5. Coherent diffraction imaging of a human chromosome.** [Reprinted with permission from Nishino, Y., et al. 2009. "Three-Dimensional Visualization of a Human Chromosome Using Coherent X-Ray Diffraction," *Physical Review Letters* **102**(1), 018101. Copyright 2009 by the American Physical Society.]

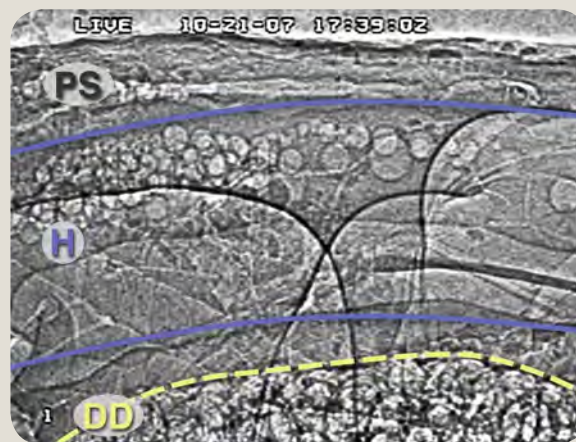
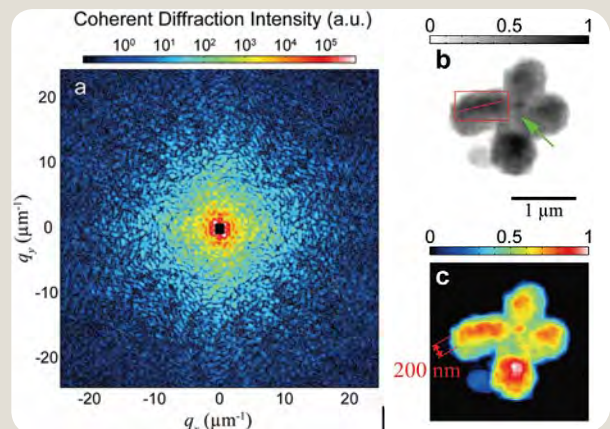


**Fig. C6. Particle tracking of biological flow in a section of the tubular heart of a grasshopper.** [From Lee, W.-K., and J. J. Socha. 2009. "Direct Visualization of Hemolymph Flow in the Heart of a Grasshopper (*Schistocerca americana*)," *BMC Physiology* **9**(2). (Open-access article distributed under the Creative Commons Attribution License.)]

## FXI – Full-Field X-Ray Imaging from Micron to Nanometer Scales

This beamline will host a transmission x-ray microscope (TXM) that will operate in a full-field imaging configuration to enable 2D and 3D dynamic imaging with 30 nm spatial resolution. The user community will be large and diverse, serving national needs and addressing fundamental issues across many fields.

### FXI Beamline Capabilities

Source:	Damping wiggler
Energy range and resolution:	5 to 11 keV
Spatial resolution:	30 nm

### Examples of Science Areas and Impact

- **Paleontology.** Unlocking ancient secrets in rare or fragile fossils.
- **Energy.** Real-time 3D imaging of solid oxide fuels, bio-fuels, and energy storage materials under real operating conditions.
- **Materials science and engineering.** *In situ* imaging of functional nanomaterials and materials in extreme environments.
- **Biology and biomimetics.** Deriving inspiration from nature, such as structural biological materials or internal flows in insects, for novel engineering solutions.

## HXN – Hard X-Ray Nanoprobe

The HXN beamline and end station instruments are being designed and constructed within the NSLS-II project to explore new frontiers of hard x-ray microscopy applications with the highest achievable resolution. Currently, resolutions are limited to ~50 nm, which is still insufficient for probing interfacial structures critical in determining properties and functionalities of material and biological systems. The HXN beamline aims to enable x-ray experiments at spatial resolutions ranging from 10 to 30 nm, with an ultimate goal of ~1 nm. It also will provide four modalities of x-ray microscopy: x-ray fluorescence, nano-diffraction, coherent diffraction imaging, and differential phase-contrast imaging.

### Examples of Science Areas and Impact

- **Hierarchical relationships between structure and functional properties.** Such relationships exist in nearly all classes of materials—from **metals** to **biological samples**—and are key components in furthering the development of next-generation technological materials.

### HXN Beamline Capabilities

Source:	U20 undulator
Energy range and resolution:	6 to 25 keV / $1 \times 10^{-4}$ at 25 keV
Spatial resolution:	10 to 30 nm (V) by 10 to 30 nm (H)
Flux on sample:	$>5 \times 10^8$ ph/s

## SRX – Submicron Resolution X-Ray Spectroscopy

This beamline is being designed and constructed within the NSLS-II project to provide a unique combination of high spectral resolution over a very broad energy range and very high beam intensity in a submicrometer spot. The first branch is optimized for higher energies and uses Kirkpatrick-Baez (KB) mirrors; a second branch, optimized for lower energies from 2 to 10 keV, will use zone plate optics to create a focal spot below 30 nm. Available techniques will include x-ray absorption and x-ray fluorescence imaging, x-ray tomography, x-ray fluorescence trace element mapping, XANES absorption and XANES fluorescence spectroscopy, x-ray spectromicroscopy, and x-ray microdiffraction.

### Examples of Science Areas and Impact

- **Diverse samples from multiple disciplines.** Beginning with geoscientists' micro- and nanoparticles in suspension to microbial and other biological specimens, the sample stage will be able to accommodate a wide variety of samples from different scientific areas.

#### SRX Beamline Capabilities (KB Branch)

Source: Undulator  
 Energy range and resolution: 4.65 to 25 keV / 1.5 to 2.5 keV at 12 keV  
 Spatial resolution: Down to 60 by 60 nm at  $0.6 \times 10^{12}$  ph/s

## XFM – X-Ray Fluorescence Microprobe

A workhorse for biological screening, this beamline will provide spatially resolved characterization of elemental abundances and speciation in “as-is” samples at the micrometer scale with high throughput. It will be optimized to provide users with microfocused extended x-ray absorption fine structure ( $\mu$ -EXAFS) spectroscopy between 4 and 20 keV. The NSLS-II three-pole wiggler is an excellent source for  $\mu$ -EXAFS and XFM, providing—in a 1 to 10  $\mu$ m beam—flux densities two orders of magnitude higher than those at NSLS. This beamline will be a world leader for full  $\mu$ -EXAFS.

#### XFM Beamline Capabilities

Source: Three-pole wiggler  
 Energy range and resolution: 4 to 20 keV / 1 eV  
 Spatial resolution: 1 to 10  $\mu$ m variable

### Examples of Science Areas and Impact

- **Molecular speciation** of contaminants in the environment at the microscale.
- **Genetic control** of metal ion uptake, transport, and storage in plants relevant to agriculture and bioenergy.

- **Biogeochemistry** of nanotoxins in the environment.
- **Metal ions** in health and disease.
- **Mineral-fluid interface** reactions relevant to carbon sequestration.
- **Characterization** of paleontological, archeological, and cultural heritage artifacts.

## IRI – Full-Field Infrared Spectroscopic Imaging

This beamline will enable *in situ* studies of the organic composition of materials by vibrational spectroscopy, producing measurements from microseconds to days with micromolar detection sensitivity and submicron spatial resolution. It also will combine the high brightness and low noise of NSLS-II with a world-leading high-throughput imaging system.

### Examples of Science Areas and Impact

- **Catalysis.** In zeolite catalysis, simultaneously image reactants and products in real time for a mechanistic picture of *in situ* zeolite reaction chemistry.
- **Polymers.** In polymer-fiber composites, image the interface morphology under shear and stretch conditions *in situ*.
- **Microbiology.** In cellulose degradation by bacteria, rapidly image reaction location, rate, and chemical intermediates for improved biofuel production.
- **Medicine.** In Lou Gehrig's disease, simultaneously image the formation, structure, and associated cellular toxicity of intracellular superoxide dismutase aggregates.

#### IRI Beamline Capabilities

Source: Dual dipole magnets  
 Energy range and resolution: 500 to 4,000  $\text{cm}^{-1}$  / 1  $\text{cm}^{-1}$   
 Spatial resolution: ~1 to 5  $\mu$ m

## AIM – Advanced Infrared Microspectroscopy

AIM will enable high-resolution studies of the organic composition of materials by vibrational spectroscopy, producing measurements with submicromolar detection sensitivity and submicron spatial resolution. This beamline also will combine the high brightness and low noise of NSLS-II with a world-leading confocal imaging system.

#### AIM Beamline Capabilities

Source: Dipole magnet  
 Energy range and resolution: 500 to 4,000  $\text{cm}^{-1}$  / 1  $\text{cm}^{-1}$   
 Spatial resolution: ~1 to 5  $\mu$ m (diffraction-limited)

## Examples of Science Areas and Impact

- **Geosciences.** In small particulates from Earth and space, determine the composition of soil contaminants, space dust, and fluid inclusions.
- **Cultural heritage.** In artifacts such as paint cross-sections, evaluate the chemical makeup of each submicron-thick layer.
- **Microbiology.** In microbial remediation of the Gulf oil spill, determine reaction intermediates and resulting metabolites.
- **Medicine.** In bone disease, image the collagen and mineral structure and composition in microdamaged, treated, and repaired bone.

## Biology Village at NSLS-II

NSLS-II is a facility but also will be a community. Indeed, designers and planners envision a community of villages embracing the diverse but interconnected sciences that will be represented at NSLS-II beamlines, each of which aspires to be a best-in-class facility in its own realm. To provide for the full range of experiments needed to address 21st century science, an accommodating user access policy and a complement of science villages have been planned. The Biology Village is a concept that emerged while developing life sciences at NSLS-II beginning in 2007 ([www.bnl.gov/nsls2/sciOps/LifeSci/chronology.asp](http://www.bnl.gov/nsls2/sciOps/LifeSci/chronology.asp)). Planners anticipate that users will have facile access to multiple beamlines that might be needed for multitechnique approaches, and an integration of techniques and scientific discourse is expected to promote better scientific opportunities. A 2010 white paper for BER elaborates such opportunities ([www.bnl.gov/nsls2/docs/PDF/BER-whitepaper-Jan10.pdf](http://www.bnl.gov/nsls2/docs/PDF/BER-whitepaper-Jan10.pdf)).

In many respects, the concept of the Biology Village is a virtual one because meaningful interactions for all beamlines cannot always be physically proximate. Nevertheless, designers strive for compatible geographical placements of beamlines as much as possible. A significant aspect of physical coordination at NSLS-II will relate to the Laboratory Office Buildings (LOBs). Three LOBs are being built in the baseline project to house beamline staff and users and to provide laboratory resources in support of synchrotron experiments; two of these will be fully outfitted. The remaining LOBs will be constructed and completed later. To a large extent, these LOBs will serve as village centers, even though some Biology Village citizens may reside around the ring. Users and staff will have both physical and virtual homes in their village center.

## References

- Chen, Y.-H., et al. 2010. "Homologue Structure of the SLAC1 Anion Channel for Closing Stomata in Leaves," *Nature* **467**, 1074–80.
- Konuma, T., et al. 2011. "Time-Resolved Small-Angle X-Ray Scattering Study of the Folding Dynamics of Barnase," *Journal of Molecular Biology* **405**(5), 1284–94.
- Lee, W.-K., and J. J. Socha. 2009. "Direct Visualization of Hemolymph Flow in the Heart of a Grasshopper (*Schistocerca americana*)," *BMC Physiology* **9**(2). DOI: 10.1186/1472-6793-9-2.
- Nishino, Y., et al. 2009. "Three-Dimensional Visualization of a Human Chromosome Using Coherent X-Ray Diffraction," *Physical Review Letters* **102**(1), 018101.
- Yuan, P., et al. 2010. "Structure of the Human BK Channel Ca<sup>2+</sup>-Activation Apparatus at 3.0 Å Resolution," *Science* **329**(5988), 182–86.

## National Synchrotron Light Source-II

### Overview of Significant New Biological Research at NSLS-II

A primary mission of the DOE Office of Biological and Environmental Research (BER) is to provide research opportunities and scientific user facilities that advance the understanding of complex biological and environmental systems. Today, BER's scientific user facilities span a wide range of capabilities; however, the challenges associated with biological complexity create a need for new and innovative tools. The National Synchrotron Light Source-II (NSLS-II) will provide such tools by offering a range of new or improved techniques enabling multiscale exploration. These tools will aid studies at (1) the molecular level to understand how genes determine biological structure and function, (2) the cellular level to understand how molecular processes are coordinated to execute cell function, and (3) the level of microbial communities and higher organisms to understand how cells interact and respond to their environment.

This paper presents examples of significant new experiments with potentially high impact in biological research that will be enabled by NSLS-II. Specifically, the examples illustrate how the unique characteristics of the NSLS-II facility will:

- Enable the determination of atomic-resolution structures of macromolecular complexes involved in a wide range of areas, including those relevant to BER missions such as bio-fuel production, light harnessing, and contaminant cleanup.
- Facilitate measurements of structural and chemical dynamics with the time resolution necessary to fully characterize new enzymes and complex assemblies for understanding their functions as “macromolecular machines.”
- Provide a range of nanometer-resolution probes to image the complex structures and molecular chemistry of biological materials, including lignocellulosic biomass, microbes and microbial communities, and microbe-plant interfaces.
- Allow *in vivo* chemical imaging and dynamics of heterogeneous systems in their natural environments.
- Make available high-throughput technologies and a multitechnique approach for correlating genomics with structural and functional information.

### Atomic-Resolution Structures of Complex Macromolecular Systems

Macromolecular crystallography (MX) is the preeminent method for structural biology worldwide. Its intrinsic value is recognized by the selection committees who, in recent years, awarded five Nobel Prizes in Chemistry to Walker (1997); MacKinnon (2003); Kornberg (2006); Tsien (2008); and Ramakrishnan, Steitz, and Yonath (2009)—researchers who all heavily relied upon synchrotron radiation.

The frontier challenges in structural biology now include large macromolecular systems and viruses, membrane proteins, protein-protein complexes, and protein–nucleic acid complexes. However, these systems are very difficult to crystallize, and the crystals that are obtained often measure only a few microns along an edge. NSLS-II is expected to provide an ideal opportunity to use microcrystals for diffraction studies due to the facility's small electron-beam profile within the storage ring and, consequently, its world-leading x-ray brightness and flux density. Furthermore, for complex biological systems incompatible with conventional MX methods, new experimental approaches are under development that will take advantage of other unique characteristics of NSLS-II.

### Multiprotein Complexes

To date, the most common approach for determining structures of multiprotein complexes is to isolate the individual components, solve their structures separately, and reassemble the complex based on the structures of the individual components. However, stably isolating individual proteins for crystallization often is impossible. Moreover, the complex may not be a simple sum of the individual units; protein-protein interactions, for example, can cause structural alterations during assembly. Thus, crystallization of the entire protein complex is a much more desirable and accurate approach. Yet, diffraction from large multiprotein complexes is generally weak, and crystals, if obtained, are often small.

For example, microbial enzymes, including cellulases and hemicellulases, have been shown to efficiently degrade the microcrystalline cellulose structure as multiprotein complexes. *Caldicellulosiruptor* is a group of extreme thermophilic bacteria known to ferment polymeric carbohydrates at high rates. Integrated genomic and proteomic datasets identified the presence of highly active cellulolytic enzymes and revealed their unusual thermostability. Thus, *Caldicellulosiruptor* is a promising anaerobic bacterium for improving high-temperature biomass conversion (Dam et al. 2011). To date, mass spectrometric analyses have identified numerous multiprotein complexes involved in this fermentation, but no structural details are available. Successful crystallographic analysis of these complexes will require a source whose brightness can be focused efficiently into micron-sized x-ray beams. Indeed, one key advantage that NSLS-II will bring to the global MX community is its ability to determine structures from microcrystalline samples, such as the enzymes that catalyze critical transformation steps in lignocellulose breakdown.

## Membrane Protein Structures

Representing approximately one-third of the known gene sequences, membrane proteins are involved in numerous biological processes that take place at cell and organelle membranes, including cell recognition, signal transduction, chemical sensing, and transportation. Despite the importance of membrane proteins, determining their structure remains a grand challenge in structural biology. The key issue is that these proteins usually have to be extracted from their native environment of cellular and organelle membranes and reconstituted into detergent micelles for structural studies. In addition to potential loss of biological activity during solubilization, the presence of detergents makes crystallizing these proteins difficult and precludes extraction of protein-only information from the solution scattering data.

Embedding membrane proteins in 2D planar lipid bilayers that resemble their native environment in a liquid-like state represents a promising alternative for examining the structures of membrane proteins and their interactions with the lipid membrane. This approach already has had some success in cryo-electron microscopy studies of 2D membrane protein crystals (Thomas 2001). It also has been adapted for grazing incidence x-ray scattering and diffraction measurements, analogous to the transmission solution scattering and crystallographic methods for soluble proteins. In these structures, the x-ray scattering signal is determined by the electron density contrast of the protein against the constant background of the bilayer membrane structure. The contrast not only depends on the protein structure itself, but also varies as a function of protein orientation in the membrane and is even sensitive to membrane deformation from hydrophobic mismatching.

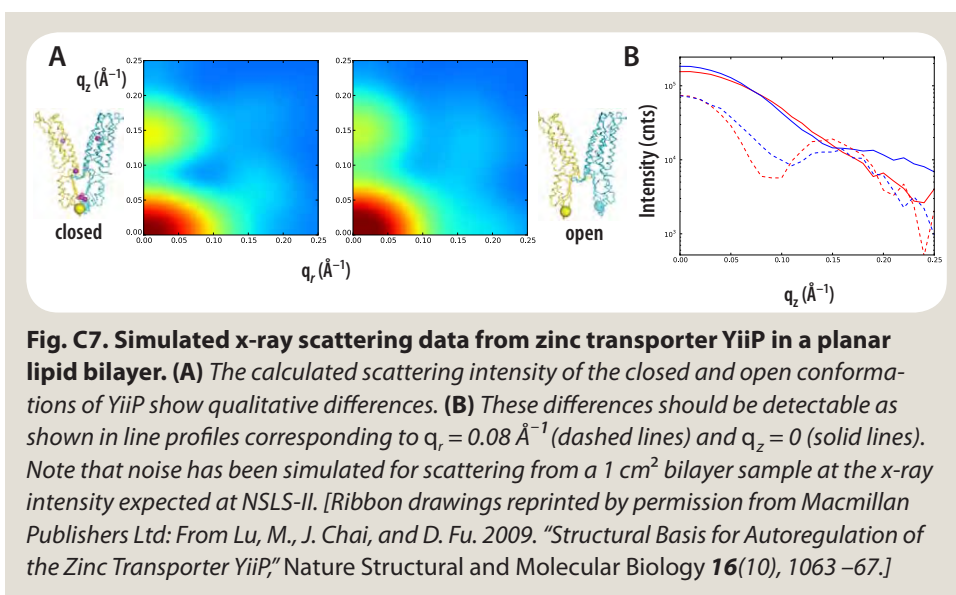
For example, YiiP is a membrane transporter that catalyzes  $\text{Zn}^{2+}/\text{H}^+$  exchange across the inner membrane of *Escherichia coli*. With its Y-shaped architecture, YiiP dramatically differs from most cylindrically shaped membrane proteins (Lu and Fu 2007). The incorporation of YiiP into the membrane necessitates reorganization of lipids surrounding the irregular transmembrane domain surface to minimize hydrophobic mismatch. The ensuing bilayer deformation would directly impact the active site for zinc transport. Molecular responses to hydrophobic mismatch may have great functional significance. Emerging evidence suggests that a large collection of lipophilic channel modulators act by deforming the bilayer

and directly binding to the protein-lipid interface. X-ray scattering data from YiiP in planar lipid membranes (see Fig. C7, this page) can reveal how protein conformations change depending on the presence of zinc ions. More importantly, due to the sensitivity of the scattering data to deformation in the lipid membrane structure, modeling these data may reveal the YiiP protein-lipid interface to help understand how lipids may reshape the active site for zinc transport.

To date, there have been reports of x-ray diffraction studies on 2D crystals of membrane-associated proteins (Lenne et al. 2000; Miller et al. 2008) and x-ray scattering studies of plant viruses adsorbed to a lipid membrane resembling a 2D solution (Yang et al. 2009). However, routine application of these methods in structural biology will necessarily entail exceedingly small scattering volumes (e.g.,  $\sim 5 \text{ nm} \times 1 \text{ cm} \times 1 \text{ cm}$ ). Such studies will require continued technical development and, more importantly, a bright source like NSLS-II to produce enough protein scattering signal above the water scattering background.

## Correlated Atomic and Electronic Structure of Metalloenzymes

Recent bioinformatics surveys show that approximately 47% of all enzymes with known 3D structures contain metal ions or complex centers (Waldron et al. 2009). Therefore, understanding the relationship between atomic and electronic structure is crucial for obtaining fundamental mechanistic insights into biology. This includes macromolecules involved in processes critical to DOE missions such as photosynthesis and water oxidation; nitrogen gas ( $\text{N}_2$ ) fixation and nitrogen oxide metabolism; carbon metabolism (e.g., methane and carbon dioxide); hydrogen gas ( $\text{H}_2$ ) metabolism; oxygen ( $\text{O}_2$ ) activation; and the sulfur cycle ( $\text{S}_0$  and  $\text{SO}_x$  metabolism). For example,  $\text{H}_2$  has enormous potential to serve as a renewable



and environmentally friendly energy alternative to fossil fuels. Nature has produced enzymes (hydrogenases) that drive the hydrogen cycle in the biosphere.  $H_2$  also is produced as a byproduct of  $N_2$  fixation by nitrogenase enzymes. In all microbial systems studied to date, the enzymes that catalyze the production of  $H_2$  from  $2H^+$  and two electrons are metallo-enzymes, which are among the most efficient  $H_2$ -forming and -consuming catalysts known.

Bioproduction of  $H_2$  using microbes must overcome several hurdles before it is commercially viable. For example, hydrogenase enzymes are rapidly inactivated in aerobic solution. Targeted bioprospecting thus is necessary to identify and characterize particularly active or stable hydrogenases that can be readily adapted for use in biosolar hydrogen production. One example is *Anabaena* sp. strain 7120, in which the enzyme is localized to the microaerobic environment. To increase this strain's  $H_2$  production, site-directed mutagenesis near the iron-molybdenum cofactor was performed and resulted in several variants that significantly increased their rates of  $H_2$  production (Masukawa et al. 2010). Single-crystal spectroscopy correlated with x-ray diffraction provides a way to promote, trap, and study reaction intermediates within the macromolecular crystal. Such studies will provide strategies to improve  $H_2$  production and further engineer microbial strains for enhanced photobiological production of  $H_2$  in an aerobic, nitrogen-containing environment.

## Synthetic Biology

A major difficulty in converting biomass into biofuels lies in its recalcitrance—the resistance of cellulose to enzymatic breakdown. Sequencing efforts and biochemistry have demonstrated that microbial enzymes are rather slow on their own, but nature has greatly enhanced their reactivity by linking them into large multienzyme collections known as “cellulosomes.” However, efforts to reproduce these effects *in vitro* using purified components have moved slowly (Nordon, Craig, and Foong 2009). As a result, such large multicatalytic complexes have not yet materialized in large-scale bioreactors.

Efforts in synthetic biology are under way for creating artificial cellulosomes of very high stability, defined composition, and reactivity tailored for specific substrates. However, structural characterization of these multienzyme complexes is extremely challenging. Though MX has been very successful at determining the structure of individual cellulosome components, a complete cellulosome has not yet been solved. Despite high-resolution structures of all individual cellulosome modules, the mechanism of enzymatic synergy remains poorly understood. Alternatively, solution x-ray scattering can provide direct shape information on artificial cellulosomes too large for MX. The

high-brilliance and high-throughput formats being developed at NSLS-II are ideally suited to the combinatorial nature of artificial cellulosome synthesis (see Fig. C8, this page). With automated high-throughput methods, structural information can be obtained rapidly from thousands of different designed cellulases. These capabilities have the potential not only to screen the constructs for activity (by enzyme assays), but also to read out shape complementarity directly and tune reactivity to complex substrates.

## Structural and Chemical Dynamics with Fast Time Resolution

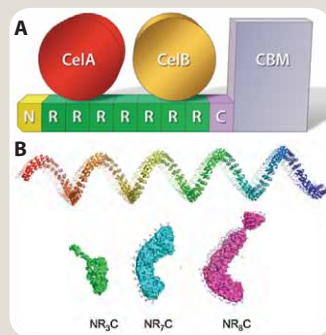
Fully understanding the function of multidomain proteins and multiprotein complexes requires understanding the dynamics of protein folding and protein-protein interactions. Though studying protein crystals is difficult, these complex systems can be studied in solution using x-ray scattering, footprinting, and spectroscopy.

## Transmembrane Protein Signaling

Membrane proteins play critical roles in cellular signaling processes and ion (or water) transport across the biological membrane. Many transmembrane proteins contain hydrophobic cores with strategically placed, charged residues that appear critical for their proper function. Observation of the structural dynamics surrounding these residues, as well as more global conformational changes in the macromolecule on biologically relevant time scales, can provide crucial information for understanding the mechanisms by which these proteins function.

X-ray footprinting of macromolecules is a unique approach for analyzing the solvent accessibility of individual residues in proteins as a function of protein conformation. X-rays generate hydroxyl radicals that covalently label solvent-exposed sites, which subsequently can be detected by mass spectrometry. By using the high x-ray flux from synchrotron radiation, microsecond time resolution can be achieved, providing a time-resolved high-resolution structural picture of solvent-accessible amino acid residues and “bound” water molecules.

**Fig. C8. Synthetic cellulosomes.** (A) Schematic diagram of a short artificial cellulosome unit. (B) Large cellulosomes with well-defined structures that can be constructed using repeated ankyrin domain templates. Solution scattering measurements on fragments of the template have confirmed the expected curved structure. [Courtesy of T. Aksel and D. Barrick, Johns Hopkins University]



An example is rhodopsin, a member of a group of proteins called the G protein-coupled receptor (GPCR) superfamily. GPCRs exhibit a conformational change when turned “on,” leading to interactions with other proteins and sending information across cell membranes to regulate many important molecular pathways (see Fig. C9, this page). Synchrotron x-ray footprinting has been used to study these different conformational states, providing a molecular map that pinpoints where water molecules sit inside the protein when it is off and on (Angel et al. 2009). Results indicate that water molecules rearrange in response to the protein being turned on and interact with key areas necessary for the protein’s function. Understanding how these proteins and associated signaling pathways are controlled can have a large impact.

Achieving higher x-ray flux density is the major barrier to providing high signal-to-noise footprinting data for the exploration of protein dynamics on shorter time scales. The damping wiggler insertion device at NSLS-II is expected to provide world-leading flux in the energy range of interest and would represent an entirely unique international resource.

### Combinatorial Enzyme Kinetics

Developing pretreatment chemistries with the associated enzymes to convert plant biomass to fermentable sugars for the cellulosic biofuels industry is a multifaceted effort. Work involves identifying enzymes expressed in bacteria and fungi; extracting, characterizing, and modifying the resulting proteins; and producing and testing them in a realistic biochemical assay. New methods are desired for all of these characterization steps to better understand deconstruction mechanisms.

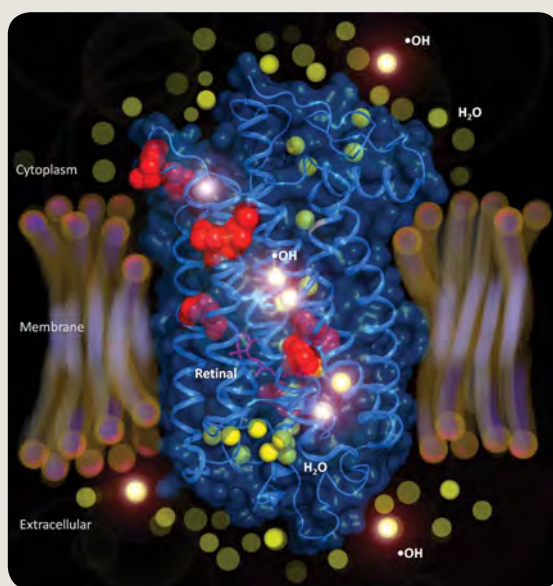
High enzyme loading is a major economic bottleneck for the commercial processing of pretreated lignocellulosic biomass to produce fermentable sugars (Gao et al. 2011). Optimizing the enzyme cocktail for specific types of pretreated biomass enables a significant reduction in enzyme loading without sacrificing hydrolysis yield. One approach to enzyme mixture development uses liquid robotics to explore full-factorial combinations of multiple (>10) enzymes, a method that can be efficiently performed in multiwell plates. This approach is suited to complementary high-throughput synchrotron structural measurements of plant materials during and after enzyme action. MX may be used to determine enzyme structures and thus help to elucidate function. SAXS and WAXS measurements can be conducted through an aqueous medium and quantify the breakdown of crystalline cellulose, hemicellulose, and other tissue structures. X-ray footprinting can probe tertiary structures in physiologically relevant solutions on millisecond time scales, and synchrotron spectroscopy techniques are available for probing different aspects of chemical and physical order in samples.

### Electron Transport

Flavin-dependent proteins catalyze a wide range of biochemical reactions—including aerobic and anaerobic metabolism, light emission, photosynthesis, DNA repair, plant phototropism, and the activation of oxygen for hydroxylation and oxidation reactions. While flavin adducts are critical intermediates in many flavoenzyme reactions, they rarely are detected even by rapid transient kinetics methods because of their high reactivity. Thus, electron transport in these systems requires a combination of structural and spectrophotometric analyses for characterizing the transient intermediates.

As an example, choline oxidase from *Arthrobacter globiformis* catalyzes the four-electron oxidation of choline to glycine betaine via two sequential reactions dependent on flavin adenine dinucleotide (FAD), with betaine aldehyde as an obligatory enzyme-bound intermediate. The crystal structure of choline oxidase revealed the presence of a C4a-oxygen adduct. The structure of the trapped flavin adduct derives from aerobic crystals of choline oxidase at cryogenic temperatures. Correlated single-crystal microspectrophotometry showed that the adduct forms rapidly *in situ* at 100 K. The high reduction potential of the enzyme-bound flavin is proposed to promote FAD reduction in the x-ray beam. This also facilitates C4a-O(OH) adduct formation, but an insufficient proton inventory at cryogenic

**Fig. C9. Radiolytic footprinting of membrane-bound rhodopsin.** This approach demonstrates the structural activation of bound waters as a function of receptor signaling status. X-rays ionize water molecules inside and outside the membrane protein to radicals (see  $\cdot\text{OH}$ , glowing spheres) that react with adjacent amino acid side chains. As the protein changes its structure during signaling, the pattern of water reactivity within the protein changes, reflecting the transmission of the signal through the membrane (see Angel et al. 2009).



temperatures prevents the decay of the complex. Thus, the use of complementary methods with time-resolved spectroscopic data and cryogenic temperatures provides a powerful strategy to study reactive intermediates in enzyme catalysis.

## Nanometer-Resolution Probes for Structural and Chemical Imaging

In addition to understanding the molecular-level structures of enzyme systems and how they relate to function, the next step in a systems biology approach is to understand the location and interactions of these molecules at the cellular level.

### Lignocellulose Ultrastructure, Chemistry, and Recalcitrance

Current understanding of the structural properties of plant cell walls that impart strength and resistance to degradation is limited, hindering development of better strategies for biomass deconstruction. For example, lignin greatly reduces the availability of cellulose for conversion into fermentable simple sugars, therefore lowering the efficiency of biomass conversion to ethanol or other biofuels. Lignocellulosic structure is heterogeneous on the nanoscale, challenging structural visualization.

Existing nanoscale imaging techniques, such as electron microscopy, have proven difficult for artifact-free imaging of biomass materials because of the possibly invasive sample preparation needed to meet the electron imaging condition of “thin sample.” Thus, new nanoscale imaging approaches are required for visualizing the lignocellulosic network to improve its breakdown efficiency.

A newly developed technique, x-ray diffraction microscopy (XDM), is a strong candidate for imaging samples that are tens of microns in size and thickness and close to their natural state (see Fig. C10, this page). XDM relies on the high coherence of advanced synchrotron sources like NSLS-II to image objects at a spatial resolution approaching the diffraction limit of the x-ray photons. The expected resolution with biological samples is 5 to 10 nm. In the past, XDM has shown the nanoscale structures of yeast (Shapiro et al. 2005; Huang et al. 2009; Nelson et al. 2010), bacteria (Lima et al. 2009), and chromosomes (Nishino et al. 2009). More recent development of scanning XDM provides unlimited field of view, allowing the technique to be applied to samples in more natural environments (Giewekemeyer et al. 2010; Dierolf et al. 2010). With the high brightness of NSLS-II, XDM can provide high-resolution imaging in structural investigations of biological materials—such as crystalline

cellulose within plant cell walls—that are not easily accessible by other existing methods.

Understanding the chemistry behind the recalcitrance of lignocellulose also is important. Enzymatic degradation offers one solution to the challenges of economically separating cellulose from lignin, motivating the need to study enzymatic degradation *in situ*. Scanning transmission x-ray microscopy (STXM) can provide chemically specific images of the organic composition of plant cell walls and be used for assessing the chemical effects of enzymatic degradation (Bernard et al. 2009). With the high brightness and broadband nature of NSLS-II, x-ray beams can be focused efficiently to sub-30 nm. This resolution will enable the visualization of specific locations within the cell wall where cellulosic enzymes are most active and the determination of the nature of the reaction’s chemical byproducts.

### Microbial Biofilm Ultrastructure, Composition, and Function

Microbial communities are known to significantly alter both physical and geochemical conditions in the subsurface. One continuously debated characteristic of a biofilm is its physical structure or morphology, which varies with the microbial species comprising the biofilm and other factors. Naturally, different types of biofilm structures can lead to very different biofilm functions, such as carbon dioxide sequestration and bioremediation capacity. Much of the research on microbial biofilm structure, both from the mathematical modeling and observational perspectives, has been carried out for microorganisms growing on flat substrates in the absence of

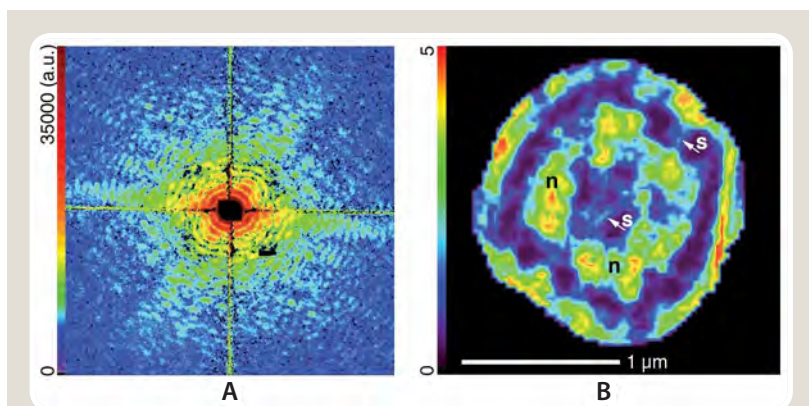


**Fig. C10. (A) Assembled diffraction pattern of a frozen-hydrated *Deinococcus radiodurans* bacterium.** The total exposure time is 7 minutes using focused 8 keV x-rays. The measured diffraction signals at the edge of the array extend to a 30 nm spatial half-period in the sample. **(B)** 2D reconstruction of *D. radiodurans*. Arrows with an “s” highlight a diagonal structure that may be the septum; areas labeled with “n” indicate possible nucleoid regions. [Reprinted with permission from Lima, E., et al. 2009. “Cryogenic X-Ray Diffraction Microscopy for Biological Samples,” *Physical Review Letters* **103**(19), 198102. Copyright 2009 by the American Physical Society.]

a porous medium. Two-dimensional studies have provided very important insights, but biofilm structures adhering in channel-and-cluster geometry, for example, cannot be described well in two dimensions. Likewise, mass transfer will be very different in 3D versus 2D.

Synchrotron-based imaging provides a unique methodology for quantifying microbial structure in 3D porous media. Conventional x-ray micro-computed tomography (CT) provides a spatial resolution of 5 to 10  $\mu\text{m}$ , insufficient to visualize individual microbes in porous media (Davitt et al. 2011). However, synchrotron nano-CT and fluorescence tomography are capable of imaging objects in 3D with a spatial resolution approaching 100 nm (Iltis et al. 2011). Imaging can be performed by attaching a suitable x-ray contrast agent to the biophase, either directly or via metal-labeled antibodies to the microorganisms. Ultimately, this approach will allow visualization of a variety of microbial biofilms in natural soils, as well as key contaminants readily imaged by synchrotron x-rays (e.g., U, Tc-99, Sr-90, Cs-137, and I-129).

### Symbiosis at the Plant-Microbe Interface

Recent studies have shown that endophytic bacteria in the environment of the plant root can enhance the rate of biomass production (Taghavi 2010). However, very little is known about the mechanism of plant growth promotion or the symbiotic relationship between plant roots and bacteria. Complex interactions between plant roots, microbes, and soil minerals occur in the rhizosphere—an intricate microenvironment consisting of the few millimeters of soil in the immediate vicinity of plant roots. The rhizosphere is directly influenced by root activity and the associated microbes; a detailed understanding of the biogeochemical interactions occurring within it has been limited by difficulties in observing these micro- and nanoscale processes *in situ* and in real time. Nanoscale x-ray imaging provides a nondestructive means to study the structure and transport of materials at the plant-microbe interface (Lombi and Susini 2009).

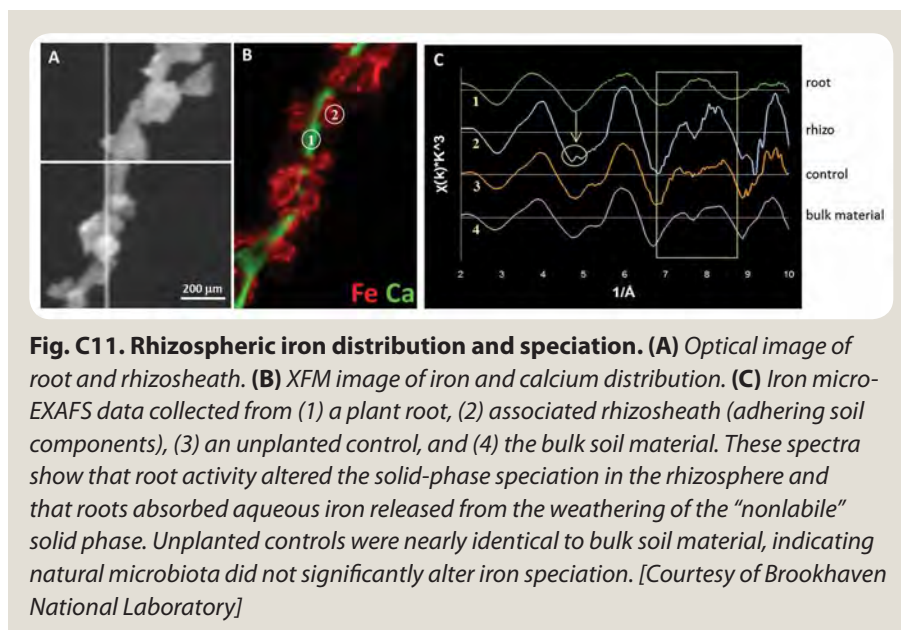
One particular issue for biofuels feedstock production on marginal lands (i.e., those with poor soil fertility) is to understand how endophytic bacteria assist plants in coping with nutrient-limited soil conditions (e.g., iron deficiency). Although needed for photosynthesis, iron is practically insoluble in most soils and natural waters and often is the “limiting” micronutrient for plant growth (Awad, Römheld, and Marschner 1994). Studying the role of endophytic bacteria in iron acquisition for

plants grown on marginal soils requires the *in situ* investigation of the heterogeneity in iron distribution and speciation within the rhizosphere (see Fig. C11, this page).

X-ray fluorescence microscopy (XFM) and fluorescence computed nanotomography (fCNT) are unique and powerful methods to study 2D and 3D elemental distributions and associations on the submicron scale. In addition, nanobeam x-ray absorption spectroscopy (XAS) can be used to determine the molecular speciation of an element (e.g., iron) at each pixel of an x-ray fluorescence image. With NSLS-II, biogeochemical processes will be observable for the first time at the subcellular level, providing new information on growth mechanisms. The facility’s advanced x-ray detectors also will provide rapid data rates, allowing quick examination of a wide range of root-microbe systems.

### Microbe-Mineral Interface Interactions

A great challenge in biogeochemistry is to understand processes at the microbe-mineral interface (Fredrickson and Zachara 2008). Although the ramifications of microbe-mineral interactions can be seen on a macroscopic scale, a microscopic approach is necessary to understand the underlying processes. Extremely helpful for this challenge is a nanoprobe instrument that can image the interface with very high spatial resolution and concurrently characterize it chemically (Benzerara et al. 2005). With its unmatched small emittance, NSLS-II is uniquely suited for high-resolution STXM experiments that will clearly improve knowledge of these processes. As an example, interactions at the microbe-mineral interface in soils and sediments can influence contaminant behavior. DOE’s Genomic Science program has identified a number of microbial systems that have the potential to remediate environmental contaminants. For example, *Shewanella* and *Geobacter*—two model systems—can



enzymatically transform uranium(VI), which is soluble and moves in groundwater, to uranium(IV), which is insoluble and precipitates out of groundwater as a biologically unavailable solid (Sheng and Fein 2010). Conversely, recent studies have indicated that microorganisms capable of bio-oxidation of U(IV) inhabit uranium-contaminated and -uncontaminated DOE sites. These organisms, including *Acidovorax ebreus* strain Tpsy and *Cosmobacter millennium*, can utilize U(IV) as the sole electron donor, potentially producing mobile uranium in anoxic environments. Essential to predictably modeling remediation efforts based on U(VI) reduction is an understanding of the microorganisms and physiology of anaerobic U(IV) bio-oxidation and the impact of this microbial metabolism on long-term sequestration of uranium in the environment.

### **Genetic Control of Metal Ion Uptake, Transport, and Storage**

Opportunities to examine how genetic variations in organisms affect their interactions with the environment are driven by the rapidly increasing quantity of nucleotide sequence data provided by DOE's Genomic Science program. In the future, reliance on plants for energy and food will place a strain on already-scarce prime agricultural land, shifting plant production to nutrient-limited soils, and will require growing crops with fewer inputs of primary macronutrients. Optimizing nutrient acquisition and use will rely on information about the genetic control of metal ion uptake, transport, and storage. Functions of ion-transport and -storage genes thus need to be determined. Identifying the organelle in which a particular element accumulates will allow rapid targeting of the genes responsible for these functions.

The ability to characterize the function of genes involved in elemental homeostasis requires instrumentation that provides suitably high detection sensitivity at submicrometer spatial resolutions. Additionally, a fundamental requirement for ionomic instrumentation is the ability to implement high-throughput analyses to achieve the required functional analysis of the genes and gene networks directly controlling the ionome. Results then need to be integrated with bioinformatic tools. Synchrotron-based x-ray fluorescence imaging techniques are extremely well suited to studies of these interactions at the cellular and subcellular level, potentially *in vivo*. Focused x-ray fluorescence beamlines at NSLS-II will be able to achieve dynamically variable spatial resolutions from just under 1  $\mu\text{m}$  to tens of nanometers. These beamlines simultaneously will provide world-leading photon flux to enable high-throughput analysis with an elemental detection sensitivity at the attogram level. Ultimately, relevant data can be obtained using whole-plant, high-resolution x-ray fluorescence computed microtomography (fCMT). Three-dimensional fCMT gives users a noninvasive, spatially resolved, and multielemental analysis technique that images the metal concentration of specific cell layers and organelles in plants as close to their natural state as possible.

### **In Vivo Imaging of Cellular Chemistry**

Following the tradition of NSLS, NSLS-II will provide the broadest spectrum of synchrotron light available to scientists in the United States. The low-energy, nonionizing infrared beams are ideally suited for *in vivo* imaging without the complications of radiation damage. Even with intense x-rays, techniques like x-ray footprinting will take advantage of the radiolytic cleavage of water to probe structural and functional biology in living cells.

### **Real-Time Chemical Imaging of Biomass Conversion**

In addition to understanding the structural and functional genomics of cellulolytic bacteria, elucidating how these processes occur in real time on real-world substrates such as lignocellulose also is necessary. New, noninvasive chemical imaging methods are needed to address spatially heterogeneous environments.

Synchrotron-based Fourier transform infrared (FT-IR) imaging provides a unique opportunity to image chemical changes in a heterogeneous system at high (micron) spatial resolution as a function of time. For example, the cell-wall architecture of *Zinnia elegans* was examined following acidified chlorite treatment and exhibited a breakdown of lignin and loss of polysaccharides (Lacayo et al. 2010). To date, real-time synchrotron-based FT-IR imaging has been performed only with single-pixel infrared detectors, which generate images in a raster-scan fashion, (i.e., one pixel at a time). This approach is exceedingly slow, limiting the time resolution of the experiments to a time scale of hours. However with NSLS-II, infrared light from multiple dipole sources will be used to illuminate a 128 by 128 pixel array detector, enabling millisecond (or better) time resolution. In addition, pixel oversampling can be employed to improve the spatial resolution by a factor of ten (i.e., to  $< 1 \mu\text{m}$ ). Lastly, the stability of the electron beam at NSLS-II will provide a 100-fold improvement in data signal-to-noise, a capability also necessary to achieve fast time resolution.

### **Structural Dynamics in Living Cells**

Despite the value of *in vitro* experiments, questions often remain as to whether observations from them truly represent events occurring within living organisms. *In vivo* observation of biomolecular structure, dynamics, and intermolecular interactions is thus a daunting but extremely desirable goal for understanding the natural function of biological molecules. Synchrotron x-ray footprinting is a promising technique for studying structural dynamics in living cells because it rapidly generates hydroxyl radicals with short pulses of intense x-rays. As proof of principle, x-ray footprinting was used to probe the structure of ribosomal RNA in frozen *E. coli* cells (Adilakshmi, Soper, and Woodson

2009), providing tertiary structural information and allowing observation of protein-RNA contacts with nucleotide resolution in living cells.

Living cell systems contain significant amounts of hydroxyl radical scavengers and thus require exposure times of hundreds of milliseconds with current technology. Such long exposure times may produce radiation-induced alterations that perturb the cellular machinery under investigation, resulting in poor data quality and limiting time resolution for observation of dynamics. Short exposure times are essential to drive this technology forward and allow *in vivo* x-ray footprinting of more complex systems and on physiologically relevant time scales. To reach these shorter exposure times, the high flux density of an NSLS-II damping wiggler source will enable the use of transient submillisecond or single-digit millisecond pulses, revolutionizing *in vivo* x-ray footprinting.

## Multimodal and High-Throughput Technologies

Becoming increasingly clear is that understanding the complexity of biological systems requires multimodal exploration. Thus, the next generation of scientific user facilities will need to provide integrated approaches that accommodate a wide variety of complementary techniques. NSLS-II will meet this important need by offering a wide range of capabilities that will enable multitechnique integration and cross-disciplinary approaches to doing science at the facility. Specifically, NSLS-II is planning on achieving this mode of research through a “biology village” environment. This village will strategically locate beamlines for scientific interaction and take advantage of programmatic synergies through shared equipment, technology, and human resources. As a jump-start to this concept, researchers are using complementary techniques from different NSLS beamlines to study the same sample,

enabling them to approach a scientific problem from several angles. Examples of technologies used in this integrative approach follow.

- **MX and SAXS** to understand the structure and function of a zinc peptidase (Aleshin et al. 2009).
- **SAXS and x-ray footprinting** to study the structure and folding of the tetrahymena ribozyme (Woodson 2010).
- **MX and XAS** to demonstrate the photoreduction of ferric myoglobin nitrate (Yi et al. 2010).
- **STXM and FT-IR** spectromicroscopy to study the organic composition and distribution of interplanetary dust particles (Sandford et al. 2006).
- **FT-IR and XFM** to examine bacterial reduction of chromium (Holman et al. 1999).
- **XFM and XRD** to elucidate the distribution and speciation of iron in the rhizosphere of *Alyssum murale* (Tappero et al. 2007).

In addition to a multitechnique approach for characterizing complex biological systems, NSLS-II also will make available high-throughput technologies for rapidly correlating genomics with structural and functional information. The tremendous amount of genetic information obtained through DOE’s Genomic Science program understandably has generated a huge number of variants to be screened and characterized. Without advanced photon sources, detectors, computers, robotics, and routines for data collection and analysis, a high-throughput approach would not be possible. Today, high-throughput technologies are becoming widely used in MX (Joachimiak 2009), SAXS (Hura et al. 2009), and XAS (Shi et al. 2005). At NSLS-II, these approaches also are expected to be extended to the imaging beamlines, where the high brightness of the source will permit—for the first time—rapid tomographic (3D) imaging at the nanoscale.

## References

- Adilakshmi, T., S. F. C. Soper, and S. A. Woodson. 2009. "Structural Analysis of RNA in Living Cells by *In Vivo* Synchrotron X-Ray Footprinting." In *Methods in Enzymology*, Vol. 468: "Biophysical, Chemical, and Functional Probes of RNA Structure, Interactions, and Folding—Part A," pp. 239–58. Elsevier Academic Press Inc., San Diego.
- Aleshin, A. E., et al. 2009. "Crystal and Solution Structures of a Prokaryotic M16B Peptidase: An Open and Shut Case," *Structure* **17**(11), 1465–75.
- Angel, T. E., et al. 2009. "Structural Waters Define a Functional Channel Mediating Activation of the GPCR, Rhodopsin," *Proceedings of the National Academy of Sciences of the United States of America* **106**(34), 14367–72.
- Awad, F., V. Römheld, and H. Marschner. 1994. "Effect of Root Exudates on Mobilization in the Rhizosphere and Uptake of Iron by Wheat Plants," *Plant and Soil* **165**(2), 213–18.
- Benzerara, T. H., et al. 2005. "Nanoscale Environments Associated with Bioweathering of a Mg-Fe-Pyroxene," *Proceedings of the National Academy of Sciences of the United States of America* **102**(4), 979–82.
- Bernard, S., et al. 2009. "Ultrastructural and Chemical Study of Modern and Fossil Sporoderms by Scanning Transmission X-Ray Microscopy (STXM)," *Review of Palaeobotany and Palynology* **156**(1–2), 248–61.
- Dam, P., et al. 2011. "Insights into Plant Biomass Conversion from the Genome of the Anaerobic Thermophilic Bacterium *Caldicellulosiruptor bescii* DSM 6725," *Nucleic Acids Research*. DOI: 10.1093/nar/gkq1281.
- Davit, Y., et al. 2011. "Imaging Biofilm in Porous Media Using X-Ray Computed Microtomography," *Journal of Microscopy* **242**(1), 15–25.
- Dierolf, M., et al. 2010. "Ptychographic X-Ray Computed Tomography at the Nanoscale," *Nature* **467**(7314), 436–39.
- Fredrickson, J. K., and J. M. Zachara. 2008. "Electron Transfer at the Microbe-Mineral Interface: A Grand Challenge in Biogeochemistry," *Geobiology* **6**(3), 245–53.
- Gao, D. H., et al. 2011. "Hemicellulases and Auxiliary Enzymes for Improved Conversion of Lignocellulosic Biomass to Monosaccharides," *Biotechnology for Biofuels* **4**(5). DOI: 10.1186/1754-6834-4-5.
- Giewekemeyer, K., et al. 2010. "Quantitative Biological Imaging by Ptychographic X-Ray Diffraction Microscopy," *Proceedings of the National Academy of Sciences of the United States of America* **107**(2), 529–34.
- Holman, H. Y. N., et al. 1999. "Real-Time Characterization of Biogeochemical Reduction of Cr(VI) on Basalt Surfaces by SR-FTIR Imaging," *Geomicrobiology Journal* **16**(4), 307–24.
- Huang, X. J., et al. 2009. "Soft X-Ray Diffraction Microscopy of a Frozen Hydrated Yeast Cell," *Physical Review Letters* **103**(19), 198101.
- Hura, G. L., et al. 2009. "Robust, High-Throughput Solution Structural Analyses by Small Angle X-Ray Scattering (SAXS)," *Nature Methods* **6**(8), 606–12.
- Itlis, G. C., et al. 2011. "Imaging Biofilm Architecture within Porous Media Using Synchrotron-Based X-Ray Computed Microtomography," *Water Resources Research* **47**, W02601. DOI:10.1029/2010WR009410.
- Joachimski, A. 2009. "High-Throughput Crystallography for Structural Genomics," *Current Opinion in Structural Biology* **19**(5), 573–84.
- Lacayo, C. I., et al. 2010. "Imaging Cell Wall Architecture in Single *Zinnia elegans* Tracheary Elements," *Plant Physiology* **154**(1), 121–33.
- Lenne, P. F., et al. 2000. "Synchrotron Radiation Diffraction from Two-Dimensional Protein Crystals at the Air/Water Interface," *Biophysical Journal* **79**(1), 496–500.
- Lima, E., et al. 2009. "Cryogenic X-Ray Diffraction Microscopy for Biological Samples," *Physical Review Letters* **103**(19), 198102.
- Lombi, E., and J. Susini. 2009. "Synchrotron-Based Techniques for Plant and Soil Science: Opportunities, Challenges and Future Perspectives," *Plant and Soil* **320**(1–2), 1–35.
- Lu, M., and D. Fu. 2007. "Structure of the Zinc Transporter YiiP," *Science* **317**(5845), 1746–48.
- Masukawa, H., et al. 2010. "Site-Directed Mutagenesis of the *Anabaena* Sp. Strain PCC 7120 Nitrogenase Active Site to Increase Photobiological Hydrogen Production," *Applied and Environmental Microbiology* **76**(20), 6741–50.
- Miller, C. E., et al. 2008. "Part I: An X-Ray Scattering Study of Cholera Toxin Penetration and Induced Phase Transformations in Lipid Membranes," *Biophysical Journal* **95**(2), 629–40.
- Nelson, J., et al. 2010. "High-Resolution X-Ray Diffraction Microscopy of Specifically Labeled Yeast Cells," *Proceedings of the National Academy of Sciences of the United States of America* **107**(16), 7235–39.
- Nishino, Y., et al. 2009. "Three-Dimensional Visualization of a Human Chromosome Using Coherent X-Ray Diffraction," *Physical Review Letters* **102**(1), 018101.
- Nordon, R. E., S. J. Craig, and F. C. Foong. 2009. "Molecular Engineering of the Cellulosome Complex for Affinity and Bioenergy Applications," *Biotechnology Letters* **31**(4), 465–76.
- Sandford, S. A., et al. 2006. "Organics Captured from Comet 81P/Wild 2 by the Stardust Spacecraft," *Science* **314**(5806), 1720–24.
- Shapiro, D., et al. 2005. "Biological Imaging by Soft X-Ray Diffraction Microscopy," *Proceedings of the National Academy of Sciences of the United States of America* **102**(43), 15343–46.
- Sheng, L., and J. B. Fein. 2010. "The Effects of Uranium Speciation on the Rate of U(VI) Reduction by *Shewanella oneidensis* MR-1," *Geochimica et Cosmochimica Acta* **75**(12), 3558–67.
- Shi, W. X., et al. 2005. "Metalloproteomics: High-Throughput Structural and Functional Annotation of Proteins in Structural Genomics," *Structure* **13**(10), 1473–86.
- Taghavi, S. 2010. "Genome Sequence of the Plant Growth Promoting Endophytic Bacterium *Enterobacter* sp 638," *PLoS Genetics* **6**(5), e1000943.
- Tappero, R., et al. 2007. "Hyperaccumulator *Alyssum murale* Relies on a Different Metal Storage Mechanism for Cobalt than for Nickel," *New Phytologist* **175**(4), 641–54.
- Thomas, G. H. 2001. "New Routes to Membrane Protein Structures, Practical Course: Current Methods in Membrane Protein Research," *Embo Reports* **2**(3), 187–91.
- Waldron, K. J., et al. 2009. "Metalloproteins and Metal Sensing," *Nature* **460**(7257), 823–30.
- Woodson, S. A. 2010. "Compact Intermediates in RNA Folding," *Annual Review of Biophysics* **39**, 61–77.
- Yang, L., et al. 2009. "Structure and Interaction in 2D Assemblies of Tobacco Mosaic Viruses," *Soft Matter* **5**(24), 4951–61.
- Yi, J., et al. 2010. "Synchrotron X-ray-Induced Photoreduction of Ferric Myoglobin Nitrite Crystals Gives the Ferrous Derivative with Retention of the O-Bonded Nitrite Ligand," *Biochemistry* **49**(29), 5969–71.

## Next Generation Light Source

# NGLS: A Transformative Tool for X-Ray Science\*



## Introduction: Need for the Next Generation Light Source

As a transformative tool for science, the Next Generation Light Source (NGLS) at Lawrence Berkeley National Laboratory (LBNL) will comprise an array of x-ray lasers providing temporally and spatially coherent pulses with unprecedented average brightness extending beyond 1 kiloelectron volt (keV). Individual lasers and beamlines will be optimized for specific applications requiring, for example, high repetition rates, time resolution to the attosecond regime, high spectral resolution, tunability, and polarization control. This powerful combination of capabilities will enable cinematic imaging of dynamics, determination of the structure of heterogeneous systems, and development of novel nonlinear x-ray spectroscopies. These unique resources will lead to a new understanding of how electronic and nuclear motions in molecules and solids are coupled and how functional systems perform and evolve *in situ*.

NGLS will dramatically impact a wide range of energy applications—from natural and artificial photosynthesis to catalysts, batteries, superconductors, carbon sequestration, and biofuels. Solving the complex long-term energy challenges facing both the nation and world is the subject of a wide-ranging set of reports from the DOE Office of Basic Energy Sciences ([science.energy.gov/bes/news-and-resources/reports/](http://science.energy.gov/bes/news-and-resources/reports/)). These reports highlight the urgent need for deeper understanding of the basic science underpinning energy technologies. NGLS—with its combination of high average power, ultrashort pulses, and coherence—is a revolutionary observational tool that will bridge the critical gaps in our understanding.

Today is a golden age for light sources. Storage ring-based synchrotrons routinely provide x-ray beams exploited by thousands of scientists annually to answer fundamental questions in diverse fields including human health, energy, and electronics and information processing. Synchrotron x-ray light sources have enabled scientists to (1) unravel the structures of biological macromolecules, essential for the design of new drugs; (2) reveal the properties of electronic materials for devices underlying the information technology revolution; and (3) provide the first glimpse of how energy conversion systems work at the atomic level. While these advances have been dramatic, there is much more to learn, and the array of x-ray lasers at NGLS will provide a foundation for major scientific advances in the 21st century.

\*Lawrence Berkeley National Laboratory prepared this and a companion document (p. 89) and approved post-workshop revisions to each.

DOE has built upon its 40-year legacy of x-ray light sources, continuously upgrading existing synchrotron facilities to keep them at the frontier. Recently, a remarkable new tool, the world's first hard x-ray laser, began operation. This resource—the Linac Coherent Light Source (LCLS) at the SLAC National Accelerator Laboratory—has exceeded performance expectations and opened the door to the x-ray laser era. Early experiments from LCLS are illustrating the promise of x-ray lasers and establishing a strong user community for them; yet a next-generation x-ray laser already is clearly needed to realize the full potential of this new tool. Based on a modern superconducting linear accelerator and leveraging the latest laser-seeding technologies, a next-generation source will provide the high repetition rate and high average coherent power needed to go beyond the initial stage of x-ray lasers. These capabilities will enable scientists to answer fundamental questions in a wide range of disciplines.

The current design concept for NGLS is a coherent, x-ray free-electron laser (FEL) array powered by a superconducting accelerator capable of delivering electron bunches to a suite of up to 10 independently configured FEL beamlines. Each beamline, operating simultaneously at a nominal repetition rate of 100 KHz, will be optimized for specific science needs. With multiple beam capabilities in each FEL beamline, up to 20 primary x-ray experimental end stations can operate in parallel, serving up to some 2,000 users per year.

Figure D1, p. 82, shows the major components of NGLS: the injector, laser heater, continuous-wave superconducting linac sections, linearizer and bunch compression systems, beam distribution, array of independent FELs, and x-ray beamlines.

The NGLS approach combines significant recent advances in high-brightness photocathode beam generation, acceleration, and transport with state-of-the-art superconducting radio frequency (RF) technology, as well as revolutionary concepts for laser-seeded FEL operation and undulator designs. The uniform pulse spacing at a high repetition rate will provide unprecedented capabilities at startup, accommodating more diverse and challenging experiments than those enabled by current or planned sources. This feature also offers the potential to exploit conceptual and technical advances in areas such as seed lasers, superconducting undulators, x-ray optics, and FEL oscillators. The distributed multibeam approach enables enhanced capacity by expanding the number of end stations. There also is tremendous opportunity to exploit advances in machine control and operation to provide greater flexibility and new capabilities for generating x-ray pulses tailored to specific science needs.

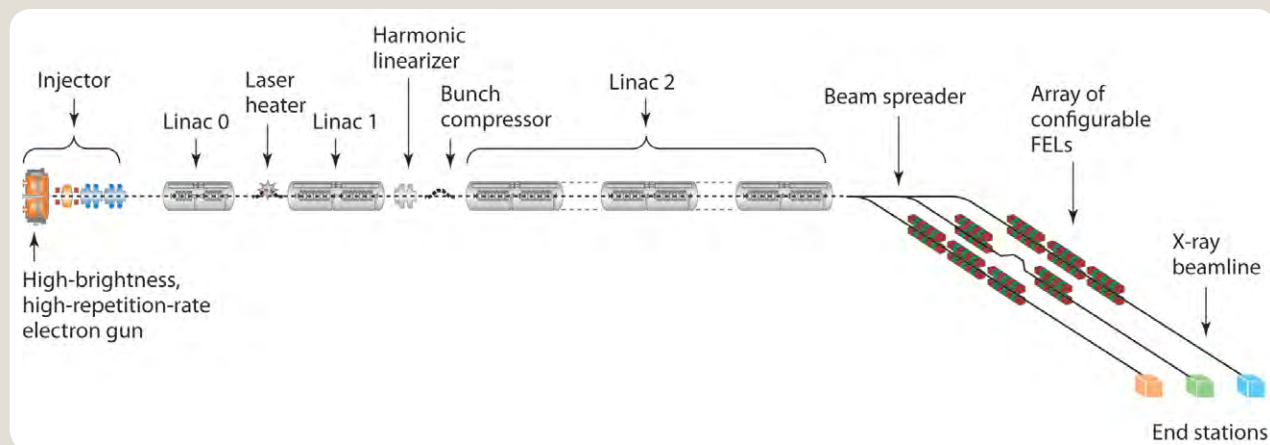


**Fig. D1. Schematic layout of the main components of NGLS (not to scale).** [Courtesy of Lawrence Berkeley National Laboratory]

No other technology can provide the average power, precision, and simultaneous utilization of multiple beams by many researchers. First-generation x-ray FELs with low repetition rates provide orders-of-magnitude improvement over existing sources, primarily in *peak* brightness and temporal resolution. However, *peak* brightness is not a substitute for *average* brightness, particularly when probing valence electron structure, chemical bonding, electron correlation, and charge dynamics in condensed matter systems. A next-generation light source is needed that provides (1) high average brightness along with ultrafast temporal resolution down to the attosecond regime; (2) polarization control; and (3) tunability through the important absorption edges of carbon, oxygen, nitrogen and the *L*-edges of first-row transition metals (i.e., beyond 1 keV in the first harmonic). High repetition rates are essential for capturing events that are rare or have low scattering rates and for probing the structures of heterogeneous ensembles *in situ*. Such rates also are needed to maintain the required *average* brightness for experiments in which the *peak* brightness is necessarily restricted to avoid significant perturbation of the sample.

These scientific requirements can be uniquely met by an array of x-ray lasers with high repetition rates, as envisioned for NGLS. As a unique tool for exploring the structure and dynamics of matter at fundamental scales of length, time, momentum, and energy, NGLS will provide many benefits and advantages over existing and planned light sources. The facility ultimately will feature the following capabilities:

- High pulse repetition rates (100 kHz or higher at each experimental end station and, ultimately, 100 MHz at specific end stations, approaching storage ring rates).
- Very high average flux and brightness [several orders of magnitude greater than third-generation rings and first-generation FELs, with peak powers of gigawatts and average powers of up to about 100 watts (W) per beamline].
- Pulse durations ranging from hundreds of attoseconds to hundreds of femtoseconds (fs).

- High temporal coherence of FEL output pulses (close to the Fourier transform limit).
- High transverse coherence (approaching diffraction limits).
- Control of time duration, bandwidth, and other longitudinal features of the pulses (i.e., the possibility of envelope shaping, modulation, or structuring and, ultimately, feedback-based control of these parameters).
- Excellent spectral resolving power without the need for monochromators.
- Synchronization of the FEL pulses to a seed laser or to other infrared (IR) or THz sources (with jitter or timing errors on the order of 1 to 10 fs).
- FEL output wavelengths (including harmonics) ultimately extending over more than two orders of magnitude, from  $\sim 10$  nm to  $\sim 1.2$  angstroms (Å).
- Precision, two-color x-ray pump–x-ray probe experiments.
- Precision pump-probe experiments with combined probes in the soft x-ray or extreme ultraviolet (EUV) range and pumps in the UV, optical, IR, THz, or other bands.
- Rapid polarization control.
- Multiple independent beamlines supporting a large user community.

The following sections describe NGLS baseline parameters for one preliminary design point while acknowledging the significant flexibility around these point parameters. No other existing or proposed facility can deliver the NGLS combination of ultrafast capability, high longitudinal coherence, high average power, multiuser operability, and flexibility in time structure (both repetition rate and pulse duration). Moreover, the facility's upgrade potential could provide both additional *capacity* (up to seven more FELs) and new *capabilities*—including (1) higher repetition rates and resolving power; (2) higher average and peak x-ray power; (3) longer pulses; (4) shorter- and longer-wavelength FELs; (5) additional synchronization and shaping possibilities; and (6) x-ray pulse

feedback control. The design options discussed in this Facility Paper are meant to illustrate the exciting scientific opportunities presented by the convergence of rapidly advancing FEL technology; superconducting accelerator technology; and sophisticated micromanipulation of high-energy, high-brightness electron beams. A detailed optimization of cost, performance, and risk has yet to be performed but will build on the baseline preconceptual design outlined here.

## Capabilities of Present Facilities

Briefly compared here are the capabilities of x-ray research tools that use ring-based sources, FELs, and high harmonic generation (HHG) lasers. Ring-based sources—particularly storage rings and energy recovery linacs (ERLs)—provide modest average power with low peak power. They support tunable devices that provide photon pulses at very high repetition rates and may be considered continuous wave (CW) sources for many applications. Storage ring-based sources are a proven technology, have well-established user communities, and will remain essential to a broad range of x-ray science. ERLs are an emerging technology not yet operating in the x-ray range. FELs can provide very high peak power as well as high average power and now operate in the x-ray range at lower repetition rates. As rapidly developing new capabilities, HHG sources provide modest average power in almost tabletop-sized sources but are not yet available in the x-ray range.

Existing storage ring-based, spontaneous x-ray sources produce a maximum degeneracy parameter (or photon number emitted per “coherence volume”) of about  $10^{-2}$  photons in a six-dimensional (6D) phase-space set by the Heisenberg-Fourier uncertainty principle. This degeneracy parameter is a fundamental description of what often is called brightness and reflects how far the pulse is from the ultimate Fourier transform and diffraction limits. Compared to third-generation synchrotron sources, future ERLs may produce more photons inside a smaller total phase-space volume and may achieve degeneracies on the order of  $10^2$  or  $10^3$ . FEL sources, through the coherent amplification process, produce highly degenerate x-ray pulses, with  $10^{10}$  or more photons per coherence volume. Seeded FELs further increase degeneracy by orders of magnitude.

Compared to storage rings, FEL sources provide increased *peak* flux (up to six orders of magnitude greater) and brightness or degeneracy (up to 10 orders of magnitude greater) because of the FEL amplification process. An additional advantage of FELs over ring-based sources is that electron pulses are prepared by a linear accelerator (linac) and then used only once to create x-rays. This enables precise control and tailoring of each individual x-ray pulse for particular scientific requirements. For example, 10 fs pulses with a large number of x-ray photons can be achieved only with FEL sources. The NGLS FEL complex will surpass the capabilities of existing x-ray facilities in numerous ways:

- Increased average photon flux and multiple, simultaneously operable x-ray beamlines will be provided.
- A moderately high peak flux will help avoid undesired damage to or perturbation of sensitive samples, thereby maximizing the fraction of useful photons in each pulse in many experiments.
- The combination of very high repetition rates with high photon flux in short pulses will open up entirely new areas of science.
- The multiple x-ray beamlines will provide flexibility to serve many different types of experiments with x-ray probes of tailored pulse structures.
- The potential for precise synchronization will allow for multidimensional spectroscopy and pump-probe experiments with multicolor probes in the x-ray range and pump pulses in the THz, IR, visible, UV, or x-ray range.
- Use of FEL seeding schemes will enable excellent tunability and, ultimately, feedback-based control of x-ray pulse stability and characteristics.

Normal-conducting, linac-driven FELs under realistic operating conditions are quite limited in repetition rate, resulting in an *average* coherent x-ray power comparable to storage rings. In comparison, the high repetition rate of NGLS will provide an *average* coherent power three orders of magnitude higher than storage rings and normal-conducting linac facilities of comparable beam energy and six orders of magnitude greater than HHG sources. The European XFEL (x-ray free-electron laser) will be based on cryogenic superconducting accelerator technology. This technology will provide average x-ray power similar to NGLS but by operating in a burst mode with 3,000 microbunches spaced by 200 ns and repeating at 10 Hz. Figure D2, p. 84 shows a comparison of the time structure of ring-based sources, HHG lasers, and FELs. A comparison of NGLS parameters with those of other existing and planned FEL facilities is shown in Table D1, p. 85.

HHG sources currently provide nanojoule (nJ) pulses up to about 100 eV, with 10 kHz repetition rate pulses. Future HHG sources are expected to improve in repetition rate and energy per pulse and reach soft x-ray wavelengths. NGLS capabilities for providing high average power and ultrafast pulses also will develop. These improvements will arise both as seed laser technology advances (potentially including the use of HHG for seeding) and as operation of low-charge, high-repetition-rate self-amplified spontaneous emission (SASE) is implemented—with a bunch charge of a few picocoulombs (pC), potentially at 100 MHz in a dedicated operating configuration. In this mode of operation, the short electron bunches radiate in a single or few optical modes, producing intense coherent radiation of a few femtoseconds duration and at an extremely high repetition rate limited by the total electron beam power (installed  $\sim 2$  MW capability). Producing  $\sim 10^8$  photons per pulse at 1 keV, an

average power of  $\sim 2$  W will be produced (three orders of magnitude greater than that projected for HHG sources).

## Machine Overview and Performance

NGLS will operate in a novel parameter regime, providing a suite of unique features compared with existing or planned x-ray light sources. Most notable among these capabilities are a high-repetition-rate (1 MHz), high-brightness electron source and a superconducting radio frequency (SCRF) electron linac operating in CW mode that will provide bunches at high average beam power with uniform bunch spacing. These bunches will be distributed via a spreader system to an array of independently configurable FELs. Each FEL will operate at pulse repetition rates three or more orders of magnitude higher than existing x-ray FELs and feature adjustable photon pulse power, central wavelength, polarization, and ultrafast temporal resolution down to the attosecond regime. The NGLS facility (see Fig. D1, p. 82, for major components) is designed to meet the most critical of anticipated science needs and provide a large user capacity. At the same time, the design takes into account the physics and engineering constraints of the accelerator and FELs as well as facility and

operating costs. The baseline design for a set of three simultaneously operable x-ray beamlines will serve a large number of experiments per year, with the capability of providing up to  $\sim 100$  W of average power to each of six end stations (two per FEL). Tunability will span the important absorption edges of carbon, oxygen, nitrogen, and the *L*-edges of first-row transition metals (i.e., to 1.2 keV in the fundamental and ultimately to 10 keV in the third harmonic). First-generation x-ray FELs with low repetition rates provide orders-of-magnitude improvement over third-generation synchrotron sources, primarily in *peak* power and temporal resolution. However, peak power is not a substitute for the level of *average* power or coherent power that will be provided by NGLS.

The primary spectral range of the NGLS baseline design will extend from 280 eV to 1.2 keV at the fundamental of the undulator emission (using undulators with different periods) and up to  $\sim 3$  keV at reduced intensity with the generation of harmonics. Flux may be controlled from  $\sim 10^8$  to  $\sim 10^{12}$  photons per pulse in the fundamental, depending on the desired wavelength, pulse duration, and repetition rate. Laser seeding will be implemented to produce pulses with duration as short as 250 attoseconds, with (1) temporal coherence

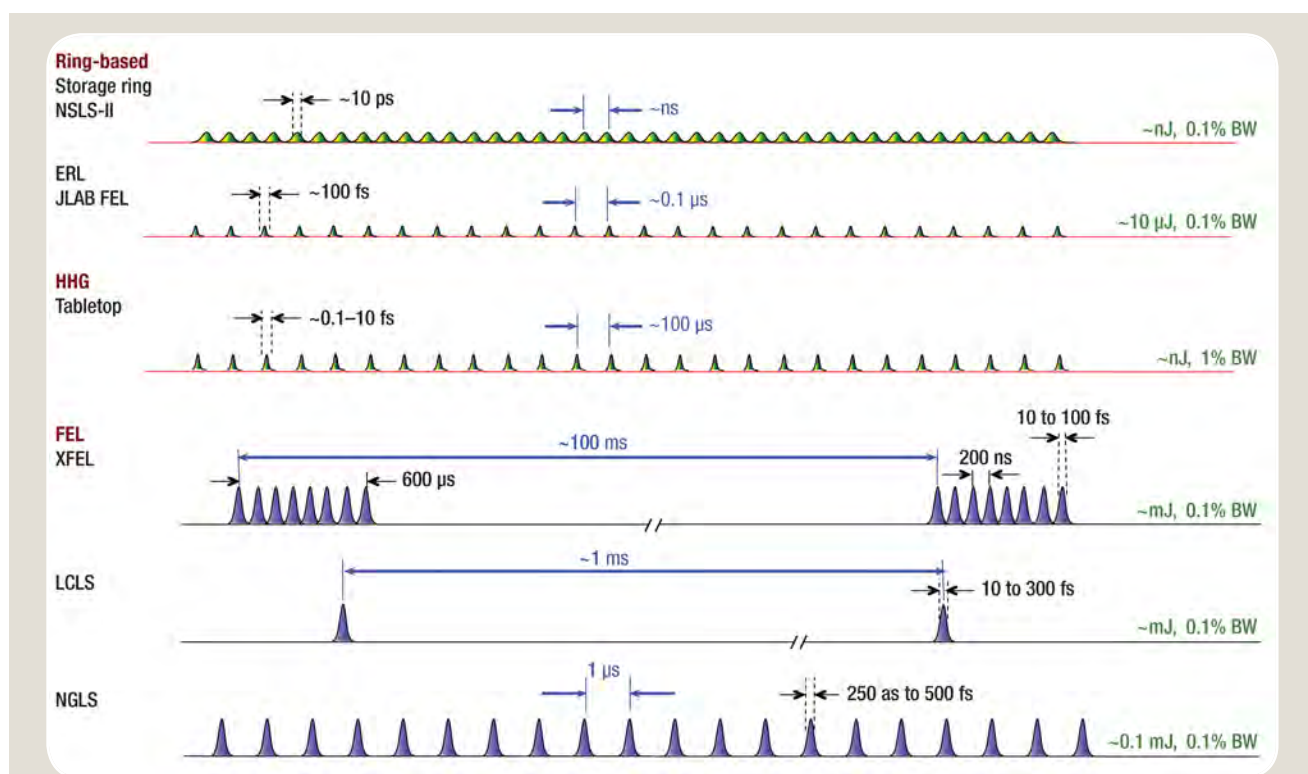


**Fig. D2. Comparison of x-ray pulse structure of different light source types based on current capability or near-term capability of facilities under construction.** Storage ring and FEL performance is for soft x-rays (around 1 nm). ERLs and HHG sources currently are not operating at soft x-ray wavelengths, and thus performance is shown for UV and EUV wavelengths. Pulse energy is in the central cone of undulator radiation, and NGLS values reflect the baseline design self-amplified spontaneous emission (SASE) FEL repetition rate. (The seeded FELs operate at up to 100 kHz and may produce similar pulse energy in some operating modes; NGLS may operate in SASE mode at an even higher repetition rate with reduced per-pulse energy.) [Courtesy of Lawrence Berkeley National Laboratory]

approaching fundamental transform limits, (2) the possibility of some control over chirp or longitudinal pulse-shape, and (3) synchronization of the x-ray pulses to end station lasers with femtosecond precision. One of the two seeded FELs will be capable of producing “two-color” x-ray pulses; the other will provide better energy resolution with longer pulses and high temporal coherence. The third FEL will be a nonseeded SASE device capable of operating at the full repetition rate of the linac, thereby providing very high average power x-ray beams. At about constant average electron beam power, NGLS can operate at a higher pulse repetition rate using bunches of lower charge and shorter duration but higher brightness. These bunches might enable lasing at shorter wavelengths or possibly the operation of a SASE beamline in so-called “single-spike” configuration, with each short electron pulse naturally radiating into, at most, a very few longitudinal modes. Table D2, p. 86 summarizes major FEL performance parameters for the baseline machine, assuming a point design of 300 pC bunch charge (potentially varying from a few picocoulombs to 1 nC). The nominal number of photons per pulse produced in each of the three baseline FELs (as a function of wavelength tuning) is shown Fig. D3, p. 86.

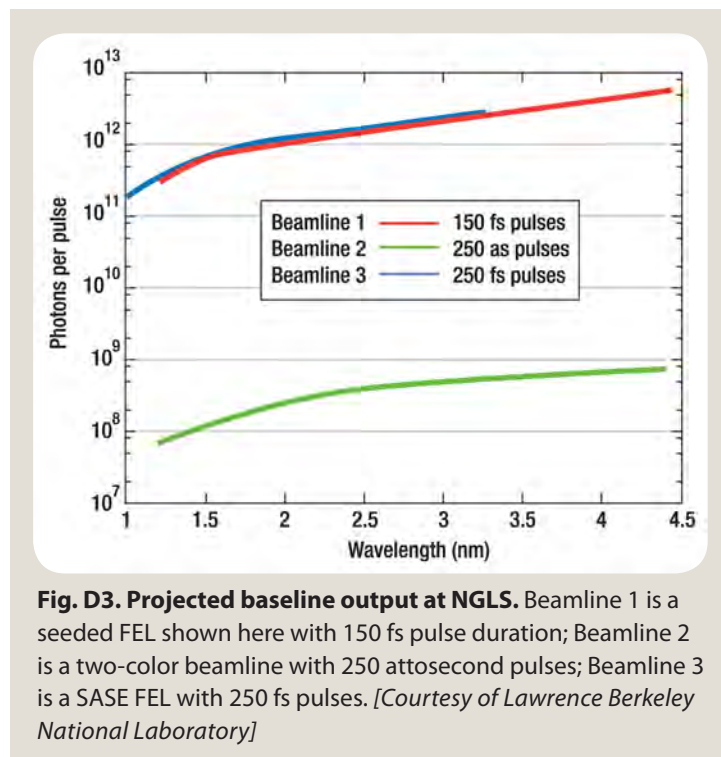
Bunches with the required high brightness will be generated at the desired high repetition rate by a state-of-the-art “very high frequency” (VHF) electron photogun, also undergoing emittance compensation and compression by ballistic and velocity bunching through the injector. Further compression will occur through a magnetic chicane in the linac before acceleration to the final beam energy. The machine is designed for an average current capability up to 1 mA, which is beyond the initial parameters of 300 pC and 1 MHz but consistent with a wide range of bunch charge and time structures. Beam brightness can be increased at lower bunch charge, and the gun and linac can accommodate a wide variety of beam conditions—including operation with low-charge, high-brightness, and ultrashort bunches for SASE-based, ultrafast x-ray production. The *baseline* design has been developed assuming a lower bunch charge of 300 pC but allows flexibility to increase versatility in performance. Higher-charge operation is anticipated for longer pulse durations or for higher peak current to improve efficiency of photon production. Further studies will be required to delimit the exact boundaries of the beam parameter space accessible by NGLS.

**Table D1. Comparison of NGLS FEL Baseline Parameters and Technical Features with Those of Other FEL Facilities Worldwide**

		Wavelength (nm)	Photon Energy (keV)	Pulse Duration (fs, FWHM)	Effective Repetition Rate (Hz)	Photons per Pulse	Bandwidth (approx.)	Energy per Pulse ( $\mu$ J)	Photons per Second	Average Power (W)
NGLS 1.8 GeV baseline parameters	High-power SASE	1	1.2	250	1.E + 06	1.E + 11	10 <sup>-3</sup>	2.E + 01	1.E + 17	19
		3.3	0.38	250	1.E + 06	1.E + 12	10 <sup>-3</sup>	6.E + 01	1.E + 18	61
	Seeded, limited	1.2	1	150	1.E + 05	1.E + 11	10 <sup>-4</sup>	2.E + 01	1.E + 16	2
		4.5	0.28	150	1.E + 05	1.E + 12	10 <sup>-4</sup>	4.E + 01	1.E + 17	4
Attosecond	1.2	1	0.25	1.E + 05	1.E + 08	10 <sup>-2</sup>	2.E - 02	1.E + 13	0.002	
	4.5	0.28	0.25	1.E + 05	1.E + 09	10 <sup>-2</sup>	4.E - 02	1.E + 14	0.004	
NGLS 2.4 GeV (estimated)	(Third harmonic)	0.75	1.8	250	1.E + 06	1.E + 11	10 <sup>-3</sup>	3.E + 01	1.E + 17	29
		0.125	5	250	1.E + 06	1.E + 09	10 <sup>-3</sup>	8.E - 01	1.E + 15	0.8
LCLS and LCLS-II		0.15	8.2	10 to 100	1.E + 02	2.E + 12	10 <sup>-3</sup>	2.E + 03	2.E + 14	0.24
		5	0.25	10 to 300	1.E + 02	7.E + 13	10 <sup>-3</sup>	3.E + 03	8.E + 15	0.34
FLASH		6.8	0.18	10 to 50	2.E + 04	2.E + 12	10 <sup>-2</sup>	6.E + 01	4.E + 16	1.15
		47	0.026	10 to 50	2.E + 04	2.E + 12	10 <sup>-2</sup>	8.E + 00	4.E + 16	0.17
European XFEL		0.1	12.4	100	3.E + 04	1.E + 12	10 <sup>-3</sup>	2.E + 03	4.E + 16	71
		6.4	0.2	100	3.E + 04	4.E + 14	10 <sup>-3</sup>	1.E + 04	1.E + 19	413
FERMI@ Elettra		3	0.41	~40	5.E + 01	1.E + 11	10 <sup>-4</sup>	7.E + 00	5.E + 12	0.0003
		10	0.12	~40	5.E + 01	1.E + 12	10 <sup>-4</sup>	2.E + 01	5.E + 13	0.001
SPring-8 XFEL		0.1	12.4	50	6.E + 01	1.E + 11	10 <sup>-3</sup>	2.E + 02	6.E + 12	0.01
SwissFEL		0.1	12	0.6 to 28	1.E + 02	1.E + 11	10 <sup>-3</sup>	2.E + 02	1.E + 13	0.02
		7	0.18	~1 to 28	1.E + 02	2.E + 13	10 <sup>-2</sup>	7.E + 02	2.E + 15	0.07
Pohang FEL		0.1	12	~50	6.E + 01	1.E + 12	10 <sup>-3</sup>	2.E + 03	6.E + 13	0.12
		1	1.2	~50	6.E + 01	4.E + 12	10 <sup>-3</sup>	8.E + 02	2.E + 14	0.05
Shanghai FEL		0.1	12	~75	5.E + 01	7.E + 10	10 <sup>-3</sup>	1.E + 02	3.E + 12	0.01
		9	0.13	~200	1.E + 01	5.E + 12	10 <sup>-3</sup>	1.E + 02	5.E + 13	0.001

The electron beam energy of 1.8 GeV has been chosen in the baseline design in order to produce 1.2 keV (1 nm) photons with readily available undulator technology (periods of

about 18 mm and minimum  $K$ -values of 0.8) but with a minimal accelerator footprint and cost. A more thorough analysis will be performed to select the optimal beam energy



for NGLS based on performance, costs, and systems optimization. Beamlines using different undulator parameters and technologies could achieve different performance or cost goals. For example, the same type of undulator with a 26 mm period and 4 mm gap will cover wavelengths from 13.4 nm (93 eV) to 1.8 nm (688 eV). An advanced planar polarized light emitted (APPLE) type of undulator with a period of 38 mm and magnetic gap of 5.5 mm (providing a beam clearance of 4 mm) will cover wavelengths from 12.5 nm (99 eV) to 2.6 nm (476 eV) and with arbitrary polarization. Very short period, superconducting undulators will allow even more options.

Choices for beam energy and pulse repetition rates necessitate adopting SCRF technology for the linac. Designs for the cryomodule and RF systems are based on the 1.3 GHz tera electron volt energy superconducting linear accelerator (TESLA) type of multicell cavities. The NGLS designers' choice of an accelerating gradient of approximately 14 MV/m is conservative in terms of present-day cavity capabilities; however, it is within a broad optimum of accelerating gradients when full construction and operating costs are considered.

**Table D2. Baseline Performance Parameters for the Three FEL Designs\***

	Beamline 1	Beamline 2	Beamline 3
<b>Type</b>	Seeded, narrow bandwidth	Two-color seeded	SASE
<b>Feature</b>	Short coherent pulses	Two-color x-ray pump-probe with adjustable delay and attosecond pulses	High average flux and brightness
<b>Pulse length (fs, FWHM)</b>	5 to 150	0.25 to 25	~5 to 250
<b>Wavelength range (fundamental, nm)</b>	1.2 to 4.5 (1.0 to 0.28 keV)	1.2 to 4.5 (1.0 to 0.28 keV)	1.0 to 3.3 (1.2 to 0.38 keV)
<b>Maximum repetition rate (kHz)</b>	100	100	1,000
<b>Total photons/pulse</b>	~10 <sup>11</sup> (150 fs, 1.2 nm) ~10 <sup>12</sup> (150 fs, 4.5 nm)	~10 <sup>8</sup> (sub-fs)	~10 <sup>11</sup> (250 fs, 1 nm) ~10 <sup>12</sup> (250 fs, 3.3 nm)
<b>Photons per 6D coherence volume</b>	~10 <sup>11</sup>	~10 <sup>8</sup>	~10 <sup>10</sup>
<b>Peak power (GW)</b>	~0.1 (1.2 nm) 1 (4.5 nm)	~0.05 (1.2 nm) 0.1 (4.5 nm)	~0.1 (1 nm) 1 (3.3 nm)
<b>Average power (W)</b>	~1 (150 fs, 1.2 nm) 10 (150 fs, 4.5 nm)	~0.001 (sub-fs) 0.1 (fs)	~0.1 (5 fs, 1 nm) 100 (250 fs, 3.3 nm)
<b>Power in third harmonic relative to fundamental (%)</b>	~0.1 (1.2 nm) 1 (4.5 nm)	~1	~0.1 (1 nm) 1 (3.3 nm)
<b>Relative bandwidth (% FWHM)</b>	~0.005 (150 fs, 1.2 nm) 0.02 (150 fs, 4.5 nm)	≥1.4 (sub-fs)	~0.2 (1 nm) 0.5 (3.3 nm)
<b>Polarization</b>	Variable, linear/circular	Variable, linear/circular	Variable, linear/circular

\*Details are given for example design points of pulse duration and wavelength and for the baseline 300 pC bunch charge. NGLS will be capable of a broad range of operating configurations, potentially extending the range of pulse lengths, photons per pulse, and repetition rate.

Further studies will determine an optimal set of operating parameters for NGLS performance, balancing risk among the injector, linac, and FEL. Besides offering the desired high pulse repetition rates, CW operation of the SCRF linac has another significant benefit: it allows for automated high-frequency feedback control to ensure quality and uniformity of the electron bunches. Consequently, jitter in x-ray pulse parameters is perhaps 10 times smaller than currently achieved.

## Design Optimization and Future Upgrades

The NGLS design concept embraces a strategy of phased implementation of FEL beamlines and is configured to take advantage of future advances in high-brightness beams, new concepts in FEL operation, and improvements in undulators and x-ray optics. The electron beam spreader is intrinsically modular. Capacity can be increased by adding additional spreader elements, FELs, and x-ray beamlines together with the corresponding housing, as shown in Fig. D4, this page. Capability can be increased not only by adding advanced FELs, but also by increasing the electron beam energy with a combination of extra linac sections and gradient increases. For example, increasing beam energy to  $\sim 2.5$  GeV and using undulators of  $\sim 12$  mm period will produce more than 3 keV in the fundamental and 10 keV in the third harmonic at power levels estimated to be 1% of those achievable in the fundamental. Future performance estimates are reflected in Table D1, p. 85. Similarly, an increase in beam energy to  $\sim 4$  GeV—together with developments in undulator technology that provide for 10 mm period devices—would permit lasing in the fundamental at 10 keV. In addition, modest improvements in cavity-quality factors could translate into significantly higher beam energies at fixed operating costs. Novel undulator designs—including very-short-gap superconducting undulators or possibly even electromagnetic undulators—could dramatically expand the NGLS wavelength with only small increments in beam energy.

Many of these areas of impact are, or will be, the subject of significant research efforts worldwide, and the NGLS project will be poised to take advantage of any incremental or revolutionary improvements.

## Layout, Conventional Facilities, and Utilities

The initial NGLS machine will consist primarily of a straight section (for electron acceleration and transport) of  $\sim 450$  m, which then will fan out over 180 m into multiple beamlines and end stations, as shown in Fig. D5, p. 88.

The major civil construction components are the linac vault and klystron gallery, spreader hall, FEL vault, and experimental hall. An exceptionally stable foundation will be needed to support the entire NGLS machine. Long-term settlement and vibration must be minimized for efficient machine operation and optimum performance. Additional space will be required for the cryogenics plant, including associated gas storage, a test facility for cryomodule acceptance, and machine maintenance activities. Space also will be needed for conventional facilities like cooling towers, low-conductivity and chilled water systems, and electrical switching and transformer stations.

Roughly 10 m of combined concrete and earth shielding will enclose NGLS. Beam dumps, located at the ends of both the spreader and each FEL, will be positioned below floor level and inclined downward. Concrete vaults surrounding the beam dumps will further isolate these units from the main portion of the machine and soil in which they are buried.

The width and height of the injector and linac enclosure will be sufficient to house beamline components and support equipment and utilities while maintaining a walkway for installation and removal of a full cryomodule. The shielding enclosure in the spreader region will have an increased width necessitated by the shallow initial angle between the branch lines and main beam axis. This wide hall will transition to individual branch enclosures for the FELs downstream of the final bend magnet on each branch. The FEL vaults extend an additional  $\sim 120$  m to the shielding end-wall and the beginning of the experimental hall.

Spacing between FELs will be about 6 m, adequate for two or more photon branch lines. X-ray beamlines will extend about 50 m from the first optic, housed within the shield wall, and will reach end stations near the far wall of the experimental hall. A walkway of  $\sim 10$  m at the end of the photon beamline will provide access for the installation

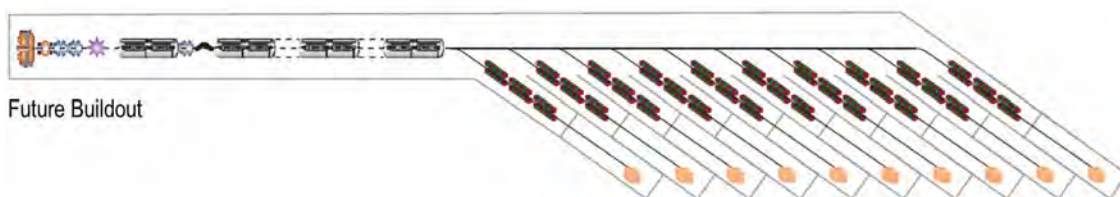


**Fig. D4. Future NGLS buildout with a 2.5 GeV linac and additional spreader elements and x-ray beamlines.**

[Courtesy of Lawrence Berkeley National Laboratory]

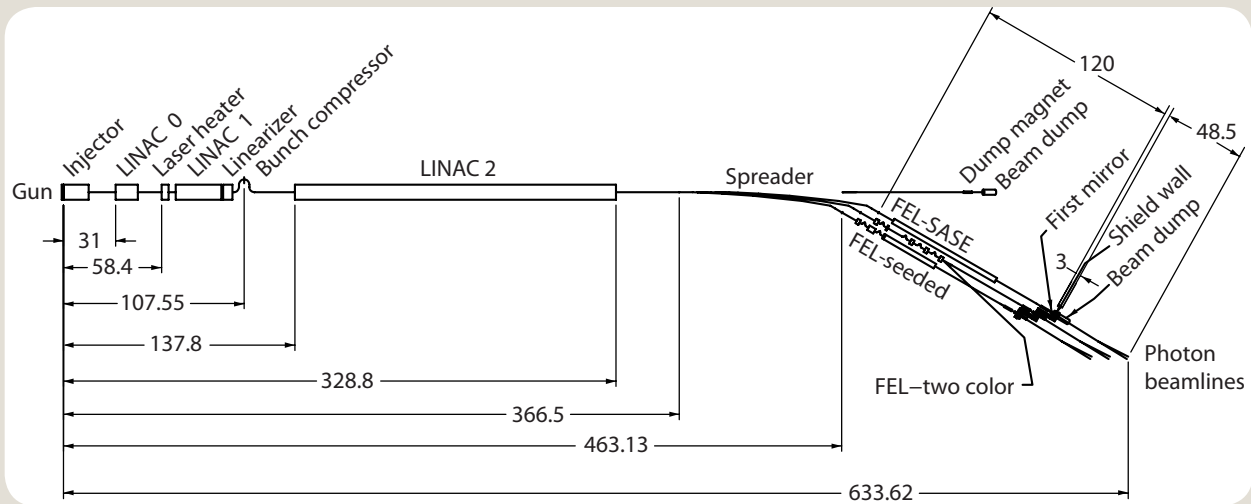


**Fig. D5. NGLS layout (in meters).** [Courtesy of Lawrence Berkeley National Laboratory]

and removal of experimental equipment. Electronic racks, utilities, and support equipment will be on the floor above the experimental floor, leaving the ground floor clear of heat and noise sources. Laser systems for the photocathode

source, FEL seeding, and end station experiments will be housed in separate, temperature-controlled rooms outside the radiation-shielded enclosure.

## Next Generation Light Source

# New Biological Research Enabled by NGLS

## Imaging Structure and Function in Heterogeneous Ensembles

### Overview

**B**iological function is profoundly influenced by changes in molecular conformation that span many decades, at periods from picoseconds to milliseconds. Such dynamics are central to the function of biological systems and macromolecular machines—including enzymes involved in DNA repair and replication; ribosomes responsible for protein synthesis; dynamic membrane protein channels and signaling complexes; and organelles and the hierarchical structures of the cell, the fundamental unit of life. An enhanced understanding of the role of dynamics in biological function has both fundamental and practical importance, ranging from understanding how cells work to designing better therapeutics.

Modern synchrotrons with scattering and diffraction techniques have revolutionized the field of structural biology by enabling the routine structure determination of isolated or simple complexes of macromolecules. The Next Generation Light Source (NGLS) will enable entirely new methods for imaging biomolecules in native environments (i.e., in solution rather than crystal form) and capturing their dynamics during functional cycles. Of paramount importance to achieving these advances will be the ability of NGLS to deliver ultrafast x-ray pulses at a high repetition rate. This, in combination with newly developed sample delivery systems and x-ray detectors, will allow researchers to collect billions of images of single molecules. From these images, probing thousands of conformational states accessible to biomolecules in solution will be possible.

The combination of high repetition rate and high pulse power will make NGLS a natural resource for a number of imaging and spectroscopic techniques, including the “diffract and destroy” nanocrystallographic method currently under development at free-electron lasers worldwide. The following sections describe the complementary techniques of fluctuation x-ray scattering (fXS), billion-snapshot coherent diffractive imaging, and associated advanced computational methods of manifold mapping that will be realized for the first time using the high-repetition-rate x-ray lasers at NGLS.

### Fluctuation SAXS – Molecular Structures in Native Environments

Understanding biological processes at a cellular level requires detailed knowledge of the structure and dynamics of large

macromolecular machines. Currently lacking are the tools necessary for dynamic imaging of such biological machines—in operation, in native environments, and at the nanoscale. Small- and wide-angle x-ray scattering (SAXS and WAXS) techniques (Andersson et al. 2009) offer tremendous potential and are being used to great advantage in combination with crystallography (Putnam et al. 2007). However, the full potential of these scattering techniques remains unrealized because the required exposure times at existing x-ray sources are orders of magnitude longer than the rotational diffusion times of the sample particles. Thus, the scattering data are spherically averaged, effectively projecting the three dimensions of the structure onto one dimension. The restricted information available from these one-dimensional (1D) projections is insufficient for unambiguous structure determination.

NGLS x-ray lasers will provide the first capability for high-quality SAXS and WAXS with exposure times much faster than rotational diffusion time scales, thereby eliminating the spherical averaging limitation. For example, the rotational diffusion time for an ~300 nm by 20 nm test sample of tobacco mosaic virus (TMV) in pure room-temperature water will be <140 ns; for smaller macromolecules, the time will be from picoseconds to nanoseconds. The high-speed SAXS and WAXS scattering snapshots will reveal a wealth of additional structural information. This information—contained in fluctuations about the mean SAXS signal (i.e., modulations in the nominally radially symmetric SAXS signal)—cannot be obtained by conventional techniques. Unlike SAXS and WAXS, which project three dimensions onto one, the snapshot “WAXS” patterns from NGLS will show 2D variation, projecting three dimensions onto two and thus providing much more information.

This powerful approach, known as “fluctuation x-ray scattering” (fXS), originally was proposed by Kam 30 years ago (Kam 1977; Kam, Koch, and Bordas 1981). To date, this method has been considered intractable—due not to the pulse speed per se, nor the difficulty of analysis, but because at least one scattered x-ray per particle per snapshot must be measured within a rotational diffusion time. A recent experimental test (Saldin et al. 2010a) using a fixed distribution of gold nanorods as a model 2D system at the Advanced Light Source (ALS) has shown that *ab initio* reconstruction is possible without relying on any of the modeling assumptions normally required for analysis of SAXS data. However, the model experiment using TMV (still a highly favorable case) in water at room temperature is not yet feasible at existing storage rings. The capabilities of NGLS x-ray lasers will finally enable this powerful fXS

approach for determining 3D structures of macromolecules in their native environments.

**Theory.** The resurgence of interest in Kam's correlation-averaging approach has not happened in a vacuum. The long-planned single-molecule diffraction (SMD) method (diffract and destroy) poses significant data analysis problems that have been under study. In this case, the idea to use correlation averaging was rediscovered independently by Saldin and coworkers (Saldin et al. 2007). Indeed, it may be that SMD data can be reconstructed only by correlation averaging (Shneerson, Ourmazd, and Saldin 2008). The reconstruction in fXS requires solving two phase problems: (1) getting from the experimentally determined autocorrelation function to the 3D single-particle diffraction pattern and (2) inverting the diffraction pattern to retrieve the 3D image (as in coherent diffraction imaging). However, in spite of this increase in research activity, the latest publications have offered no solution of the full 3D reconstruction problem for a modern fXS experiment, even in simulations.

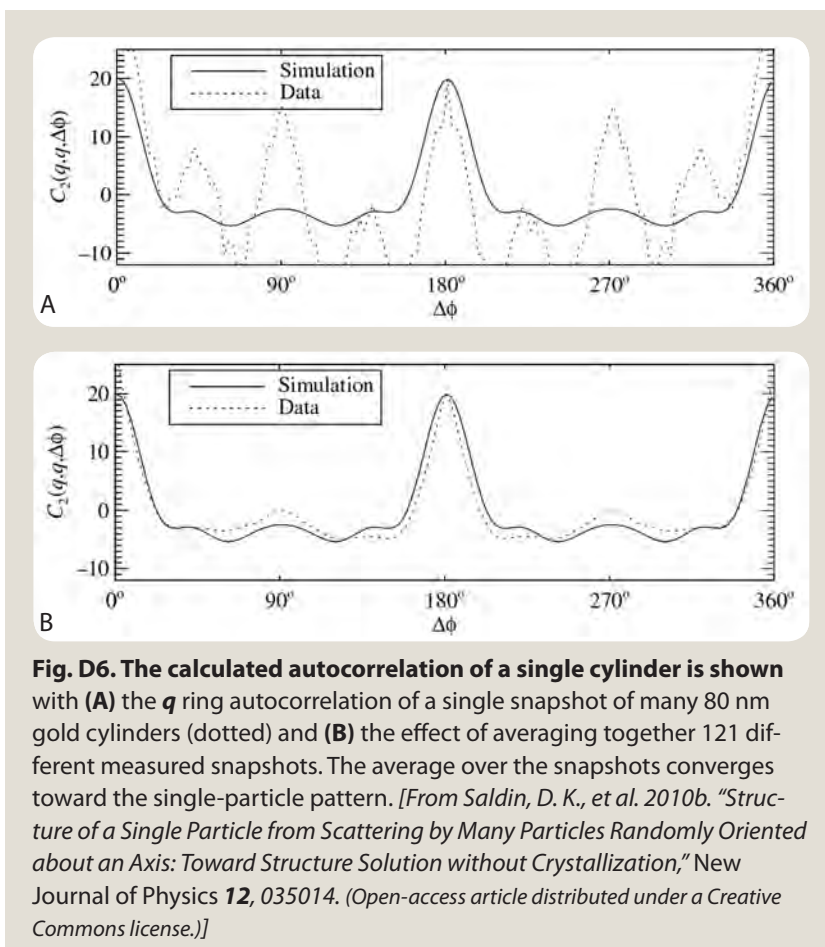
**Prior Experiments.** Good progress has been made on the 2D analogue of fXS, in which identical particles lie in a plane differing only by rotation about an axis parallel to the x-ray beam. In an fXS experiment at ALS, 80 nm-long gold rods were dispersed on membranes, with the rod orientations being random about one axis only. About 100 diffraction patterns of different areas were recorded, and the autocorrelation around a single  $q$  ring was calculated for each pattern. The averaged autocorrelations “converged” toward the autocorrelation of one particle. This derivation of a one-particle pattern from a measurement of an ensemble of particles is the essence of correlation averaging (see Fig. D6, this page). The final step consisted of phasing these data to reconstruct a 2D image of one typical gold rod. This work represents the first successful *ab initio* experimental demonstration of the Kam fXS method, albeit in two dimensions (Saldin et al. 2010b; Saldin et al. 2011).

**Theory Developments.** A full 2D theory was described and used successfully to reconstruct a set of simulated diffraction patterns of  $K$ -channel membrane protein molecules, again randomly oriented about one axis (Saldin et al. 2010a). Researchers used this same theory to reconstruct the set of patterns from the gold rod samples in the experiment cited above. A 3D theory, still using spatial correlation averaging, also was developed for the SMD experiment and used successfully to reconstruct the 3D image of a protein molecule (Saldin et al. 2009). Recent theoretical developments show that *ab initio*

image reconstruction of 3D objects (randomly oriented) is possible from fXS data using algorithms developed for protein crystallography and coherent diffractive imaging. Furthermore, current algorithms available for shape reconstruction from SAXS data can be extended to incorporate fXS data. Although the computational complexity of the problem is significant, modern computational approaches are expected to eliminate the most significant bottlenecks. To determine the structure of intermediate states during the reaction cycle of macromolecular machines, the theory of fXS can be extended following the lines of Andersson et al. 2009 (see also Kam 1977). The latter work demonstrates that a time-resolved series of WAXS data from an evolving mixture of species (as observed in time-resolved measurements) can be decomposed into curves of individual species of (meta) stable intermediates. A similar technique can be applied to fXS data, enabling the investigation of time-resolved structural changes of large macromolecular machines in near-native environments.

**Source Requirements.** Proposed parameters of NGLS x-ray lasers fit the following fXS requirements.

- *Ultrafast x-ray pulse durations*—Scattering patterns must be measured with x-ray exposures that are faster than molecular rotational diffusion times (typically subpicosecond under native conditions).



- *High average photon flux and high flux per pulse*—The number of scattering particles and scattering efficiency are limited. Proposed NGLS flux per pulse is comparable to an exposure time of roughly 1 s on state-of-the-art SAXS beamlines, indicating that, with sufficient data, high-resolution 2D fXS patterns can be efficiently obtained. Scattering patterns from multiple exposures can be summed together (with appropriate processing of individual patterns).
- *Coherence*—A fully coherent beam provides significant simplifications in data analysis of mixtures and does not impede analysis of samples with a single structural species.

The optimal choice of energy for an fXS experiment will be determined by the nature of the problem investigated. Available photon energies at NGLS, ranging from hard x-rays (using harmonics) to the water window (wavelength  $\sim 2$  nm), allow for imaging relatively small systems such as enzymes (using hard x-rays) or very large systems such as viruses and large macromolecular assemblies like polysomes. NGLS will enable studying samples in buffer at physiological conditions, without viscosity enhancers, and at room temperature with no need for cooling to slow particle diffusion.

**Sample Environment and Data Acquisition.** By using a liquid-water mixing jet (DePonte et al. 2008) running single file across the NGLS beam—combined with suitable substrates, protein concentrations, jet velocity, and delay lines—fXS data can be obtained at intermediate time points spanning subnanoseconds to seconds within the duty cycle of a macromolecular machine. The high repetition rate of NGLS will allow collection of hundreds of thousands of patterns at suitably chosen time points along the continuous or droplet beam. NGLS will operate in the diffract and destroy mode to avoid any effects of radiation damage on the diffraction patterns (Chapman 2009). Given data rates associated with these experiments, efficient detector technology is instrumental to the success of these studies. An exciting possibility is the development of hardware solutions for data reduction. Obtaining fXS data involves computing angular correlations of the scattering patterns. If this essential step can be performed on the detector with dedicated hardware while data are collected, a significant infrastructure bottleneck is resolved.

**Outlook.** The fXS technique overlaps with single-molecule diffraction studies that typically provide more detailed information than the ensemble-based fXS method. Due to the underlying experimental design of an fXS study, the technique lends itself to a higher level of automation. Assuming a conservative, particle injector–limited data acquisition rate of 10 kHz, 10 million images can be obtained within 20 minutes, sufficient time to assemble a high-resolution fXS dataset. Given its high-throughput nature (akin to industry-standard protein crystallographic data acquisition), automated fXS can be an essential tool in discovering novel drugs acting on membrane proteins or other large macromolecular machines

not amenable to routine biophysical techniques used in structure-based drug design.

## Gigashot Imaging of Heterogeneous Ensembles with Manifold Mapping

NGLS will produce  $\sim 10^{10}$  diffraction snapshots per day. Combined with advanced manifold-based analytical techniques, this capability will elucidate the role of heterogeneity in biological systems; enable 4D imaging of molecular machines; and provide unprecedented, statistically validated access to the operation of molecular factories.

Radiation damage severely limits the information that can be gathered from a single copy of soft-matter objects before they are destroyed. To boost the weak scattered signal, current structural techniques average the data gathered from many objects assumed to be identical. Examples include well-established techniques such as crystallography and cryo-electron microscopy (cryo-EM; Frank 2006), as well as “scatter and destroy” methods recently enabled by x-ray FELs (Shneerson, Ourmazd, and Saldin 2008; Solem and Baldwin 1982; Neutze et al. 2000; Gaffney and Chapman 2007; Fung et al. 2009). Mounting evidence, however, indicates that structural variability not only is common at the molecular level, but also important to function and that “structure” in soft matter is neither static nor immutable (Ludtke et al. 2008; Fischer et al. 2010; Scheres et al. 2007; Brink et al. 2004; Yu et al. 2008; Levin et al. 2007). Although vital for controlling soft-matter processes, understanding structural variability and dynamics has remained elusive.

*The ability to collect and comprehend information from systems spanning a broad heterogeneity landscape is essential to control complex dynamic processes for efficient energy conversion, carbon sequestration, and enzymatic reactions honed by nature over millennia.*

## Accessing Dynamic, Heterogeneous Systems by Manifold Mapping

Random snapshots obtained from members of a heterogeneous ensemble are correlated, otherwise there would be nothing to characterize the set. In the absence of noise, these correlations force the snapshots to lie on a hypersurface—a manifold—whose dimensionality is determined by the number of degrees of freedom available to the system. A rotating rigid body observed in far-field diffraction, for example, has three (orientational) degrees of freedom and thus produces a 3D manifold (Fung et al. 2009). The additional degrees of freedom of a dynamic, nonrigid system give rise to higher dimensional manifolds (Schwander et al. 2010) as illustrated in Fig. D7, p. 92. Similarly, the reaction coordinates of an ongoing process are reflected in the dimensionality of the data manifold (Nadler et al. 2006).

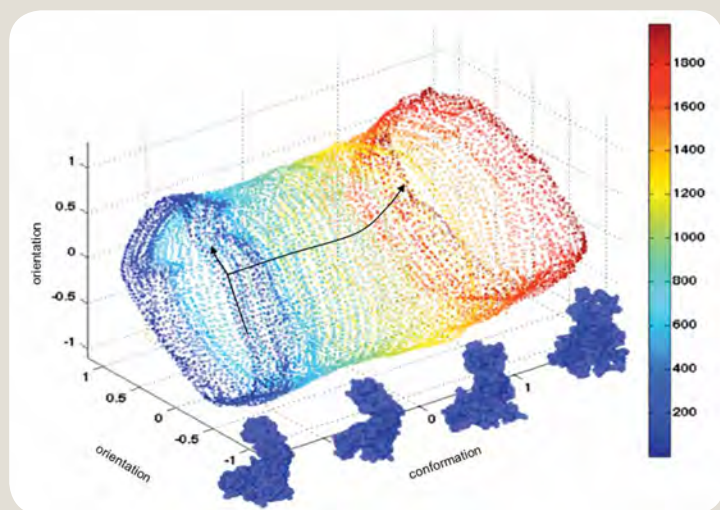


**Fig. D7. Manifold traced out by simulated diffraction snapshots of an adenylate kinase molecule as it unfolds due to heating.**

*Insets show the molecular structure at points on the manifold. Advanced analytical techniques offer a route to reconstructing the 3D structure of the molecule during its evolution, essentially generating a 3D movie of the unfolding process. [From Schwander, P., et al. 2010. "Mapping the Conformations of Biological Assemblies," New Journal of Physics **12**, 035007. (Open-access article distributed under a Creative Commons license.)]*

The data manifold contains the entire information content of the dataset. Often, this manifold must be determined in the presence of overwhelming noise. Noise-robust algorithms for manifold mapping have been demonstrated with simulated and experimental data down to  $\sim 10^{-2}$  scattered photons per pixel in the presence of background scattering, with signal-to-noise ratios as low as about  $-20$  decibels (Fung et al. 2009; Schwander et al. 2010; Moths and Ourmazd 2009).

Comprehending the information content of the dataset is tantamount to being able to "navigate on the manifold" to reach any desired point. For example, a researcher may wish to reconstruct the 3D structure of an enzyme at a particular point in its conformational landscape. A 3D model is equivalent to the ability to produce any 2D projection at will. On the data manifold, this involves navigating from a certain point (i.e., a given conformation) along directions of pure orientational change, thus producing any desired 2D projection of the given conformation (see Fig. D7, this page). Similarly, one goal may be to extract the conformational changes observed from a certain direction, equivalent to moving along the manifold in a direction of pure conformational change.

*Manifolds swept out by random sightings of heterogeneous dynamic systems can be used to compile 4D maps (i.e., "3D movies") of these systems. Key to this approach is the availability of a sufficient number of snapshots to define the manifold to the required granularity. The unique characteristics of NGLS, particularly the combination of high flux per pulse and high repetition rate, are essential to this capability.*

## **Conformational Heterogeneity and Dynamics: Molecular Machines**

Molecular machines undergo discrete and continuous conformational excursions and induce similar changes in the substrate. Using ultralow-signal snapshots with no orientational or timing information, these changes can be mapped by manifold-based analytical techniques (Schwander et al. 2010; Giannakis et al. 2010).

When a molecular machine possesses discrete conformational states, such as the closed and open conformations of the energy-relevant enzyme adenylate kinase, simulations show that snapshots are automatically and accurately sorted into two different manifolds.

The error probability is  $8.5 \sigma$  at  $4 \times 10^{-2}$  scattered photons per Shannon pixel in the presence of Poisson noise (Levin et al. 2007) as shown in Fig. D8, p. 93. The ability to separate discrete conformations with remarkable fidelity and determine the orientation from which each snapshot emanates is an indication of the efficient use that manifold-based approaches make of the information content of the entire dataset. The natural eigenfunctions of the scattering manifold allow identification of directions corresponding to orientational and conformational changes. In this framework, 4D maps (3D movies in time) can be compiled of continuous conformational changes in molecules and their assemblies. Such approaches currently are being used to map conformations of molecular machines using cryo-EM images (Fischer et al. 2010; Schwander et al. 2010) and x-ray FEL diffraction snapshots (Schwander et al. 2010).

The fundamental limit to this approach is set by information-theoretic considerations. Roughly speaking, the experimental snapshots have been "sorted" into classes (i.e., "bins"), and the state of the system from which each class originated identified. The number of bits required for each class is determined by the size of the object, number of distinguishable states accessible to the system, and resolution of the method of observation (Shneerson, Ourmazd, and Saldin 2008; Fung et al. 2009; Schwander et al. 2010; Moths and Ourmazd 2009). When the signal is so low that the information content of the dataset is smaller than the number of bits required to label its classes, the process breaks down. At this very low limit (Elser 2009), total accumulated

snapshots can be traded against the dose per pulse (i.e., compensate for extremely low scattered signals by collecting more snapshots).

The practical limit is set by the number of snapshots in the collection, which, in turn, depends on the source repetition or detector readout rates. As a specific example, recovering the structure of a rigid object to  $\sim 1$  nm resolution typically requires  $\sim 10^4$  snapshots (Fung et al. 2009). Distinguishing between 100 different conformations of a molecule with a single conformational degree of freedom increases the number of snapshots to  $\sim 10^6$  (Schwander et al. 2010). By comparison, LCLS currently produces  $\sim 10^7$  snapshots per day, limiting the size, complexity, and resolution at which the conformations, configurations, and dynamics of a system can be studied.

*NGLS will be capable of generating more than  $10^{10}$  snapshots per day. Systems with  $\sim 10^6$  conformational states can be studied, assuming a one-day experiment and  $10^4$  snapshots are required to recover the 3D structure of each configuration to  $\sim 1$  nm resolution. The largest number of conformational states mapped so far is  $\sim 50$  (Fischer et al. 2010).*

The projected capabilities outlined above must be compared with those expected from alternative techniques when NGLS commences operation. Cryo-EM undoubtedly will continue to make progress in investigating molecular machines; datasets obtained with this method currently span  $\sim 10^6$  snapshots. While further progress is possible in key steps such as sample preparation and microscope operation, increases of more than 100-fold in the size of cryo-EM datasets are difficult to envisage. Such increases still would be 100 times smaller than capabilities offered by NGLS. More importantly, introducing time resolution in cryo-EM has not been possible other than by slowing reactions chemically.

*The high repetition rate and time-resolved capabilities of NGLS represent an inherent advantage in studying dynamic systems on nano to atto scales. Gigashot digital cellular microscopy with NGLS offers an unprecedented capability to reconstruct selected regions of a large number of objects with orientational, conformational, and configurational degrees of freedom. This capability provides a route to statistically validated examination of molecular factories beyond the limits set by radiation damage.*

## Diffraction and Destroy at High Repetition Rates

An important consideration for diffractive imaging applications is that they will rely on fundamentally new implementations of

the diffract and destroy method pioneered at FLASH (the Free-Electron Laser in Hamburg) and LCLS. Both fXS and billion-shot diffractive imaging deal with the problem of random sample orientation in new ways that capitalize on the capabilities of NGLS x-ray lasers. These techniques will exploit the tremendous advances in experimental capabilities that have been driven by first-generation x-ray FELs. In particular, the Spence laboratory at Arizona State University has developed a liquid “aerojet” injector for generating a 1 MHz stream of  $\sim 1$   $\mu\text{m}$  liquid droplets at velocities of  $\sim 10$  m/s (see Fig. D9, p. 94). This tool has been successfully demonstrated in initial experiments at LCLS (using protein nanocrystals in solution). The temporal stability and uniform pulse spacing derived from the NGLS superconducting linac operating in CW mode will be essential for synchronization with future high-speed aerojet injectors.

## Potential Biological Targets

Modern synchrotrons and macromolecular crystallographic methods have revolutionized the field of structural biology by enabling the routine structure determination of isolated or simple complexes of macromolecules. However, conventional structural determinations of biological macromolecules disregard the presence of heterogeneous conformations by assuming identical objects. Moreover, current x-ray methods for structural determination depend

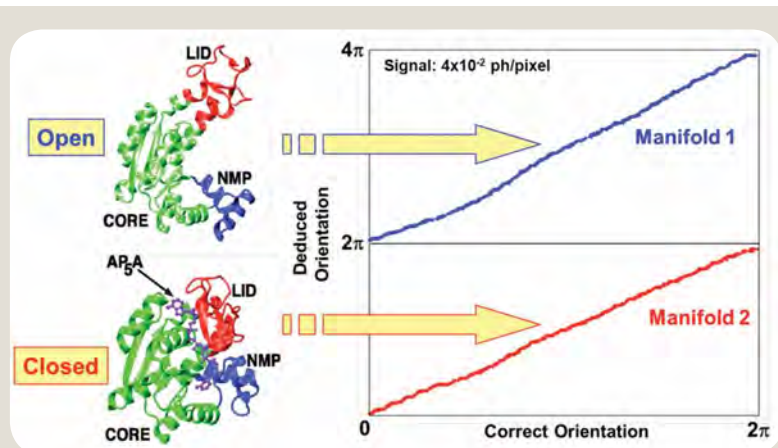


**Fig. D8. Manifold mapping of conformational states in molecular machines.** This mapping technique separates snapshots from different conformations and finds the orientations within each set with no a priori knowledge. A mixture of diffraction snapshots from the adenylate kinase molecule in its open and closed conformations is presented to noise-robust versions of graph-theoretic techniques at signal levels corresponding to 0.04 photons per pixel at 0.18 nm. The snapshots are automatically sorted into different manifolds and their orientations determined. The  $8.5\sigma$  separation between the two manifolds implies extreme fidelity in separating different conformations. [From Schwander, P., et al. 2010. “Mapping the Conformations of Biological Assemblies,” *New Journal of Physics* **12**, 035007. (Open-access article distributed under a Creative Commons license.)]

**Fig. D9. Hydrated bioparticle jet for interaction with the FEL beam.** The jet provides a controlled chemical environment (e.g., for living cells or membrane proteins). A coaxial high-pressure gas sheath focuses the entrained liquid from a nozzle large enough to avoid clogging.

The concentration of the particles is arranged to ensure 100% hit rate, with each FEL pulse striking one particle, or several particles in the case of fXS.



[From DePonte, D. P., et al. 2008. "Gas Dynamic Virtual Nozzle for Generation of Microscopic Droplet Streams," *Journal of Physics D: Applied Physics* **41**(19), 195505.]

on growing ordered crystals of proteins that necessarily inhibit the investigation of different conformations and the dynamic motions connecting them. Yet, biological function is known to be profoundly influenced by subtle (and not so subtle) changes in conformation that span many decades in time, from picoseconds to milliseconds.

To advance the understanding of biological processes at a cellular level, detailed knowledge of the structure of very large macromolecular machines is an absolute necessity. The high repetition rate of x-ray lasers at NGLS will enable entirely new methods for (1) imaging biomolecules in native environments (e.g., in solution rather than crystal form), (2) capturing the dynamics of molecules during their functional cycles, and (3) visualizing cellular components in their native context. The dream of "imaging biological function" will be realized for the first time. The following sections present a few representative examples of key areas of biology that will be transformed by NGLS capabilities for imaging heterogeneous ensembles and conformational dynamics of biomolecules in native environments.

## Nanogeobiology

Recent advances in microbiology have demonstrated that microorganisms are intimately involved in the transformation of inorganic minerals at or near the Earth's surface (Weber, Achenbach, and Coates 2006). Microbe-catalyzed electron transfer (ET) to metal ions in these minerals lies at the heart of many such transformations, which are performed by redox-active proteins that efficiently transport electrons over long distances with minimal loss of free energy (Fredrickson

and Zachara 2008). These redox proteins are exquisitely tuned for facile ET to different solid-phase electron acceptors. A basic research goal in biogeochemistry is understanding the natural diversity and impact of microbial redox proteins and the processes by which microorganisms have been shaping Earth over geologic periods. Because microbe-mineral ET processes influence the carbon cycle and contaminant distribution and mobility, understanding them is crucial for safeguarding our natural environment.

Multiheme *c*-type cytochromes expressed by iron(III)-reducing bacteria are among the best-characterized redox-active microbial proteins that interact with minerals and soluble metal ions (Shi et al. 2009). Physiological studies of these bacteria have identified a number of outer-membrane multiheme *c*-type cytochromes (e.g., MtrC) that interact with mineral surfaces. However, no high-resolution structure of MtrC or related proteins exists to rationalize the pathway of electron transfer. Consequently, detailed mechanisms of ET often are derived from model studies on simpler redox-active proteins that are easier to handle and for which crystallographic structures can be obtained (Kerisit et al. 2007). Yet, such model systems cannot address structure-activity relationships in relevant systems. A major contribution to understanding these complex nanogeobiological systems will be new methods, enabled by NGLS x-ray lasers, for determining the structure of environmentally and technologically important electron-transfer proteins, including multiheme *c*-type cytochromes such as OmcA. Dynamic pump-probe studies that visualize the structural changes occurring on the time scales of intraprotein and interfacial ET are essential.

Experiments that can visualize the structural dynamics of the protein–inorganic material interface before and during intermolecular ET will vastly expand our understanding of this process. To determine how ET kinetics and pathways are altered by association with a mineral surface, the sensitizer-protein bioconjugate could be complexed to a polyoxometalate cluster, which can serve as a model for a metal oxide mineral (see Fig. D10, p. 95). These kinds of studies will provide the first-ever systematic understanding of the structure and kinetics of interfacial ET. This fundamental science is envisioned to enable rational engineering of the redox protein–crystal interface and, in turn, have significant applications in biosynthesis, bioenergy, and biosensing.

## Carboxysomes

Carboxysomes are self-assembling proteinaceous organelles that play a key role in bacterial carbon dioxide (CO<sub>2</sub>) fixation (see Fig. D11, p. 95). Ranging from ~90 to 170 nm in diameter and from 100 to 350 MDa in mass (Schmid et al. 2006; Iancu et al. 2007; Iancu et al. 2010), carboxysomes encapsulate hundreds of copies of two key enzymes involved in CO<sub>2</sub> fixation: RuBisCO and carbonic anhydrase (see Fig. D11 c and d, p. 95; Iancu et al. 2007; Heinhorst, Cannon, and Shively 2006). Given the urgent global need to reduce

CO<sub>2</sub> emissions and develop carbon sequestration technologies, there is great interest in understanding carboxysomes and using them to enhance CO<sub>2</sub> capture and fixation rates in bioengineering applications. Thus far, structural information about carboxysomes has been limited to structures of isolated component proteins or low-resolution electron microscopy images. The dynamic imaging capabilities of NGLS x-ray lasers present unprecedented opportunities to characterize whole functional carboxysomes; observe dynamic structural changes during catalysis; understand the cellular context in which carboxysomes assemble; and track changes in carboxysome structure in response to environmental changes.

New time-resolved x-ray imaging techniques are required for a full understanding of the structure and catalytic dynamics of CO<sub>2</sub> fixation by carboxysomes. For example, structural data at the nanometer-resolution limit for a single carboxysome will reveal how RuBisCO and carbonic anhydrase pack together inside a functional carboxysome to mediate substrate and product channeling. Docking atomic-level structures of RuBisCO, carbonic anhydrase, and shell proteins into a nanometer-resolution map of the whole carboxysome will provide a detailed view of how RuBisCO and carbonic anhydrase are arranged for CO<sub>2</sub> fixation as well as how they interact with the protein shell.

The internal structure of the carboxysome also is anticipated to change with available light, the metabolic state of the cell, or the state of biogenesis. A powerful result of single-particle imaging thus will be the ability to compare reconstructions of carboxysomes from many cells or cells grown under different environmental conditions. This capability will enable the characterization of conserved and heterogeneous features of carboxysome structure and identification of structural changes that occur in response to shifting environmental conditions. Nanometer-resolution carboxysome structures also will provide an initial foundation to understand how the structures of carboxysome proteins change during catalysis.

## Membrane Proteins

Cells are surrounded by membranes that separate the cellular interior from the outside world. The lipids and proteins that dominate the composition of membranes exhibit a characteristic architecture in which the lipids adopt a bilayer arrangement (~40 Å thick) penetrated by integral membrane proteins. The flows of molecules, energy, and information across this barrier are mediated by these proteins embedded in the bilayer. Membrane proteins represent a fertile area for structural study; an estimated 25% of the proteins encoded in the genomes of organisms are membrane proteins, yet they constitute less than

**Fig. D10. Schematic representation of an optical pump-probe experiment with the sensitizer-protein-acceptor bioconjugate.** [Courtesy of Lawrence Berkeley National Laboratory]

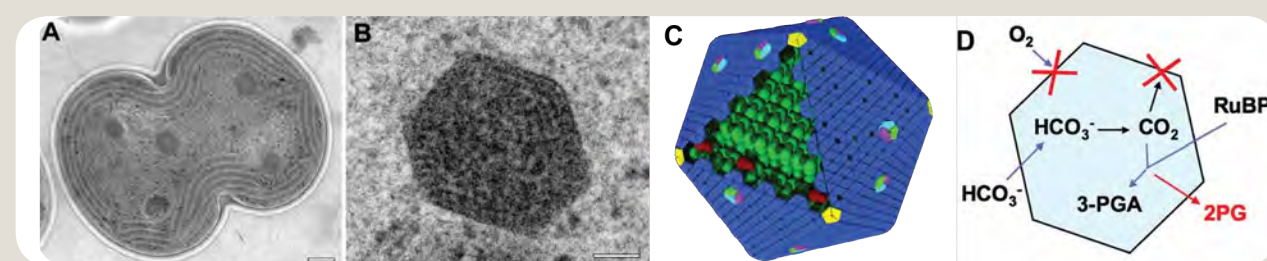
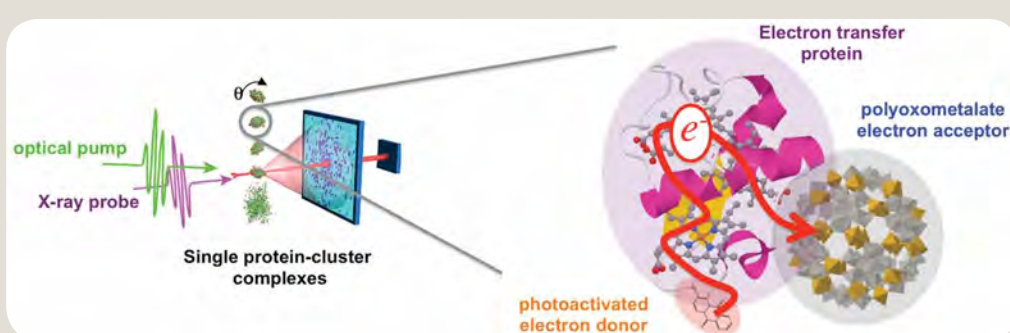


**Fig. D11. Transmission electron micrographs of (A) carboxysomes in a dividing cyanobacteria and (B) single carboxysome (scale bars, 50 nm). (C) Predicted model of a whole carboxysome showing RuBisCO (green), carbonic anhydrase (red), single-domain hexameric shell proteins (dark blue), tandem-domain shell proteins (light blue), and pentameric shell proteins (yellow). (D) Schematic of CO<sub>2</sub> fixation reactions inside the carboxysome (PGA, phosphoglycerate; RuBP, ribulose bis-phosphate). [A and B from Kerfeld, C. A., et al. 2005. "Protein Structures Forming the Shell of Primitive Bacterial Organelles," *Science* **309**(5736), 936–38. Reprinted with permission from AAAS. C from Kinney, J. N., S. D. Axen, and C. A. Kerfeld. 2011. "Comparative Analysis of Carboxysome Shell Proteins," *Photosynthesis Research*. DOI: 10.1007/s1120-011-9624-6.]**

1% of current entries in the Protein Data Bank (Berman et al. 2002). The biological significance of membrane proteins mirrors their pharmacological significance because they are targets for a majority of the most popularly prescribed drugs (Davey 2004).

The same properties that enable membrane proteins to function in this heterogeneous milieu also have profound consequences for their structural analysis. Reflecting the small ratio of membrane surface area to cellular volume, membrane proteins generally are present in low abundance, and extracting them from the membrane typically involves using detergents to solvate the hydrophobic surfaces. Consequently, the most detailed structural information on membrane proteins is typically in their detergent-extracted state (Poolman et al. 2005). While detergents have been extremely useful, they are not always faithful mimics of the membrane bilayer and can perturb the structure and dynamics of membrane proteins. Transformative new methods will be enabled by NGLS x-ray lasers that provide information on the structure and dynamics of membrane proteins in a native-like bilayer environment, including proteoliposomes or supported bilayers.

The characteristic properties of the ion-channel class of membrane proteins reflect their conductance, ion selectivity, and gating. These proteins typically are regulated by conformational switching of their structures between “open” and “closed” states. This conformational switching may be gated in response to changes in membrane potential (Jiang et al. 2003), ligand binding (Kawate et al. 2009), or application of mechanical forces (Liu, Gandhi, and Rees 2009). Structural studies have been able to visualize end points and, rarely, intermediate states in conformational switching (for example, see Fig. D12, this page).

Voltage-gated channels (Doyle et al. 1998) represent one of the basic circuit elements of neurobiology, and their response to changes in membrane potential serves as a key event in the propagation of electrical signals through the nervous system. Over the past decade, the structural framework for addressing the opening and closing of voltage-gated channels has been developed (Doyle et al. 1998). However, the dynamics of these processes (the temporal response of structural changes) has been lacking. Also notable is that the influence of the membrane potential on a protein requires a membrane, and these effects cannot be studied with detergent-extracted proteins in the absence of a membrane. Thus, time-resolved structural studies characterizing the membrane and the response of

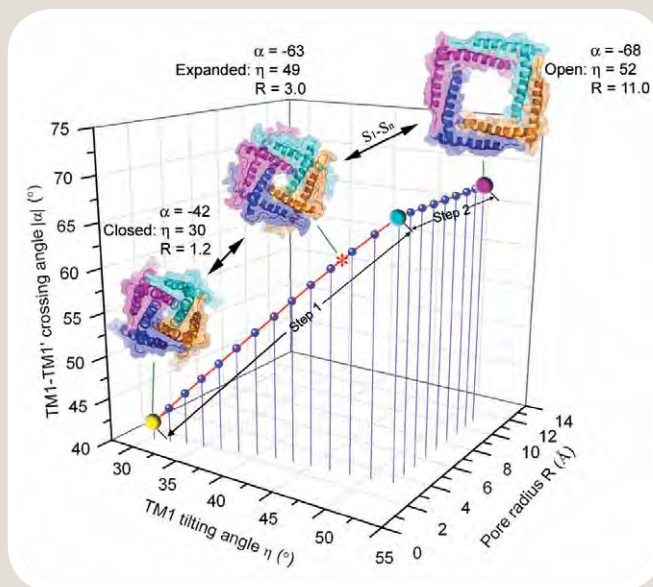


**Fig. D12. Different conformational states of a mechanosensitive ion channel, moving from closed to open.** [Reprinted by permission from Macmillan Publishers Ltd: From Liu, Z., C. S. Gandhi, and D. C. Rees. 2009. “Structure of a Tetrameric MscL in an Expanded Intermediate State,” *Nature* **461** (7260), 120–24.]

the voltage-gated channels embedded in the membrane to changes in membrane potential will be essential in establishing the mechanistic details of this fundamental event in cell signaling. Questions to be answered include, “How does a protein domain move through the membrane to create an all-or-none change in channel conductance without compromising membrane integrity?”

## Beamlines for Imaging Biological Dynamics and Function

Biological imaging research will rely on diffract and destroy methods using the third and fifth harmonics with the highest flux per pulse on two NGLS beamlines:

- Seeded beamline 1 at 100 kHz repetition rates.
- Unseeded SASE beamline 3 at MHz repetition rates (as high-speed detectors allow).

Choice of wavelength will be determined by balancing the scattering efficiency with the required resolution for particular samples. A key component of these experiments will be a high-speed particle injector synchronized to the continuous-wave, superconducting radio frequency linac, which will provide for sample replacement on a pulse-by-pulse basis.

## References

- Andersson, M., et al. 2009. "Structural Dynamics of Light-Driven Proton Pumps," *Structure* **17**(9),1265–75.
- Berman, H. M., et al. 2002. "The Protein Data Bank," *Acta Crystallographica D: Biological Crystallography* **58**(1), 899–907.
- Brink, J., et al. 2004. "Experimental Verification of Conformational Variation of Human Fatty Acid Synthase as Predicted by Normal Mode Analysis," *Structure* **12**(2), 185–91.
- Chapman, H. N. 2009. "X-Ray Imaging Beyond the Limits," *Nature Materials* **8**, 299–301.
- Davey, J. 2004. "G-Protein-Coupled Receptors: New Approaches to Maximise the Impact of GPCRs in Drug Discovery," *Expert Opinion on Therapeutic Targets* **8**(2),165–70.
- DePonte, D. P., et al. 2008. "Gas Dynamic Virtual Nozzle for Generation of Microscopic Droplet Streams," *Journal of Physics D: Applied Physics* **41**(19), 195505.
- Elser, V. 2009. "Noise Limits on Reconstructing Diffraction Signals from Random Tomographs," *IEEE Transactions on Information Theory* **55**(10), 4715–22.
- Doyle, D. A., et al. 1998. "The Structure of the Potassium Channel: Molecular Basis K<sup>+</sup> Conduction and Selectivity," *Science* **280**(5360), 69–77.
- Fischer, N., et al. 2010. "Ribosome Dynamics and tRNA Movement by Time-Resolved Electron Cryomicroscopy," *Nature* **466**(7304), 329–33.
- Frank, J. 2006. "Electron Microscopy of Macromolecular Assemblies," pp. 15–70. In *Three-Dimensional Electron Microscopy of Macromolecular Assemblies: Visualization of Biological Molecules in Their Native State*. Oxford University Press, New York.
- Fredrickson, J. K., and J. M. Zachara. 2008. "Electron Transfer at the Microbe-Mineral Interface: A Grand Challenge in Biogeochemistry," *Geobiology* **6**, 245–53.
- Fung, R., et al. 2009. "Structure from Fleeting Illumination of Faint Spinning Objects in Flight," *Nature Physics* **5**, 64–67.
- Gaffney, K. J., and H. N. Chapman. 2007. "Imaging Atomic Structure and Dynamics with Ultrafast X-Ray Scattering," *Science* **316**(5830), 1444–48.
- Giannakis, D., et al. 2010. "The Symmetries of Image Formation by Scattering," [arxiv.org/abs/1009.5035](https://arxiv.org/abs/1009.5035).
- Heinhorst, S., G. C. Cannon, and J. M. Shively. 2006. "Carboxysomes and Carboxysome-Like Inclusions," pp. 141–65. In *Microbial Monographs Vol. 2: Complex Intracellular Structures in Prokaryotes*. Springer-Verlag, Berlin, Germany.
- Iancu, C. V., et al. 2007. "The Structure of Isolated *Synechococcus* strain WH8102 Carboxysomes as Revealed by Electron Cryotomography," *Journal of Molecular Biology* **372**(3), 764–73.
- Iancu, C. V., et al. 2010. "Organization, Structure, and Assembly of Alpha-Carboxysomes Determined by Electron Cryotomography of Intact Cells," *Journal of Molecular Biology* **396**(1), 105–17.
- Jiang, Y. X., et al. 2003. "The Principle of Gating Charge Movement in a Voltage-Dependent K<sup>+</sup> Channel," *Nature* **423**, 42–48.
- Kam, Z. 1977. "Determination of Macromolecular Structure in Solution by Spatial Correlation Averaging," *Macromolecules* **10**(5), 927–34.
- Kam, Z., M. H. Koch, and J. Bordas. 1981. "Fluctuation X-Ray Scattering from Biological Particles in Frozen Solution by Using Synchrotron Radiation," *Proceedings of the National Academy of Sciences of the United States of America* **78**(6), 3559–62.
- Kawate, T., et al. 2009. "Crystal Structure of the ATP-Gated P2X4 Ion Channel in the Closed State," *Nature* **460**, 592–98.
- Kerfeld, C. A., et al. 2005. "Protein Structures Forming the Shell of Primitive Bacterial Organelles," *Science* **309**(5736), 936–38.
- Kerisit, S., et al. 2007. "Molecular Computational Investigation of Electron-Transfer Kinetics Across Cytochrome-Iron Oxide Interfaces," *Journal of Physical Chemistry C* **111**(30), 11363–75.
- Liu, Z., C. S. Gandhi, and D. C. Rees. 2009. "Structure of a Tetrameric MscL in an Expanded Intermediate State," *Nature* **461**(7260), 120–24.
- Levin, E. J., et al. 2007. "Ensemble Refinement of Protein Crystal Structures: Validation and Application," *Structure* **15**(9), 1040–52.
- Ludtke, S. J., et al. 2008. "De Novo Backbone Trace of GroEL from Single Particle Electron Cryomicroscopy Structure," *Structure* **16**(3), 441–48.
- Moths, B., and A. Ourmazd. 2009. "Bayesian Algorithms for Recovering Structure from Single-Particle Diffraction Snapshots of Unknown Orientation: A Comparison," *Acta Crystallographica A: Foundations of Crystallography* **A67**. DOI:10.1107/S0108767311019611.
- Nadler, B., et al. 2006. "Diffusion Maps, Spectral Clustering and Reaction Coordinates of Dynamical Systems," *Applied and Computational Harmonic Analysis* **21**(1), 113–27.
- Neutze, R., et al. 2000. "Potential for Biomolecular Imaging with Femtosecond X-Ray Pulses," *Nature* **406**, 752–57.
- Poolman, B., et al. 2005. "Functional Analysis of Detergent-Solubilized and Membrane-Reconstituted ATP-Binding Cassette Transporters," *Methods in Enzymology* **400**, 429–59.
- Putnam, C. D., et al. 2007. "X-Ray Solution Scattering (SAXS) Combined with Crystallography and Computation: Defining Accurate Macromolecular Structures, Conformations and Assemblies in Solution," *Quarterly Reviews of Biophysics* **40**(3), 191–285.
- Saldin, D., et al. 2007. *Crystallography Without Crystals: Structure from Diffraction Patterns of Randomly Oriented Molecules*. Coherence 2007: International Workshop on Phase Retrieval and Coherent Scattering, Asilomar, Calif., USA.
- Saldin, D., et al. 2009. "Structure of Isolated Biomolecules Obtained from Ultrashort X-Ray Pulses: Exploiting the Symmetry of Random Orientations," *Journal of Physics: Condensed Matter* **21**(13), 134014.
- Saldin, D. K., et al. 2010a. "Beyond Small-Angle X-Ray Scattering: Exploiting Angular Correlations," *Physical Review B* **81**, 174105.
- Saldin, D. K., et al. 2010b. "Structure of a Single Particle from Scattering by Many Particles Randomly Oriented about an Axis: Toward Structure Solution without Crystallization," *New Journal of Physics* **12**, 035014.
- Saldin, D. K., et al. 2011. "New Light on Disordered Ensembles: *Ab Initio* Structure Determination of One Particle from Scattering Fluctuations of Many Copies," *Physical Review Letters* **106**(11), 115501.
- Scheres, S. H. W., et al. 2007. "Disentangling Conformational States of Macromolecules in 3D-EM Through Likelihood Optimization," *Nature Methods* **4**, 27–29.

Schmid, M. F., et al. 2006. "Structure of *Halothiobacillus neapolitanus* Carboxysomes by Cryo-Electron Tomography," *Journal of Molecular Biology* **364**(3), 526–35.

Schwander, P., et al. 2010. "Mapping the Conformations of Biological Assemblies," *New Journal of Physics* **12**, 035007.

Shi, L. A., et al. 2009. "The Roles of Outer Membrane Cytochromes of *Shewanella* and *Geobacter* in Extracellular Electron Transfer," *Environmental Microbiology Reports* **1**(4), 220–27.

Shneerson, V. L., A. Ourmazd, and D. K. Saldin. 2008. "Crystallography Without Crystals I: The Common-Line Method for Assem-

bling a Three-Dimensional Diffraction Volume from Single-Particle Scattering," *Acta Crystallographica A* **64**, 303–15.

Solem, J. C., and G. C. Baldwin 1982. "Microholography of Living Organisms," *Science* **218** (4569), 229–35.

Weber, K. A., L. A. Achenbach, and J. D. Coates. 2006. "Microorganisms Pumping Iron: Anaerobic Microbial Iron Oxidation and Reduction," *Nature Reviews Microbiology* **4**, 752–64.

Yu, I. M., et al. 2008. "Structure of the Immature Dengue Virus at Low pH Primes Proteolytic Maturation," *Science* **319**(5871), 1834–37.

**Table D3. Contributing Scientists**

Authors	Affiliations
Paul D. Adams	Physical Biosciences Division and DOE Joint BioEnergy Institute, Lawrence Berkeley National Laboratory (LBNL)
Caroline Ajo-Franklin	Molecular Foundry, LBNL
Jillian F. Banfield	Environmental Science, Policy, and Management and Earth and Planetary Science, University of California–Berkeley
Jamie Cate	Departments of Chemistry and Molecular and Cellular Biology, University of California–Berkeley
Benjamin Gilbert	Earth Science Division, LBNL
Malcolm Howells	Advanced Light Source, LBNL
Cheryl A. Kerfeld	DOE Joint Genome Institute, LBNL
Janos Kirz	Advanced Light Source, LBNL
Abbas Ourmazd	University of Wisconsin–Milwaukee
Douglas C. Rees	California Technical Institute
Dilano K. Saldin	University of Wisconsin–Milwaukee
Annette E. Salmeen	DOE Joint Genome Institute, LBNL
Robert W. Schoenlein	Advanced Light Source, LBNL
Steven W. Singer	Earth Science Division and DOE Joint BioEnergy Institute, LBNL
John C. H. Spence	Physics Department, Arizona State University
Peter H. Zwart	Physical Biosciences Division, LBNL

## Spallation Neutron Source

### *SNS: A Powerful Tool for Biological Research\**



**N**eutron scattering is one of the most powerful research techniques available to scientists studying the structure and dynamics of materials. Crystallography, small-angle scattering, diffraction, and reflectometry are ideal methods for studying structure and organization on length scales from atoms to microns, and neutron spectroscopic methods characterize self- and collective motions on time scales from picoseconds to microseconds. These techniques are applicable to the length and time scales intrinsic to biological systems but, unlike most other methods, are uniquely sensitive to hydrogen (and its isotopes), an atom abundantly present throughout biological materials and a key effector in many biological processes.

Oak Ridge National Laboratory (ORNL) hosts two of the world's most powerful and advanced neutron scattering research facilities, the Spallation Neutron Source (SNS) and the High Flux Isotope Reactor (HFIR), which attract scientists worldwide. The accelerator-based, 1 megawatt (MW) SNS produces the most intense pulsed neutron beams in the world. It is designed to be upgraded to 3 MW and accommodate a second target station, doubling the number of experimental end stations. The 85 MW HFIR has one of the highest continuous neutron fluxes of any research reactor, and its cold neutron source is the most intense in the world. With these two leading-edge facilities, ORNL is positioned for leadership in addressing a diverse set of scientific problems in biology whose solutions are essential to future progress in health, medicine, and energy.

## Introduction

A variety of neutron scattering techniques can be used to characterize the structural and dynamical properties of biomaterials across length scales from microns ( $\mu\text{m}$ ) to angstroms ( $\text{\AA}$ ) and time scales from microseconds ( $\mu\text{s}$ ) to picoseconds ( $\text{ps}$ ). Although the neutron's interaction with atomic nuclei is weak, the scattering "power" (cross-section) of an atom is not related to its atomic number, as is the case for x-rays. As a result, neighboring elements in the periodic table can have substantially different scattering cross-sections and correspondingly different contributions to a measured neutron signal. Moreover, the interaction of a neutron with an atomic nucleus differs for an element's various isotopes. The scattering cross-section of hydrogen, which is ubiquitous in biology, differs dramatically from that of its isotope deuterium. This difference, coupled with the ability to substitute deuterium for hydrogen, enables powerful contrast variation methods that allow subunits

\*Oak Ridge National Laboratory prepared this and a companion document (p. 105) and approved post-workshop revisions to each.



[Courtesy of Oak Ridge National Laboratory]

within intact, functional macromolecular complexes to be highlighted. Furthermore, neutron energies are similar to the biologically relevant energies of atomic translations, rotations, and vibrations, enabling spectroscopic studies of these dynamic processes as well as both self- and collective diffusive motions. Neutron scattering has the ability to provide unique, novel insights into structural and dynamic transitions related to biologically important processes.

SNS is the United States' newest and most advanced neutron scattering facility. It contains a broad suite of instruments, including small-angle neutron scattering (SANS), reflectometers, diffractometers, and spectrometers. ORNL's research reactor, HFIR, has been substantially upgraded in recent years. Its cold neutron source provides the long-wavelength neutrons that enable two world-class SANS instruments, and HFIR soon will serve a crystallography station well suited to studying biological macromolecules. The neutron beams produced at SNS complement and expand on the suite of instruments available at HFIR, thus enabling new science with neutrons that could not have been realized a decade ago. In particular, the intense pulsed nature of the SNS neutron beams opens up opportunities to collect structural and dynamical data on time scales previously unachievable at neutron scattering facilities (i.e., from subseconds to hours). The suite of neutron scattering instruments at SNS—including those designed for and dedicated to interrogating biological samples—will be used to address a wide variety of problems in structural biology. These challenges range from atomic-resolution analysis of enzyme structure and dynamics to meso- and macroscale analyses of complex biological structures, membranes, or assemblies and their kinetic processes. Neutrons' weak interaction with matter makes them highly penetrating and nondestructive. This feature enables the use of complex sample environments that simulate biologically relevant conditions (e.g., pH, salinity, and humidity), including those that often are poorly suited to other structural biology techniques (e.g., high pressures and extreme

temperatures). The Neutron Sciences Directorate at ORNL has a dedicated sample environment group that works with users and beamline scientists to develop and advance the state of the art in sample environments suitable for biological materials.

Despite the clear benefits that neutrons offer for biology, their broader application in the biological sciences has been constrained by a number of factors. These include the limited flux of available neutron beams; the very limited (or nonexistent) availability of suitable neutron instruments and sample environments; and, to an extent, a lack of cohesive scientific direction in biological sciences at neutron facilities. New opportunities exist in supporting data reduction and analysis for members of the structural biology community, many of whom are not experts in neutron scattering. ORNL has invested in establishing a cohesive neutron structural biology program that expands upon the Center for Structural Molecular Biology, which is funded by DOE's Office of Biological and Environmental Research (BER). This expansion includes the establishment of the Biology and Soft Matter Division, one of three specific multidisciplinary scientific areas established to foster scientific programs and partnerships at SNS and HFIR. This Facility Paper describes the suite of current and future ORNL capabilities for structural biology using neutron scattering and imaging that enable world-leading science at SNS and HFIR.

## Research

### *Protein Crystallography*

Macromolecular crystallography continues to be the leading technique for atomic-resolution analysis of proteins and nucleic acids. Because of their unique sensitivity to hydrogen and its isotope deuterium, neutrons can be used to locate hydrogen atoms within biological macromolecules. Locating hydrogen atoms provides special insight into enzymatic processes that are difficult, if not impossible, to obtain via other structural biology techniques. By 2013, ORNL will provide access to a suite of three state-of-the-art single-crystal diffractometers ideal for macromolecular crystallography and designed and optimized for analyzing submillimeter-size single crystals. Currently at SNS, the first of these instruments, the TOPAZ single-crystal diffractometer, is completing commissioning and will be available in 2012 for high-resolution chemical and biological crystallography on systems with unit cell edges <math><100 \text{ \AA}</math>. A second instrument, MaNDi (macromolecular neutron diffractometer), will enter the user program in 2013 and be capable of collecting, at near-atomic resolution, the data from 0.1 mm<sup>3</sup> crystals with lattice repeats of ~150 Å. MaNDi's large-area detector (see Table E1, p. 101), coupled with the high neutron flux at SNS, will enable collection of a complete dataset within a few days. Also suitable for structural biology is IMAGINE, a quasi-Laue image plate diffractometer under construction at HFIR and funded by the National Science Foundation (NSF). Instrument capabilities for macromolecular crystallography are summarized in Table E1.

### *Macromolecular Complexes, Flexible Systems, and Hierarchical Structures*

The intrinsic structures of disordered macromolecular complexes have long posed challenges for structural biology. These systems can be resistant to crystallization—precluding high-resolution structural determination—and typically are too large for study by nuclear magnetic resonance. Their flexibility, often important to their biological functions, also can prevent their crystallization by traditional methods. SANS is well suited for studying such systems because it can provide structural information under near-native biological conditions. Like all neutron scattering techniques, SANS is sensitive to the hydrogen content of materials. The structures of subunits within a functional, intact complex can be probed by combining SANS with selective deuterium labeling of the subunits or by leveraging the intrinsic difference in the neutron scattering power of proteins, nucleic acids, and lipids. ORNL has three SANS instruments (see Table E2, p. 102)—the recently completed Extended Q-range SANS (EQ-SANS) at SNS and the Bio-SANS and General-Purpose SANS (GP-SANS) instruments at HFIR, which both began operation in late 2007. EQ-SANS is designed to study noncrystalline nanomaterials such as polymers, micelles, proteins, and large biomolecular complexes in solution. Its capabilities include high neutron flux, high wavelength resolution (precision), and wide Q coverage. The higher Q values accessible to EQ-SANS make it uniquely suited to probing shorter length scales, such as those important to crystallization during annealing and other significant processes in biological materials science. These instruments provide complementary capabilities (see Table E2) that position ORNL to address a diverse number of problems in structural biology.

### *Biological Membranes and Macroscopic Systems*

The biological function of cell membranes is intrinsically linked to structure. Cell membranes are complex, dynamic, responsive, and self-repairing assemblies that are spatially and temporally heterogeneous and regulate transport, signaling, and energy processes in living systems. As complex systems composed of lipids, proteins, and other molecules (e.g., cholesterol), cell membranes have proven difficult to study. However, the study of membranes can be facilitated by taking advantage of the self-assembly tendencies of their cellular components to produce samples with well-defined geometries. One technique ideally suited to leveraging this inherent feature of membranes is neutron reflectometry. By adsorbing a membrane to a planar surface, interrogation of the membrane structure and its interactions with other biomolecules, such as proteins and cholesterol, is possible. The Liquids Reflectometer (see Table E3, p. 103), one of the first instruments commissioned at SNS, is well suited to studying lipid membranes in a planar geometry under biologically relevant conditions. The high flux available on the Liquids Reflectometer enables time-resolved studies of specific structure features

Table E1. Instruments for Protein Crystallography

Instrument	Availability	Instrument Data	Applications
TOPAZ (SNS)	Available in 2012	<b>Wavelength:</b> $0.5 < \lambda < 7.2 \text{ \AA}$ <b><math>\Delta\lambda/\lambda</math>:</b> 0.2% <b>Q range:</b> 0.25 to $20 \text{ \AA}^{-1}$ <b>Detector angle:</b> 20 to $160^\circ$ <b>Detector resolution:</b> 1 by $1 \text{ mm}^2$	TOPAZ is optimized specifically for high-resolution chemical crystallography and can resolve unit cell edges of up to $50 \text{ \AA}$ . It is therefore ideal for studying oligonucleotides and small proteins [ $< 25$ to $30$ kilodaltons (kDa)] at or near atomic resolution ( $1.0$ to $1.5 \text{ \AA}$ ). However, TOPAZ can be configured to study larger proteins at lower resolution with cell edges up to $100 \text{ \AA}$ .
MaNDi (SNS)	Under construction	<b>Bandwidth:</b> $2.16 \text{ \AA}$ <b>Wavelength:</b> $1 < \lambda < 10 \text{ \AA}$ <b>Detectors:</b> 27 Anger cameras <b>Detector size:</b> 150 by $150 \text{ mm}^2$ <b>Detector resolution:</b> 1 by $1 \text{ mm}^2$ <b>Solid angle coverage:</b> 2 steradian (sr)	MaNDi is capable of collecting atomic-resolution data ( $1.5 \text{ \AA}$ ) using protein crystals as small as $0.1 \text{ mm}^3$ with unit cell edges up to $150 \text{ \AA}$ in length.
IMAGINE (HFIR)	Under construction	<b>Wavelength:</b> $2.0 < \lambda < 4.5 \text{ \AA}$ <b><math>\Delta\lambda/\lambda</math>:</b> 25% <b>Detector:</b> 1,200 by $450 \text{ mm}^2$ image plate <b>Detector resolution:</b> 125, 250, $500 \text{ \mu m}$	IMAGINE will support a broad range of fundamental science, spanning the location of individual hydrogen atoms in enzymes to parametric studies of complex materials under extremes of temperature and pressure.

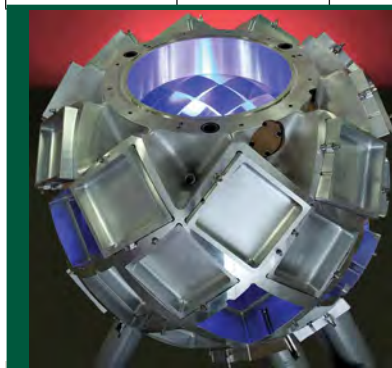


Fig. E1. Detector array for the TOPAZ instrument.



Fig. E2. Detector array for the MaNDi instrument.

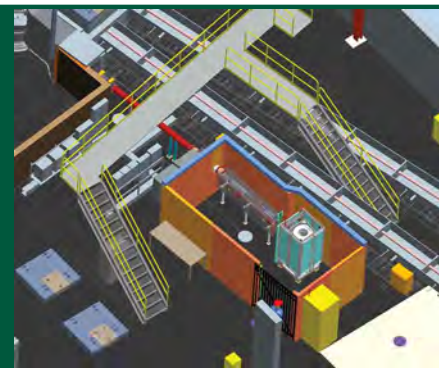


Fig. E3. Schematic of the IMAGINE instrument.

not accessible to other instruments. At the other end of the length scale, the VENUS neutron imaging facility proposed at SNS (see Table E3, p. 103) will be capable of providing detailed structural information at resolutions from submillimeters down to  $1 \text{ \mu m}$ . The large field of view (up to  $1 \text{ m}$  by  $1 \text{ m}$ ) will allow unprecedented studies of real biological systems. Using SNS's pulsed neutrons, VENUS will be able to take real-time measurements (i.e., events of a few milliseconds) with stroboscopic imaging techniques.

### Dynamical Measurements in Biological Systems

The dynamics of atomic groups or molecules that make up materials contain key information indispensable for understanding and controlling the properties of biological materials. Unlike other techniques for probing structural dynamics, neutron scattering is sensitive not only to the temporal, but also the spatial characteristics of dynamical processes through the scattering signal's dependence on neutron momentum

transfer. The large incoherent neutron scattering cross-section of hydrogen, compared with that of other elements, allows researchers to use partial sample deuteration to probe the dynamics of selected structural units in biological systems inherently rich in hydrogen. Moreover, the highly penetrating nature of neutrons enables the use of sample environments not compatible with other experimental techniques, such as those providing very high pressures or magnetic and electric fields. The Backscattering Spectrometer (BASIS) at SNS features a unique combination of high-energy resolution and a wide variety of accessible energy transfers that enables experiments over a broad range of biological motions, from nanosecond to picosecond time scales. The Cold Neutron Chopper Spectrometer (CNCS) is particularly well suited for investigating collective dynamics such as the fluctuations of biological membranes and the diffusive motions of small molecules like water and many drugs. The Neutron Spin Echo spectrometer (NSE) is capable of measuring lower energies (slower processes) and longer length scales, with the maximum achievable Fourier time extended to at least  $1 \text{ \mu s}$ .

**Table E2. Instruments for Macromolecular Complexes and Flexible Systems**

Instrument	Availability	Instrument Data	Applications
<b>EQ-SANS (SNS)</b>	Available	<b>Bandwidth:</b> 3 to 4.3 Å <b>Q range:</b> $0.004 < Q < 1.5 \text{ \AA}^{-1}$ <b>Detector:</b> $1 \text{ m}^2 \text{ } ^3\text{He}$ <b>Detector resolution:</b> 8 mm by 5.1 mm pixels	EQ-SANS is capable of studying the solution structures of proteins, DNA, and molecular complexes (e.g., protein-protein and protein-ligand interactions). The instrument also is well suited for multiscale studies of biological supramolecular assemblies and biomimetic materials.
<b>Bio-SANS (HFIR)</b>	Available	<b>Wavelength:</b> $6 < \lambda < 25 \text{ \AA}$ <b><math>\Delta\lambda/\lambda</math>:</b> 12% to 45% <b>Q range:</b> $0.001 < Q < 1 \text{ \AA}^{-1}$ <b>Detector:</b> $1 \text{ m}^2 \text{ } ^3\text{He}$ <b>Detector resolution:</b> 5.1 by 5.1 mm <sup>2</sup> pixels	Bio-SANS is capable of probing structures from 6 to 6,000 Å. Applications in biology range from mapping low-resolution structures and structural transitions of individual proteins and large macromolecular complexes in solution to the multiscale analysis of complex hierarchical structures.
<b>GP-SANS (HFIR)</b>	Available	<b>Wavelength:</b> $4 < \lambda < 30 \text{ \AA}$ <b><math>\Delta\lambda/\lambda</math>:</b> 9% to 45% <b>Q range:</b> $0.001 < Q < 1.0 \text{ \AA}^{-1}$ <b>Detector:</b> $1 \text{ m}^2 \text{ } ^3\text{He}$ <b>Detector resolution:</b> 5.1 by 5.1 mm <sup>2</sup> pixels	GP-SANS is optimized for analysis of the structure, interaction, and assembly of particles and systems with characteristic length scales ranging from 6 to 6,000 Å. Applications in biology and biomedical research include probing the structural changes in biomembranes, bone mineralization studies, complex fluid systems for drug delivery, and synthesis and delivery of nanoparticles of biomedical interest. Low-resolution structure and structural transitions of individual proteins and large macromolecular complexes in solution are also suited to GP-SANS.



Fig. E4. EQ-SANS instrument.



Fig. E5. Bio-SANS instrument.



Fig. E6. GP-SANS instrument.

Using wavelengths of  $0.25 < \lambda / \text{nm} < 2.0$ , an unprecedented dynamical range of six decades from  $1 \text{ ps} < \tau$  to  $\tau < 1 \mu\text{s}$  can be achieved, greatly enhancing the range of biological systems that can be studied at SNS. (For details of these instruments, see Table E4, p. 104).

### Infrastructure and Support

Although world-class neutron scattering instrumentation is critical for leading an effective neutron structural biology program, the instruments must be supported by sample preparation and characterization facilities staffed by expert researchers. ORNL has established the Bio-Deuteration Laboratory to help biologists and biophysicists maximize the potential of their neutron scattering experiments. Additionally, its data analysis and modeling effort will enable ORNL to take a leadership role in the use of modeling and simulation for interpreting neutron scattering data.

### The Bio-Deuteration Laboratory

The particular sensitivity of neutrons to hydrogen and its isotopes makes selective deuteration in complex biological systems a necessary tool for maximizing the impact of neutron scattering experiments. For example, in SANS experiments, the use of a deuterium-labeled subunit in a complex allows researchers to deconvolute the scattering of the labeled and unlabeled subunits, along with their relative dispositions within the complex. Similar approaches are equally powerful in studying biological membranes with neutron reflectometry. The use of deuterated proteins also improves the sensitivity of crystallography experiments and makes working with smaller crystals possible. In inelastic neutron scattering experiments, specific deuterium labeling can be used to highlight dynamics of interest within a system.

The mission of the Bio-Deuteration Laboratory is to support and develop the facilities and expertise required for

Table E3. Instruments for Biological Membranes

Instrument	Availability	Instrument Data	Applications
<b>Liquids Reflectometer (SNS)</b>	Available	<b>Bandwidth:</b> 3.5 Å <b>Wavelength:</b> $2.5 < \lambda < 17.0$ Å <b><math>\Delta Q/Q</math>:</b> 2% <b>Q range:</b> $0.002 < Q < 1.5$ Å <sup>-1</sup> <b>Detector:</b> 0.2 by 0.2 m <sup>2</sup> <sup>3</sup> He <b>Detector resolution:</b> 1.3 by 1.3 mm <sup>2</sup>	The Liquids Reflectometer is optimized to measure neutron reflectivity from solid and free-liquid surfaces and from buried solid-liquid interfaces. It can address a broad range of questions in interfacial biological science, including structure, orientation, and placement of membrane proteins in lipid bilayers and raft formations.
<b>VENUS (SNS)</b>	In planning	<b>Wavelength:</b> $0 < \lambda < 40$ Å <b>Energy resolution:</b> < 0.1% <b>Neutron flux:</b> (n/cm <sup>2</sup> /s): 10 <sup>10</sup>	VENUS will be optimized for energy-selective neutron imaging radiography and computed tomography for a diverse number of applications, ranging from plants to geothermal systems to biological and biomedical samples. Access to epithermal and thermal neutrons will enable the investigation of samples of varying thickness.



Fig. E7. Liquids Reflectometer instrument.



Fig. E8. Schematic of the VENUS instrument.

expressing and purifying deuterium-labeled proteins and macromolecules. In typical applications, microbial protein expression systems (such as *Escherichia coli*) have been adapted to grow in heavy water (D<sub>2</sub>O) and deuterated carbon sources, allowing functional, isotopically deuterium-labeled proteins to be expressed reliably and in large quantities. More advanced techniques are being developed that will enable the design and production of specific, random, and uniformly hydrogen- or deuterium-labeled macromolecules for specific applications.

### Computational Modeling and Simulation

In addition to being home to two world-class neutron scattering facilities, ORNL hosts the National Center for Computational Sciences. Its “Jaguar” Cray XT5 supercomputer is one of the world’s most powerful machines for unclassified research and is the cornerstone of ORNL’s Leadership Computing Facility (LCF). The combination of neutron scattering

instruments at SNS and HFIR and the computing power offered by LCF enables ORNL to perform multiscale analysis of the structure and dynamics of biological systems. Jaguar and the NSF-funded Kraken supercomputer are petaflop-class computing systems capable of modeling biological systems over length and time scales not previously accessible. ORNL’s Neutron Sciences Directorate is establishing the Simulation and Modeling Division that will lead an effort to bridge ORNL’s supercomputing facilities with the neutron scattering research at SNS and HFIR. The members of this division will work with researchers studying biological systems using the various neutron scattering techniques. Also, ORNL’s Center for Molecular Biophysics uses computational techniques to investigate biological systems—including enzymatic processes and the structural dynamics of biomass—via simulations of up to one million atoms. The center actively collaborates with researchers using neutron scattering to probe the dynamics of biological systems.

Table E4. Instruments for Probing Dynamics in Biological Materials

Instrument	Availability	Instrument Data	Applications
<b>BASIS (SNS)</b>	Available	<p><b>Elastic energy:</b> 2.08 millielectron volts (meV)</p> <p><b>Bandwidth:</b> (optimized standard configuration) <math>\pm 100 \mu\text{eV}</math>; (special configuration) <math>\pm 250 \mu\text{eV}</math></p> <p><b>Q range (elastic):</b> <math>0.2 &lt; Q &lt; 2 \text{ \AA}^{-1}</math></p> <p><b>Q resolution:</b> 0.05 to <math>1.0 \text{ \AA}^{-1}</math></p> <p><b>Detector:</b> <math>^3\text{He}</math></p> <p><b>Resolution (elastic):</b> <math>3.5 \mu\text{eV}</math></p> <p><b>Solid angle coverage :</b> 1.2 sr</p>	BASIS is a high energy resolution backscattering neutron spectrometer for studies of dynamic processes from the nanosecond to picosecond time scales. Applications in biology and biomedical sciences include the (1) dynamics of proteins and other biomolecules both in solution and the partially hydrated state, (2) dynamics of various small-molecule solvents in contact with biomolecules, (3) diffusion of molecules in systems designed for drug delivery, and (4) dynamic processes in lipid membranes.
<b>Neutron Spin Echo (SNS)</b>	Available	<p><b>Wavelength:</b> <math>2 &lt; \lambda &lt; 21 \text{ \AA}</math></p> <p><math>\Delta\lambda/\lambda</math>: 1%</p> <p><b>Q range:</b> <math>0.03 &lt; Q &lt; 2.5 \text{ \AA}^{-1}</math></p> <p><b>Detector:</b> 300 by 300 mm<sup>2</sup> <math>^3\text{He}</math></p> <p><b>Detector resolution:</b> 20 by 20 mm<sup>2</sup></p> <p><b>Solid angle coverage:</b> 1.2 sr</p>	NSE is capable of measuring the dynamics of biologically relevant materials, including proteins, over a broad range of time scales up to 400 ns, or an equivalent energy resolution of 1.8 neV.
<b>Cold Neutron Chopper Spectrometer (SNS)</b>	Available	<p><b>Incident energy:</b> 1 to 50 meV</p> <p><b>Energy resolution:</b> 10 to 500 <math>\mu\text{eV}</math></p> <p><b>Q range:</b> 0.05 to <math>10.0 \text{ \AA}^{-1}</math></p> <p><b>Detector:</b> <math>^3\text{He}</math></p> <p><b>Solid angle coverage:</b> 1.7 sr</p>	CNCS is a direct-geometry, multichopper, inelastic, time-of-flight spectrometer that provides good energy and momentum transfer resolution at low-incident neutron energies (1 to 50 meV). It is suitable for studying biological samples with collective excitations and diffusive processes in the picosecond time range.

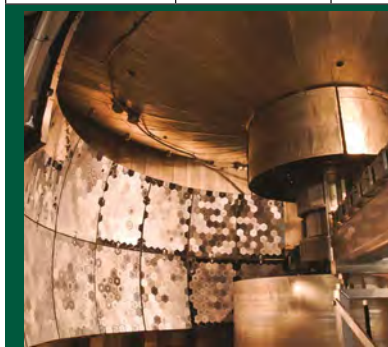


Fig. E9. BASIS instrument.



Fig. E10. NSE instrument.

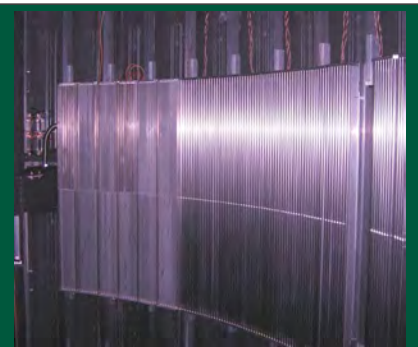


Fig. E11. Detector array for the CNCS instrument.

For further information on the SNS and HFIR user program, please contact [neutronusers@ornl.gov](mailto:neutronusers@ornl.gov).

For further information on the Center for Structural Molecular Biology and Bio-Deuteration Laboratory, please contact [csmb@ornl.gov](mailto:csmb@ornl.gov).

## Spallation Neutron Source

# SNS: Addressing the Next Challenges in Biology

Neutron scattering is one of the most powerful research techniques available to scientists studying the structure and dynamics of materials. Crystallography, small-angle scattering, diffraction, and reflectometry are ideal methods for studying atomic and subatomic structures, and several types of neutron spectroscopy are used for characterizing material dynamics. Neutron scattering is applicable to the length and time scales intrinsic to biological systems. Unlike other structural techniques, it is uniquely sensitive to hydrogen (and its isotopes), an atom abundantly present in biological materials and a key effector in many biological processes.

ORNL's two neutron scattering research facilities, the Spallation Neutron Source (SNS) and the High Flux Isotope Reactor (HFIR) attract scientists worldwide. The accelerator-based, 1 MW SNS produces the most intense pulsed neutron beams in the world. It is designed to be upgraded to 3 MW and accommodate a second target station. The 85 MW HFIR has one of the highest continuous neutron fluxes of any research reactor, and its cold neutron source is the most intense in the world. These two leading-edge facilities position ORNL for leadership in addressing a diverse set of scientific problems in structural biology whose solutions are essential to future progress in health, medicine, and energy.

## Introduction

Structural biology has a prolific and proven track record of providing key molecular-level insights into life's essential processes. Through the application of several complementary physical techniques—particularly x-ray crystallography and nuclear magnetic resonance (NMR) spectroscopy—the structures of many molecular components of biological systems are being solved at near-atomic resolution. The increasing availability of genomic sequences along with advances in technologies that manipulate and translate genes into molecular structures are presenting a clearer picture of the structural complexity of molecules, such as proteins and nucleic acids, within living organisms. These new capabilities in structural and molecular biology have enabled researchers to better understand the relationship between molecular structure and function, knowledge that in turn has provided insights into the role of that relationship in evolution and disease. These new insights have enabled the development of rational approaches to genetic engineering and therapeutics. The next great challenge in structural biology is to understand how these molecules dynamically interact, change shape, and assemble with each other and how they carry out their detailed biochemical or physical functions at an atomic level. Structural biology must continue to evolve if it is to address the increasingly

challenging problems that arise as scientists strive to understand the interplay of systems that drive living cells. These cellular systems need to be understood over length scales ranging from the atomic to the cellular and over time scales spanning atomic vibrations to macromolecular processes such as protein folding. Such knowledge is important for tackling disease and for industrial manipulation of cellular systems to introduce new pathways and functionalities through biology.

The importance of neutron scattering for addressing challenging problems in biology is that it provides unique structural and dynamic information on complex systems. The *structural* information provided is directly complementary to that provided by other experimental methods such as NMR spectroscopy; electron microscopy; and x-ray scattering techniques like diffraction, small-angle scattering, and reflectometry. The *dynamic* information provided is complementary to that provided by spectroscopic techniques. Neutrons can be used to probe length scales ranging from angstroms to microns and can elucidate dynamic processes occurring over time scales from picoseconds to milliseconds. They also are capable of investigating the kinetic behavior of systems over time scales from milliseconds to hours. This combination of both structural and dynamic data over enormous length and time scales cannot be achieved with any other single experimental technique. Neutrons thus allow researchers to probe cellular processes that range from fast reactions at the atomic level (e.g., enzyme catalysis) to slower processes that involve complex molecular assemblies and machines (e.g., light harvesting, signaling, membrane translocation, and cell-wall synthesis).

Several of their properties enable the use of neutrons to acquire information unobtainable by other structural biology methods. X-rays are scattered primarily by electrons; neutrons are fundamental particles scattered by their interaction with atomic nuclei. While the scattering “ability” of x-rays increases simply with atomic number, the scattering “ability” of neutrons varies in a complex manner that depends on the mass, spin, and energy level of the target nucleus. However, this scattering ability remains comparable for all atoms, making light atoms visible. Because neutrons interact uniquely with different nuclei, including various isotopes of elements, neutron scattering enables the powerful and commonly used method of contrast variation. Particularly important for biological samples, which are inherently rich in hydrogen, neutrons are very sensitive to the strong but different scattering from hydrogen and its isotope deuterium. This difference allows for the classical example of contrast variation by the substitution of hydrogen with deuterium. The variation in scattering power between hydrogen and deuterium is one of the largest differences existing among the isotopes of any

element and affords structural biology with opportunities for novel experimental design. Deuteration will be a key to fully exploiting the power of neutron techniques in addressing future challenges in structural biology.

The sensitivity of neutrons to hydrogen and deuterium enables studies of biological structure, dynamics, and function that span a wide range of length and time scales involved in cellular processes. Neutron crystallography can be applied to locate functionally important individual hydrogen atoms with near-atomic precision in biological molecules such as enzymes, DNA, and cell-wall carbohydrates. Locating such atoms provides information on the protonation states of amino-acid residues and ligands, identity of solvent molecules, and nature of bonds involving hydrogen. At the longer length scales probed by small-angle scattering, membrane and fiber diffraction, and reflectometry, the sensitivity of neutrons to the bulk hydrogen content of materials enables researchers to determine the structures of lipids, proteins, and larger nucleic acids within intact assemblies. Such assemblies range from membrane proteins in detergent micelles to protein-DNA complexes (e.g., viruses and complexes involved in DNA damage repair). Through deuterium-labeling methods, this ability can be extended to protein-protein complexes. Importantly, because neutrons are highly penetrating yet nondestructive, large biological complexes can be examined in extreme environments and as they function or undergo changes. Most neutron spectroscopic methods rely on hydrogen to provide the inelastic neutron scattering processes that arise from structural dynamics. Such studies are further enhanced by the application of selective deuterium labeling at the levels of molecules and specific amino acids. The combination of neutron scattering and deuterium labeling opens a vast array of possibilities for experimental design.

Exemplifying DOE's investment in the future of neutron scattering in the United States, SNS represents the next generation of neutron facilities by combining a powerful pulsed neutron source with state-of-the-art time-of-flight scattering instrumentation. The DOE Office of Biological and Environmental Research (BER) and ORNL also have invested in infrastructure to foster structural biology at SNS and HFIR by establishing the Center for Structural Molecular Biology (CSMB). The center operates the Bio-SANS instrument at HFIR and the Bio-Deuteration Laboratory (BDL) for producing isotopically enriched biological macromolecules for neutron scattering studies. These investments provide new opportunities for structural biologists interested in using neutron scattering to support their scientific programs. The staff at SNS, CSMB, and BDL are active researchers who serve and collaborate with the facilities' user communities, including scientists who are new to neutron scattering methods.

New instruments at SNS, enhanced support facilities at CSMB and BDL, and the established and new capabilities at HFIR will add experimental capacity and allow for the study

of smaller samples of more complex materials. The current and future suite of instruments available for studying biological systems is detailed in the Facility Paper, beginning on p. 99, and represents the most significant advance in neutron scattering instrumentation for biology in decades. For example, the crystallography instruments TOPAZ and MaNDi at SNS and IMAGINE at HFIR are projected to significantly increase data collection efficiency. These and other instrument capabilities, together with access to routine perdeuteration of proteins at CSMB, will prove to be a key for studying enzyme mechanisms. To a great extent, such studies have been limited by large sample size requirements, long data collection times, and the lack of availability (or complete absence) of suitable neutron beamlines. Other instruments at SNS will enable experiments previously not feasible with neutrons. For example, the Nanoscale Ordered Materials Diffractometer (NOMAD) and EQ-SANS will allow time-resolved studies of local and supramolecular structures over atomic to cellular length scales as biological systems are subjected to changing conditions, such as during industrial processes used in biofuel production. NSE will allow experimental access, for the first time, to dynamic time scales that correspond to the functionally important collective slow motions of biological macromolecules and their complexes.

In this Science Paper, researchers describe high-impact science of interest to DOE, the National Institutes of Health (NIH), and the National Science Foundation that will be enabled by current and future capabilities at SNS and HFIR. As is common in studies of complex systems, the projects described in the following sections require the application of several complementary experimental and theoretical techniques to truly understand system behavior. X-ray scattering, NMR spectroscopy, and electron microscopy provide complementary information that—when combined with the unique data obtained by using neutrons—results in a holistic picture of these systems. Such a synergistic synthesis cannot be obtained by any one experiment. Additionally, these projects require computational modeling approaches to combine the information from different experimental techniques and to aid the interpretation of neutron scattering data. The key role that neutron scattering will play in the success of these projects demonstrates the growth of its importance in structural biology, a field expected to have a bright future at HFIR and SNS.

## Research

### *Understanding the Molecular Machines of Genomic Maintenance*

**Walter Chazin**

All organisms must maintain the integrity of their genomes to survive. Dividing cells must faithfully replicate and distribute their chromosomes, and all cells must prevent the

accumulation of DNA damage to ensure the protein code remains accurate. DNA can be damaged during replication by reactive metabolic byproducts and mutagens present in the environment. Responding to and repairing DNA damage are critical for cell viability and disease prevention. Accumulated mutations from unrepaired damage in oncogenes and tumor suppressor genes can lead to cancer. As a result, organisms have evolved elegant mechanisms for genomic maintenance. Neutron scattering at SNS affords new ways to probe these molecular machines.

DNA replication, damage response, and repair processes all involve multiple biochemical steps that cannot be accomplished by a single protein, not even a protein composed of several domains with specific functionalities. All living organisms, therefore, have evolved multiprotein machines that exert a coordinated action to achieve these various outcomes. For example, accumulated evidence to date confirms that DNA processing machinery is dynamically assembled and disassembled in conjunction with the cell cycle and in response to encountering DNA damage. Damage response and subsequent repair of all types of DNA lesions must occur in tandem with the replication and transcription of DNA, otherwise the genes and gene products will be compromised. Thus, all aspects of DNA processing are integrated events in cellular life. The grand challenge is to understand the individual machines involved in DNA processes and their interactions as they function.

Technological developments allow investigation of the function of DNA-processing machinery at an ever-increasing level of detail and with a growing number of atomic-resolution domain structures of the proteins involved. Researchers now can begin to address the correlations among molecular structure, cellular outcomes, and disease. A fundamental advance in understanding protein machinery is the realization of the pervasive role of dynamics. Not only is the machine undergoing dynamic transformation, but the proteins themselves are flexible and constantly adapting to the progression through the steps of each process. There are many advantages to dynamic assembly and disassembly, some of which relate to overall cellular efficiency. For example, fewer copies of keystone proteins such as replication protein A (RPA) and proliferating cell nuclear antigen (PCNA) are needed because they can be recycled. Other advantages relate to the need for temporal and spatial regulation and the cross-talk between various DNA processing events in the cell. Within this dynamic context, the activity of the constituent proteins is coordinated to bring about the ordered progression of each process. Many important characteristics of the proteins and a few concepts about the operation of the machinery have been discerned. Concepts such as protein modularity, versatility of common folds, direct competition between sites, and the critical role of allostery are integrated into a framework that forms the underlying basis for the actions of DNA repair machinery.

Neutron scattering experiments will play a key role in understanding DNA processing machinery. In particular, critical gaps remain in our understanding of protein enzymatic action and the remodeling of the architecture of complex machinery as it moves from step to step in a given pathway or at the switch points between pathways. Neutron protein crystallography using the MaNDi instrument at SNS can provide powerful complementary information to x-ray crystallography to elucidate unprecedented detail about the catalytic mechanism of DNA lesion repair. The structure and dynamics of complete, multidomain proteins composed of well-structured domains can be understood through combined application of NMR spectroscopy, small-angle x-ray scattering (SAXS), and small-angle neutron scattering (SANS) using EQ-SANS at SNS with contrast variation and deuterium labeling. Interpreting such data also requires the development and application of new modeling methods. Neutron crystallography and scattering, along with the other tools of structural biology, provide the ability to quantitatively characterize molecular machines to make the connection between their structure and disease. SNS is envisioned as offering key horizon technologies necessary for pursuing investigations of these challenging systems.

## ***Signaling Pathways: Complex Molecular Interactions and Assemblies of Protein Kinases***

**Susan Taylor, Don Blumenthal, Patrick Hogan, and Phineus Markwick**

More and larger structures are being solved by conventional x-ray crystallography and NMR spectroscopy. Yet, becoming increasingly clear with these advances are the major roadblocks still challenging the multilevel understanding of cellular processes involving (1) changes in the chemical profiles of proteins, (2) ligand interactions, (3) assembly of multiprotein complexes, and (4) proteins with flexible linkers and tails. These challenges are particularly true when attempting to model signaling pathways and signaling proteins. A major focus of our work is to understand the structure and function of protein kinase A (PKA), a cAMP-dependent signaling protein. Cyclic adenosine monophosphate (cAMP) is an important second messenger ligand responsible for converting an extracellular stimulus into a cascade of intracellular signaling events. The primary sensor for cAMP in mammalian cells is PKA, whose function is to phosphorylate numerous proteins, resulting in diverse pathways and biological responses. PKA is an inactive tetramer composed of two catalytic (C) subunits bound to a dimer of regulatory (R) subunits. Binding of two cAMP molecules to each R-subunit releases two catalytically active C-subunits. The C-subunit was the first kinase structure to be solved and continues to serve as a prototype for understanding the structure and function of the large kinase enzyme family. Not only is PKA one of the largest gene

families in mammalian cells, it also is critically important for regulating almost every biological process in the cell.

At SNS, there is an enormous opportunity to move beyond the roadblocks of traditional structural biology and address one of the biggest challenges facing the signaling community. Neutron crystallography with the MaNDi instrument at SNS could provide crucial information on the catalytic mechanism of the C-subunit. The impact on the chemical and computational community would be profound, and the relevance of such structures for the biological community would be equally significant. The ability to solve structures of complexes consisting of the C-subunit and R-subunits adds further opportunities for neutron diffraction. Understanding the role of protons and hydrogen-bonding networks in activating an R:C complex by the binding of cAMP is another exciting opportunity. By employing the power of SNS, scientists may be able to analyze larger complexes of assembled proteins.

PKAs typically function as part of large macromolecular complexes that assemble in proximity to their protein substrates. Although higher-order structures are beginning to be solved, challenges remain because of the flexible linkers and loops that often are internal to these complexes and that connect domains or dock to other proteins in the complex. SNS will allow the use of SANS to define the position of the C-subunits in the tetramer, thus providing a powerful way to define the organization of these complexes. As research now moves forward in trying to understand the allostery created by a tetrameric holoenzyme, SAXS and SANS will be used to understand the consequences of single mutations and domain movements associated with targeting and activation. In addition, PKA is targeted to specific sites by scaffold proteins [A-kinase anchoring proteins (AKAPs)] that bind to the small helical dimerization and docking domain in the R-subunit. Thus, with PKA, there is an opportunity to go not only from individual subunits to tetrameric holoenzymes but also to large macromolecular assemblies. As a prototype for such assemblies, we are characterizing the interactions of the RII subunits of PKA that are targeted near calcineurin (CN)—a calcium-dependent phosphatase containing two subunits, CN-A and CN-B—via a small portion of the AKAP79/150 protein. AKAP79/150 localizes PKA and CN to the tails of ion channels, such as the voltage-gated calcium channel. By anchoring the kinase and phosphatase to a small AKAP peptide containing the docking site for both proteins, we have been able to isolate stoichiometric complexes of CN (both the A and B subunits) and PKA (both the R-subunit dimer and the tetrameric R2C2 complex). The opportunities for using SNS to explore the effects of cAMP and calcium on these two proteins are very exciting and provide a wonderful chance to apply SAXS and SANS technologies.

In addition to SANS and crystallography, there also are new opportunities for inelastic neutron scattering and computational studies of PKA. These molecules have considerable functionally important, electrostatics-driven structural plasticity, a feature centrally important for drug discovery. The

conformational flexibility of PKAs provides an opportunity for both traditional inelastic neutron scattering using the BASIS instrument to probe local dynamics and the CNCS and NSE instruments to probe larger collective motions. Considerable progress has been made very recently in the development of computational methods to probe the structures, solvation, and dynamics of proteins and their complexes (Shaw et al. 2010; Markwick et al. 2011). Methods include those based on special-purpose computer hardware and associated software (Shaw et al. 2010) and on complementary approaches based on advances in the statistical mechanical methods underlying molecular dynamics simulations (Markwick et al. 2011). The advances in SANS resources offered by SNS will make available corresponding experimental data on the structures, solvation, and dynamics of proteins and their complexes, allowing rapid progress in understanding the origins of biological activity. Merging results from different time and length scales with the computational tools of molecular dynamics will bridge the experimental and theoretical understanding of how these proteins work.

## References

- Markwick, P. R. L., et al. 2011. “Adaptive Accelerated Molecular Dynamics (Ad-AMD) Revealing the Molecular Plasticity of P450cam,” *Journal of Physical Chemistry Letters* **2**(3), 158–64.
- Shaw, D. E., et al. 2010. “Atomic-Level Characterization of the Structural Dynamics of Proteins,” *Science* **330**(6002), 341–46.

## Structure and Function of a Membrane-Containing Virus

Dennis Brown and Raquel Hernandez

Arthropod-borne viruses (arboviruses), such as those vectored by mosquitoes or ticks, are major causes of human disease. For example, dengue fever virus produces several hundred million cases of human disease per year, and 2.5 billion people are at risk.

The Sindbis virus, transmitted by mosquitoes, is a prototypic member of the arboviruses. Structurally, it is composed of three proteins, two of which are glycoproteins making up an outer icosahedral protein shell. A single protein forms an inner icosahedral shell containing RNA of the virus. Between the two protein shells is a membrane bilayer derived from the host in which the virus is produced. Because arthropods are the vectors for these viruses, the membrane derived from the insect or vertebrate host can have different compositions and yet retain infectious activity between host species (Burge and Strauss 1970; Knight et al. 2009). Similarly, the glycosylation pattern of the outer shell protein derives from the host species (Renkonen et al. 1972; Renkonen et al. 1971). Previously, our group used SANS to characterize structural differences between Sindbis virus particles grown in insect and mammalian cells and found that the host influences more than the structure of the membrane in the virus (see Fig. E12, p. 109; He et al. 2010).

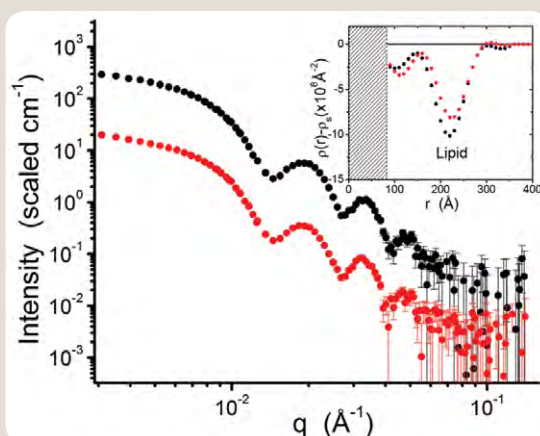
The process of infection by Sindbis virus is complex (Paredes et al. 2004). The structure of the mature virus is metastable and capable of dramatic reorganization of its surface and inner core as it delivers its RNA into a host cell. We believe that changes in its physical and chemical environment can induce many of these morphological changes in the virus. The virus can respond to heat and changes in ionic strength and pH in ways that can be measured by a variety of methods. Understanding the three-dimensional structure of the mature virus and the changes it can undergo is critical to elucidating the process of infection and subsequently designing antiviral compounds to prevent it.

Developing a complete understanding of the process of Sindbis virus infection of cells is one goal of our research. We are studying the structure of Sindbis virus and its ability to change configuration using a combined experimental approach that includes mass spectrometry, electron cryo-microscopy, x-ray crystallography, and SANS. SANS has proven to be a particularly powerful tool for a number of reasons. We have developed a method of purifying Sindbis viruses so that they remain 100% infectious. The exposure to neutrons, in contrast to x-rays, does not decrease virus infectivity (He et al. 2010). By using SANS together with contrast variation methods uniquely enabled by neutrons, we thus can study changes in the virion and its lipid, protein, and RNA components in response to environmental shifts—confident that the analysis is not damaging virus infectivity. Furthermore, the inherent time-resolved nature of measurements at SNS using EQ-SANS raises the possibility of being able to probe conformational changes in Sindbis virus *in situ*. This would allow, for example, continuous monitoring of conformational changes in the structure of the virus as the pH of the solution is lowered. Such studies are impossible with other experimental techniques.

## References

- Burge, B. W., and J. H. Strauss, Jr. 1970. "Glycopeptides of the Membrane Glycoprotein of Sindbis Virus," *Journal of Molecular Biology* **47**(3), 449–66.
- He, L., et al. 2010. "The Structure of Sindbis Virus Produced from Vertebrate and Invertebrate Hosts as Determined by Small-Angle Neutron Scattering," *Journal of Virology* **84**(10), 5270–76.
- Knight, R. L., et al. 2009. "Role of N-Linked Glycosylation for Sindbis Virus Infection and Replication in Vertebrate and Invertebrate Systems," *Journal of Virology* **83**(11), 5640–47.

**Fig. E12. SANS profiles for Sindbis virus particles grown in a mammal (black) and insect (red). Inset shows profiles of the radial scattering length density difference derived from SANS data. The strong feature results from the lipid bilayer of the virus, and the differences therein result from the higher cholesterol content in the mammalian-grown virus particle.** [From He, L., et al. 2010. "The Structure of Sindbis Virus Produced from Vertebrate and Invertebrate Hosts as Determined by Small-Angle Neutron Scattering," *Journal of Virology* **84**(10), 5270–76. DOI: 10.1128/JVI.00044-10. Reproduced with permission from the American Society for Microbiology.]



Paredes, A. M., et al. 2004. "Conformational Changes in Sindbis Virions Resulting from Exposure to Low pH and Interactions with Cells Suggest that Cell Penetration May Occur at the Cell Surface in the Absence of Membrane Fusion," *Virology* **324**, 373–86.

Renkonen, O., et al. 1971. "The Lipid Class Composition of Semliki Forest Virus and Plasma Membranes of the Host Cells," *Virology* **46**(2), 318–26.

Renkonen, O., et al. 1972. "The Lipids of the Plasma Membranes and Endoplasmic Reticulum from Cultured Baby Hamster Kidney Cells (BHK21)," *Biochimica et Biophysica Acta* **255**(1), 66–78.

## Investigating Light-Energy Trapping and Transfer in Photosynthesis

Robert Blankenship

The photosynthetic apparatus of plants, algae, and bacteria is a multicomponent, complex, and hierarchical assembly that converts solar energy into chemical energy. The first step in photosynthesis is light capture by antenna systems that absorb and transfer solar energy to the reaction centers where photochemistry occurs. The antenna systems found in photosynthetic organisms are strikingly diverse structures highly specialized to optimize capture of the maximum light energy available to an organism in its native environment. This diversity is evident in the range of different antenna complexes found in (1) cyanobacteria (phycobilisomes), (2) plants (light-harvesting complexes LHC I and LHC II), (3) purple photosynthetic bacteria (LH1 and LH2), and (4) green photosynthetic bacteria [chlorosomes and Fenna-Matthews-Olson (FMO) protein]—all of which have different structural architectures and even different types of light-absorbing pigment molecules.

Funded by the DOE Office of Basic Energy Sciences, the Photosynthetic Antenna Research Center is an Energy Frontier Research Center dedicated to understanding the basic scientific principles of light harvesting and energy

funneling in antenna systems as applied to natural, biohybrid, and biomimetic photosynthetic systems. Aspects of this problem include:

- Studying the effects of size and pigment composition of natural antenna systems on the efficiency of energy conversion.
- Understanding antenna regulation, control, and repair.
- Extending the range of photosynthetically active radiation into other regions of the solar spectrum.
- Designing hybrid and biomimetic systems so that they use the principles of natural antennae to enhance energy collection and storage.

Native and recombinant antenna complexes have been studied using a range of structural techniques, including x-ray crystallography, various types of microscopies, and steady-state and ultrafast spectroscopies. These studies provided a wealth of information on and insight into the structure and function of components such as the LH2 complex and the reaction center. However, the inherent structural heterogeneity in these systems has hampered efforts to determine how the components interact to form integrated functional pathways. In particular, the multimembrane, supramolecular organization of these photosynthetic pathways makes ascertaining information about the precise organization of the individual complexes difficult. Details of how the FMO antenna complex is organized in the complex architecture of the green bacterial photosynthetic apparatus are just now being elucidated. These examples illustrate the challenges in understanding the complex hierarchical machinery of photosynthetic organisms. To comprehensively understand the overall energy-trapping and -transfer processes, structural information at many different length scales is required.

ORNL offers a powerful new suite of instruments for small-angle scattering, diffraction, spectroscopy, and reflectometry—all of which promise 10- to 1,000-fold gains in performance. Neutron scattering techniques such as small-angle scattering (EQ-SANS and Bio-SANS), reflectivity (Liquids Reflectometer), and crystallography (TOPAZ, MaNDi, and IMAGINE) can play important roles in investigating natural antenna systems, such as their assembly, packing fraction, distribution, organizational structure, and pigment composition. These studies will provide insight into many facets of the photosynthetic process, including efficiency of light-energy conversion in plant photosynthetic machinery; antenna regulation, control, and repair; and design of hybrid and biomimetic antenna systems for enhanced energy collection and storage.

## ***Enzymes for Carbon Sequestration and Renewable Energy: Carbonic Anhydrases***

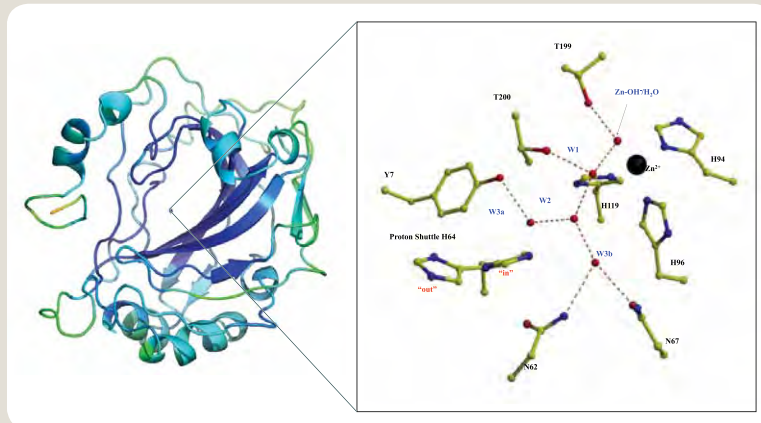
**David Silverman and Zöe Fisher**

Carbonic anhydrases (CAs) are ubiquitous enzymes found in diverse organisms from humans to archaeobacteria. We are investigating several CAs that have potential applications in renewable energy and the environment, aiming to understand their detailed catalytic mechanisms. The important biochemical reaction in this system involves transferring hydrogen, an atom difficult to locate using crystallography with x-rays but easy to locate with neutrons. This capability allows us to answer many questions about CAs that have been unresolved for years despite extensive study by other complementary methods. Some key questions about CA mechanisms involve the nature of the transition state, ionization state of the zinc-bound aqueous ligand and other groups in the active-site cavity that influence catalysis, and the conformation of the proton transfer pathway.

We plan to address these questions by preparing deuterated crystals of various CA mutants at four or five different pH (pD) values and then determine the neutron structures of each state. Such an approach simply would not have been possible even 3 years ago but is now becoming feasible due to SNS development and the increasing number of macromolecular neutron crystallography beamlines coming online. The resulting SNS-enabled discoveries on the catalytic mechanisms of CAs will be exploited to manipulate enzyme performance and use for renewable energy and carbon sequestration. In the recent past, researchers were fortunate to have been able to pursue a single neutron structure, which then could take years to complete. Now, with the advent of 10- to 100-fold increases in flux, scientists can actually prepare and collect neutron data from several deuterated samples under different conditions to trap intermediates and mimic catalysis by varying pH (pD) or other conditions.

**The Nature of the Transition State.** A long-standing issue concerning transition-state structure in catalysis of carbon dioxide (CO<sub>2</sub>) hydration relates to the position of the hydrogen and mode of binding to the zinc (the Lindskog versus Lipscomb model; Silverman and McKenna 2007). At least two sites on the forming bicarbonate (HCO<sub>3</sub><sup>-</sup>) are possibilities for hydrogen binding: one proximal to the zinc and likely hydrogen-bonded to the side-chain hydroxyl of Thr-199, and the other distal to the zinc and hydrogen-bonded at another site such as a water molecule in the active-site cavity. An x-ray structure of substrate bicarbonate bound to T200H HCA II is reported (Xue et al. 1993). Examination of such a structure by neutron diffraction that can locate hydrogen-deuterium exchangeable sites would do much to resolve this issue that has been the subject of countless experimental and computational approaches. Such capabilities are important not only for CA but also for enzymes of similar structure and mechanism, such as the zinc-containing beta-lactamases that

**Fig. E13. Carbonic anhydrase catalyzes the reversible interconversion of  $\text{CO}_2$  to  $\text{HCO}_3^-$  and is rate-limited by a proton transfer (PT) event between a zinc-bound solvent and internal proton shuttle, His64. PT is thought to be mediated by a hydrogen-bonded network of solvent molecules (ZnH<sub>2</sub>O, W1, W2, W3a, and W3b) that spans the ~8 Å distance between the catalytic zinc and bulk solvent. Despite the availability of atomic-resolution x-ray structures, it is still unknown whether the zinc-bound solvent is water or hydroxide, if H64 is charged or neutral, and how the solvents are oriented with respect to each other and active-site residues. Understanding how the enzyme facilitates  $\text{CO}_2$  hydration and proton transfer**



will help in devising methods for using biological systems for carbon sequestration and ultimately will assist with reducing carbon emissions. This information can be used to make a better, faster enzyme that will help accomplish these goals more efficiently. [Close-up of active site from Budayova-Spano, M., et al. 2006. "Production and X-Ray Crystallographic Analysis of Fully Deuterated Human Carbonic Anhydrase II," *Acta Crystallographica F: Structural Biology and Crystallization Communications* **62**(1), 6–9.]

hydrolyze penicillins, cephalosporins, and carbapenems and are mechanisms of drug resistance.

**The Ionization State of Active-Site Groups.** Neutron diffraction also has the capability to resolve long-standing uncertainties as to the ionization state of the zinc-bound water, the carboxyl group of Glu106, the phenol side chain of Tyr7, and the imidazole side chain of His64. All of these active-site groups play critical roles in the catalysis, and new and surprising results are being obtained from the single neutron structure so far achieved (Fisher et al. 2010). Experiments need to be performed for a series of different conditions of pH (pD), with a series of site-specific mutants related to known catalytic rates. Such results could lead to a paradigm shift in understanding the zinc-hydroxide mechanism of CA and related enzymes such as beta-lactamase and alkaline phosphatase. This plan requires a more rapid turnaround of structures and would be enabled by SNS.

**The Proton Transfer Pathway.** Detailed examination of the ionization states of both residues and the structure and hydrogen-bonding schemes of ordered water molecules in the active-site cavity is necessary to understand the proton transfer mechanism in CA (see Fig. E13, this page). Information about the specific orientations of waters and the hydrogen bonding in ground-state CA structures is vital to relate structure to function. Many catalytic rates of proton transfer are currently available (Silverman and McKenna 2007; Fisher et al. 2007), but an underlying and unifying understanding would be provided by structural details revealed by neutron diffraction. In particular, such structural data would be significant in estimating the relevance of the Marcus Theory of proton transfer in the active site (Silverman et al. 1993). CA serves as an important model for proton

transfer through long distances in a protein environment and hence is relevant to proton transfer in more complex and vital biosystems such as ATP synthase, cytochrome oxidase, and the photosynthetic reaction center.

## References

- Budayova-Spano, M., et al. 2006. "Production and X-Ray Crystallographic Analysis of Fully Deuterated Human Carbonic Anhydrase II," *Acta Crystallographica F: Structural Biology and Crystallization Communications* **62**(1), 6–9.
- Fisher, S. Z., et al. 2007. "Speeding Up Proton Transfer in a Fast Enzyme: Kinetic and Crystallographic Studies on the Effect of Hydrophobic Amino Acid Substitutions in the Active Site of Human Carbonic Anhydrase II," *Biochemistry* **46**, 3803–13.
- Fisher, S. Z., et al. 2010. "Neutron Structure of Human Carbonic Anhydrase II: Implications for Proton Transfer," *Biochemistry* **49**(3), 415–21.
- Silverman, D. N., and R. McKenna. 2007. "Solvent-Mediated Proton Transfer in Catalysis by Carbonic Anhydrase," *Accounts of Chemical Research* **40**(8), 669–75.
- Silverman, D. N., et al. 1993. "Rate-Equilibria Relationships in Intramolecular Proton Transfer in Human Carbonic Anhydrase III," *Biochemistry* **32**(40), 10757–62.
- Xue, Y. F., et al. 1993. "Crystallographic Analysis of Thr-200 → His Human Carbonic Anhydrase II and Its Complex with the Substrate,  $\text{HCO}_3^-$ ," *Proteins: Structure, Function, and Bioinformatics* **15**(1), 80–87.

## Investigating Structural Changes During Voltage-Gating in a Potassium Channel

Stephen H. White, A. Richard Chamberlin, Douglas J. Tobias, Ella Mihailescu, David Worcester, Dmitriy Krepkiy, and Kenton Swartz

Throughout the biological world, cell membranes are crucial to the life of individual cells. In animal cells, the plasma membrane is a selectively permeable barrier (primarily made up of proteins and lipids) that separates the cytosol from the cell's extracellular environment. Ionic channels constitute an important part of the cell membrane by forming a small voltage gradient across the membrane as a result of ions flowing down their electrochemical gradients. The basis of membrane excitability (e.g., in neurons and muscle cells) is the flow of ions through voltage-gated ion channels, which consist of a single pore domain and four voltage-sensing domains (VSDs).

Conformational changes to VSDs in response to changes in transmembrane potential lead to the opening and closing of the ion-conducting pore. A team of scientists from the University of California–Irvine, the University of Pennsylvania, the National Institute of Standards and Technology Center for Neutron Research (NCNR), and NIH is investigating the molecular-scale details of this process, with support from an NIH Program Project grant. The primary goal of the project is to elucidate the structure and dynamics of VSDs—as well as their surrounding membrane and associated water molecules—in response to changes in transmembrane potential. Neutron diffraction and reflectometry measurements will be used in conjunction with molecular dynamics (MD) simulations. Researchers recently demonstrated the potential of the combined neutron scattering–MD simulation approach using the Advanced Neutron Diffractometer / Reflectometer (AND/R) at NCNR (Krepkiy et al. 2009); this work can be readily expanded through the capabilities offered by SNS.

In September 2010, the research team carried out a neutron reflectometry experiment on the Magnetism Reflectometer at SNS using vectorially oriented VSDs and channels in membranes with *in situ* manipulation of electrochemical potential. Preliminary data show that the reflectivity from the team's inorganic multilayer substrates was significantly better than data from the AND/R instrument at NCNR over the accessible region of higher  $Q$  (0.15 to 0.30  $\text{\AA}^{-1}$ ). The team is scheduled to begin the first experiments with the VSD protein vectorially oriented within fully hydrated, single bilayer membranes tethered to the surface of silicon-nickel-silicon multilayer substrates in an electrochemical cell. If the planned experiments are successful, the unique capabilities of SNS, coupled with the deuteration of selected residues within the VSDs, are anticipated to help the team realize the goals of its ambitious project.

### Reference

Krepkiy, D., et al. 2009. "Structure and Hydration of Membranes Embedded with Voltage-Sensing Domains," *Nature* **462**, 473–79.

## Understanding the Cellulose-Degrading Mechanisms of Cellulosome Enzyme Complexes

Yannick J. Bomble, Michael E. Himmel, and Michael F. Crowley

Cellulosic biomass is the most abundant biological material on Earth. As such, it is a vast, renewable resource for human energy needs, for both fuels and power. Substantial U.S. and international research efforts are focused on engineering bacterial enzymes to convert lignocellulosic biomass more efficiently to sugars, which then can be fermented to liquid fuels. Neutrons already are being used extensively to study various aspects of this conversion process. Those aspects include (1) The structure and hydrogen bonding in cellulose using SANS and fiber diffraction, (2) the detailed catalytic mechanisms of enzymes involved in biomass hydrolysis and sugar metabolism using neutron crystallography, and (3) the pretreatment of cellulosic biomass using SANS and neutron spin echo spectroscopy. In addition to broadening and enhancing these existing studies, SNS will make possible new and more complex areas of research such as understanding and developing cellulosomes for biofuels. In nature, many bacteria break down lignocellulosic biomass using large, extracellular enzyme complexes—cellulosomes—that consist of cellulose-degrading enzymes noncovalently bound to long peptide scaffolds.

Although the structures of many cellulase enzyme domains have been solved, there are few studies that probe the solution structure of fungal enzymes or large, complexed cellulosomes. We already have used SAXS to examine enzymes from the cellulosomal bacterium *Clostridium thermocellum*. This work provided invaluable insights into the function of the cellulosome. However, the direct comparison to our extensive set of molecular dynamics simulations exhibited a crucial limitation: within the framework of SAXS, conducting these experiments is extremely difficult if not impossible while the cellulosome or cellulosomal enzymes are degrading cellulose. This difficulty arises mainly because of radiation damage by x-rays and a lack of scattering contrast between enzyme complex and substrate. Combining neutron scattering with deuterated cellulosomes would enable us to obtain direct measurements of the radius of gyration of these enzymes' complex "molecular envelopes" on cellulose substrates. This information is extremely important for our primary investigation of the multimodular enzyme CbhA (see Fig. E14, p. 113), a study in which we hypothesize that this enzyme adopts a radically different conformation on cellulose than in solution (i.e., a conformation in which its seven modules can work in concert). Additionally, neutron scattering is essential to probe the flexibility of the populated cellulosome and the accessible surface coverage of the cellulosomal complex on cellulose. Neutrons represent our best hope of imaging this process in motion. Overall, this work will support our ongoing modeling

efforts and drive rational protein engineering approaches to design enhanced cellulosomes for biofuels applications in the DOE BER–sponsored BioEnergy Science Center (BESC).

BESC, a multi-institutional collaboration consisting of 19 partners, is using a multidisciplinary research program to understand and eliminate biomass recalcitrance. The program spans the biological, chemical, physical, and computational sciences, as well as mathematics and engineering. Scientists in BESC seek to improve the accessibility of the sugars within biomass through the design of plant cell walls for rapid deconstruction. Specifically, BESC is working with two potential bioenergy crops, switchgrass and *Populus*, to develop varieties that are easier to break down into fermentable sugars. BESC also is developing multitasking microbes for converting plant biomass into biofuels through consolidated bioprocessing. Addressing the roadblock of biomass recalcitrance to improve the yields of biofuels will require developing a multiscale

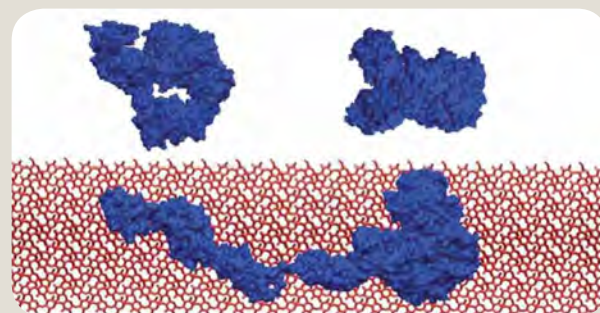


**Fig. E14. The multimodular enzyme CbhA (blue) in its active and extended form on a cellulose surface (red) and in a more compact configuration in solution.**

understanding of plant cell walls during both biosynthesis and various deconstruction pathways, such as the work with the cellulosome described here.

**Table E5. Contributing Scientists**

Name	Position and Affiliation	E-mail
Robert Blankenship	Lucille P. Markey Professor of Biology and Chemistry, Washington University	blankenship@wustl.edu
Don Blumenthal	Associate Professor of Pharmacology and Toxicology, University of Utah	don.blumenthal@pharm.utah.edu
Yannick J. Bomble	Research Scientist, National Renewable Energy Laboratory	yannick.bomble@nrel.gov
Dennis Brown	Professor and Head of Biochemistry, North Carolina State University	dennis_brown@ncsu.edu
A. Richard Chamberlin	Professor, Chemistry School of Physical Sciences; Professor and Chair of Pharmaceutical Sciences, University of California–Irvine	richard.chamberlin@uci.edu
Walter Chazin	Professor of Biochemistry and Chemistry, Director of Structural Biology, Vanderbilt University	walter.chazin@vanderbilt.edu
Michael F. Crowley	Senior Scientist, National Renewable Energy Laboratory	michael.crowley@nrel.gov
Wolfgang Dostmann	Professor of Pharmacology, University of Vermont College of Medicine	wolfgang.dostmann@uvm.edu
S. Zöe Fisher	Research Scientist, Los Alamos National Laboratory	zfisher@lanl.gov
Raquel Hernandez	Senior Research Scientist in Biochemistry, North Carolina State University	raquel_hernandez@ncsu.edu
Michael E. Himmel	Team Leader of the award-winning cellulase enzyme technology effort, National Renewable Energy Laboratory	mike.himmel@nrel.gov
Patrick Hogan	Professor of Signaling and Gene Expression Research, La Jolla Institute for Allergy and Immunology	hogan@liai.org
Dmitriy Krepkiy	Research Scientist, National Institutes of Health	krepkiyd@ninds.nih.gov
Phineus Markwick	Senior Research Scientist, University of California–San Diego	pmarkwick@ucsd.edu
Ella Mihailescu	Institute for Bioscience and Biotechnology Research, a joint institute of the National Institute of Standards and Technology and the University of Maryland	ella.mihailescu@nist.gov
David Silverman	Distinguished Professor of Pharmacology, University of Florida	silvrnm@ufl.edu
Kenton Swartz	Senior Investigator in Neuroscience, National Institutes of Health	swartzk@ninds.nih.gov
Susan Taylor	Investigator, Howard Hughes Medical Institute; Professor of Chemistry and Biochemistry, and Pharmacology, University of California–San Diego	staylor@ucsd.edu
Douglas J. Tobias	Professor of Chemistry, School of Physical Sciences, University of California–Irvine	dtobias@uci.edu
Stephen H. White	Professor, Department of Physiology and Biophysics, University of California–Irvine	stephen.white@uci.edu
David Worcester	Associate Professor of Biological Sciences, University of Missouri	worcesterd@missouri.edu



# Workshop Agenda

*U.S. Department of Energy  
Office of Biological and Environmental Research*

## Applications of New DOE National User Facilities in Biology Workshop

Plaza III Room, Hilton Hotel, Rockville, Maryland

May 9–11, 2011

### Monday, May 9

- 6:30 p.m. Dinner for panel, chairs, DOE staff  
 7:30 p.m. Introductions  
 7:40 p.m. **Roland Hirsch** Background and motivation for workshop and report  
 8:00 p.m. **Dagmar Ringe** Workshop preview and report overview, assignments, and schedule

### Tuesday, May 10

Meetings with delegations from the new and planned user facilities

#### David Eisenberg, Chair

- 8:30 a.m. Brookhaven National Laboratory, National Synchrotron Light Source-II (NSLS-II)  
 9:45 a.m. Panel discussion  
 10:00 a.m. Break  
 10:15 a.m. Argonne National Laboratory, Advanced Photon Source Upgrade (APS-U)  
 11:30 a.m. Panel discussion  
 11:45 a.m. Lunch for panel, chairs, staff

#### Dagmar Ringe, Chair

- 12:45 p.m. SLAC National Accelerator Laboratory, Linac Coherent Light Source (and LCLS-II)  
 2:00 p.m. Panel discussion  
 2:15 p.m. Break  
 2:30 p.m. Lawrence Berkeley National Laboratory, Next Generation Light Source (NGLS)  
 3:45 p.m. Panel discussion  
 4:00 p.m. Break  
 4:15 p.m. Oak Ridge National Laboratory, Spallation Neutron Source (SNS)  
 5:30 p.m. Panel discussion  
 5:45 p.m. Panel executive session  
 6:15 p.m. Adjournment (informal dinner arrangements by panel members)

### Wednesday, May 11

- David Eisenberg, Chair** Meeting of panel and agency staff  
 8:00 a.m. NSLS-II  
 8:30 a.m. APS-U  
 9:00 a.m. LCLS-II  
 9:30 a.m. NGLS  
 10:00 a.m. SNS  
 10:30 a.m. Major needs that no planned facility will meet  
 10:45 a.m. Break into groups for report writing  
 12:00 p.m. Lunch  
 3:00 p.m. Close of workshop

# Workshop Participants and Observers

## Workshop co-chairs

**David Eisenberg**  
University of California–Los Angeles

**Dagmar Ringe**  
Brandeis University

**Janet Smith**  
University of Michigan

**Matthias Wilmanns\***  
European Molecular Biology Laboratory

**Masaki Yamamoto**  
SPring-8

**Kamal Shukla**  
National Science Foundation  
Directorate for Biological Sciences

**Ward Smith**  
National Institutes of Health  
National Institute of General Medical Sciences

## Participants

**J. Kent Blasie**  
University of Pennsylvania

**Valeri Copie**  
Montana State University

**Jennifer DuBois**  
University of Notre Dame

**Joachim Frank**  
Columbia University

**James Fredrickson**  
Pacific Northwest National Laboratory

**Petra Fromme**  
Arizona State University

**Sol Gruner**  
Cornell University

**Janos Hajdu**  
Uppsala University

**Steve Harrison\***  
Harvard University

**Ken Keegstra**  
Michigan State University

**Alfonso Mondragon**  
Northwestern University

**Doug Rees\***  
California Institute of Technology

**Christian Riek**  
European Synchrotron Research Facility

**Clemens Schulze-Briese**  
Dectris AG

\*Did not attend full workshop but assisted with writing the report.

## Observers

**Todd Anderson**  
U.S. Department of Energy  
Office of Biological and Environmental Research

**Benjamin Brown**  
U.S. Department of Energy  
Office of Science

**Susan Gregurick**  
U.S. Department of Energy  
Office of Biological and Environmental Research

**Roland Hirsch**  
U.S. Department of Energy  
Office of Biological and Environmental Research

**Jeff Krause**  
U.S. Department of Energy  
Office of Basic Energy Sciences

**Peter Lee**  
U.S. Department of Energy  
Office of Basic Energy Sciences

**Gail McLean**  
U.S. Department of Energy  
Office of Basic Energy Sciences

**Dan Neumann**  
U.S. Department of Commerce  
National Institute of Standards and Technology

**Robert Stack**  
U.S. Department of Energy  
Office of Basic Energy Sciences

**Amy Swain**  
National Institutes of Health  
National Center for Research Resources

**Guebre Tessema**  
National Science Foundation  
Directorate for Mathematical and Physical Sciences

**David Thomassen**  
U.S. Department of Energy  
Office of Biological and Environmental Research

**Sharlene Weatherwax**  
U.S. Department of Energy  
Office of Biological and Environmental Research

**Mary Ann Wu**  
National Institutes of Health  
National Center for Research Resources

**Shireen Yousef**  
U.S. Department of Energy  
Office of Biological and Environmental Research

**Report Preparation**  
**Biological and Environmental Research Information System**  
Oak Ridge National Laboratory  
Holly Haun, Judy Wyrick, Marissa Mills, Kris Christen, Brett Hopwood, Jennifer Bownas, Betty Mansfield



Workshop panel, DOE observers, and science communications staff at the May 2011 meeting.

## Acronyms and Abbreviations

3D	three dimensional (also 1D, 2D, 4D, and 6D)	fCNT	fluorescence computed nanotomography	NYX	NYSBC microdiffraction beamline
3PW	three-pole wigglers	FEE	Front End Enclosure	OEC	oxygen-evolving complex
Å	angstrom	FEL	free-electron laser	OPA	optical parametric amplifier
ABS	automated biomolecular solution scattering	FERMI	Free Electron Laser for Multidisciplinary Investigations	ORNL	Oak Ridge National Laboratory
AD	Alzheimer's disease	FLASH	Free-Electron Laser in Hamburg	PAD	pixel array detector
AIM	advanced infrared microspectroscopy	FMO	Fenna-Matthews-Olson protein	pC	picoCoulomb
AKAP	A-kinase anchoring protein	FMX	frontier macromolecular crystallography	PCNA	proliferating cell nuclear antigen
ALS	Advanced Light Source	fs	femtosecond	PKA	protein kinase A
AMO	Atomic, Molecular, and Optical Science instrument at LCLS	fSAXS	fluctuation small-angle x-ray scattering	PRP	Proposal Review Panel
AMX	flexible access macromolecular crystallography	FT-IR	Fourier transform infrared	PS I	photosystem I
ANL	Argonne National Laboratory	FTE	full time equivalent	PS II	photosystem II
APAD	analog-integrating pixel array detector	FWHM	full width at half maximum	PSD	position-sensitive x-ray detector
APCF	Advanced Protein Crystallization Facility	FXI	long beamline for full-field imaging	PT	proton transfer
APPLE	advanced planar polarized light emitted	fXS	fluctuation x-ray scattering	PYP	photoactive yellow protein
APS	Advanced Photon Source	GeV	gigaelectron volt	Q	wave vector transfer
APS-U	Advanced Photon Source Upgrade Project	GFP	green fluorescent protein	R&D	research and development
ASAXS	anomalous small-angle x-ray scattering	GISAXS	grazing incidence small-angle x-ray scattering	RF	radio frequency
BASIS	Backscattering Spectrometer	GM/CA-CAT	National Institute of General Medical Sciences and National Cancer Institute Collaborative Access Team at the Advanced Photon Source	RIP	radiation damage-induced phasing
BDL	Bio-Deuteration Laboratory	GPCR	G protein-coupled receptors	RNA	ribonucleic acid
BER	Office of Biological and Environmental Research	GP-SANS	General-Purpose small-angle neutron scattering	RPA	replication protein A
BES	Office of Basic Energy Sciences	GTF	general transcription factor	SAC	Scientific Advisory Committee
BESAC	Basic Energy Sciences Advisory Committee	HFIR	High Flux Isotope Reactor	SAD	single-wavelength anomalous dispersion
BioCARS	biology-focused part of the Center for Advanced Radiation Sources	HHG	high harmonic generation	SANS	small-angle neutron scattering
BM	bend magnet	HXN	hard x-ray nanoprobe	SASE	self-amplified spontaneous emission
BPM	beam position monitor	Hz	Hertz	SAXS	small-angle x-ray scattering
°C	degrees Centigrade	IR	infrared	SCRf	superconducting radio frequency
CA	carbonic anhydrase	IRI	full-field infrared spectroscopic imaging	SHAB	second harmonic afterburner
cAMP	cyclic adenosine monophosphate	IXS	inelastic x-ray scattering	SMD	single-molecule diffraction
CAMP	CFEL Advanced Study Group Multipurpose Chamber	K	degrees Kelvin	SM3	correlated spectroscopy and MX beamline at NSLS-II
CCD	charge-coupled device	KB	Kirkpatrick-Baez	SNS	Spallation Neutron Source
CD	critical decision	keV	kiloelectron volt	SONIC	second-order nonlinear optical imaging of chiral crystals
CDI	coherent diffraction imaging	LAX	low-energy anomalous x-ray diffraction	SRX	submicron resolution x-ray spectroscopy
CFEL	Center for Free-Electron Laser Science	LCF	Leadership Computing Facility	SSRL	Stanford Synchrotron Radiation Lightsource
CHX	coherent hard x-ray scattering	LCLS	Linac Coherent Light Source	STXM	scanning transmission x-ray microscopy
CN	calcineurin	LHC	light-harvesting complex	SRX	submicron resolution x-ray spectroscopy
CNCS	Cold Neutron Chopper Spectrometer	LIX	x-ray scattering for life sciences beamline at NSLS-II	SXR	Soft X-ray Materials Science instrument at LCLS
CSMB	Center for Structural Molecular Biology	LOB	Laboratory Office Building	T	tesla
CS-PAD	Cornell SLAC Pixel Array Detector	μ-EXAFS	microfocused extended x-ray absorption fine structure	TAML	tetra-amido macrocyclic ligand
CT	computed tomography	μ-XANES	micro-x-ray absorption near-edge spectroscopy	TB	terabytes
CXDI	coherent x-ray diffraction imaging	mA	milliamperes	TF	trigger factor
CXI	Coherent X-Ray Imaging instrument at LCLS	MAD	multiwavelength anomalous dispersion	TMV	tobacco mosaic virus
CW	continuous wave	MaNDi	macromolecular neutron diffractometer	THz	terahertz
CXS	correlated x-ray scattering	MD	molecular dynamics	TXM	transmission x-ray microscope
CypA	cycophilin A enzyme	MEC	Matter in Extreme Conditions instrument at LCLS	UEC	Users' Executive Committee
cryo-EM	cryo-electron microscopy	MIT	medical imaging and radiation therapy (NSLS-II)	UV	ultraviolet
cryo-FIB	cryo-focused ion beam	mL	milliliter	VHF	very high frequency
Da	Dalton	MRI	magnetic resonance imaging	VISAR	velocity interferometer system for any reflector
DESY	Deutsches Elektronen Synchrotron	MX	macromolecular crystallography	VSD	voltage-sensing domain
DNA	deoxyribonucleic acid	NCNR	National Institute of Standards and Technology Center for Neutron Research	WAXS	wide-angle x-ray scattering
DOE	U.S. Department of Energy	Nd:YAG	neodymium-doped yttrium aluminium garnet	XANES	x-ray absorption near-edge structure
DW	damping wigglers	NIH	National Institutes of Health	XAS	x-ray absorption spectroscopy
EEHG	Enhanced Echo Harmonic Generation	NGLS	Next Generation Light Source	XCS	X-Ray Correlation Spectroscopy instrument at LCLS
EGF	epidermal growth factor	NMR	nuclear magnetic resonance	XDM	x-ray diffraction microscopy
EGFR	epidermal growth factor receptor	NOMAD	Nanoscale Ordered Materials Diffractometer	XES	x-ray emission spectroscopy
EM	electron microscopy	NSE	Neutron Spin Echo spectrometer	XFEL	x-ray free-electron laser
EMBL	European Molecular Biology Laboratory	NSF	National Science Foundation	XFM	x-ray fluorescence microscopy
EQ-SANS	Extended Q-range small-angle neutron scattering	NSLS	National Synchrotron Light Source	XFP	x-ray footprinting
ERL	energy recovery linac			XPCS	x-ray photon correlation spectroscopy
ESRF	European Synchrotron Radiation Facility			XPP	X-Ray Pump Probe instrument at LCLS
ET	electron transfer			XRS	x-ray scattering
EUV	extreme ultraviolet			XUV	extreme ultraviolet
eV	electron volt				
EXAFS	extended x-ray absorption fine structure				
FAD	flavin adenine dinucleotide				
fCMT	fluorescence computed microtomography				

